STUDIES OF THE THERMODYNAMICS OF SOME NATIVE AND RUTHENATED METALLOPROTEINS BY SPECTROELECTROCHEMISTRY

Thesis by

Huey-jenn Chiang

In Partial Fulfillment of the Requirements

for the Degree of

Doctor of Philosophy

California Institute of Technology

Pasadena, California

1987

(Submitted May 4, 1987)

DEDICATED TO

MY HERO, COMMANDER, AND FATHER

MR. TAO CHIANG

A GIANT WHO KEEPS HIMSELF GOING ON FOR SUCCESS

WITH ONLY LIMITED LUCK AND RESOURCES

ACKNOWLEDGEMENTS

My years at Caltech as a graduate student are the most cherished of my student career. I am glad to have had my prime time of learning in concert with this wonderful experience. I would like to express my appreciation to those people, without whose help and inspiration, it would not have been possible for me to make progress during my years here. Forgive me for being unable to pay my gratitude to each one of them by name.

First of all, Professor Harry B. Gray, my research advisor. He deserves my deepest gratitude. I appreciate the scientific guidance and the financial support he has provided for me during these years. His great personality will continue to affect my future life. No matter what and where I will be, he will always be the hero image that I shall try to follow.

Many thanks to Professor Terry J. Collins and Professor John J. Hopfield for their guidance and help throughout my graduate studies at Caltech. I appreciate their excellent service as members of my Ph.D. committee. I also want to thank Professor Rudy A. Marcus for being a committee member for my final oral examination on my hasty invitation.

I want to thank Dr. Vernon T. Taniguchi for leading me into the field of spectroelectrochemistry. His contribution can be felt throughout the whole thesis. To Dr. Chi-Ming Che, my longtime collaborator, I would like to say thank you for everything he has done

for me. I would also like to thank Professors Nenad M. Kostić and Robert J. Crutchley. I have enjoyed having the opportunity to cooperate with them on projects involving azurin and with ruthenated myoglobin, respectively. I would also like to thank Dr. Hsue-Yang Liu for his assistance in the field of electrochemistry. My thanks also go to Ms. Ting-Lin Kao for her help in the laboratory, I wish her the best of luck in her future career.

I would like to thank two of my chemistry teachers at Tamkang University. Professor Kee-Chuan Pan was the key person who educated me to be a scientist. He is still the best physicist and mathematician I have ever met. Professor Bor-Her Chen, even though I have never taken any classes from him officially, encouraged me to travel to the United States to study. To these people, I shall always be grateful.

In those years at Auburn University, I thank Professor S. Davis Worley for being my research advisor. I appreciate everything he has done for me. I learned a lot, and owe a lot to Professors Curtis H. Ward and Philip B. Shevlin. They treated me as one of their own students, and without their recommendations I do not think I would have been able to go one step further.

The enthusiasm and cordiality of Dr. Arthur Er-terg Chiou set a standard for me to follow. I appreciate his friendship, guidance and tolerance during these years. Mr. and Mrs. Tony Chang also deserve the thanks for their warm friendship and hospitality. Drs. Yu-Min Tsou and Y. Henry Sun are the best friends I could possibly have. I

have also enjoyed many conversations with Professors Chao-Ying Meng and Yuk Ling Yung and Dr. Mary Zi-ping Luo; I appreciate the intellectual characteristics of our friendship. Mr. Chih-herng Yin, the guy has warmed me up for twenty five years. The only feeling I have is to keep it going forever and enjoy.

Professor Ambrose Yaw-Shong Jong and Mr. Chien-Tsung Mickey Hu are my tutors on molecular biology. I appreciate their enthusiasm in educating me to be a biological scientist. Especially Professor Jong, he even designed a laboratory course solely for me without getting any credit and, of course, without pay.

I appreciate the companionship of all the present and past members of Professor Gray's group. I want to thank especially Drs. Jay R. Winkler, Walther R. Ellis, Jr., Michael D. Hopkins, Charlie M. Lieber, Michael Albin, and Mr. Tad L. S. Fox for their understanding and help. Dr. Jimmy A. Cowan deserves my special thanks for being proofreader of my thesis. I can certainly think of how painful the job is. I appreciate his enthusiasm and patience.

Professor Aron Kuppermann also deserves my special thanks. I am sorry that I was not able to keep up my interest of being a theoretician while I was a member in his group. I will always appreciate his understanding and support.

I would like to dedicate my limited success to my families, my father Tao Chiang, my mother Chu-ying Cheng, my father-in-law Chien-kuo Ming, my mother-in-law Yueh-er Ting, my sisters Huey-fang, Huey-feng, and Huey-ying, my elder cousin Shih-hsiung Cheng, for every-

thing they have ever done for me. I would also like to dedicate this thesis to the memory of my younger brother Huey-lin. Sixteen years, it still hurts me so deeply. I thank my wife Ming Feng-ying who has been with me since I arrived at Caltech. For being my producer, stage director, supporter, and cheerleader throughout my Ph.D. studies; she deserves half of the credit for this thesis.

ABSTRACT

The thermodynamic parameters of redox centers in some metalloproteins have been investigated using spectroelectrochemical techniques, with the employment of an OTTLE (Optically Transparent Thin-Layer Electrode) cell. With the aid of various carefully selected mediators, the temperature dependence of the formal redox potentials of type I copper (blue copper) ions in *Rhus vernicifera* (tree) laccase, as well as in native and in pentaammineruthenium-modified azurins from *Pseudomonas aeruginosa*, have been measured. Similar experiments have been carried out for the heme site of *cis*-[$Ru(en)_2(OH)(His)$]-horse heart cytochrome *c* (en: ethylenediamine; His: histidine). Cyclic voltammetry has been used to study the pH-dependence of the formal redox potentials of the appended ruthenium ion in *cis*-[$Ru(en)_2(OH)(His)$]-horse heart cytochrome *c*. Finally, the synthesis and spectroelectrochemistry of sperm whale myoglobin reconstituted with [Ru(MpIX)(DMSO) dicarboxylic acid]- moiety (MpIX: mesoporphyrin IX; DMSO: dimethyl sulfoxide) have also been carried out.

TABLE OF CONTENTS

LIST OF FIGURES

Chapter I

Chapter II.

Chapter III

Chapter IV

Chapter VI

LIST OF TABLES

CHAPTER III

Chapter IV

LIST OF SCHEMES

CHAPTER IV

CHAPTER I

INTRODUCTION

Overview

Long-range electron transfer studies[1-12] of biological molecules have drawn considerable attention in recent years. This forms the basis for an understanding of oxidative phosphorylation[13,14] and photosynthesis[15,16], which are the most important metabolic processes involved in biological energetics.[17] Electron transport chains function as a series of consecutive electron transfer reactions between pairs of proteins. These proteins have evolved to couple efficiently, so that they conserve energy in the electron transfer events. Figures 1 and 2[18] depict a simplified view of the flow of electrons in mitochondria and in photosynthesis, respectively. The most outstanding characteristic in these processes is that though they often involve relatively large distances,[19,20] say 10 Å or more, between the redox centers, the reaction rates are surprisingly fast.[21] Because it is so unique in terms of what is known about conventional redox chemistry, many scientists are interested in understanding the factors that control the rates of long-range electron transfers.

Biological electron transfer reactions can occur in two different ways: either intermolecular electron transfer between sites residing in two protein molecules, or intramolecular electron transfer between distinct sites within a single protein molecule. There have been numerous investigations of intermolecular electron transfer reactions between single-site metalloproteins and inorganic complexes.[22-33] A profile of these experiments is shown in Figure 3, how-

Figure 1. The electron transport chain in mitochondrial oxidative phosphorylation. The diagram shows the last stages in the conversion of sugars to CO_2 and H_2O; the transfer of electrons (and hydrogen ions) to oxygen to form water. In the course of this process several protons are transferred across the membrane, and these can then return via the ATPase complex, generating molecules of ATP, which serve as an energy source for other biochemical processes.

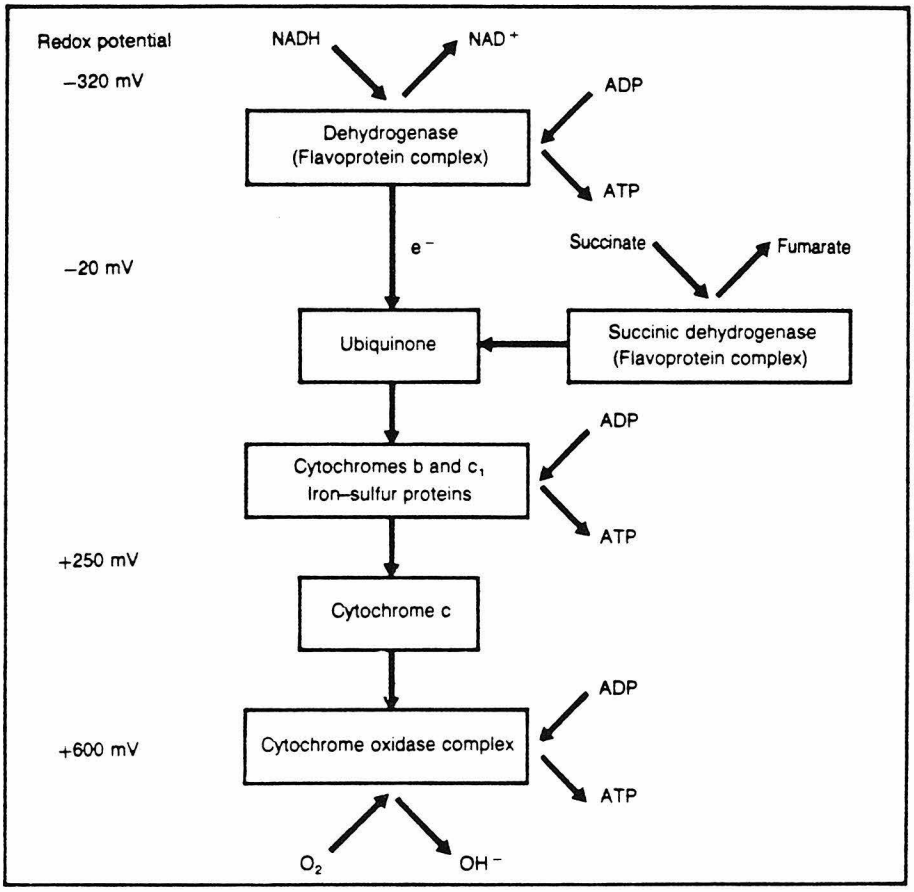
Redox potential
NADH
NAD+
−320 mV
ADP
Dehydrogenase
(Flavoprotein complex)
ATP
e−
Succinate
Fumarate
−20 mV
Ubiquinone
Succinic dehydrogenase
(Flavoprotein complex)
ADP
Cytochromes b and c1
Iron–sulfur proteins
ATP
+250 mV
Cytochrome c
ADP
+600 mV
Cytochrome oxidase complex
ATP
O2
OH−

Figure 2. The electron transport chain in photosynthetic bacteria. The diagram shows the first stage in the conversion of sunlight to chemical energy. The chlorophyll and pheophytin molecules, together with some others, make up the bacterial reaction center found in the plasma membrane of these bacteria. One molecule of ATP per photon is formed when protons, transferred across the membrane during the light-induced electron transfer reactions, return via the ATPase complex.

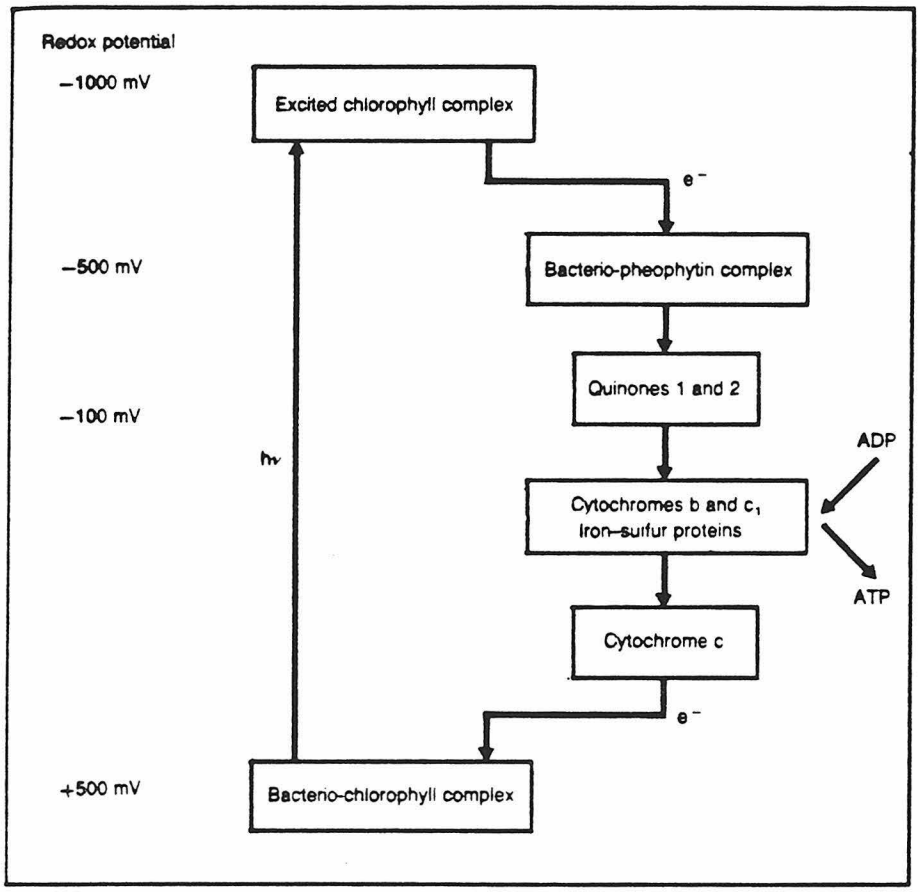
Redox potential
−1000 mV
−500 mV
−100 mV
+500 mV
Excited chlorophyll complex
e⁻
Bacterio-pheophytin complex
Quinones 1 and 2
hν
ADP
Cytochromes b and c1
Iron–sulfur proteins
ATP
Cytochrome c
e⁻
Bacterio-chlorophyll complex

Figure 3. Bimolecular electron transfer reactions between metalloproteins and small inorganic complexes. The complexes with hydrophobic ligands can penetrate into the interior of the native protein structure, seeking the shortest possible distance for intermolecular electron transfer. However, both types of complexes exchange electrons with proteins via outer-sphere electron transfer mechanism.

Metalloprotein Electron Transfer Rates

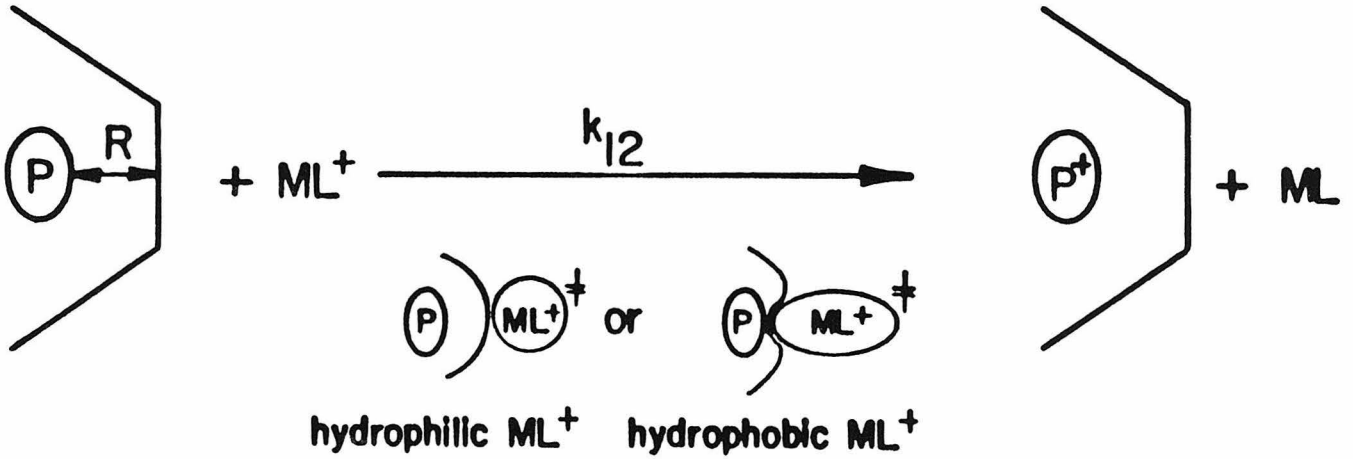

1. k_{12} (hydrophobic ML^+) > k_{12} (hydrophilic ML^+)
2. k_{12} (hydrophilic ML^+) decreases rapidly as R increases

ever, the rate constants of intermolecular electron transfer in these cases contained bimolecular contributions from diffusion rates and electrostatic effects in addition to the unimolecular contributions of intramolecular electron transfer.

The following factors have been recognized as key parameters governing the electron transfer reactions:

(1) Donor-to-acceptor distance.[3]

(2) Thermodynamic driving force for the reaction, *i.e.*, the difference between the reduction potentials of the acceptor and donor.[34,35]

(3) Geometric changes of redox centers, *i.e.*, inner sphere reorganization of donor and acceptor.

(4) Relative orientation of the involved orbitals between the acceptor and donor sites.[36-38]

(5) Nature of the intervening medium.[39-41]

(6) Solvation.[42-44]

In order to explore the effects of these factors in long-range unimolecular electron transfer processes, experiments have been designed in which the intramolecular electron transfer reaction between two fused redox centers, in a modified metalloprotein, is observed.[45-55] Figure 4 illustrates the idea of a semi-synthetic electron transfer metalloprotein. Due to current experimental limitations, most of the studies have concentrated on the effects of distance, driving force, and geometric reorganization on the electron transfer kinetics.

Figure 4. Semi-synthetic metalloproteins containing two redox centers with fixed and known distances. The intramolecular electron transfer proteins are made by chemically modifying the surface residues of single site metalloproteins with transition metal complexes. These metal complexes are substition inert in both the oxidized and reduced form.

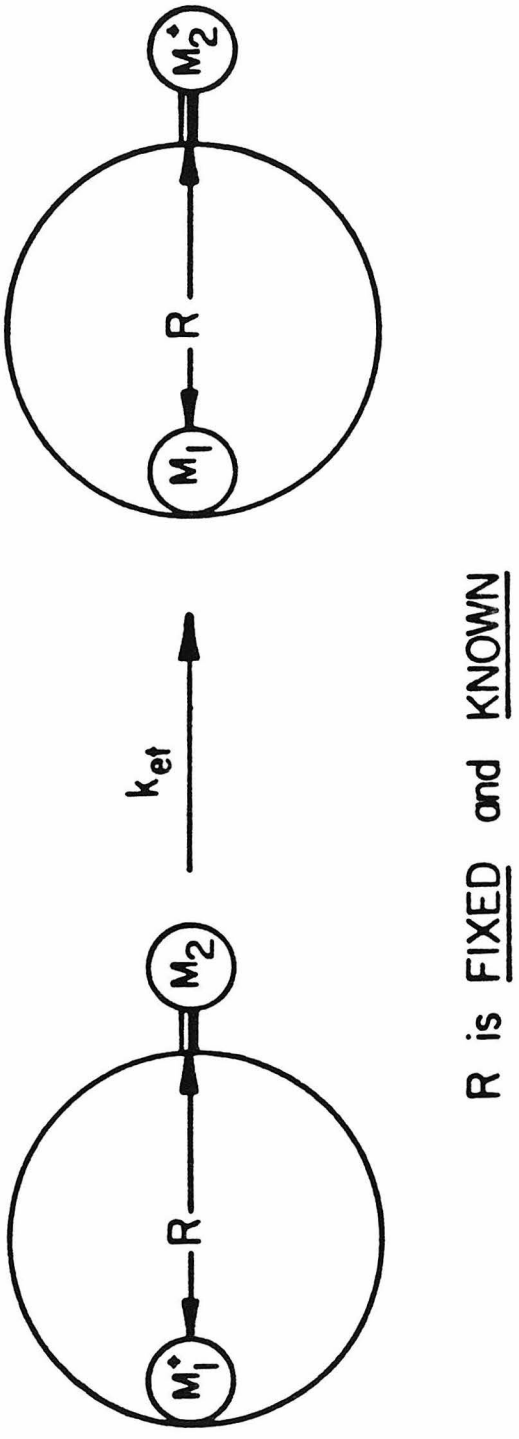

R is FIXED and KNOWN

Distance data between donors and acceptors are extracted from X-ray crystallographic results, although the debate concerning the structural differences between molecules in the solid and solvated states remains unresolved. With the assumption that both the solid and solvated state of the proteins are structurally identical, we can estimate the edge-to-edge distances between redox centers for the electron transfer experiment performed in solution. Figures 5 and 6 demonstrate the distance estimation, based on the crystallographic results from native horse heart cytochrome *c*, for pentaammineruthenium-(histidine 33) cytochrome *c*.[49,54] Based on spectroscopic and electrochemical studies, the evidence is overwhelming that the protein's native conformation is not significantly perturbed[56] by modification. However, this argument may change in other cases due to the hydrophobicity of the modifying complexes used. At this level of resolution, the structural changes due to different oxidation states are inevitably ignored.

Crystallography can also provide details of the relative orientation and intervening medium between donors and acceptors. The role of these factors in biological electron transfer processes is extremely interesting. There are several important issues, such as through-bond/through-space mechanisms (Figure 7) and donor-acceptor electronic coupling which are closely related to them. The main source of information pertaining to driving forces of redox centers, such as formal potentials or free energy changes, comes from electrochemistry. Thermodynamic parameters, such as changes of enthalpy

Figure 5. X-ray crystallographic structure of horse heart cytochrome *c*, in which the non-heme-bound histidine and methionine residues are highlighted. The distance from each amino acid side chain, to the closest heme edge, is given in parentheses.

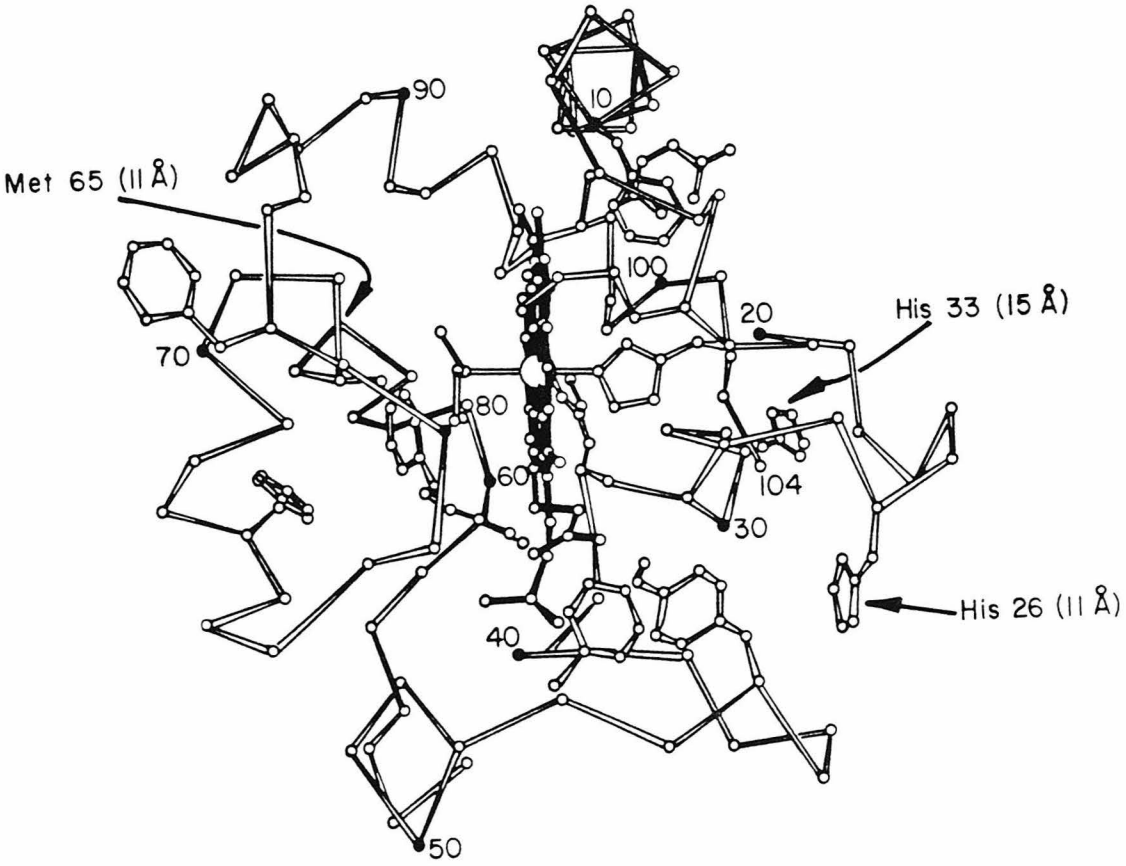
Met 65 (11 Å)
His 33 (15 Å)
His 26 (11 Å)
10
20
30
40
50
60
70
80
90
100
104

Figure 6. Structural model for selected parts of [$Ru(NH_3)_5$ (histidine-33)]-ferricytochrome *c*, based on coordinates for the tuna protein. In this view it has been assumed that the imidazole of His-33 is coincident with the five-membered ring of Trp-33 in the tuna cytochrome *c* structure.

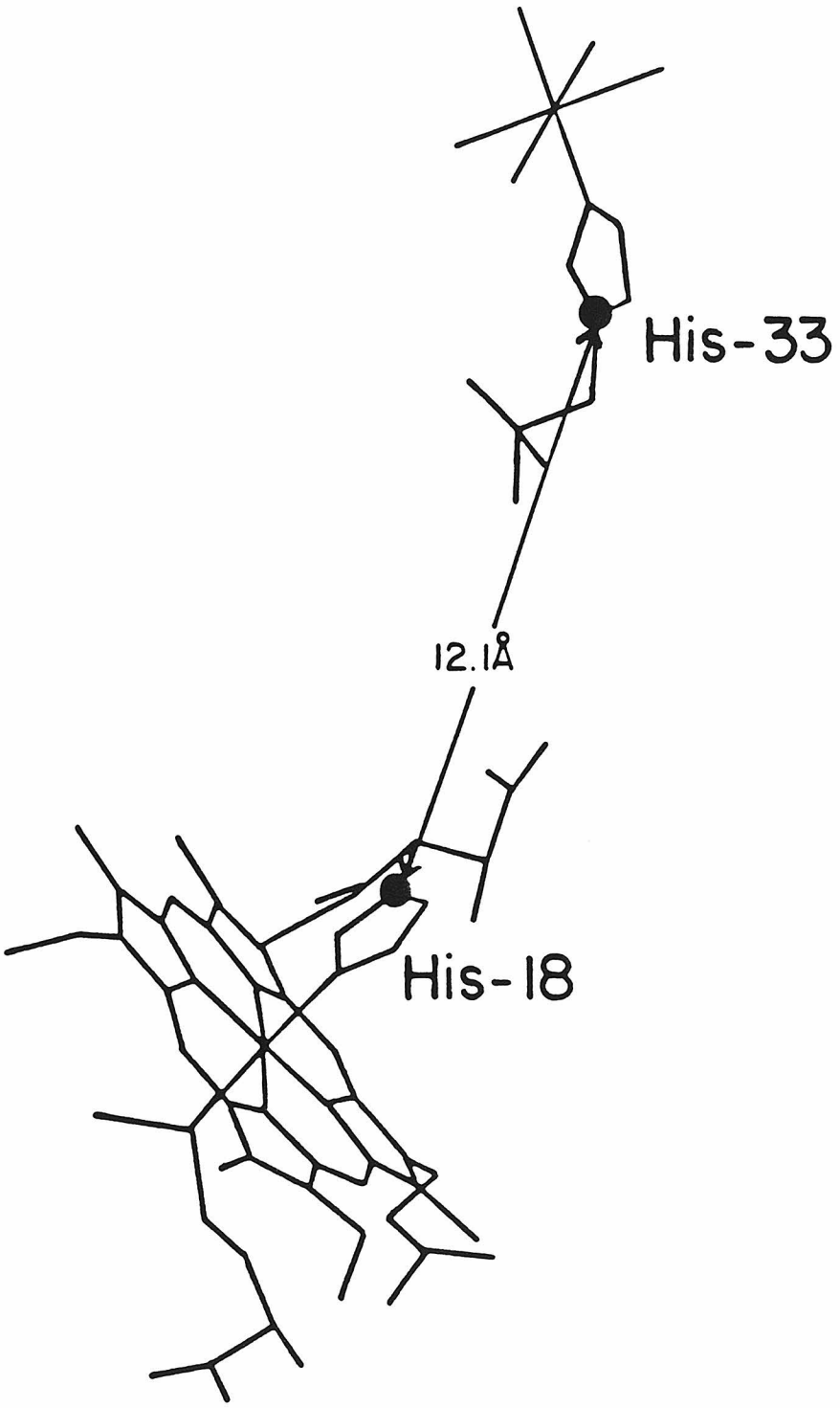
His-33
12.1Å
His-18

Figure 7. This figure depicts the idea of through-bond (the curved line connecting His-18 and His-33) and through-space (the shortest distance between His-18 and His-33) mechanisms of intramolecular electron transfer reactions in pentaammineruthenium (histidine-33)-horse heart cytochrome *c*.

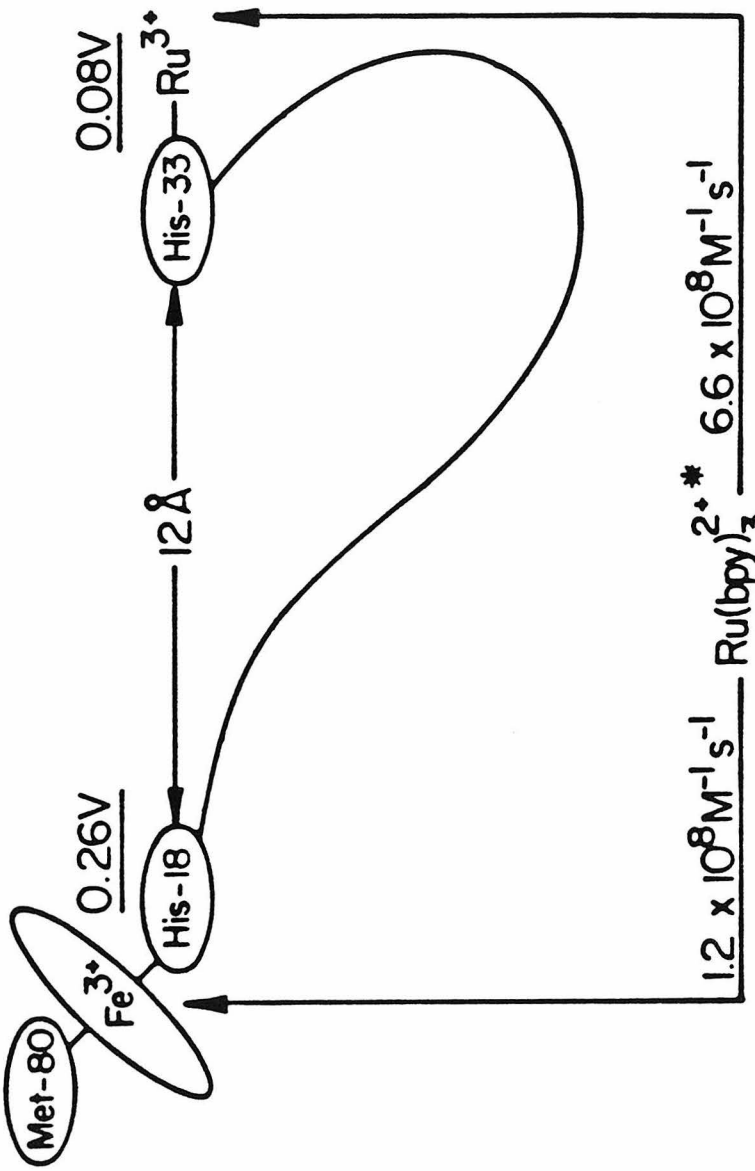
0.08V
Ru3+
His-33
12 Å
His-18
0.26V
Fe3+
Met-80
1.2 x 10^8 M^-1 s^-1
Ru(bpy)3 2+*
6.6 x 10^8 M^-1 s^-1

and entropy, can be calculated based on the relationship of formal potential *vs.* temperature. These thermodynamic data, in particular the entropy, are very important in terms of obtaining a mechanistic understanding of electron transfer processes.

Kinetic studies can be carried out in one of two different ways, each using a different method for perturbing the system. The first method, flash photolysis, involves an electronically excited species which is generated by a pulse of light. Using this species as a strong oxidizing or reducing agent, a nonequilibrium state of electron distribution among the redox centers is created (Figure 8). The relaxation of this state is then monitored spectroscopically in a time domain (Figure 9). The second method, called pulse radiolysis,[57] employs a short pulse (~ 30 ps) of an electron beam instead of photons, the solvated electrons then acting as a reducing agent. Again, the relaxation of the nonequilibrium distribution of electron density between the redox centers is followed as a function of time. The rate constants obtained by these two methods are in reasonable agreement. The temperature dependence of the rate constants (Figure 10) can give valuable information on the activation parameters for electron transfer, and can often be the vital link in the comparison of experiments and theories. Structural reorganization can also be understood on the basis of thermodynamic and kinetic studies.

Hopefully, a clear picture of protein-mediated electron transfer reactions will be revealed by systematic studies of experiments using

Figure 8. The illustration shows the intramolecular electron transfer pathway of pentaammineruthenium (histidine-33)-ferricytochrome *c*. Here, the surface histidine bound $Ru^{3+/2+}$ stands for $[Ru(NH_3)_5(His\text{-}33)]^{3+/2+}$, Ru^{2+*} stands for $[Ru(bpy)_3]^{2+*}$, free Ru^{2+} stands for $[Ru(bpy)_3]^{2+}$ and free Ru^{3+} stands for $[Ru(bpy)_3]^{3+}$, respectively.

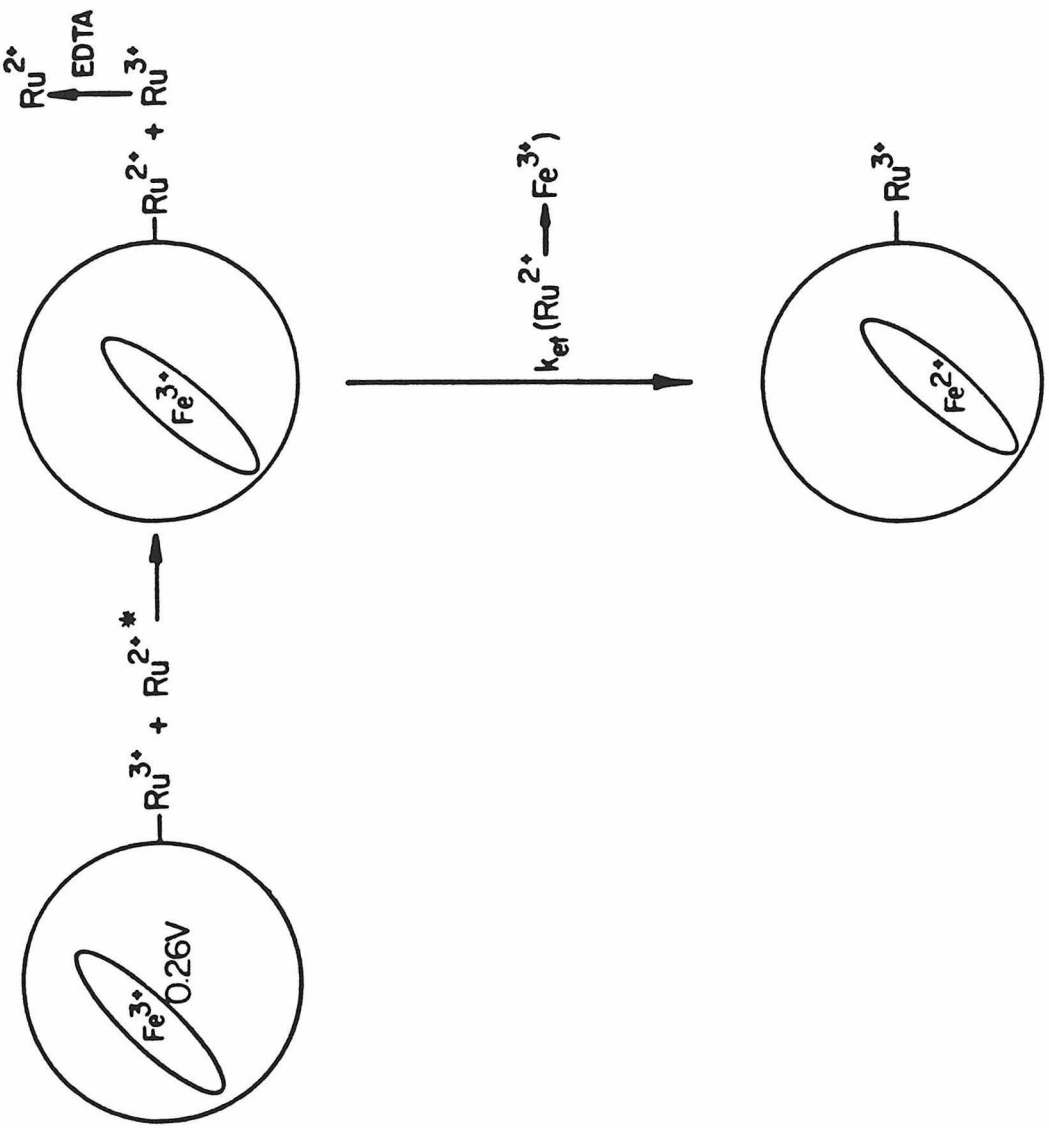
Ru2+
EDTA
Ru3+
Ru3+ + Ru2+*
Ru2+ + Ru3+
Fe3+
0.26V
Fe3+
ket (Ru2+ → Fe3+)
Ru3+
Fe2+

Figure 9. Traces of the change in 550 nm optical density resulting from flash photolysis of (A) $PFe^{III}/[Ru(bpy)_3]^{2+}/EDTA$ and (B) $PFe^{III}\text{-}Ru^{III}/[Ru(bpy)_3]^{2+}/EDTA$ solutions at 22 ^{o}C. The vertical axis refers to light intensity at the detector, and t = 0 on the horizontal axis coincides with the flash pulse. The intensities of the two traces have been normalized to reflect the differences in quenching rate constants.

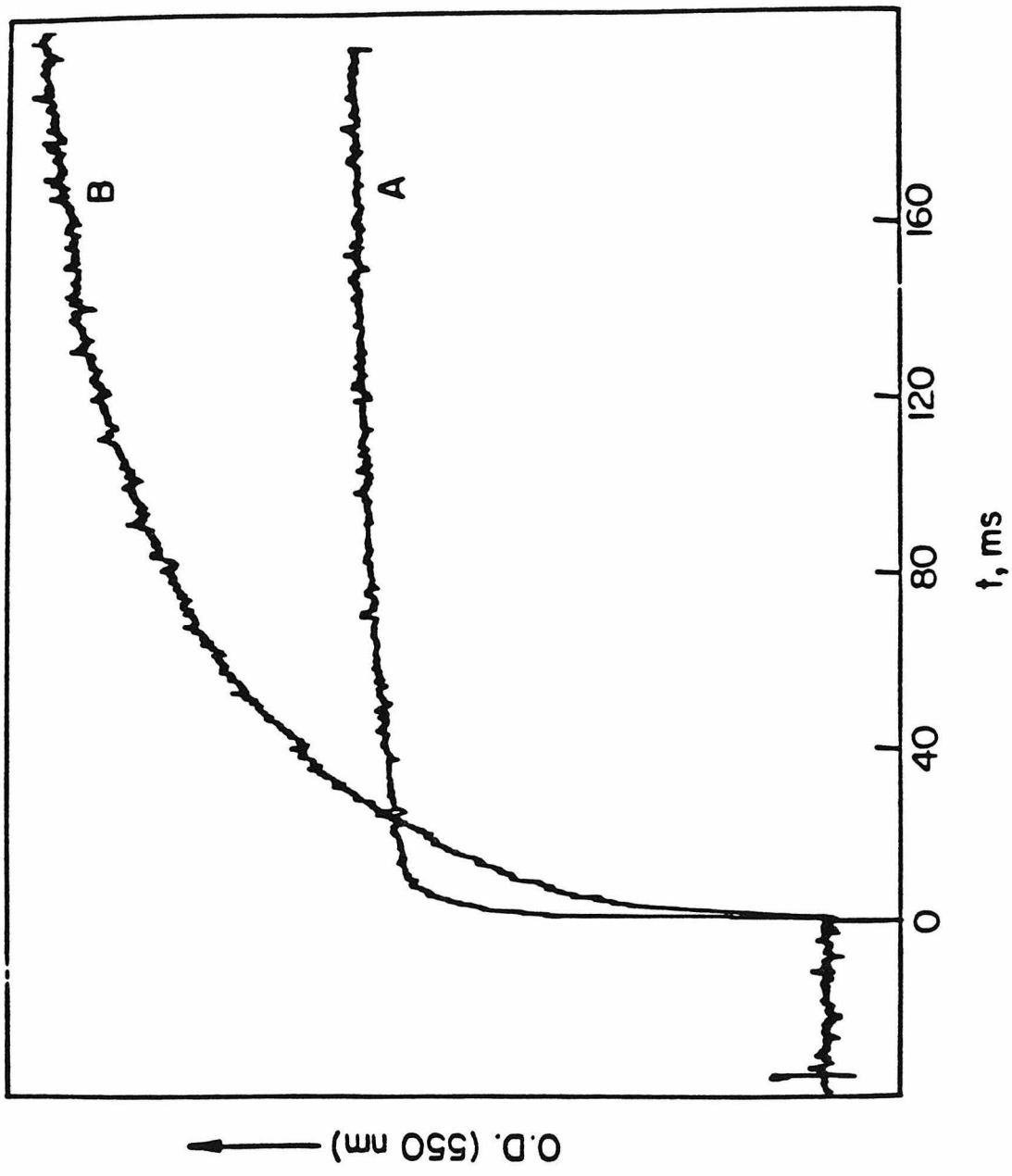
B
A
0
40
80
120
160
t, ms
O.D. (550 nm)

Figure 10. Temperature dependence of the rate constant for the intramolecular electron transfer reaction $PFe^{III}\text{-}Ru^{II} \longrightarrow PFe^{II}\text{-}Ru^{III}$ at pH 7, μ = 100 mM, phosphate buffer. The inset is a duplication of Figure 9.

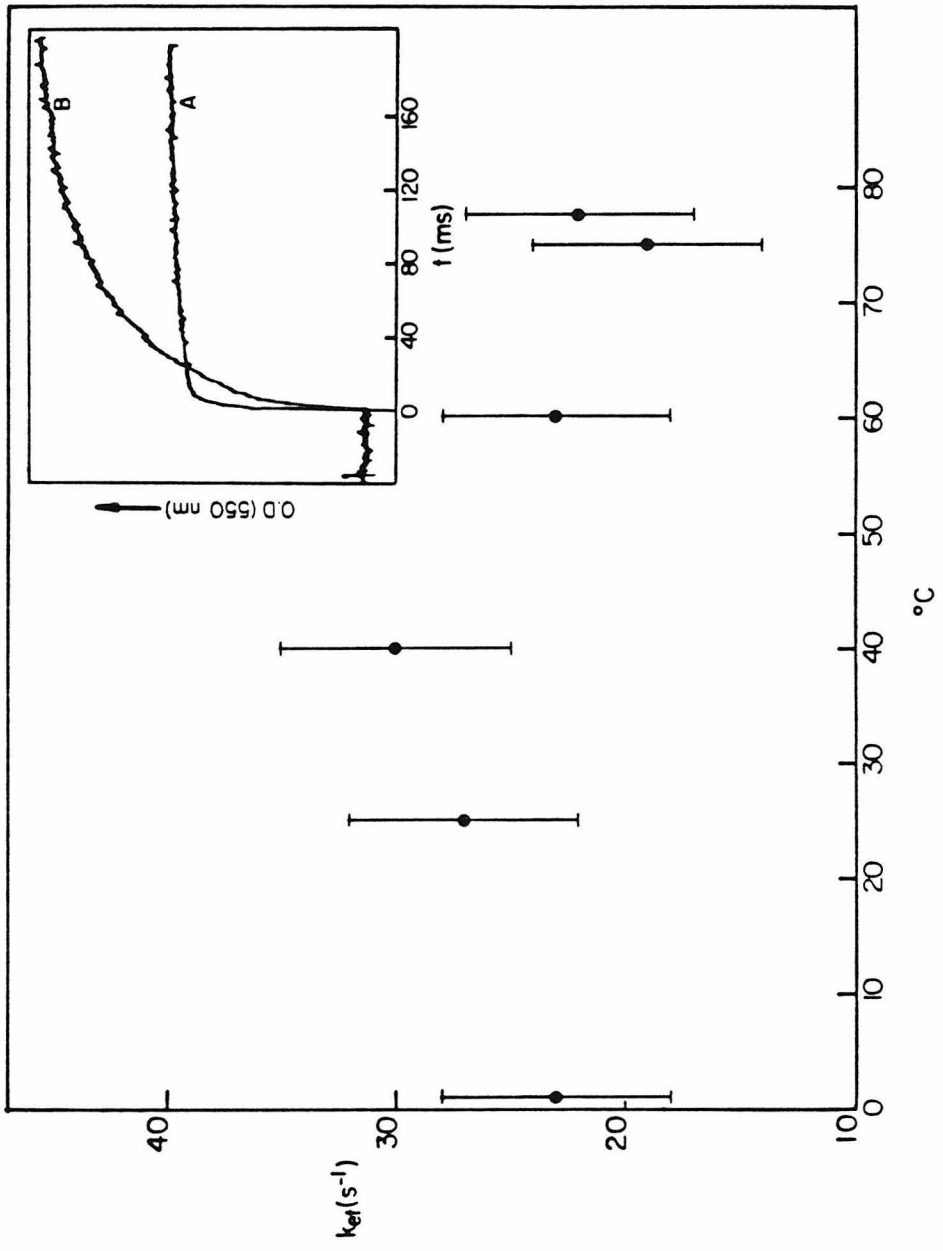
B
A
0
40
80
120
160
t (ms)
O.D (550 nm)
$k_{ef}(s^{-1})$
10
20
30
40
0
10
20
30
40
50
60
70
80
°C

various combinations of proteins and complexes. New strategies are also needed, in order to settle questions that are beyond current experimental capabilities.

Scope of the Thesis

The material contained in this thesis is confined to the thermodynamic aspects of electron transfer metalloproteins, native or chemically modified by ruthenium complexes, which have been studied by electrochemical techniques such as cyclic voltammetry and spectroelectrochemistry.

Chapter II summarizes the fundamentals of electrochemical techniques for determining redox formal potentials. Some of the details of spectroelectrochemistry have also been presented. The fabrication procedures of an OTTLE (Optically Transparent Thin-Layer Electrode) cell are also mentioned.

Chapter III presents the spectroelectrochemistry of type I blue-copper ion in *Rhus vernicifera* (tree) laccase. The formal redox potentials of these proteins have been studied in the range 4 to 40 ^{o}C. Apparently, there are two different mechanisms that the four copper ions in laccase exhibit. The comparison in temperature dependence of formal potentials between tree laccase and fungal laccase has been made.

Chapter IV[1,48] describes the thermodynamic data from native azurin, as well as singly and doubly pentaammineruthenium-modified

azurins, from *Pseudomonas aeruginosa* at pH 5.0, 6.0, and 7.0, respectively. A few comparisons have been made in terms of the effect of modification, and the effect of pH on the redox potentials of azurin have also been shown.

Chapter V[58] demonstrates the possibilities for protein modifications using ruthenium ammine complexes other than ruthenium pentaammine. *cis*-$[Ru(en)_2(OH)]$- and *cis*-$[Ru(NH_3)_4(OH)]$- are the two examples in this new direction.

Chapter VI illustrates the synthesis and thermodynamic studies of sperm whale myoglobin reconstituted with [Ru(MpIX)(DMSO) dicarboxylic acid]- moiety. This experiment provides possible opportunities for new lines of study on biological long-range electron transfer processes.

References

1. Gray, H. B., *Chem. Soc. Rev.*, ***15***, 17 (1986).

2. Mayo, S. L., Ellis, W. R., Jr., Crutchley, R. J., and Gray, H. B., *Science*, ***233***, 948 (1986).

3. Hush, N. S., *Coord. Chem. Rev.*, ***64***, 135 (1985).

4. Marcus, R. A., and Sutin, N., *Biochem. Biophys. Acta*, ***811***, 265 (1985).

5. Scott, R. A., Mauk, A. G., and Gray, H. B., *J. Chem. Educ.*, ***62***, 932 (1985).

6. DeVault, D., *Quantum Mechanical Tunnelling in Biological Systems*, Cambridge University Press, Cambridge, ed. 2, 1984.

7. Dreyer, J. L., *Experientia*, ***40***, 653 (1984).

8. Isied, S. S., in *Progress in Inorganic Chemistry*, Volume 32, Lippard, S. J., ed., Wiley, New York, 1984, p. 443.

9. Chance, B., DeVault, D. C., Frauenfelder, H., Marcus, R. A., Schrieffer, J. R., and Sutin, N., eds., *Tunneling in Biological Systems*, Academic Press, New York, 1979.

10. Hopfield, J. J., in *Electrical Phenomena at the Biological Membrance Level*, Roux, E., ed., Elsevier, Amsterdam, 1978, P. 471.

11. Wherland, S., and Gray, H. B., in *Biological Aspects of Inorganic Chemistry*, Addison, A. W., Cullen, W. R., Dolphin, D., and James, B. R., eds., Wiley, New York, 1977, P. 289.

12. Hopfield, J. J., *Proc. Natl. Acad. Sci. USA*, ***71***, 3640 (1974).

13. Hatefi, Y., in *Annual Review of Biochemistry*, Richardson, C. C., ed., Annual Reviews Inc., Palo Alto, 1985, P. 1015.

14. Dixit, B. P. S. N., and Vanderkooi, J. M., in *Current Topics in Bioenergetics*, Volume 13, Lee, C. P., ed., Academic, Orlando, 1984, P. 159.

15. Michel-Beyerle, M. E., ed., *Antennas and Reaction Centers of Photosynthetic Bacteria*, Springer-Verlag, Berlin, 1985.

16. Govindjee, ed., *Photosynthesis: Energy Conversion by Plants and Bacteria*, Volume 1, Academic Press, New York, 1982.

17. Ernster, L., ed., *Bioenergetics*, Elsevier, Amsterdam, 1984.

18. Chance, B, Mueller, P., DeVault, D., and Powers, L., *Physics Today*, ***33***, 32 (1980).

19. Deisenhofer, J., Michel, H., and Huber, R., *Trends Biochem. Sci.*, ***10***, 243 (1985).

20. Deisenhofer, J., Epp, O., Miki, K., Huber, R., and Michel, H., *J. Mol. Biol.*, ***180***, 385 (1984).

21. DeVault, D., and Chance, B., *Biophys. J.*, ***6***, 825 (1966).

22. Brunschwig, B. S., DeLaive, P. J., English, A. M., Goldberg, M., Gray, H. B., Mayo, S. L., and Sutin, N., *Inorg. Chem.*, ***24***, 3742 (1985).

23. English, A. M., Lum, V. R., DeLaive, P. J., and Gray, H. B., *J. Am. Chem. Soc.*, ***104***, 870 (1982).

24. Mauk, A. G., Bordignon, E., and Gray, H. B., *J. Am. Chem. Soc.*, ***104***, 7654 (1982).

25. Gray, H. B., Coyle, C. L., Dooley, D. M., Grunthaner, P. J., Hare, J. W., Holwerda, R. A., McArdle, J. V., McMillin, D. R., Rawlings, J., Rosenberg, R. C., Sailasuta, N., Solomon, E. I., Stephens, P. J., Wherland, S., and Wurzbach, J. A., in *Advances in Chemistry Series, No. 162, Bioinorganic Chemistry-II*, Raymond, K. N., ed., American Chemical Society, Washington, D. C., 1977, P. 145.

26. McArdle, J. V., Coyle, C. L., Gray, H. B., Yoneda, G. S., and Holwerda, R. A., *J. Am. Chem. Soc.*, ***99***, 2483 (1977).

27. Holwerda, R. A., Wherland, S., and Gray, H. B., in *Annual Review of Biophysics and Bioengineering*, Volume 5, Mullins, L. J., ed., Annual Reviews Inc., Palo Alto, 1976, P. 363.

28. Cummins, D., and Gray, H. B., *Inorg. Chem.*, ***20***, 3712 (1981).

29. Holwerda, R. A., Knaff, D. B., Gray, H. B., Clemmer, J. D., Crowley, R., Smith, J. M., and Mauk, A. G., *J. Am. Chem. Soc.*, ***102***, 1142 (1980).

30. McArdle, J. V., Yocum, K., and Gray, H. B., *J. Am. Chem. Soc.*, ***99***, 4141 (1977).

31. Coyle, C., and Gray, H. B., *Biochem. Biophys. Res. Comm.*, ***73***, 1122 (1976).

32. Wherland, S., and Gray, H. B., *Proc. Natl. Acad. Sci. USA*, ***73***, 2950 (1976).

33. McArdle, J. V., Gray, H. B., Creutz, C., and Sutin, N., *J. Am. Chem. Soc.*, ***96***, 5737 (1974).

34. Ellis, W. R., Jr., Ph.D. Thesis, California Institute of Technology, Pasadena, United States, 1986.

35. Miller, J. R., Beitz, J. V., and Huddleston, R. K., *J. Am. Chem. Soc.*, ***106***, 5057 (1984).

36. Cave, R. J., Klippenstein, S. J., and Marcus, R. A., *J. Chem. Phys.*, ***84***, 3089 (1986).

37. Siders, P., Cave, R. J., and Marcus, R. A., *J. Chem. Phys.*, ***81***, 5613 (1985).

38. Makinen, M., Schichman, S. A., Hill, S. C., and Gray, H. B., *Science*, ***222***, 929 (1983).

39. Higuchi, Y., Kusunoki, M., Matsuura, Y., Yasuoka, N., and Kakudo, M., *J. Mol. Biol.*, ***172***, 109 (1984).

40. Pierot, M., Haser, R., Frey, M., Payan, F., and Astier, J.-P., *J. Biol. Chem.*, ***257***, 14341 (1982).

41. Kimura, K., Nakahara, Y., Tagi, T., and Inokuchi, H., *J. Chem. Phys.*, ***70***, 3317 (1979).

42. Onuchic, J. N., Beratan, D. N., and Hopfield, J. J., *J. Phys. Chem.*, ***90***, 3707 (1986).

43. Garg, A., Onuchic, J. N., and Ambegaokar, V., *J. Chem. Phys.*, ***83***, 4491 (1985).

44. Kosower, E. M., *J. Am. Chem. Soc.*, ***107***, 1114 (1985).

45. Crutchley, R. J., Ellis, W. R., Jr., and Gray, H. B., in *Frontiers in Bioinorganic Chemistry*, Xavier, A. V., ed., VCH erlagsgesellschaft, Weinheim, F. R. G., 1986, P. 679.

46. Crutchley, R. J., Ellis, W. R., Jr., and Gray, H. B., *J. Am. Chem. Soc.*, ***107***, 5002 (1985).

47. Isied, S. S., Kuehn, C., and Worosila, G., *J. Am. Chem. Soc.*, ***106***, 1722 (1984).

48. Margalit, R., Kostić, N. M., Che, C.-M., Blair, D. F., Chiang, H.-J., Pecht, I., Shelton, J. B., Shelton, J. R., Schroeder, W.

A., and Gray, H. B., *Proc. Natl. Acad. Sci. USA*, ***81***, 6554 (1984).

49. Nocera, D. G., Winkler, J. R., Yocom, K. M., Bordignon, E., and Gray, H. B., *J. Am. Chem. Soc.*, ***106***, 5145 (1984).

50. Kostić, N. M., Margalit, R., Che, C.-M., and Gray, H. B., *J. Am. Chem. Soc.*, ***105***, 7765 (1983).

51. Margalit, R., Pecht, I., and Gray, H. B., *J. Am. Chem. Soc.*, ***105***, 301 (1983).

52. Yocom, K. M., Winkler, J. R., Nocera, D. G., Bordignon, E., and Gray, H. B., *Chem. Scr.*, ***21***, 29 (1983).

53. Isied, S. S., Worosila, G., and Atherton, S. J., *J. Am. Chem. Soc.*, ***104***, 7659 (1982).

54. Winkler, J. R., Nocera, D. G., Yocom, K. M., Bordignon, E., and Gray, H. B., *J. Am. Chem. Soc.*, ***104***, 5798 (1982).

55. Yocom, K. M., Shelton., J. B., Shelton, J. R., Schroeder, W. A., Worosila, G., Isied, S. S., Bordignon, E., and Gray, H. B., *Proc. Natl. Acad. Sci. USA*, ***79***, 7052 (1982).

56. Toi, H., La Mar, G. N., Margalit, R., Che, C.-M., and Gray, H. B., *J. Am. Chem. Soc.*, ***106***, 6213 (1984).

57. Beitz, J. V., and Miller, J. R., *J. Chem. Phys.*, ***71***, 4579 (1979).

58. Che, C.-M., Margalit, R., Chiang, H.-J., and Gray, H. B., *Inorg. Chim. Acta*, ***135***, 33 (1987).

CHAPTER II

SPECTROELECTROCHEMISTRY AND THE OTTLE CELL

Introduction

Elucidation of the thermodynamics of metalloprotein electron transfer reactions[1-21] is a matter of fundamental importance in biochemistry.[22] The accurate measurement of the formal reduction potentials of redox centers in metalloproteins allows the determination of one of the most important parameters in biological long-range electron transfer reactions, namely the driving force. Based on the temperature coefficient of formal reduction potentials, $(dE^{0\prime}/dT)$, thermodynamic parameters such as enthalpy and entropy terms can be derived from it, and important questions, concerning the effects of solvation and inner-sphere reorganization, can be answered by the interpretation of these thermodynamic data. The redox properties of mettalloproteins cannot be studied properly by conventional techniques, such as cyclic voltammetry, due to the problem of slow electron exchange between metalloprotein and the electrode surface. This is why many measurements of formal reduction potentials rely on potentiometric titration,[23-25] even though such experiments have inherent errors, since successive addition of redox titrants change the sample volume and other properties of solution. The redox potential data based on these techniques are therefore by no means accurate.

It is known that by introducing certain small molecules to act as a redox mediator or promoter,[26-30] the electron exchange between proteins and electrodes can be achieved. With the proper selection of redox mediator or promoter, the range of possible applications of

electrochemical techniques in the study of biological molecules has been greatly enhanced.

Spectroelectrochemistry

The combination of two quite different techniques, electrochemistry and spectroscopy, has proved to be an effective approach for studying the redox chemistry of inorganic, organic, and biological molecules. Oxidation states are changed electrochemically by addition or removal of electrons at an electrode and spectral measurements, on the solution adjacent to the electrode, are thus made simultaneously with the electrogeneration process. Thus, spectroscopy is used as a probe of the consequences of electrochemical phenomena that occur in the solution undergoing electrolysis. Such spectroelectrochemical techniques[31-39] offer a convenient means for obtaining both spectra and redox potentials and also for observing subsequent chemical reactions of the electrogenerated species.

A number of optical methods that have been coupled with electrochemistry are summarized in Figure 1.[34] The most frequently used technique is absorption spectroscopy in the ultraviolet-visible-infrared region. Transmission spectroscopy involves passing the optical beam directly through a transparent or semi-transparent electrode and the adjacent solution.[38-40] In specular reflectance spectroscopy the beam is passed through solution and reflected from the electrode surface back through the solution.[41,42] Internal reflectance spec-

Figure 1. Block diagram representation of spectroelectrochemical techniques.

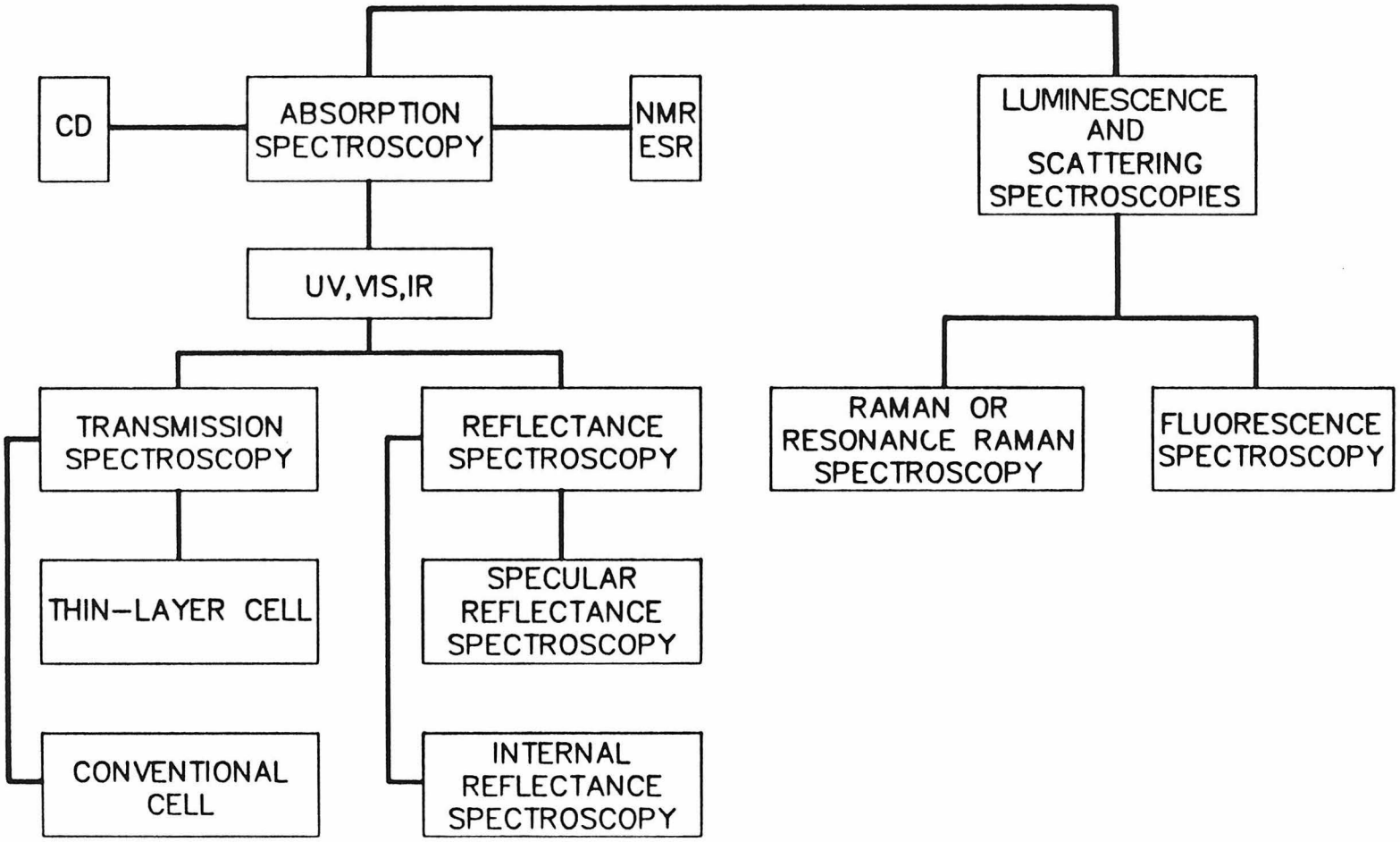
CD
ABSORPTION SPECTROSCOPY
NMR ESR
LUMINESCENCE AND SCATTERING SPECTROSCOPIES
UV, VIS, IR
TRANSMISSION SPECTROSCOPY
REFLECTANCE SPECTROSCOPY
RAMAN OR RESONANCE RAMAN SPECTROSCOPY
FLUORESCENCE SPECTROSCOPY
THIN-LAYER CELL
SPECULAR REFLECTANCE SPECTROSCOPY
CONVENTIONAL CELL
INTERNAL REFLECTANCE SPECTROSCOPY

troscopy involves introducing the optical beam through the back side of a transparent electrode at an angle greater than the critical angle at which the beam is totally reflected.[38-40,43] Sensitivity enhancement for both types of reflectance spectroscopies can be achieved by multiple reflections.

Luminescence and scattering spectroscopic techniques have been coupled with electrochemistry. In Raman and resonance Raman spectroelectrochemistry the excitation is done by a laser beam directed through solution at an electrode, and the Raman back-scattering is observed.[44] A particularly important aspect of Raman spectroelectrochemistry lies in the structural information on the electrogenerated species which is contained in the Raman spectrum. The excitation beam can be passed through an electrochemical cell, and the resulting fluorescence from the electrogenerated species observed.[45] A variety of electrode reactions are accompanied by the emission of light. Such electrogenerated chemiluminescence results from decay of an excited state formed by the solution reaction of electrogenerated cations and anions.[46]

Electrochemical cells have also been placed in the sample cavities of ESR and NMR spectrometers to record the absorption spectra of electrogenerated species.[47,48]

OTTLE (Optically Transparent Thin-Layer Electrode) Cells

There are two types of cell geometries which are commonly used

in conjunction with the various optical techniques. The normal cell is analogous to a conventional electrochemical cell in which the electrode is in contact with an electrolyte solution much thicker than the diffusion layer adjacent to the electrode. By contrast, the thin-layer cell[49-52] confines a thin (0.1 ~ 0.5 mm) solution layer adjacent to the electrode. The most significant virtues of thin-layer cells are:

(1) The rapidity with which electroactive species within this layer can be completely electrolyzed (for cell path length of 0.2 mm, the time needed for electrolytic equilibrium is *ca.* 20 ~ 120 seconds).

(2) The very small amount of sample is needed (typically 700 ~ 1000 μl).

Both of these virtues, in particular the latter, benefit the study of metalloenzymes, because the proteins are usually expensive and easily denatured.

Progress in the methodology of spectroelectrochemistry has been stimulated by the development of suitable optically transparent electrodes[38] that enable the light beam to be passed directly through the electrode and adjacent solution. Although reflectance, luminescence, and scattering techniques can be implemented with conventional electrodes, transparency is necessary for transmission and internal reflectance spectroelectrochemistry.

One type of transparent elecrtrode consists of a very thin film of conducting material, such as platinum, gold, tin oxide, or carbon,

that is deposited on a transparent substrate such as glass (visible), quartz (ultraviolet-visible), or germanium (infrared), depending on the spectral region of interest. The transparency (20 ~ 85%) of these electrodes is due to the thinness of the conducting film.

A second type of transparent electrode is the minigrid electrode which consists of a metal (gold, silver, copper, nickel or platinum) micromesh of 100 ~ 2000 wires per inch. In this case, the transparency (20 ~ 80%) is due to the physical holes in the minigrid structure. The minigrid has been used primarily in the thin-layer cell configuration in conjunction with transmission spectroscopy.

Mercury transparent electrodes have been prepared by electrodepositing a thin film of mercury onto platinum and carbon film electrodes and gold and nickel minigrids. This allows use of the excellent negative potential range of mercury.

Fabrication of OTTLE Cells

The step by step procedure for the fabrication of an OTTLE cell is described below:

(1) The cell body was machined from clear lucite plastic (methyl methacrylate). The dimensions are illustrated in Figure 2. For use with non-aqueous solvents (except methanol, it softens epoxy), a Kel-F (teflon) cell body is recommended.

(2) Carefully cleaned quartz windows (1.5 mm x 21 mm x

Figure 2. Detailed view of the dimension specifications for the OTTLE (Optically Transparent Thin-Layer Electrode) cell body. (A) Front view, (B) side view, and (C) thermocouple plug. All dimensions are in mm.

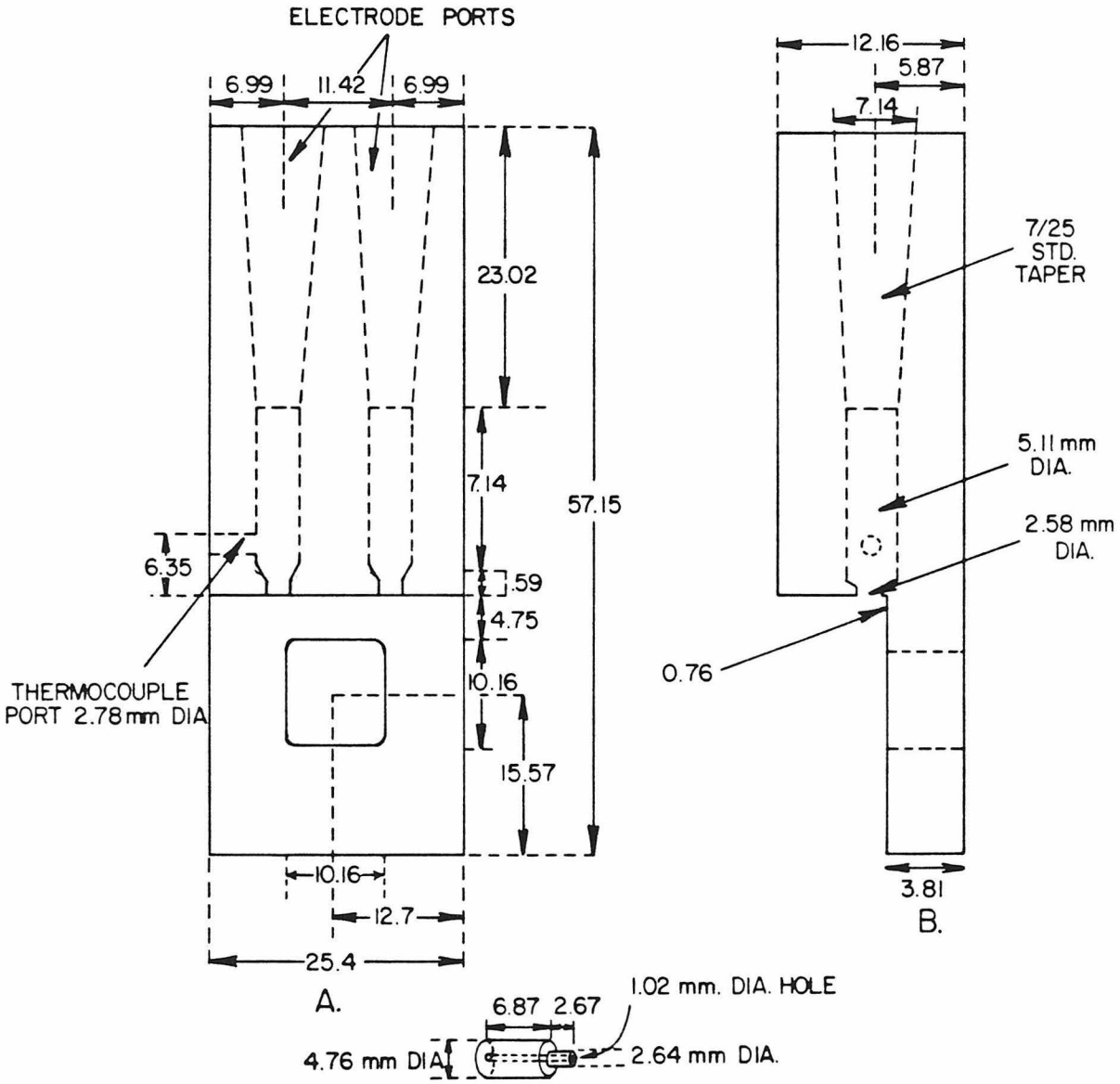

C. THERMOCOUPLE PLUG

21mm, transparency to 170 nm) were used. A thin layer of epoxy was applied to the OTTLE portion of the lucite block and one of the quartz windows was carefully glued in. A small vial filled with mercury provided a sufficient weight to set on top of the window while the epoxy set.

(3) A teflon tape[53] spacer was cut out. If two thicknesses were used, a cell path length of *ca.* 0.5 mm resulted. A small, trapezoid-shaped piece of spacer was lodged against the lucite body (centered between the electrode port openings), and epoxied to the quartz window only at the end near the lucite cell body. A second, larger piece of teflon spacer was cut approximately 20 mm x 20 mm square and then trimmed to a "U" shape. The interior opening was larger than the opening cut in the cell body.

(4) A gold minigrid[54] was fabricated. If a thick OTTLE cell is desired, then two minigrids are required. The 500 wires/inch minigrid is very delicate and was cut with scissors while sandwiched between mylar sheets. The minigrid was not touch with bare hands. The dimension of the minigrid was *ca.* 17 mm wide and 35 mm long.

(5) One minigrid was carefully inserted under the trapezoidal teflon spacer. The "U" shaped teflon was then

placed on top of the gold minigrid, followed by the second gold minigrid. Finally, the second quartz window was placed on top and a mercury-filled vial laid on top of the assembly to keep everything in place. Once this was done, the four corners of the OTTLE assembly were tacked down with epoxy. The epoxy should be used sparingly, since once it hits the minigrid(s) it flows quickly and messes up the cell interior.

(6) A thin layer of epoxy was carefully applied to all edges of the OTTLE except the end where the gold minigrid protruded. During this process, which should be done one edge at a time, the cell body should be tilted in such a way that the epoxy flows away from the direction of the OTTLE interior. Lastly the protruding minigrid was lifted up and a very thin layer of epoxy applied between the minigrid and the lucite cell body. The minigrid was pressed down with a pair of forceps and left to dry.

(7) The end of a 3" piece of 18 gauge copper wire was tinned and then laid across the ends of the gold minigrid and soldered to the grid. It was found best to sandwich the wire between the two minigrids when making a thick OTTLE cell. To avoid melting the minigrid, the tip of the soldering iron should be pressed on a portion of the wire not in contact with

the minigrid.

(8) The excess minigrid was gently rolled around the copper wire, and the wire epoxied at the base of the cell body, just below the quartz windows. A heavy coat of epoxy was then applied to all four edges of the OTTLE cell.

(9) The thermocouple tip was epoxied into a clear lucite plug which was machined slightly undersize. The plug assembly was then inserted into the thermocouple port and epoxy was layered around the inserted plug on the outside of the cell body. The OTTLE cell assembly is illustrated in Figure 3.

(10) The counter electrode (auxiliary electrode) consisted of a 9" length of platinum wire (0.0020 inch diameter) sealed into a tube of soft glass with a 5/20 outer ground glass joint, leaving approximately 1" of wire exposed at the ground end. This was supported in a compartment consisting of a 5/20 inner ground glass joint, terminated by a fine porous glass frit. A description of the nonisothermal configuration of the reference electrode is given in a later section.

Spectroelectrochemistry of Biological Molecules

Application of spectroelectrochemistry to biological molecules

Figure 3. OTTLE (Optically Transparent Thin-Layer Electrode) cell assembly. (A) Front view, (B) side view, (C) top view, and (D) enlarged illustration of thin-layer structure.

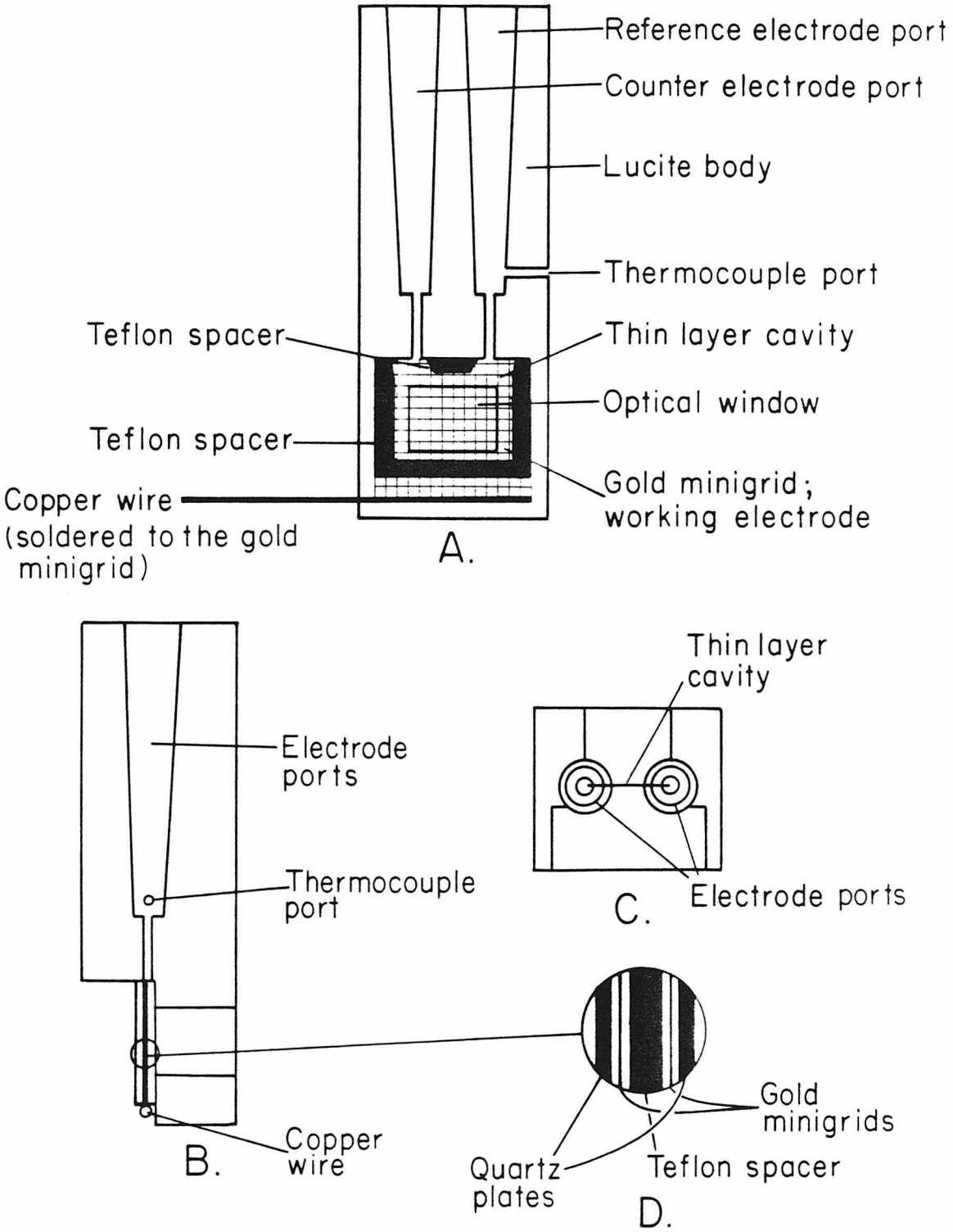
Reference electrode port
Counter electrode port
Lucite body
Thermocouple port
Teflon spacer
Thin layer cavity
Optical window
Teflon spacer
Gold minigrid; working electrode
Copper wire (soldered to the gold minigrid)
A.
Electrode ports
Thermocouple port
Copper wire
B.
Thin layer cavity
Electrode ports
C.
Gold minigrids
Quartz plates
Teflon spacer
D.

was first demonstrated by Heineman in 1975.[55] Metalloproteins often exchange electrons poorly with an electrode, presumably due to insulation of the redox center from the electrode by the surrounding amino acid residues, however, spectroelectrochemical measurements can be made by adding to the solution a small amount of another redox species, a mediator. As illustrated in Figure 4 mediators indirectly couple the metalloprotein redox species with the electrode.

In a typical spectroelectrochemical experiment, a potential, $E_{appl.}$, is applied across the thin-layer cell containing the metalloprotein-mediator solution mixture. The mediator adjusts to its equilibrium [Ox]/[Red] value by direct electrolysis at the electrode. It then in turn homogeneously oxidizes or reduces the protein in the solution until an equilibrium is reached between $E_{appl.}$ at the electrode and all the redox centers in solution. Thus, the results are mediator independent.

The use of a mediator with an $E^{0'}$ too far away from that of the metalloprotein frequently results in a midpoint potential that is either too high or too low. Hence, the selection of the mediators to be used in a spectroelectrochemical experiment is very important for the precise determination of the redox potentials of metalloproteins.

The criteria for the choice of mediators[56] are summarized below:

(1) The mediators must be able to readily oxidize and reduce the molecules under study and be able to interact readily with the electrode in order to establish their redox stages according to the applied potentials.

Figure 4. Mediator-titrant (MT), the redox species besides metalloprotein in the electrochemical experiments, mediates electron exchange between electrode and protein *via* an outer-sphere electron transfer mechanism. When the electrode potential is changed, the electrode reduces/oxidizes the mediator-titrant which in turn reduces/oxidizes the protein.

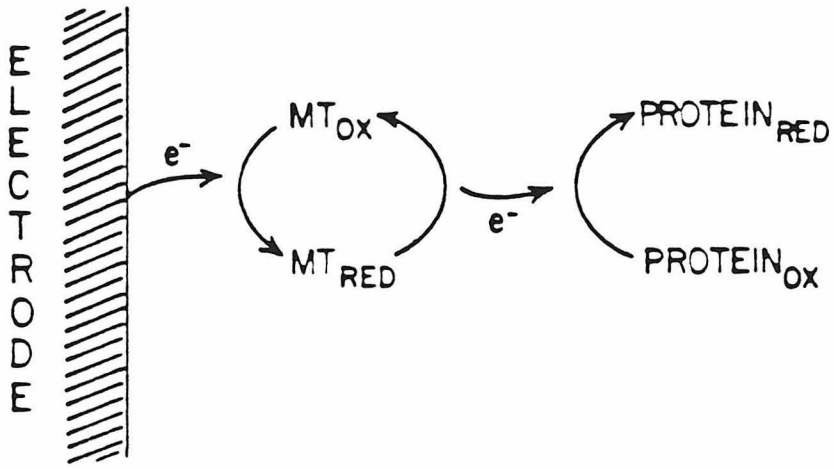
ELECTRODE
e⁻
MT OX
MT RED
e⁻
PROTEIN RED
PROTEIN OX

(2) The mediators must have reduction potentials which allow them to span the required potential range (to a first approximation an active mediator is effective from 90% reduction, equivalent to ± 60 mV (n = 1) on either side of the reduction potential).

(3) The mediators should not interact with the redox components so as to modify them chemically.

(4) The mediators should not interfere with the measurements of the component of interest.

(5) The measured values must be independent of the time allowed for measurement.

(6) The same results must be obtained by either oxidation or reduction processes.

(7) The same results must be obtained using different mediators.

Nonisothermal Configuration of the Variable Temperature OTTLE Cells

The formal reduction potential, $E^{0\prime}$, for this redox couple is determined by sequentially applying a series of potentials $E_{appl.}$, across the thin-layer cell. Each potential is maintained until electrolysis has ceased, as determined by spectroscopically, so that the equilibrium value of the ratio of the concentration of oxidized to reduced forms, [Ox]/[Red] is established as defined by the Nernst equation:

$$E_{appl.} = E^{0\prime} + (2.303RT/nF) \cdot \log([Ox]/[Red])$$

The redox couple is incrementally converted from one oxidation state to the other by the series of applied potentials, for each of which the corresponding value of [Ox]/[Red] is determined from the spectra. Both formal reduction potentials and the value of n can be determined from plots of $E_{appl.}$ *vs.* log([Ox]/[Red]).

Measurements of the temperature coefficient of the e.m.f. from electrochemical cells of the type:[57]

$$\underbrace{Hg \mid Hg_2Cl_2\ (sat.),\ KCl\ (sat.) \parallel KCl\ (sat.) \parallel M^{m+},\ M^{(m-n)+} \mid M'}_{T\ (varied)}$$

were normally employed in the earlier studies (M^{m+} and $M^{(m-n)+}$ refer to the oxidized and reduced halves respectively, of the redox couple of interest, and M' represents the working electrode material). Formal reduction potentials at each temperature were determined potentiometrically using solutions containing equi-molar concentrations of the oxidized and reduced halves of the redox couple.

Such cell arrangements contain enthalpy and entropy contributions from the reference electrode half-cell to the temperature coefficient of the cell e.m.f. and are referred to as "isothermal" cells. An inherent difficulty with this procedure lies in the long time needed for most common reference electrodes to reach temperature

equilibrium.

It has been demonstrated that a cell arrangement of the type:[58]

$$\underbrace{Hg \mid Hg_2Cl_2\ (sat.),\ KCl\ (sat.) \,||\, KCl\ (sat.)}_{T_1\ (fixed)} \mid \underbrace{KCl\ (sat.) \,||\, M^{m+},\ M^{(m-n)+} \mid M'}_{T_2\ (varied)}$$

can be utilized effectively for determining the thermodynamics of redox reactions in aqueous solution if certain thermal junction potentials are either negligible, or are constant and can be determined. Under favorable circumstances the difference in partial molal ionic entropy, between the reduced and oxidized halves of the redox couple of interest (*i.e.*, the electron transfer reaction entropy, ΔS^0_{et}), is directly proportional to the temperature coefficient of the nonisothermal cell:[58]

$$\Delta S^0_{et} = S^0_{red} - S^0_{ox} = F \cdot (dE^0/dT)$$

where F is the Faraday constant.

These two commonly used configurations for the electrochemical cell are illustrated in Figure 5.

For variable temperature studies we have employed the nonisothermal configuration in our OTTLE cells, and the following arrangement was utilized:

Figure 5. Isothermal and nonisothermal configurations for electrochemical cells. In the case of the isothermal configuration, the temperature of the reference electrode changes with that of the sample. The temperature dependence of the formal reduction potential of the sample, $E^{0\prime}$, was therefore corrected for the contribution of the temperature dependence of the reference electrode. The nonisothermal configuration required that the working and reference electrode compartments be maintained at two different temperatures. In our experiments, the temperature of the reference electrode was always held at ambient room temperature.

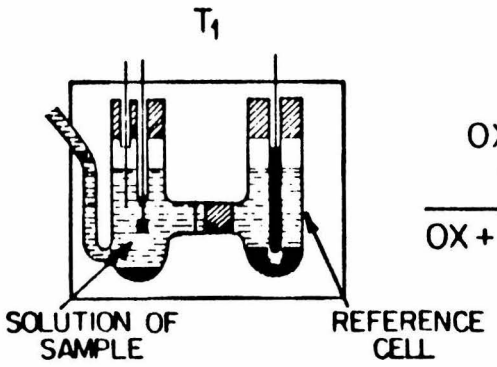

ISOTHERMAL

$$OX + E^- \rightleftharpoons RED$$
$$\tfrac{1}{2}\cdot H_2 \rightleftharpoons H^+ + E^-$$
$$OX + \tfrac{1}{2}\cdot H_2 \rightleftharpoons RED + H^+$$

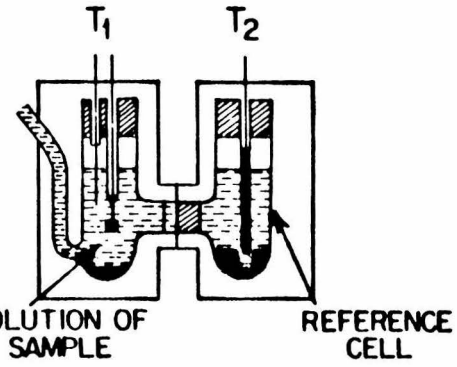

NONISOTHERMAL

$$\Delta S^0_{iso} = (S^0_{red} + S^0_{H^+}) - (S^0_{ox} + \tfrac{1}{2}\cdot S^0_{H_2})$$

$$S^0_{H_2} = 31.2 \text{ eu}$$

$$S^0_{H^+} = 0 \text{ (BY CONVENTION)}$$

$$S^0_{red} - S^0_{ox} = \Delta S^0_{iso} + 15.6 \text{ eu}$$

$$\Delta S^0_{rc} = \Delta S^0_{iso} + 15.6 \text{ eu}$$

T_2 IS HELD FIXED WHILE
T_1 IS VARIED

$$S^0_{red} - S^0_{ox} = F\cdot(dE^0/dT)$$

$$\Delta S^0_{rc} = F\cdot(dE^0/dT)$$

$$\underbrace{Hg \mid Hg_2Cl_2\ (sat.), KCl\ (sat.) \,||\, KCl\ (sat.)}_{T_1\ (fixed)} \mid \underbrace{KCl\ (sat.) \,||\, M^{m+}, M^{(m-n)+} \mid Au}_{T_2\ (varied)}$$

where Au represents the gold minigrid working electrode. The nonisothermal salt bridge consisted of a 5 mm x 25 cm glass tube filled with saturated KCl solution. The bottom end was terminated by a \$7/25 outer ground glass joint with a Pt junction sealed in. The tip end was flared to receive a Sargent-Welch SCE (miniature, Pt junction, #S-30080-17). The temperature of the OTTLE cell was varied using a specially constructed variable temperature cell holder and the cell temperatures were directly measured with an Omega Engineering, Inc. precision micro thermocouple,[59] connected to a Fluke 21754 Digital Thermometer, ± 0.2 ^{0}C, situated in the protein solution in close proximity to the thin-layer cavity. The reference electrode and part of the nonisothermal salt bridge were maintained at ambient room temperature. The Nernst plot data were analyzed using a linear least squares fit to the Nernst equation, and reduction potentials were retained only if the linear correlation coefficients were 0.999.

The temperature coefficient of the formal reduction potential, ($dE^{0\prime}/dT$), was determined as the slope of a linear least squares fit to the $E^{0\prime}$ *vs.* temperature data. The entropy change for the complete cell reaction (ΔS^0), adjusted to the NHE scale was determined from the relation:[60]

$$\Delta S^0 = (S^0_{red} + S^0_{H^+}) - (S^0_{ox} + 1/2\ S^0_{H_2})$$

$$= (S^0_{red} - S^0_{ox}) - 15.6 \text{ eu}$$

taking $S^0_{H_2}$ = 31.2 eu and adhering to the arbitrary convention that $S^0_{H^+}$ be taken as zero.[61] Standard free energy changes for the cell reaction were calculated from the $E^{0\prime}$ (V *vs.* NHE) values at 25.0 ^{0}C and the standard enthalpy changes, $\Delta H^{0\prime}$s, were determined from the corresponding $\Delta G^{0\prime}$s and $\Delta S^{0\prime}$s:

$$\Delta G^{0\prime} = \Delta H^{0\prime} - T\Delta S^{0\prime}$$

References

1. Crutchley, R. J., Ellis, W. R., Jr., and Gray, H. B., *J. Am. Chem, Soc.*, ***107***, 5002 (1985).

2. Margalit, R., Kostić, N. M., Che, C.-M., Blair, D. F., Chiang, H.-J., Pecht, I., Shelton, J. B., Shelton, J. R., Schroeder, W. A., and Gray, H. B., *Proc. Natl. Acad. Sci. USA*, ***84***, 6554 (1984).

3. Nocera, D. G., Winkler, J. R., Yocom, K. M., Bordignon, E., and Gray, H. B., *J. Am. Chem. Soc.*, ***106***, 5145 (1984).

4. Reid, L. S., Taniguchi, V. T., Gray, H. B., and Mauk, A. G., *J. Am. Chem. Soc.*, ***104***, 7516 (1982).

5. Taniguchi, V. T., Ellis, W. R., Jr., Cammarata, V., Webb, J., Anson, F. C., and Gray, H. B., in *Advances in Chemistry Series, No. 201, Electrochemical and Spectrochemical Studies of Biological Redox Components*, Kadish, K. M., ed., American Chemical Society, Washington, D. C., 1982, P. 51.

6. Taniguchi, V. T., Malmström, B. G., Anson, F. C., and Gray, H. B., *Proc. Natl. Acad. Sci. USA*, ***79***, 3387 (1982).

7. Taniguchi, V. T., Sailasuta-Scott, N., Anson, F. C., and Gray, H. B., *Pure Appl. Chem.*, ***52***, 2275 (1980).

8. Goldberg, M., Ph.D. Thesis, Weizmann Institute of Science, Rehovot, Israel, 1979.

9. Sailasuta, N., Anson, F. C., and Gray, H. B., *J. Am. Chem. Soc.*, ***101***, 455 (1979).

10. Wherland, S., and Pecht, I., *Biochemistry*, ***17***, 2585 (1978).

11. Kreishman, G. P., Su, C.-H., Anderson, C. W., Halsall, H. B., Heineman, W. R., in *Advances in Chemistry Series, No. 188, Bioelectrochemistry: Ions, Surfaces, Membranes*, Blank, M., ed., American Chemical Society, Washington, D. C., 1980, P. 169.

12. Anderson, C. W., Halsall, H. B., Heineman, W. R., and Kreishman, G. P., *Biochem, Biophys. Res. Comm.*, ***76***, 339 (1977).

13. Goldberg, M., and Pecht, I., *Biochemistry*, ***15***, 4197 (1976).

14. Jacks, C. A., Bennett, L. E., Raymond, W. N., and Lovenberg, W., *Proc. Natl. Acad. Sci. USA*, ***71***, 1118 (1974).

15. Margalit, R., and Schejter, A., *Eur. J. Biochem.*, ***32***, 492 (1973).

16. Margalit, R., and Schejter, A., *FEBS Lett.*, ***6***, 278 (1970).

17. Watt, G. D., and Sturtevant, J. M., *Biochemistry*, ***8***, 4567 (1969).

18. George, P., Eaton, W. A., and Trachtman, M., *Fed. Proc.*, ***27***, 526 (1968).

19. George, P., Hanania, G. I. H., and Eaton, W. A., in *Hemes and Hemoproteins*, Chance, B., Estabrook, R. W., and Yonetani, T., eds., Academic Press, New York, 1966, P. 267.

20. Hanania, G. I. H., Ph.D. Thesis, University of Cambridge, Cambridge, England, 1953.

21. Ball, E. G., *Biochem. Z.*, ***295***, 262 (1938).

22. Walz, D., *Biochim. Biophys. Acta*, ***505***, 279 (1979).

23. Wilson, D. F., Dutton, P. L., Erecinska, M., Lindsay, J. G., and Sato, N., *Acc. Chem. Res.*, *5*, 234 (1972).

24. Clark, W. M., *Oxidation-Reduction Potentials of Organic Systems*, Williams and Wilkins, Baltimore, 1960.

25. Rodkey, F. L., and Ball, E. G., *J. Biol. Chem.*, ***182***, 17 (1950).

26. Higgins, I. J., and Hill, H. A. O., in *Essays in Biochemistry*, Volume 21, Marshall, R. D., and Tipton, K., eds., Academic Press, London, 1985, P. 119.

27. Allen, P. M., Hill, H. A. O., and Walton, N. J., *J. Electroanal. Chem.*, ***178***, 69 (1984).

28. Eddowes, M. J., and Hill, H. A. O., in *Advances in Chemistry Series, No. 201, Electrochemical and Spectrochemical Studies of Biological Redox Components*, Kadish, K. M., ed., American Chemical Society, Washington, D. C., 1982, P. 173.

29. Alberg, W. J., Eddowes, M. J., Hill, H. A. O., and Hillman, A. R., *J. Am. Chem. Soc.*, ***103***, 3904 (1981).

30. Eddowes, M. J., and Hill, H. A. O., *J. Am. Chem. Soc.*, ***101***, 4461 (1979).

31. Heineman, W. R., Hawkridge, F. M., and Blount, H. N., in *Electroanalytical Chemistry*, Volume 13, Bard, A. J., ed., Marcel

Dekker, New York, 1984, P. 1.

32. Heineman, W. R., *J. Chem. Educ.*, ***60***, 305 (1983).

33. Heineman, W. R., and Kissinger, P. T., *Anal. Chem.*, ***52***, 138R (1980).

34. Heineman, W. R., *Anal. Chem.*, ***50***, 390A (1978).

35. Heineman, W. R., and Kissinger, P. T., *Anal. Chem.*, ***50***, 166R (1978).

36. Muller, R. H., *Electrochim. Acta*, ***22***, 951 (1977).

37. Parson, R., *Sci. Prog., Oxf.*, ***64***, 29 (1977).

38. Kuwana, T., and Heineman, W. R., *Acc. Chem. Res.*, ***9***, 241 (1976).

39. Kuwana, T., and Winograd, N., in *Electroanalytical Chemistry*, Volume 7, Bard, A. J., ed., Marcel Dekker, New York, 1974, P. 1.

40. Kuwana, T., *Ber. Bunsenges. Phys. Chem.*, ***77***, 858 (1973).

41. Aylmer-Kelly, A. W. B., Bewick, A., Cantrill, P. R., and Tuxford, A. M., *Faraday Discuss. Chem. Soc.*, No. 56, 96 (1973).

42. McIntyre, J. D. E., in *Advances in Electrochemisty and Electrochemical Engineering*, Volume 9, Muller, R. H., ed., Wiley, New York, 1973, P. 61.

43. Hansen, W. N., in *Advances in Electrochemistry and Electrochemical Engineering*, Volume 9, Muller, R. H., ed., Wiley, New York, 1973, P. 1.

44. Jeanmaire, D. L., Suchanski, M. R., and Van Duyne, R. P., *J. Am Chem. Soc.*, ***97***, 1699 (1975).

45. Hawkridge, F. M., and Ke, B., *Anal. Biochem.*, ***78***, 76 (1977).

46. Faulkner, L. F., and Bard, A. J., in *Electroanalytical Chemistry*, Volume 10, Bard, A. J., ed., Marcel Dekker, New York, 1977, P. 1.

47. McKinney, T. M., in *Electroanalytical Chemistry*, Volume 10, Bard, A. J., ed., Marcel Dekker, New York, 1977, P. 97.

48. Richards, J. A., and Evans, D. H., *Anal. Chem.*, ***47***, 964 (1975).

49. Hubbard, A. T., *CRC Crit. Rev. Anal. Chem.*, ***3***, 201 (1973).

50. Hubbard, A. T., and Anson, F. C., in *Electroanalytical Chemistry*, Volume 4, Bard A. J., ed., Marcel Dekker, New York, 1971, P. 129.

51. Reilley, C. N., *Rev. Pure Appl. Chem.*, ***18***, 137 (1968).

52. Murray, R. W., Heineman, W. R., and O'Dom, G. W., *Anal. Chem.*, ***39***, 1666 (1967).

53. Teflon film for spacers between quartz windows:
Specify type DF 1200 2 mil 1" x 36 yards.
Order from: Dilectrix Corp.
465 Ohio St.
Lockport, NY 14094

54. Electroformed gold mesh for the minigrid:
5000 lines/inch, 6" x 6" sheet.
Order from: Buckbee-Mears Co.
Industrial Products Group
245 E. Sixth St.
St. Paul, MN 55101

55. Heineman, W. R., Norris, B. J., and Goelz, J. F., *Anal. Chem.*, ***47***, 79 (1975).

56. Scott, N. S., Ph.D. Thesis, California Institute of Technology, Pasadena, United States, 1980.

57. Lin, J., and Breck, W. G., *Can. J. Chem.*, ***43***, 766 (1965).

58. Yee, E. L., Cave, R. J., Guyer, K. L., Tyma, P. D., and Weaver, M. J., *J. Am. Chem. Soc.*, ***101***, 1131 (1979).

59. Copper-Constantan thermocouple:
specify item TT-T-36-48 in.-PJ
Order from: B. J. Wolfe Enterprises
10760 Burbank Blvd.
North Hollywood, CA 91601

60. George, P., Hanania, G. I. H., and Irving, D. H., *J. Chem. Soc.*, 2548 (1959).

61. Latimer, W. M., *The Oxidation States of the Elements and Their Potentials in Aqueous Solutions, Second Edition*, Prentice-Hall, New York, 1952.

CHAPTER III

THERMODYNAMIC STUDIES OF THE TYPE-1 COPPER IN TREE LACCASE

Introduction

Copper-containing proteins occur widely in nature, displaying different spectral, chemical and functional properties. The functions of copper-proteins include the catalysis of electron transfer reactions (azurin, plastocyanin, stellacyanin), the transport of oxygen molecules (hemocyanin), the catalysis of the disproportion of the superoxide anion (superoxide dismutase), and the catalysis of the reduction of O_2 to H_2O_2 (galactose oxidase, amine oxidase) and H_2O (cytochrome *c* oxidase, laccase). Furthermore, the protein albumin is involved in the transport of copper in mammals. A selection of some important copper proteins is listed in Table 1.

Recently, several investigations have been carried out on the spectroscopic, electrochemical, structural and functional properties of copper-containing proteins. This work has been reviewed by several authors.[1-13]

Laccase is a blue-copper-containing oxidase which is widely distributed in higher plants and fungi. It belongs to a small group of oxidases which can utilize the full oxidizing capacity of dioxygen and reduce it to two molecules of water. These other enzymes are the proteins ceruloplasmin and ascorbate oxidase which have many properties in common with laccase.

Laccase is one of the most complicated copper-containing oxidases since it contains three types of quite unique copper ions. Nevertheless, it has been extensively studied by a number of differ-

Table 1. Some blue and non-blue copper-containing proteins together with the types of copper ions present and their functions.

Protein	Type of protein	Type of coppers	Function
Azurin	blue	type 1(1)*	electron carrier
Plastocyanin	blue	type 1(1)	electron carrier
Stellacyanin	blue	type 1(1)	electron carrier
Ascorbate oxidase	blue	type 1(3), type 2(1) and type 3(4)	oxidase, reducing $O_2 \longrightarrow H_2O$
Laccase	blue	type 1(1), type 2(1) and type 3(2)	oxidase, reducing $O_2 \longrightarrow H_2O$
Ceruloplasmin	blue	type 1(2), type 2(1) and type 3(4)	probably involved in iron metabolism oxidase, reducing $O_2 \longrightarrow H_2O$

*The number in parentheses designates how many specified type of copper ions per molecule.

Protein	Type of protein	Type of coppers	Function
Hemocyanin	non-blue	anti-ferromagnetically coupled Cu pair	O_2 carrier
Tyrosinase	non-blue	anti-ferromagnetically coupled Cu pair	monooxygenase; cresolase activity oxidase; catecholase activity
Superoxide dismutase	non-blue	Cu–Zn imidazole bridge	O_2 detoxification
Cytochrome *c* oxidase	non-blue	Fe–Cu anti-ferromagnetically coupled	terminal oxidase, reducing $O_2 \longrightarrow H_2O$
Galactose oxidase	non-blue	"normal" copper	oxidase, reducing $O_2 \longrightarrow H_2O_2$
Amine oxidase	non-blue	"normal" copper	oxidase, reducing $O_2 \longrightarrow H_2O_2$
Albumine	non-blue	"normal" copper	copper transport

ent techniques, and is, therefore, one of the best understood oxidases, at least in terms of its catalytic mechanism.

Laccase has a rather low specificity with regard to the reducing substrate. Therefore, a number of quite different substances are readily oxidized. Good substrates included many derivatives of phenol.

Tree laccase (*Rhus vernicifera*) (p-diphenol: O_2 oxidoreductase, E.C. 1.10.3.2) from the Japanese lacquer tree has a molecular weight of 110,000 daltons. The amino acid sequence is still unknown, although it probably consists of a single polypeptide chain of *ca.* 500 amino acid residues. No crystal structure has yet been determined. Since the enzyme is a glycoprotein, containing 45% carbohydrate, the probability that X-ray structure information will be available in the near future is low.

Laccase has four copper ions, and includes examples from each of the three subclasses: Type 1, Type 2, and Type 3. This classification was originally used to describe the composition of proteins containing more than one copper center, and was based on the characteristic optical spectra and ESR parameters for each type of center.[11,13]

Type 1 copper is present in all blue-copper-proteins and is characterized by unique spectral and redox properties:

(1) A very intense absorption (molar extinction coefficient ~ 5000 $M^{-1}cm^{-1}$, for tree laccase, ε_o = 5700 $M^{-1}cm^{-1}$) in the electronic spectrum around 600 nm (614

nm for tree laccase).

(2) A very small $A_{||}$ value in the EPR spectrum (for Cu(II), 0.004 ~ 0.04 cm^{-1}; 0.0043 cm^{-1} for tree laccase).

(3) A relatively high reduction potential (190 ~ 800 mV, generally in the 300 ~ 500 mV range *vs.* 150 mV for $Cu^{II}_{(aq)}$).[14-16]

These properties have intrigued chemists for many years because they are so different from their analogs in ordinary tetragonal Cu(II) complexes.

Recently, a different way of classifying copper proteins was suggested.[17,18] The new method has focused attention on the details of molecular structure provided by X-ray crystallography and has highlighted the function of the copper ions in the proteins. Group-I proteins are those that contain a single copper ion having four ligands in a distorted tetrahedral geometry. The ligands are coordinated to the copper via sulfur and nitrogen donor atoms, with two nitrogens and two sulfur atoms being the most common arrangement. Important physical properties, including the redox potential, are modulated by the details of the coordination environment, particularly by the number and nature of the sulfur ligands. Group-II copper proteins also contain a single copper ion at the catalytic center, although in this case the ligands are coordinated by nitrogen and oxygen donor atoms and the geometry tends to be a square-planar arrangement around the copper ion. An important feature of this arrangement is that there is at least one readily accessible

coordination site, either in the plane or along the tetragonal axis, that binds substrate or other ligands. In these proteins, the Lewis acid properties of copper(II) are employed with, or without, concomitant redox activity. Group-III proteins contain one or more binuclear copper centers with a coordination environment consisting mainly of nitrogen donor atoms. In the copper(I) form of the protein, two ligand atoms may dominate the coordination environment thereby allowing the protein to fulfill its function, *i.e.*, the coordination of dioxygen. Group-IV proteins contain two or more of the centers that characterize groups I to III. Thus the new classification method can characterize laccase as group $IV_{I,II,III}$, and the classification of a number of copper proteins is given in Table 2.

Several recent experiments on the single blue copper proteins azurin, plastocyanin, and stellacyanin have done much toward elucidating the structure of the blue copper site. Spectroscopic studies[19] have shown that the absorption spectrum can be fit using a tetragonally-distorted tetrahedral coordination environment, where the large absorbance near 610 nm has been assigned to S^-(Cys) $\longrightarrow$ Cu(II) charge transfer. This has been confirmed by crystal structure analysis of two single blue copper proteins, *i.e.*, plastocyanin[20,21] and azurin.[22,23] The X-ray crystallographic structure of poplar plastocyanin *(Populus nigra* var. *italica)* is shown in Figures 1 and 2. In both cases the copper atom is coordinated in a distorted tetrahedral environment by two δ-nitrogen atoms of the imidazole

Table 2. Alternative classification for copper proteins.

Role	Calssification	Examples
Electron transfer	Group I	Azurin, plasto-cyanin, rusticyanin, stellacyanin
Substrate oxidation with hydrogen peroxide formation	Group II	Galactose oxidase Benzylamine oxidase
Superoxide dismutation	Group II	Superoxide dismutase
Monooxygenation	Group II	Dopamine β-mono-oxygenase
	Group III	Tyrosinase
Oxygen transport	Group III	Hemocyanin
Terminal oxidase	Group IV	Laccase Ceruloplasmin Ascorbate oxidase

Figure 1. An X-ray crystallographic structure of the polypeptide backbone of poplar (*Populus nigra* var. *italica*) plastocyanin in the oxidized form.


10
90
87
Cu
92
37
30
60
84
40
70
N
80
20
C
50

Figure 2. The copper-binding site of poplar (*Populus nigra* var. *italica*) plastocyanin in the oxidized state.

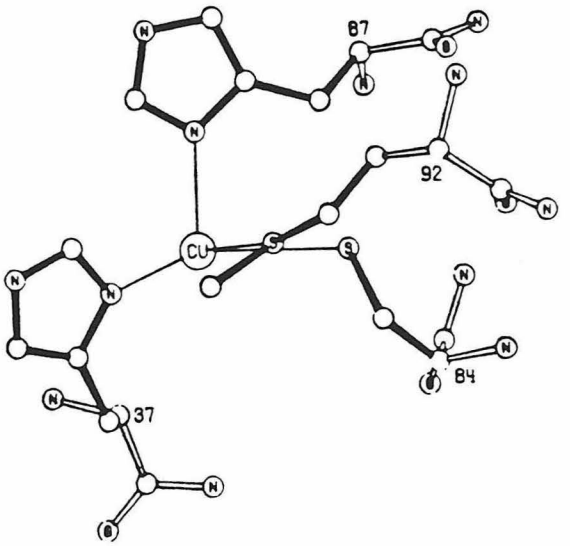
87
92
CU
84
37

rings of histidine residues (His-37 and His-87) and by two sulfur atoms, one of which is a thioether sulfur from methionine (Met-92), the other a thiol sulfur atom from cysteine (Cys-84). The crystal structure of plastocyanin in the reduced form has also been solved.[6] It appeared that the coordination of copper resembled that of the copper(II) protein: one of the histidines had moved slightly away from the copper, whereas the methionine sulfur atom was at a somewhat closer distance; however, no considerable structural rearrangement is involved in the reduction. The small change in inner-sphere structural reorganization can explain the high redox potential, favouring an easy Cu(II) ⟶ Cu(I) transition. Although stellacyanin does not have a methionine residue in the amino acid sequence,[24] all type 1 copper sites are believed to resemble the one found in plastocyanin and azurin, with probably two cysteines in the case of stellacyanin.[25]

Type 2 copper exhibits normal spectral properties and is sometimes called "colorless copper", because the d-d transitions of the Cu(II) ion are hidden under the strong 600 nm absorption of the type 1 copper. EPR studies have shown that the type 2 copper of laccase is almost certainly coordinated to four nitrogens in a square planar arrangement,[26] and displays an EPR spectrum typical of an axial Cu(II) complex.[7,11]

Type 3 copper consists of two coppers which are strongly antiferromagnetically coupled.[27,28] Prior to the report of the Goteborg's group, the type 3 site was believed to be EPR-silent in both

the resting and active states.[29] By analogy with the molluscan oxygen-carrying protein hemocyanin, which also has such a copper pair, the type 3 site is considered to be the site of oxygen binding, and it probably contains no sulfur ligands.

There have been several attempts to elucidate the mechanism of electron transfer from reducing substrates to dioxygen by laccase. The interpretation of the data is a complex and difficult task. The experiments involve:

(1) Reoxidation of fully reduced laccase.

(2) The steady state reaction of laccase with oxygen and reductant.

(3) The anaerobic reduction of laccase with various reductants.

The results from these experiments are consistent with the view that laccase can exist in at least two catalytically different forms, one active and the other inactive.[30,31] The active enzyme is converted to an inactive form at high pH. It has been shown that the enzyme becomes inhibited above pH 6.5 and that the inhibition depends on the formation of a type-2 Cu(II)-OH^- complex at high pH values. The reduction mechanism based on studies at high and low pH is shown in Scheme 1 of Figure 3. Since the structure of the enzyme is not known the protein is represented by a box. Type-1 and type-2 copper ions are placed at the upper and lower left part and type-3 is represented by a pair which can accept two electrons. The resting enzyme can be in two forms. One of them has an OH^- ion bound to

Figrue 3. Scheme 1, reduction mechanism of laccase at high or low pH, and scheme 2, reoxidation reaction mechanism for laccase.

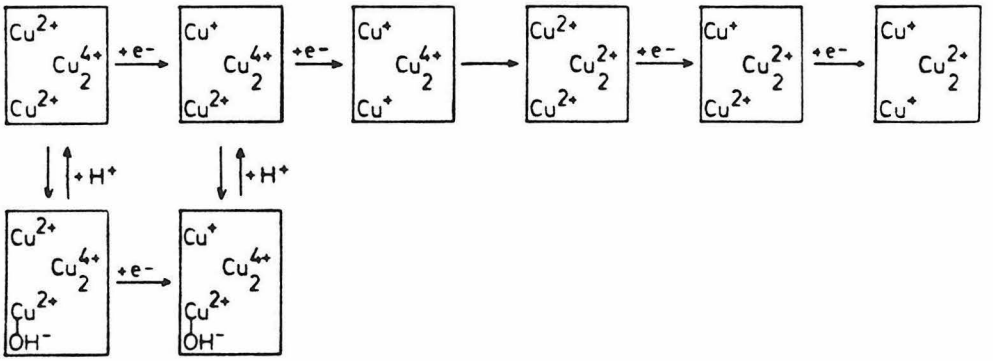

SCHEME 1.

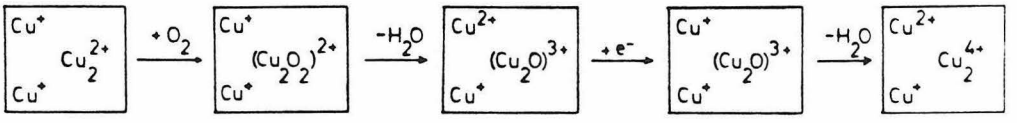

SCHEME 2.

type-2 Cu(II) and corresponds to the inactive form. The other form is active and probably has water instead of OH^- bound to this metal site.

At pH 6.5 both type-1 and type-2 Cu(II) are reduced simultaneously. This simultaneous reduction is probably due to a conformational interaction between these metal sites. The first electron from a substrate molecule reduces type-1 Cu(II). When this site is reduced it affects the reduction of type-2 Cu(II) which seems to be reduced by a second substrate molecule and not by electron transfer from type-1 Cu(I). It has been suggested that type-2 copper is coordinated to the two histidine residues on each side of the cysteine which is a proposed type-1 copper ligand. If this is the case, the reduction of type-1 Cu(II) might cause a conformational alteration of the type-2 Cu(II) site which could affect the reduction of this metal site. The reduced type-1 and type-2 coppers then simultaneously donate one electron each to the type-3 copper pair. Thereafter, the reoxidized type-1 and type-2 coppers are once more reduced and the enzyme becomes completely reduced. This reaction sequence is shown in the upper part of Scheme 1 in Figure 3.

Materials and Methods

Tree laccase was isolated from an acetone powder extract of the latex of the Japanese lacquer tree *Rhus vernicifera*,[32] with a slight modification of the published procedure.[33] Purity was checked by

the ratio A_{280}/A_{614} and a very satisfactory value (*ca.* 15.3) was obtained, as shown in Figure 4. The laccase was then stored at - 60 ^{0}C in aliquots.

The potassium ferricyanide used as the mediator in the spectroelectrochemical studies, was obtained as AR grade from Mallinckrodt. Sodium phosphate buffer, of ionic strength 100 mM and pH 6.0, was prepared from analytical grade reagents. All protein and buffer solutions were prepared using deionized water purified by a Barnstead NANOpure water purifier.

Formal reduction potentials at different temperatures for type-1 copper center were determined by using an optically transparent thin-layer electrode (OTTLE) cell in a nonisothermal configuration. A description of this technique is summarized in Chapter II. The OTTLE cell employing gold minigrid as the working electrode material. The optical path length of 0.47 mm was measured by using the molar extinction coefficient at 420 nm of $[Fe(CN)_6]^{3-}$ solution as a standard. Potentials were applied across the thin-layer cell by using a Princeton Applied Research model 174A polarographic analyzer and were accurately measured with a Keithley model 177 microvolt digital multimeter. The cell temperature was varied by using a variable temperature cell holder and measured directly with an Omega Engineering precision microthermocouple and a Fluke model 2175A digital thermometer. The thermocouple was situated in the protein solution in close proximity to the thin-layer cavity. All visible spectra were obtained with a Cary 219 recording spectrophotometer.

Figure 4. UV-VIS absorption spectrum of tree laccase. The A_{280}/A_{614} ratio is shown.

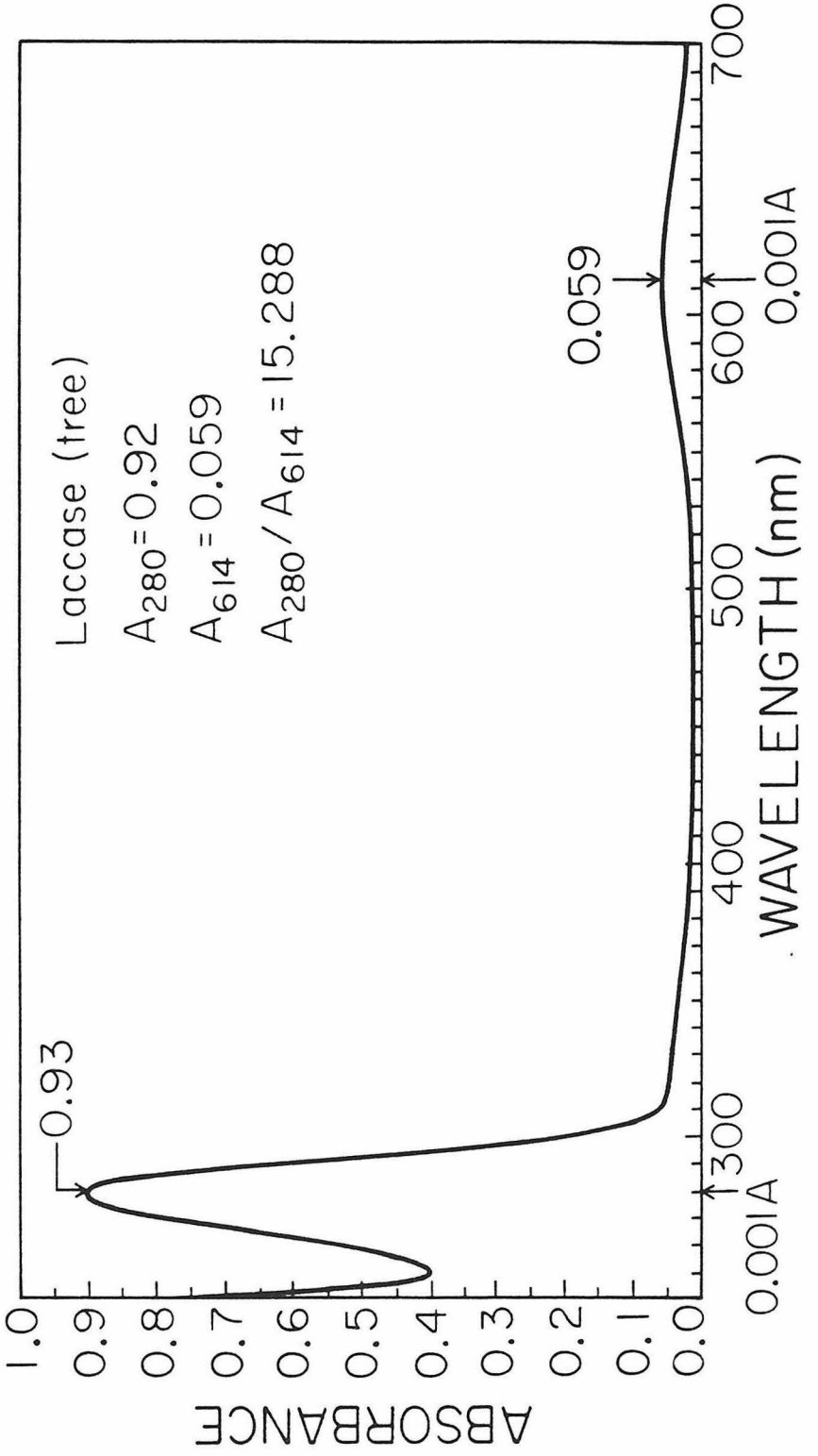
Laccase (tree)
A_{280}=0.92
A_{614}=0.059
A_{280}/A_{614}=15.288
0.93
0.059
0.001A
0.001A
ABSORBANCE
WAVELENGTH (nm)
1.0
0.9
0.8
0.7
0.6
0.5
0.4
0.3
0.2
0.1
0.0
300
400
500
600
700

Formal reduction potentials were determined by sequentially applying a series of potentials, $E_{appl.}$, to the gold minigrid electrode. Each potential was maintained until electrolysis ceased so that the equilibrium value of the ratio of concentrations of oxidized to reduced forms of all redox couples in solution, [Ox]/[Red], was established as defined by the Nernst equation. Redox couples were incrementally converted from one oxidation state to the other by the series of applied potentials, for which each corresponding value of [Ox]/[Red] was determined from the spectra. Formal reduction potentials and n values were determined from plots of $E_{appl.}$ *vs.* log([Ox]/[Red]).

All solution were deoxygenated prior to use by vacuum/argon cycling on a vacuum/purified argon double manifold and loaded into the OTTLE cell by using rubber septum caps and syringe techniques. The platinum wire auxiliary electrode was situated in a compartment containing deoxygenated mediator-titrant solution that was isolated from protein solution by a porous glass frit.

Results and Discussion

The formal reduction potential of the redox mediator couple $[Fe(CN)_6]^{3-/4-}$, was determined to be 425 mV *vs.* NHE.[34] Molar extinction coefficients at 420 nm for ferricyanide and ferrocyanide[35,36] were calculated to be 1100 and 4.7 $M^{-1}cm^{-1}$, respectively. The overlay UV-VIS spectra of $[Fe(CN)_6]^{3-}$ and $[Fe(CN)_6]^{4-}$ are shown in

Figure 5.

A typical thin layer spectroelectrochemical experiment with tree laccase is illustrated in Figure 6. The additional absorbance in the 300 ~ 450 nm region is due mainly to ferricyanide, which was present in a five-fold excess over protein. Since both $[Fe(CN)_6]^{3-}$ and $[Fe(CN)_6]^{4-}$ are transparent above 500 nm, all absorbance change at 614 nm are due entirely to the blue copper chromophore in tree laccase[11] and can be analyzed directly.

A least squares analysis of the 614 nm Nernst plot ($E_{appl.}$ *vs.* log([Ox]/[Red]) is given in Figure 7. All $E^{0\prime}$ values were determined from data that yielded linear correlation coefficients of at least 0.999. Equilibration of the blue copper center at each applied potential was determined from the stabilization of the absorbance at 614 nm.

The enzyme could be reversibly cycled between its fully oxidized and fully reduced forms, and the value of $E^{0\prime}$ calculated for the blue copper center was independent of the direction of cycling. Table 3 gives the results of $E^{0\prime}$ at 25 ^{0}C for blue copper in tree laccase determined by three different methods including this work. The temperature dependence of the formal reduction potential of the blue copper center in tree laccase is shown in Figure 8. A detailed compilation of data for this and other metalloprotein systems is listed in Table 4. It is clearly shown that there are two different thermodynamic behaviors adapted by this enzyme. A least squares fit of the data within the temperature range of 20.2 ~ 42.1 ^{0}C gives an $E^{0\prime}$ at

Figure 5. UV-VIS overlay spectra of $[Fe(CN)_6]^{3-}$ and of $[Fe(CN)_6]^{4-}$.

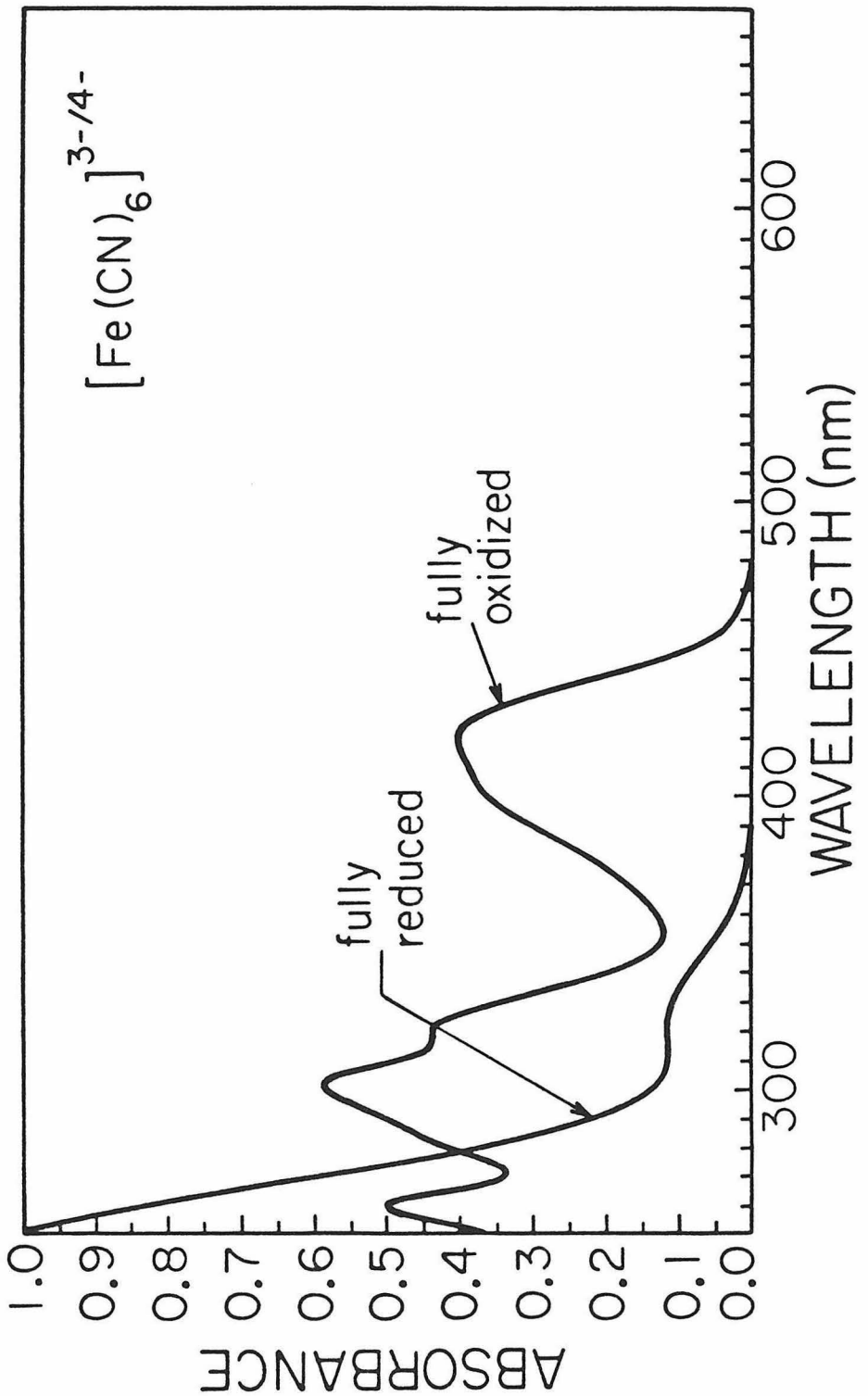
[Fe(CN)6]3-/4-
fully reduced
fully oxidized
ABSORBANCE
1.0
0.9
0.8
0.7
0.6
0.5
0.4
0.3
0.2
0.1
0.0
300
400
500
600
WAVELENGTH (nm)

Figure 6. Thin-layer spectroelectrochemistry of native tree (*Rhus vernicifera*) laccase. Solution conditions: pH 5.84, μ = 100 mM, phosphate buffer, 24.8 ^{0}C. Protein concentration: 0.27 mM. Redox mediator: $K_3[Fe(CN)_6]$, 1.35 mM. Overlay spectra and absorbance changes at different values of the applied potentials in mV *vs.* SCE.

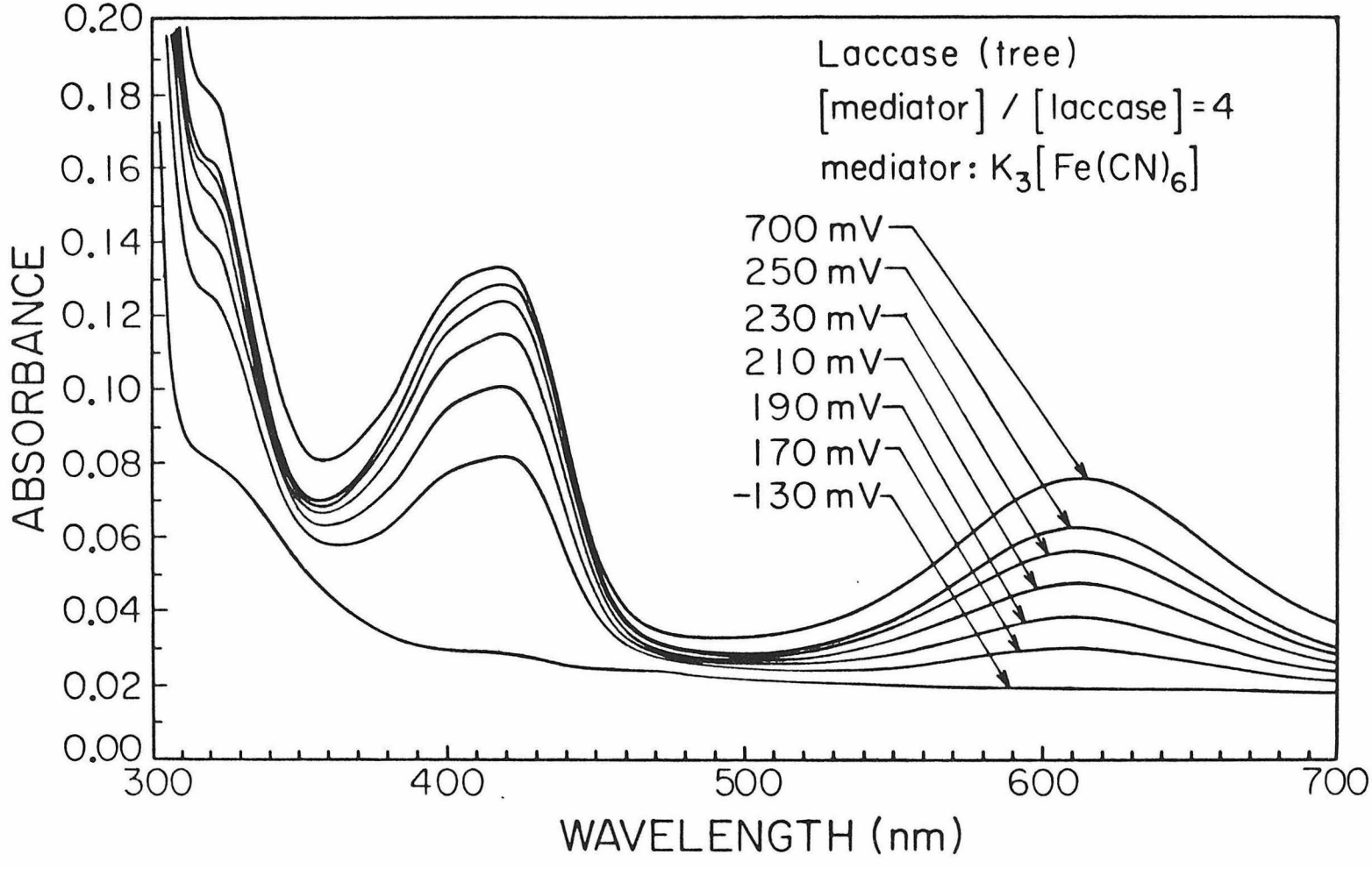
Laccase (tree)
[mediator] / [laccase] = 4
mediator: $K_3[Fe(CN)_6]$
700 mV
250 mV
230 mV
210 mV
190 mV
170 mV
-130 mV
ABSORBANCE
0.20
0.18
0.16
0.14
0.12
0.10
0.08
0.06
0.04
0.02
0.00
300
400
500
600
700
WAVELENGTH (nm)

Figure 7. Nernst plot of the absorbance changes at 614 nm during a spectroelectrochemical titration of the type-1 copper center in tree laccase *Rhus vernicifera*. The circles represent experimental points, and the line is a least squares fit of the $E_{appl.}$ *vs.* log([Ox]/[Red]). The fit yielded $E^{0\prime}$ = 452 mV *vs.* NHE and Nerst slope = 76 mV. Solution conditions: pH = 5.84, μ = 100 mM, phosphate buffer, 25.0 ^{0}C, 5 equivalents $K_3[Fe(CN)_6]$.

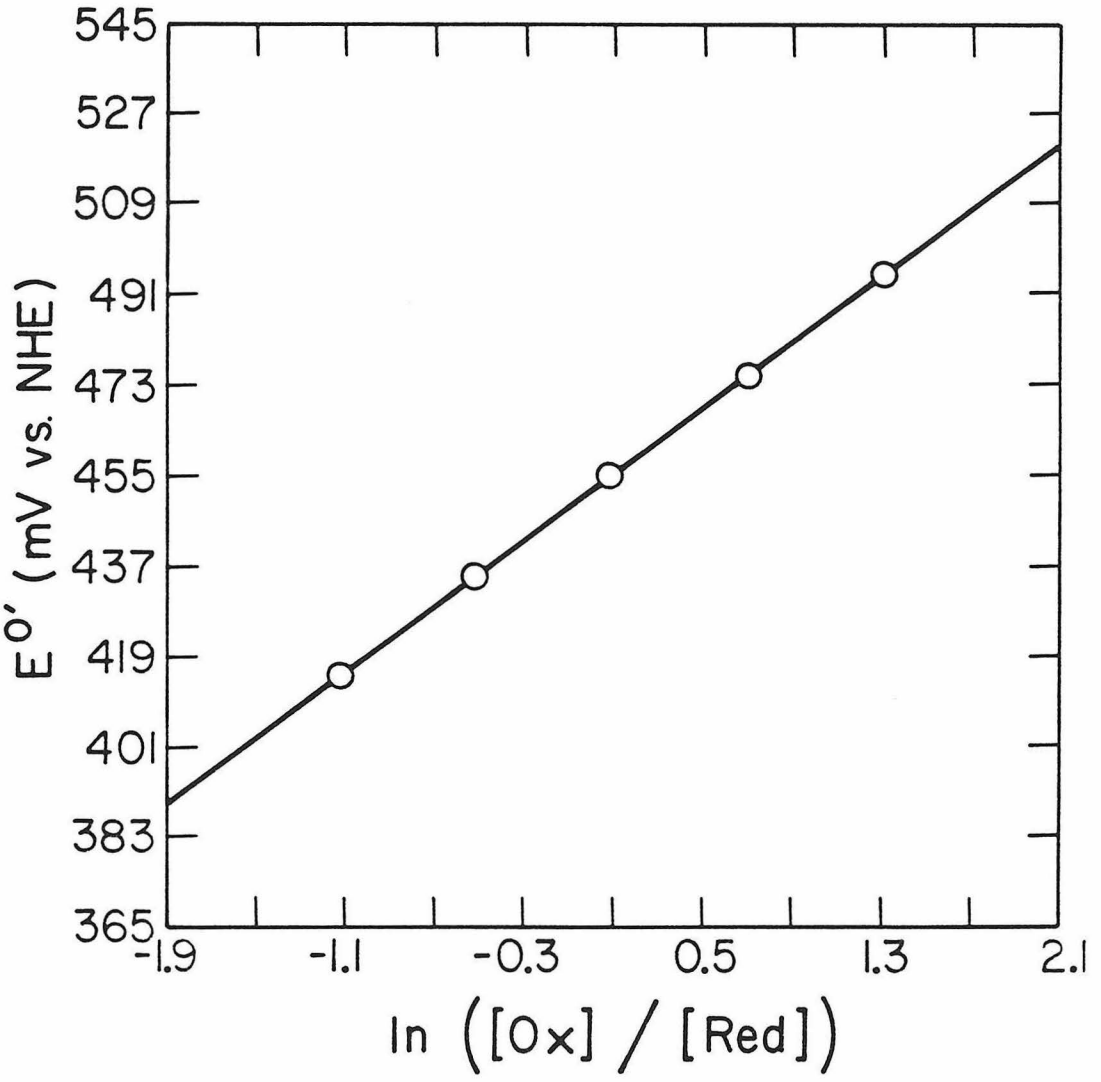
545
527
509
491
473
455
437
419
401
383
365
E°' (mV vs. NHE)
-1.9
-1.1
-0.3
0.5
1.3
2.1
ln ([Ox] / [Red])

Table 3. Formal reduction potentials for the blue copper center in *Rhus vernicifera* (tree) laccase.

$E^{0\prime}$ at 25 ^{0}C (mV vs. NHE)	Reaction Conditions	Method
415	μ = 0.2 M, pH 7.0, phosphate buffer	Chemical titration with $[Fe(CN)_6]^{3-/4-}$ as titrants[47]
394	μ = 0.2 M, pH 7.5, phosphate buffer mediator: $[Fe(CN)_6]^{3-}$ [mediator]/[laccase] = 1/3	Potentiometric titration; ascorbate, quinol, and O_2 were used as titrants[48]
434	μ = 0.2 M, pH 7.5 phosphate buffer mediator: $[Fe(CN)_6]^{3-}$ [mediator]/[laccase] = 3	Same as above
452	μ = 0.1 M, pH 5.8 ± 0.1, phosphate buffer mediator: $[Fe(CN)_6]^{3-}$ [mediator]/[laccase] = 5	Spectroelectrochemistry*

*This thesis work.

Table 4. Temperature dependence of the formal reduction potentials, $E^{0\prime}$, for the blue copper ion in *Rhus vernicifera* (tree) laccase, using nonisothermal thin-layer spectroelectrochemistry. Solution conditions: pH 5.8, μ = 100 mM, phosphate buffer.

Temperature (^{0}C)*	$E^{0\prime}$ (mV vs. NHE)†
6.4	433
6.8	434
8.4	436
11.8	442
14.0	444
15.8	447
18.1	449
20.2	450
22.2	449
25.0	452
25.0	453
27.2	452
29.1	456
30.5	453
32.9	457
34.9	455
38.8	459
40.6	457
42.1	459

* ± 0.2 ^{0}C

† ± 2 mV

Figure 8. Temperature dependence of the formal reduction potential, $E^{0\prime}$, for the type 1 copper center in tree laccase *Rhus vernicifera*, using nonisothermal thin-layer spectroelectrochemistry. Solution conditions: pH = 5.8 ± 0.1, μ = 100 mM, phosphate buffer. Temperature range: 6.4 ~ 42.1 ^{0}C. A least squares fit of the data in the temperature range of 20.2 ~ 42.1 ^{0}C gave an $E^{0\prime}$ = 452 ± 2 mV at 25.0 ^{0}C and $(dE^{0\prime}/dT)_{25\ ^{0}C} = 4.18 \times 10^{-4}$ V/^{0}C.

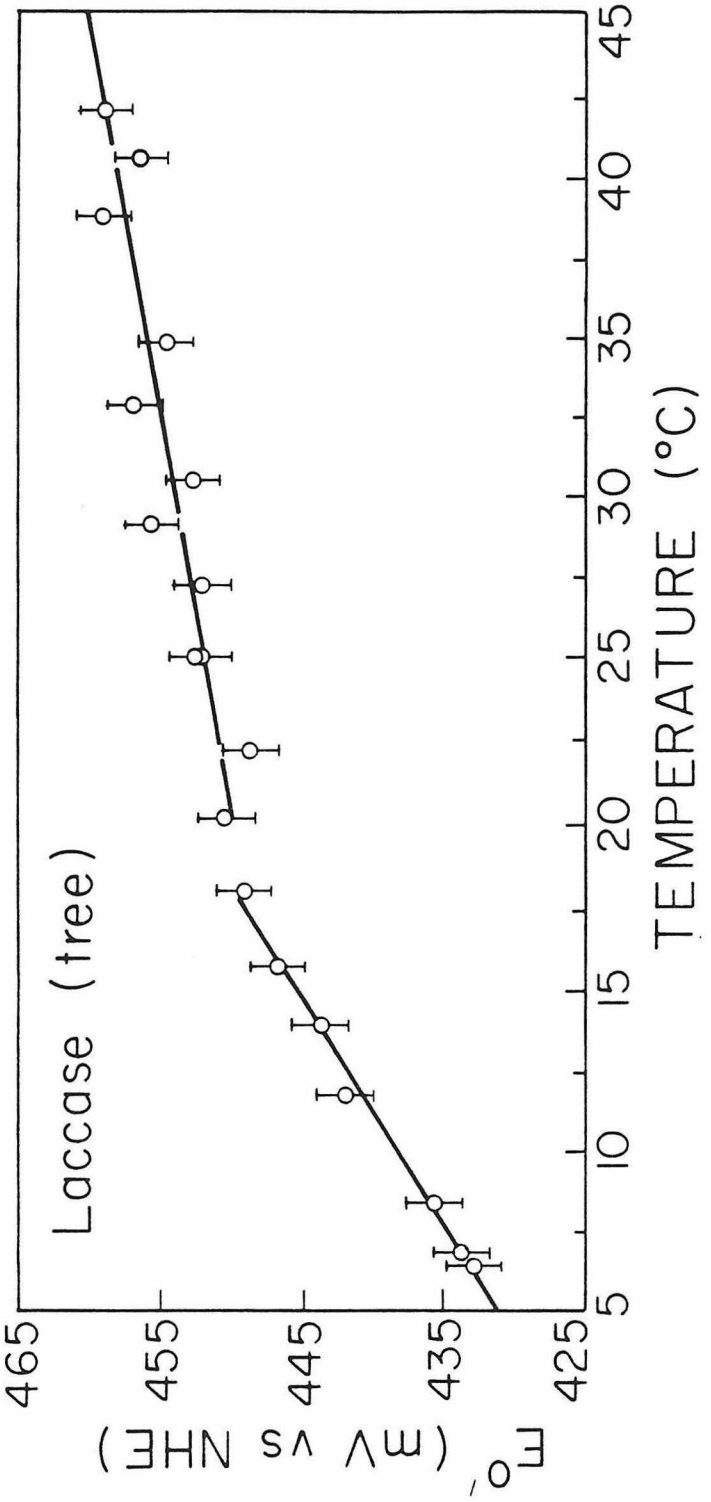
Laccase (tree)
$E^{o'}$ (mV vs NHE)
465
455
445
435
425
5
10
15
20
25
30
35
40
45
TEMPERATURE (°C)

25 ^{0}C of 452 mV and $(dE^{0\prime}/dT)_{25\ ^{0}C}$ = 4.18 x 10^{-4} V/^{0}C. The partial molal ionic entropy difference between the reduced and oxidized halves of the redox couple of interest (*i.e.*, the electron transfer reaction entropy, ΔS^{0}_{et}; ΔS^{0}_{rc}, the reaction entropy, has been used in the literature with the same meaning) is directly proportional to the temperature coefficient of the nonisothermal cell:[37-39]

$$\Delta S^{0}_{et} = S^{0}_{red} - S^{0}_{ox} = F \cdot (dE^{0}/dT)_{25\ ^{0}C}$$

where F is the Faraday constant. The value of $\Delta S^{0\prime}_{et}$ for the blue copper center in tree laccase is, therefore, calculated to be 9.6 ± 1.2 eu.

The transformation of the results from $E^{0\prime}$ *vs.* temperature (^{0}C) in Figure 8 to $\Delta G^{\prime}$ *vs.* temperature (^{0}K) is shown in Figure 9, and the value of $\Delta S^{0\prime}_{et}$ can be directly determined from the gradient of the straight-line plot.

The entropy for the complete cell reaction $\Delta S^{0\prime}$, adjusted to the NHE scale, is -6.0 ± 1.2 eu when a value of -15.6 eu is assumed for ΔS^{0}_{et} (NHE). The corresponding reaction enthalpy, $\Delta H^{0\prime}$, is -12.2 ± 0.4 kcal/mol, with $E^{0\prime}$ (25.0 ^{0}C) = 452 ± 2 mV.

In a similar manner, the 25 ^{0}C values of the thermodynamic parameters can be calculated by extrapolation from the temperature range 6.4 ~ 18.1 ^{0}C, giving $\Delta H^{0\prime}$ = -5.6 ± 0.4 kcal/mol, $\Delta S^{0\prime}$ = 16.9 ± 1.2 eu, add $\Delta S^{0\prime}_{et}$ = 32.5 ± 1.2 eu with $E^{0\prime}$ (extrapolated to 25 ^{0}C) = 459 ± 2 mV.

Figure 9. Temperature dependence of the Gibbs free energy change for the complete cell reaction of tree laccase. This is the result of transformating the data in Figure 8.

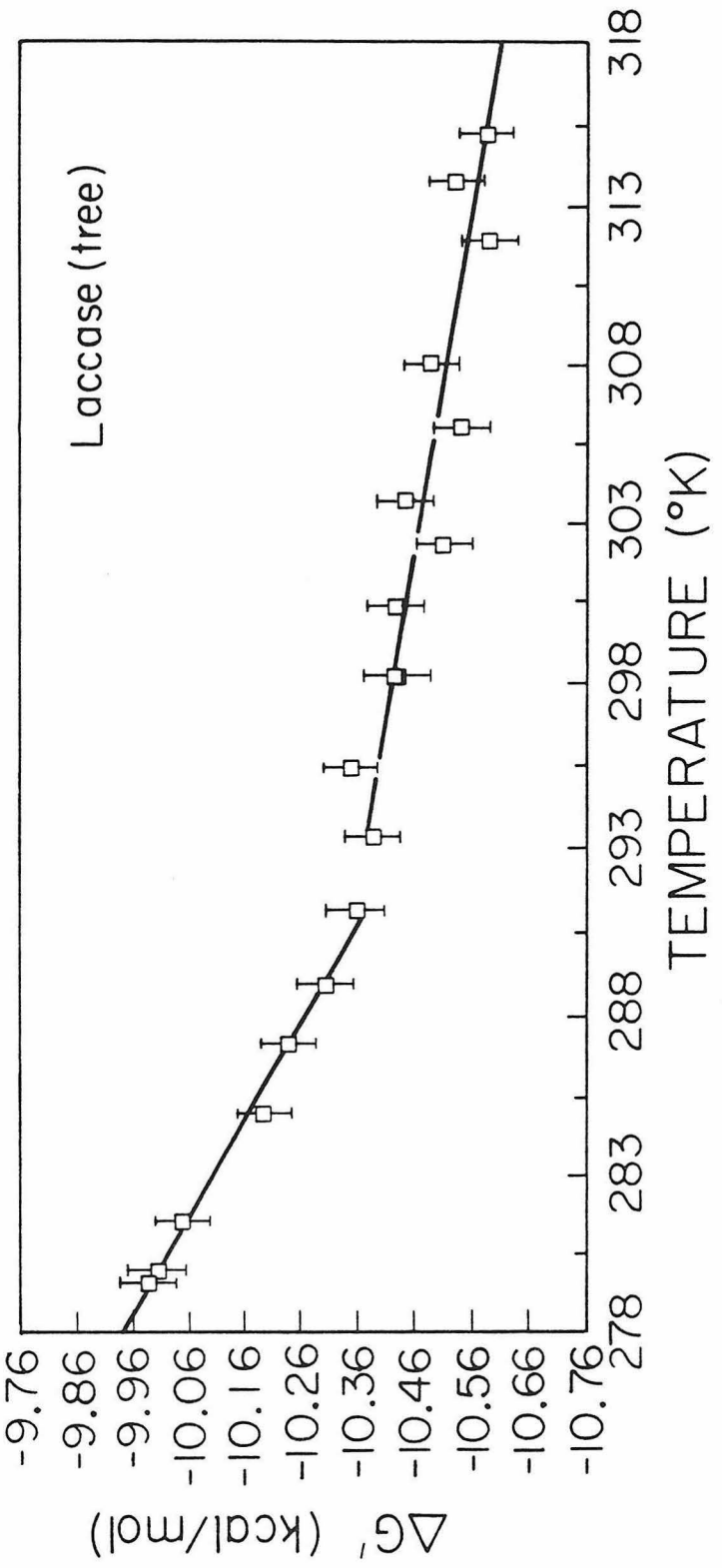
Laccase (tree)
ΔG' (kcal/mol)
-9.76
-9.86
-9.96
-10.06
-10.16
-10.26
-10.36
-10.46
-10.56
-10.66
-10.76
278
283
288
293
298
303
308
313
318
TEMPERATURE (°K)

The value of $\Delta S^{0'}_{et}$ for the type 1 copper center in tree laccase is the highest one known in the world of metalloenzymes. Hence, as shown in Tables 5, 6 and Figure 8, both the high value of $\Delta S^{0'}_{et}$, and also the two distinct thermodynamic behaviors shown by this blue copper site in different temperature ranges, are worthy of closer attention. There are only two other examples of systems having positive $\Delta S^{0'}_{et}$ values, and these values are small, *i.e.* 0.5 eu for *Rhodospirillum rubrum* cytochrome c', and 1.7 eu for type 1 copper of fungal laccase.

Fungal laccase is another blue copper containing oxidase which has received attention comparable to tree laccase. The type-1 copper center of this protein has also been studied by spectroelectrochemistry.[51] Table 7, Figure 10 as well as Table 5 summarize the electrochemical and thermodynamic properties of blue copper center in fungal laccase, respectively. Apparently, the most distinct difference between these two metalloenzymes is the huge difference of their redox potentials, as shown in Figure 11. However, there is no satisfactory explanation on this dramatic phenomenon.

In general, information about changes in solvation , conformation, and structural reorganization of the proteins, following the change from oxidized to reduced states, could be extracted from the data on $\Delta S^{0'}_{et}$. However, this kind of approach remains far from adequate for multisite enzymes. Many additional experiments, involving more subtle manipulations, such as active site binding with various foreign ligands, and site-depleted techniques, would be re-

Table 5. Thermodynamic parameters for metalloproteins.

Metalloprotein	$E^{0\prime}$ at 25 °C (mV vs. NHE)	$\Delta H^{0\prime}$ (kcal/mol)	$\Delta S^{0\prime}$ (eu)	$\Delta S_{et}^{0\prime}$ (eu)
Cytochrome c[38] (Horse Heart)	260	-14.5	-28.5	-12.9
Cytochrome c[49,50] (Tuna)	270	-13.9	-25.9	-10.3
Cytochrome c'[37] (*Rhodospirillum rubrum*)	39	-5.4	-15.1	+0.5
Cytochrome c'[37] (*Rhodopseudomonas Palus*tris)	95	-8.6	-21.1	-6.0
Cytochrome c_2[38] (*Rhodospirillum* rubrum)	324	-15.0	-25.2	-9.6
Cytochrome c_{551}[38] (*Pseudomonas aeruginosa*)	276	-15.9	-31.8	-16.2

Azurin[38] *(Pseudomonas aeruginosa)*	308	-16.6	-31.7	-16.1
Plastocyanin[38] *(Phaseolus vulgaris)*	360	-13.7	-18.0	-2.4
Stellacyanin[38] *(Rhus vernicifera)*	191	-10.3	-19.8	-4.2
Laccase[51] *(Polyporus versicolor)*	780	-22.1	-13.9	+1.7
Laccase* *(Rhus vernicifera)*	452	-12.2	-6.0	+9.6
HiPIP[38] *(Chromatium vinosum)*	352	-15.8	-25.5	-10.0
Myoglobin[52] (Sperm Whale)	60	-13.0	-39.2	-23.6
Hemoglobin[53,54]	160	-15.0	-38.0	-22

* This thesis work.

Table 6. Comparison of spectral, formal reduction potential, and other thermodynamic properties of some blue copper proteins.

Metalloproteins	λ_{max} of blue color (nm)	$\varepsilon_{\lambda_{max}}$ ($M^{-1}cm^{-1}$)	$E^{0'}$ at 25 °C (mV vs. NHE)	Coordination structure of blue copper site	$\Delta S^{0'}_{et}$ (eu)	$\Delta H^{0'}$ (kcal/mol)
Azurin (*Pseudomonas aeruginosa*)	625	5700	308 ± 2	$[Cu(N(His))_2S(Met)S(Cys)]$	-16.1 ± 1.2	-16.6 ± 0.4
Plastocyanin (*Phaseolus vulgaris*)	597	4500	360 ± 2	$[Cu(N(His))_2S(Met)S(Cys)]$	-2.4 ± 1.2	-13.7 ± 0.4
Stellacyanin (*Rhus vernicifera*)	604	4090	191 ± 2	Probably $[Cu(N(His))_2(S(Cys))_2]$	-4.2 ± 1.2	-10.3 ± 0.4
Laccase (*Rhus vernicifera*)	614	5700	452 ± 2	Unknown	9.6 ± 1.2 (32.5 ± 1.2)*	-12.2 ± 0.4 (-5.6 ± 0.4)*
Laccase (*Polyporus versicolor*)	610	4900	780 ± 3	Unknown	1.7 ± 2	-22.1 ± 0.5

*For tree laccase in the temperature range of 6.4 ~ 18.1 °C;
the number in parentheses is the one extrapolated to 25 °C.

Table 7. Temperature dependence of the formal reduction potentials, $E^{0\prime}$, for the blue copper ion in *Polyporus versicolor* (fungal) laccase, using nonisothermal thin-layer spectrochemistry. Solution conditions: pH = 5.4, 200 mM, phosphate buffer.

Temperature (^{0}C)*	$E^{0\prime}$ (mV vs. NHE)†
7.2	778
12.6	780
17.0	779
20.8	781
25.4	781
30.6	781
35.2	778
40.8	782

* ± 0.2 ^{0}C

† ± 2 mV

Figure 10. Temperature dependence of the formal reduction potentials, $E^{0\prime}$, for the type-1 copper center in fungal laccase *Polyporus versicolor*, using nonisothermal thin-layer spectroelectrochemistry. Solution conditions: pH 5.4, μ = 200 mM, phosphate buffer. Temperature range: 7.2 ~ 40.8 ^{0}C. A least squares fit of the data gave an $E^{0\prime}$ = 780 ± 2 mV at 25 ^{0}C and $(dE^{0\prime}/dT)_{25\ ^{0}C} = 6.13 \times 10^{-5}$ V/^{0}C.

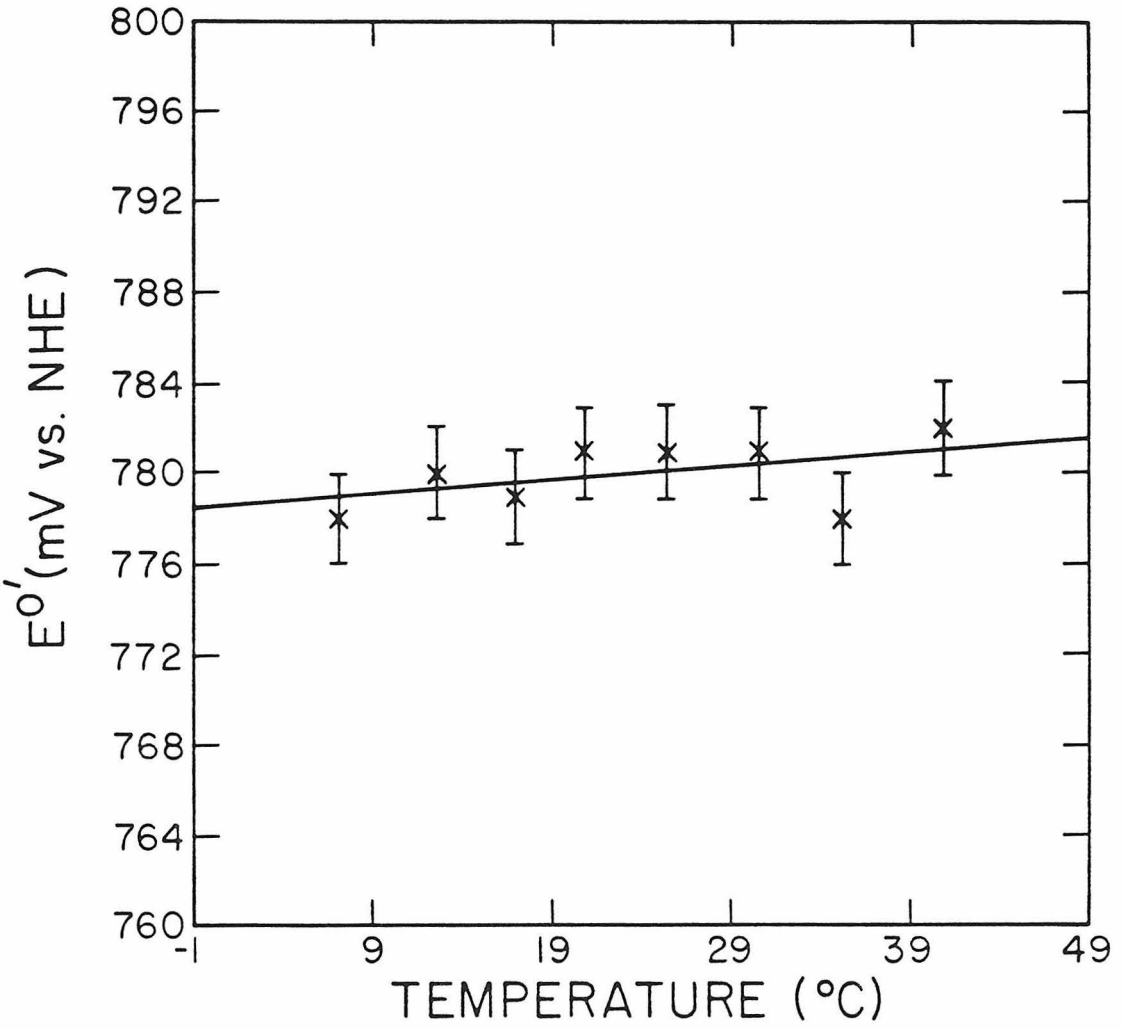
800
796
792
788
784
780
776
772
768
764
760
E°'(mV vs. NHE)
-1
9
19
29
39
49
TEMPERATURE (°C)

Figure 11. Temperature dependence of the formal reduction potentials, $E^{0\prime}$, for the type-1 copper centers in tree laccase *Rhus vernicifera* (Δ and O) and in fungal laccase *Polyporus versicolor* (X).

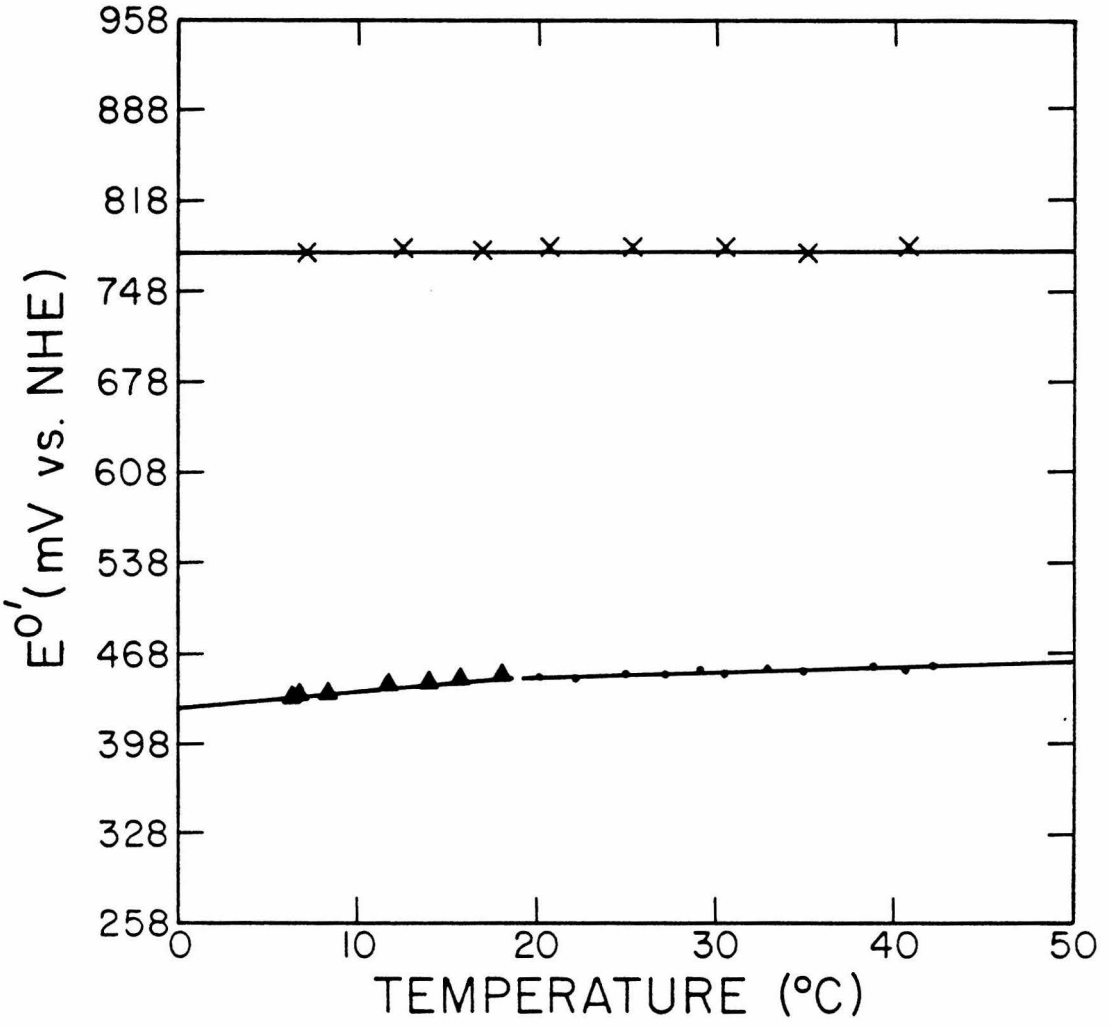
958
888
818
748
678
608
538
468
398
328
258
E°'(mV vs. NHE)
0
10
20
30
40
50
TEMPERATURE (°C)

quired in order to extract further crucial information concerning the mechanism of cooperation among different centers in multisite metalloenzymes.

There are two points I can make:

(1) Kinetic evidence suggests that the blue copper center in tree laccase is buried deep in the enzyme,[40] hence protein solvation effects play a much less important role than that of conformational change.

(2) The conformation of the polypeptide backbone of tree laccase is probably very much temperature dependent.

There are several experiments which would need to be done to make the whole picture more complete:

(1) A mediator dependence study of the formal reduction potential of the blue copper of tree laccase. Ferricyanide has been used intensively in the thermodynamic as well as kinetic studies of tree laccase. There is some evidence[11] however which shows that the cyano ligand of this complex will bind to the type 2 and type 3 copper ions. Obviously, the properties of these redox sites will be changed by the presence of this mediator. According to the criteria of choosing the mediator for spectroelectrochemical studies, ferricyanide is not a good choice for this purpose, at least for the studies of type 2 and type 3 copper ions. The redox couple $[Co(phen)_3]^{3+/2+}$ is a poten-

tial candidate for replacing ferricyanide. The formal reduction potential of $[Co(phen)_3]^{3+/2+}$ is *ca.* 401 mV *vs.* NHE[41] and the complex is known not to bind to the enzyme.

(2) A study of the temperature dependence of the blue copper redox potential of the type 2 depleted tree laccase. The type 2 copper displays an ESR spectrum typical of an axial Cu(II) complex,[7,11] and is accessible to solvent and small anions. A number of reports on the type 2 depleted enzyme have also appeared in the literature of tree laccase,[42-45] and using a slight modification of the method in Gray's laboratory has resulted in greater than 95% removal of the type 2 copper in tree laccase.[46] Recent NMR experiments indicate that type 2 copper stabilizes the tree laccase structure, so it would be of interest to study the blue copper redox thermodynamics of type 2 depleted tree laccase.

(3) Determination of the thermodynamic properties and formal reduction potential of type 3 copper pair.

References

1. Adman, E. T., in *Topics in Molecular and Structural Biology, Volume 6, Metalloproteins, Part 1: Metal Proteins with Redox Roles*, Harrison, P. M., ed., MacMillan Press, London, 1985, P. 1.

2. Reinhammar, B., in *Copper Proteins and Copper Enzymes*, Volume III, Lontie, R., ed., CRC Press, Boca Raton, 1984, P. 1.

3. Gray, H. B., and Solomon, E. I., in *Metal Ions in Biology, Volume 3, Copper Proteins*, Spiro, T. G., ed., Wiley, New York, 1981, P. 1.

4. Lappin, A. G., in *Metal Ions in Biological Systems, Volume 13, Copper Proteins*, Sigel, H., ed., Marcel Dekker, New York, 1981, P. 15.

5. Reinhammar, B., and Malmström, B. G., in *Metal Ions in Biology, Volume 3, Copper Proteins*, Spiro, T. G., ed., Wiley, New York, 1981, P. 109.

6. Beinert, H., *Coord. Chem. Rev.*, ***33***, 55 (1980).

7. Reinhammar, B., in *Advances in Inorganic Biochemistry*, Volume 1, Eichhorn, G. L., and Marzilli, L. G., eds., Elsevier, New York, 1979, P. 91.

8. Malmström, B. G., in *New Trends in Bio-inorganic Chemistry*, Williams, R. J. P., and Da Silva, J. R. R. F., eds., Academic Press, New York, 1978, p. 59.

9. Beinert, H., *Coord. Chem. Rev.*, ***23***, 119 (1977).

10. Holwerda, R. A., Wherland, A., and Gray, H. B., in *Annual Review of Biophysics and Bioengineering*, Volume 5, Mullins, L. J., ed., Annual Reviews Inc., Palo Alto, 1976, P. 363.

11. Fee, J. A., in *Structure and Bonding*, Volume 23, Dunitz, J. D., Hemmerich, P., Holm, R. H., Ibers, J. A., Jørgensen, C. K., Neilands, J. B., Reinen, D., and Williams, J. P., eds., Springer-Verlag, Berlin, 1975, P. 1.

12. Osterberg, R., *Coord. Chem., Rev.*, ***12***, 309 (1974).

13. Malkin, R., and Malmström, B. G., in *Advances in Enzymology and Related Areas of Molecular Biology*, Volume 33, Nord, F. F., ed., Wiley, New York, 1970, P. 177.

14. Gray, H. B., in *Advances in Inorganic Biochemistry, Volume 2, Methods for Determining Metal Ion Environments in Proteins: Structure and Function of Metalloproteins*, Darnall, D. W., and Wilkins, R. G., eds., Elsevier, New York, 1980, P. 1.

15. Malmström, B. G., *Pure Appl. Chem.*, ***24***, 393 (1970).

16. Malmström, B. G., and Vänngård, T., *J. Mol. Biol.*, ***2***, 118 (1960).

17. Cass, A. E. G., and Hill, H. A. O., in *Copper Proteins and Copper Enzymes*, Volume I, Lontie, R., ed., CRC Press, Boca Raton, 1984, P. 63.

18. Cass, A. E. G., and Hill, H. A. O., in *Ciba Foundation Symposium 79, Biological Roles of Copper*, Excerpta Medica, Amsterdam, 1980, P. 71.

19. Solomon, E. I., Hare, J. W., and Gray, H. B., *Proc. Natl. Acad. Sci. USA*, ***73***, 1389 (1976).

20. Guss, J. M., and Freeman, H. C., *J. Mol. Biol.*, ***169***, 521 (1983).

21. Colman, P. M., Freeman, H. C., Guss, J. M., Murata, M., Norris, V. A., Ramshaw, J. A. M., and Venkatappa, M. P., *Nature*, ***272***, 319 (1978).

22. Adman, E. T., and Jensen, L. H., *Isr. J. Chem.*, ***21***, 8 (1981).

23. Adman, E. T., Stenkamp, R. E., Sieker, L. C., and Jensen, L. H., *J. Mol. Biol.*, ***123***, 35 (1978).

24. Peisach, J., Levine, W. G., and Blumberg, W. E., *J. Biol. Chem.*, ***242***, 2874 (1967).

25. Hill, H. A. O., and Lee, W. K., *J. Inorg. Biochem.*, ***11***, 101 (1979).

26. Branden, R., Malmström, B., and Vänngård, T., *Eur. J. Biochem.*, ***36***, 195 (1973).

27. Dooley, D. M., Scott, R. A., Ellinghans, J., Solomon, E. I., and Gray, H. B., *Proc. Natl. Acad. Sci. USA*, ***75***, 3019 (1978).

28. Petersson, L., Ångström, J., Ehrenberg, A., *Biochim. Biophys. Acta*, ***526***, 311 (1978).

29. Reinhammar, B., Malkin, R., Jensen, P., Karlsson, B., André-asson, L.-E., Aasa, R., Vänngård, T., and Malmström, B. G., *J. Biol. Chem.*, ***255***, 5000 (1980).

30. Andréasson, L.-E., and Reinhammar, B., *Biochim. Biophys. Acta*, ***568***, 145 (1979).

31. Andréasson, L.-E., and Reinhammar, B., *Biochim. Biophys. Acta*, ***445***, 579 (1976).

32. The acetone powder extract of the latex of the Japanese lacquer tree can be ordered from:
Saito and Co., Ltd.
No. 9, Hommachi 1-chome
Higashi-Ku, Osaka
Japan

33. Reinhammar, B., *Biochim. Biophys. Acta*, ***205***, 35 (1970).

34. Kolthoff, I. M., and Tomsicek, W. J., *J. Phys. Chem.*, ***39***, 945 (1935).

35. Alexander, J. A., and Gray, H. B., *J. Am. Chem., Soc.*, ***90***, 4260 (1968).

36. Gray, H. B., and Beach, N. A., *J. Am. Chem. Soc.*, ***85***, 2922 (1963).

37. Taniguchi, V. T., Ellis, W. R., Jr., Cammarata, V., Webb, J., Anson, F. C., and Gray, H. B., in *Advances in Chemistry Series, No. 201, Electrochemical and Spectrochemical Studies of Biological Redox Components*, Kadish, K. M., ed., American Chemical Society, Washington, D. C., 1982, P. 51.

38. Taniguchi, V. T., Sailasuta-Scott, N., Anson, F. C., and Gray, H. B., *Pure and Appl. Chem.*, *52*, 2275 (1980).

39. Yee, E. L., Cave, R. J., Guyer, K. L., Tyma, P. D., and Weaver, M. J., *J. Am. Chem. Soc.*, ***101***, 1131 (1979).

40. Holwerda, R. A., and Gray, H. B., *J. Am. Chem. Soc.*, ***97***, 6063 (1975).

41. Farina R., and Wilkins, R. G., *Inorg. Chem.*, *7*, 514 (1968).

42. Graziani, M. T., Morpurgo, L., Rotilio, G., Mondovi, B., *FEBS Lett.*, ***70***, 87 (1976).

43. Morpurgo, L., Desideri, A., Rotilio, G., Mondovi, B., *FEBS Lett.*, ***113***, 153 (1980).

44. Morpurgo, L., Graziani, M. T., Agro, A. F., Rotilio, G., Mondovi, B., *Biochem.5 J.*, ***187***, 367 (1980).

45. Reinhammar, B., and Oda, Y., *J. Inorg. Biochem.*, ***11***, 115 (1979).

46. Dooley, D. M., unpublished results.

47. Nakamura, T., *Biochim. Biophys. Acta*, ***50***, 44 (1958).

48. Reinhammar, B. R. M., *Biochim. Biophys. Acta*, ***275***, 245 (1972).

49. Margalit, R., and Schejter, A., *Eur. J. Biochem.*, ***32***, 492 (1973).

50. Margalit, R., and Schejter, A., *FEBS Lett.*, ***6***, 278 (1970).

51. Taniguchi, V. T., Malmström, B. G., Anson, F. C., Gray, H. B., *Proc. Natl. Acad. Soc. USA*, ***79***, 3387 (1982).

52. Mayo, S. L., Ellis, W. R., Jr., Crutchley, R. J., and Gray, H. B., *Science*, ***233***, 948 (1986).

53. George, P., Hanania, G. I. H., and Eaton, W. A., in *Hemes and Hemoproteins*, Chance, B., Estabrook, R. W., and Yonetani, T., eds., Academic Press, New York, 1966, P. 267.

54. Hanania, G. I. H., Ph.D. Thesis, University of Cambridge, Cambridge, England, 1953.

CHAPTER IV

REDOX CHEMISTRY OF NATIVE, SINGLY, AND DOUBLY PENTAAMMINERUTHENIUM-MODIFIED BACTERIAL AZURIN

Introduction

Blue copper proteins are proteins containing a type I copper center, and have a characteristic intense absorption near 600 nm with a molar absorption coefficient per Cu(II) of 10^3 to 10^4 $M^{-1}cm^{-1}$.[1,2] They are also paramagnetic in the oxidized form, with an unusually small value of the parallel hyperfine splitting constant, $A_{||}$, in their EPR spectra.[1,2] Both of these properties are special to the di-valent copper in this class of protein and are quite atypical of simple inorganic Cu(II) complexes. The absorption coefficient of the blue copper center is some 100 times larger than that found for simple copper amino acid or peptide complexes. The EPR spectrum of the blue copper center in proteins is also characterized by having g-values similar to those of simple Cu(II) chelates, but with a value of the main hyperfine splitting constant, $A_{\perp}$, approximately one half of that found for the simple copper complexes.

Azurin, renamed by Sutherland and Wilkinson,[3] was originally reported as *Pseudomonas* blue protein[4] and was first isolated by Horio.[5] It can be isolated from a bacterial source, and acts as an electron transfer agent in the bacterial respiratory chain.[6-9] A long and intense study by Gray and co-workers on its electronic spectroscopy,[10-12] in addition to NMR,[13,14] EPR,[15] Resonance Raman,[16] Extended X-ray Absorption Fine Structure (EXAFS)[17,18] experiments and the reports of their crystal structures,[19,20] have now provided a solid foundation toward the understanding of this single copper me-

talloprotein. Figure 1 shows that the protein structure of azurin, based on X-ray crystallographic studies, has 8 strands of β-barrel with the sole copper ion located toward one end of the cylindrically shaped molecule. The copper coordination environment is close to tetrahedral, and from their known amino acid sequences four ligands have been identified. Two histidine nitrogens and a cystein sulfur have normal bond lengths and a fourth ligand appears to be a sulfur-coordinated methionine. The intense blue color is accounted for by an S^-(Cys) $\longrightarrow$ Cu(II) charge transfer transition in this protein, whereas the unusual EPR properties are explained by the distortion of the Cu(II) ligand environment away from planarity.[21]

In recent years, there has been much interest in the mechanism of electron transfer involving metalloproteins.[22-33] A novel approach to this study consists of modifying or labelling metalloproteins with redox-active inorganic complexes and measuring kinetic and thermodynamic parameters for intramolecular electron transfer between the inorganic label and the native metal site in the protein interior.

Pseudomonas aeruginosa azurin,[6-9] a bacterial protein, has been the main focus for these long-range electron transfer studies involving blue copper. It consists of a single polypeptide chain of 128 amino acid residues and has a molecular weight of around 14,600 daltons. It contains, in total, four histidines —— His-35, His-46, His-83, and His-117 —— in which His-46 and His-117 are coordinated to the copper center. His-35 is buried in the protein interior near

Figure 1. The folding of the polypeptide backbone in azurin with the copper ion, coordinating ligands, and histidine residues indicated. This ribbon drawing was constructed from computer plots of the atomic coordinates in azurin, based on X-ray crystallographic results.

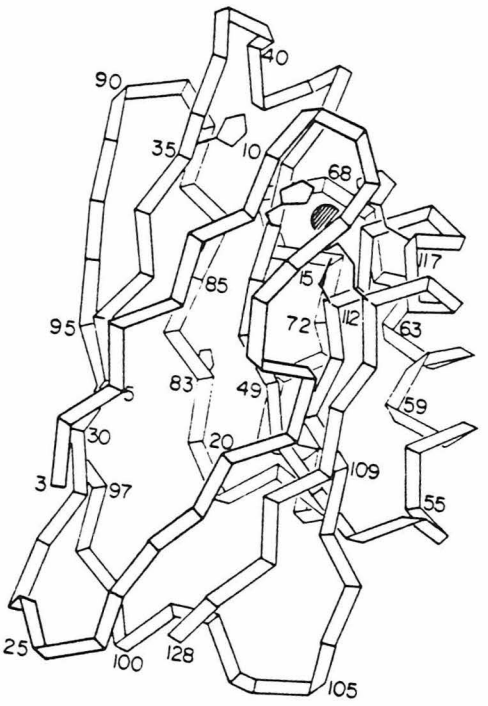
90
40
35
10
68
117
85
15
95
72
112
63
83
49
59
30
20
3
97
109
55
25
100
128
105

the blue copper site, and appears to be inaccessible to labelling. On the other hand, His-83 is exposed at the protein surface, providing an attractive site for modifier binding.

The reaction of $[Ru(NH_3)_5(OH_2)]^{2+}$ with azurin[27] is outlined in Scheme 1,[24] and produces two ruthenated products, (a_5Ru)-Az and $(a_5Ru)_2$-Az where "a" stands for NH_3. The (a_5Ru)-Az has been characterized, by peptide mapping experiments (scheme 2),[24] as $[Ru(NH_3)_5$(His-83)]-azurin, a protein which has been singly-modified at the imidazole ring of His-83. However, $(a_5Ru)_2$-Az has not been fully characterized. The absorption spectrum of the isolated $[Ru(NH_3)_5$(His-83:peptide)$]^{3+}$ fragment is virtually the same as the spectrum of an independently characterized $[Ru(NH_3)_5(His)]^{3+}$ model complex. Figure 2 illustrates the absorption spectra of these two species, respectively.

Figure 3 shows the cross-sectional view along selected parts of $[a_5Ru^{III}$(His-83)]-Az(Cu^{II}).[29] The edge-to-edge distance between the two electron tansfer sites is 11.8 Å. Tables 1 and 2 list the thermodynamic and spectroscopic data, respectively,[27] which show that the blue copper site is not perturbed by the presence of the $[a_5Ru(His\text{-}83)]^{3+}$ group. The ruthenated protein is ideally structured for a long-range electron transfer experiment. Selective reduction of the surface-accessible $[a_5Ru(His\text{-}83)]^{3+}$ group will produce $[a_5Ru^{II}$(His-83)]-Az(Cu^{II}). If the experiments are done at very low protein concentrations, then the electron transfer should be intramolecular. Scheme 3 illustrates the kinetic results, from flash

Scheme 1. Preparation and purification scheme of pentaammineruthenium modified azurins.

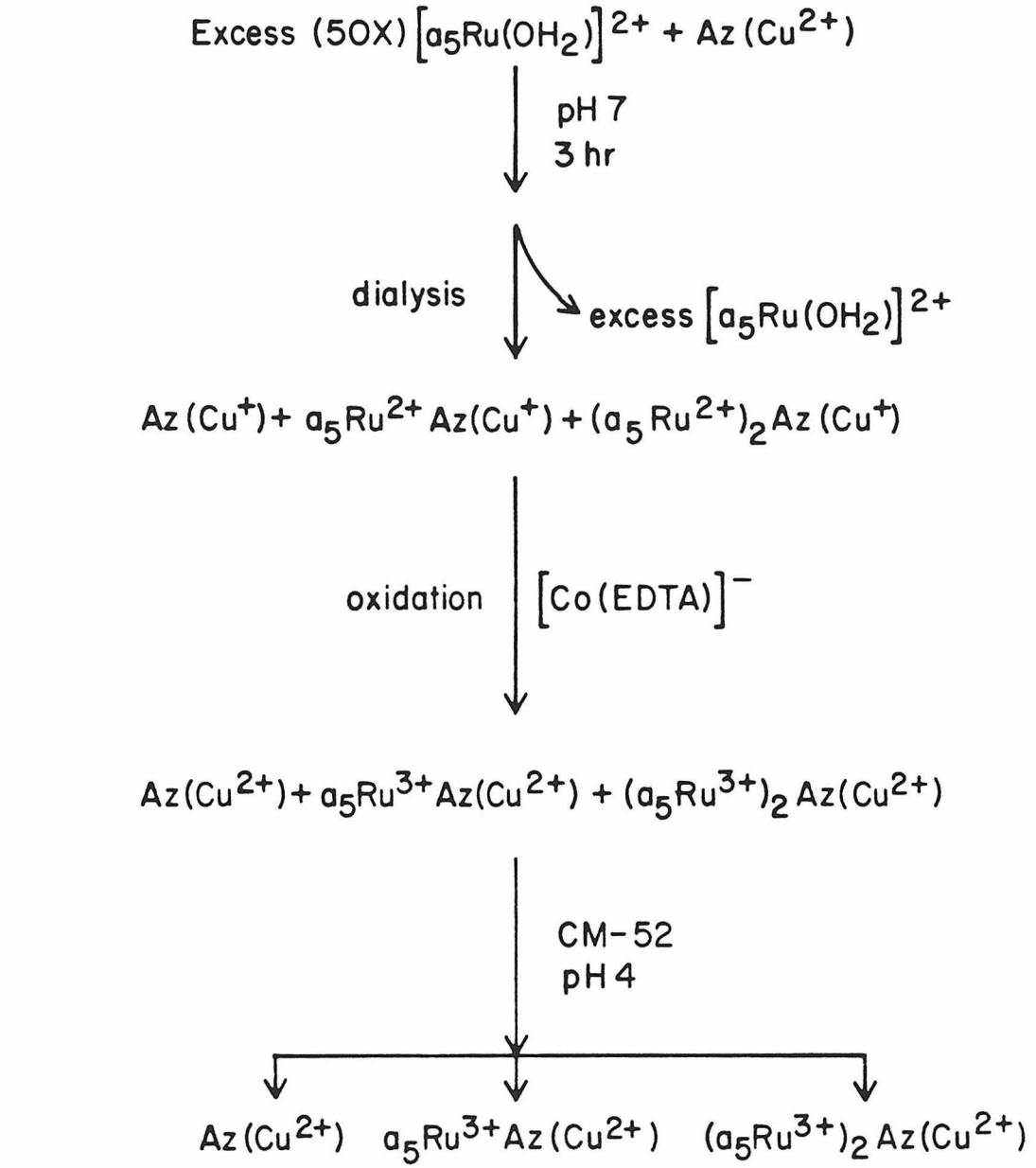

yield (%)	35	31	12
pI	5.4	7.2	8.2

Scheme 2. Peptide mapping of $[Ru^{III}(NH_3)_5(His\text{-}83)]$-Az($Cu^{II}$).

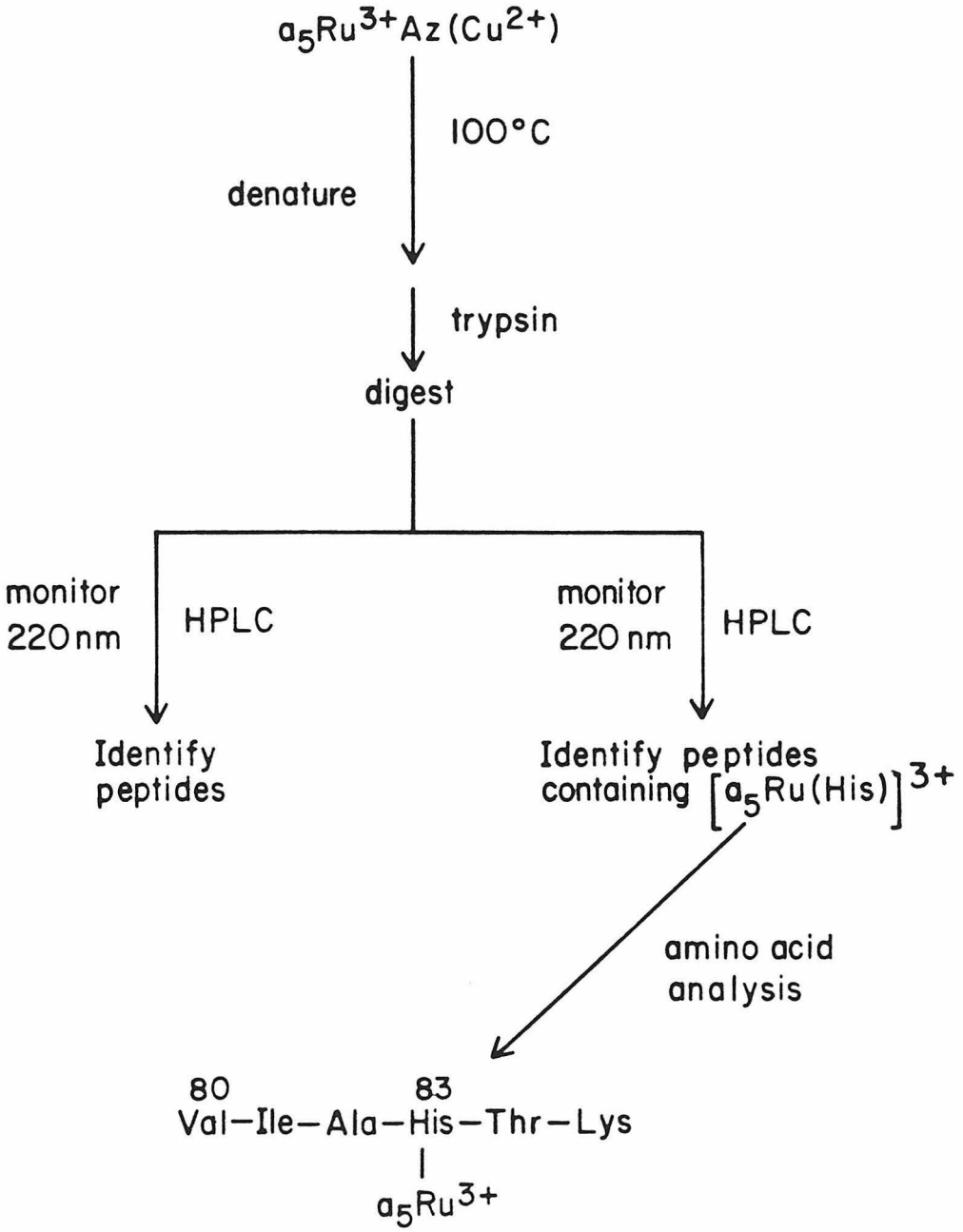
$a_5Ru^{3+}Az(Cu^{2+})$
100°C
denature
trypsin
digest
monitor 220nm
HPLC
Identify peptides
monitor 220 nm
HPLC
Identify peptides containing $[a_5Ru(His)]^{3+}$
amino acid analysis
80
83
Val–Ile–Ala–His–Thr–Lys
a_5Ru^{3+}

Figure 2. Absorption spectra of (A) the hexapeptide containing His-83, *i.e.*, Val-Ile-Ala-His-Thr-Lys, obtained by tryptic hydrolysis of the modified azurin and HPLC separation of the resulting peptide, and (B) a 0.3 mM aqueous solution of $[Ru(NH_3)_5(His)]Cl_3$.

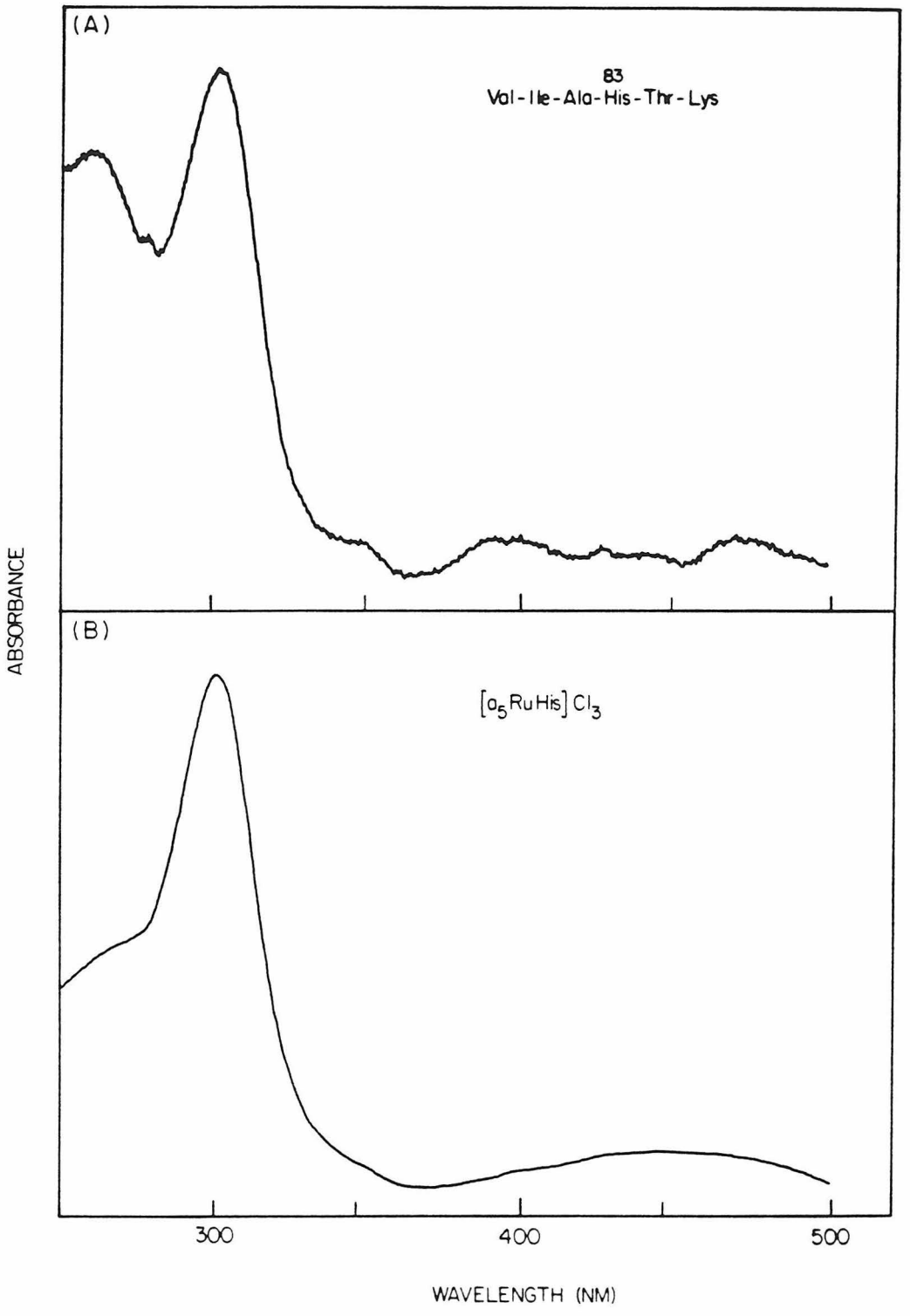
(A)
83
Val-Ile-Ala-His-Thr-Lys
(B)
[o_5RuHis] Cl_3
ABSORBANCE
300
400
500
WAVELENGTH (NM)

Figure 3. View of selected parts of the molecular skeleton of azurin, with a_5Ru^{III}-bonded to the imidazole of His-83. The copper ligands are His-46, Cys-112, His-117, and Met-121. The edge-to-edge distance between the two electron transfer units, *i.e.*, $[a_5Ru(His\text{-}83)]^{3+}$ group and the blue copper center, is 11.8 Å. The distance was calculated from N1 of the imidazole of His-83 to S of Cys-112.

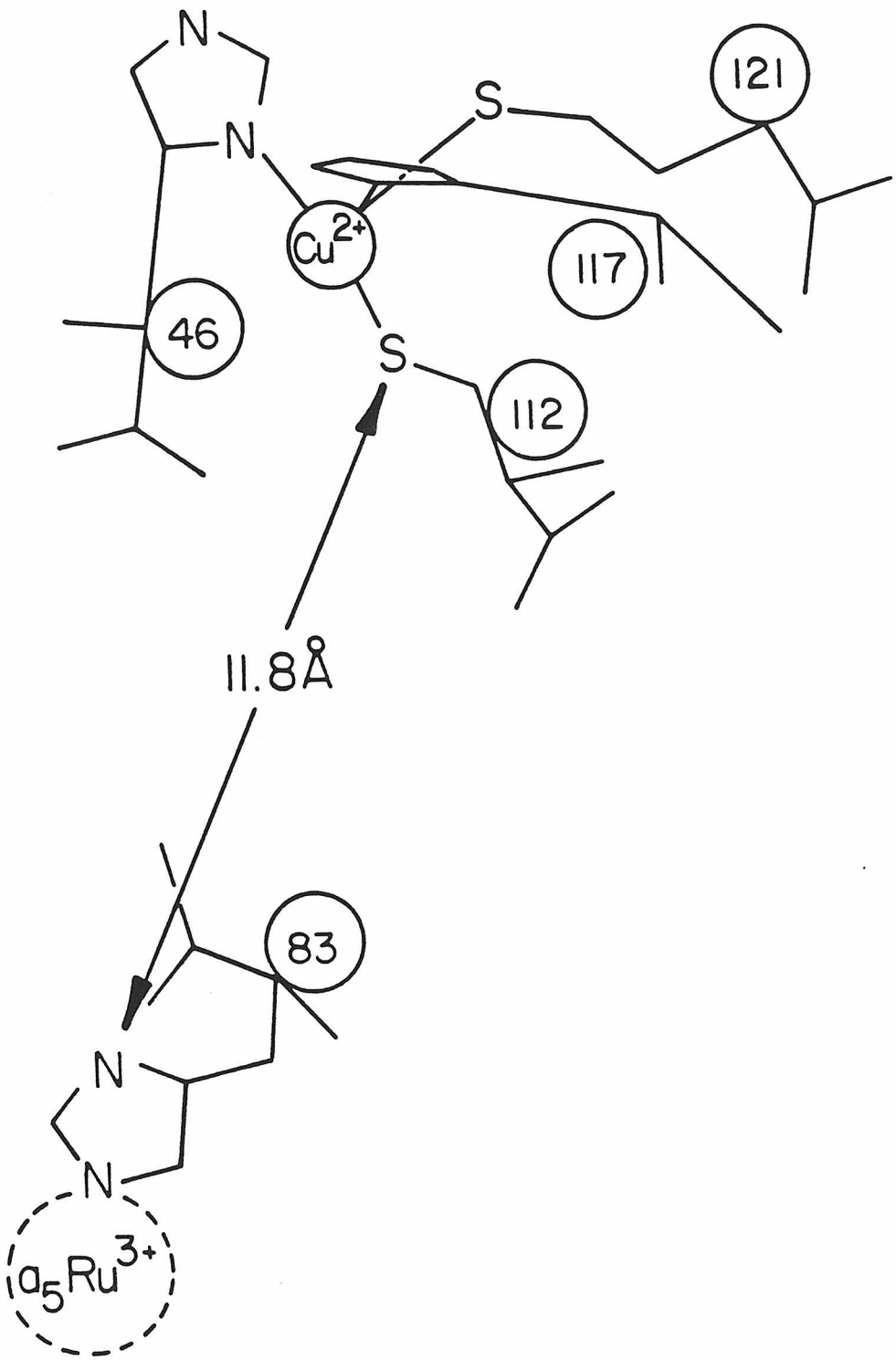
N
N
S
121
Cu2+
117
46
S
112
11.8Å
83
N
N
a5Ru3+

Table 1. Thermodynamic parameters for the reduction of $[a_5Ru(His)]^{3+}$ and the blue-copper, Cu^{II}, in native and pentaammineruthenium modified azurins. Solution conditions: pH 7.0, μ = 100 mM, phosphate buffer.

Thermodynamic parameter	Native Az($Cu^{2+/1+}$)	[a_5Ru(His-83)$^{3+}$-Az($Cu^{2+/+}$)	[a_5Ru(His)]$^{3+/2+}$
$E^{0\prime}$ (mV vs. NHE)	308 ± 2	320 ± 2	80 ± 5
$\Delta S^{0\prime}$ (eu)	-31.7 ± 1.2	-26.8 ± 1.2	-3.4 ± 2
$\Delta S^{0\prime}_{ct}$ (eu)	-16.1 ± 1.2	-11.2 ± 1.2	12.2 ± 2
$\Delta G^{0\prime}$ (kcal/mol)	-7.10 ± 0.05	-7.39 ± 0.05	-1.96 ± 0.12
$\Delta H^{0\prime}$ (kcal/mol)	-16.6 ± 0.4	-15.4 ± 0.4	-3.0 ± 0.8

Table 2. Spectroscopic properties of the blue-copper sites in native and pentaammineruthenium modified azurins.

Spectroscopy	Parameter (Cu^{II})	Native Az	$[a_5Ru^{III}$(his-83)]-Az(Cu^{II})
EPR	$g_{\|\|}$	2.271	2.271
	$a_{\|\|}$(G)	57	57
	g_x	2.065	2.065
	g_y	2.043	2.044
Resonance Raman	$\nu(cm^{-1})$ [CuN_2SS^*]	369	370
		404	404
		424	425

Scheme 3. The scheme of flash kinetic spectrometry used in the study of the intramolecular long-range electron transfer reaction in $[a_5Ru^{III}(His\text{-}83)]\text{-}Az(Cu^{II})$.

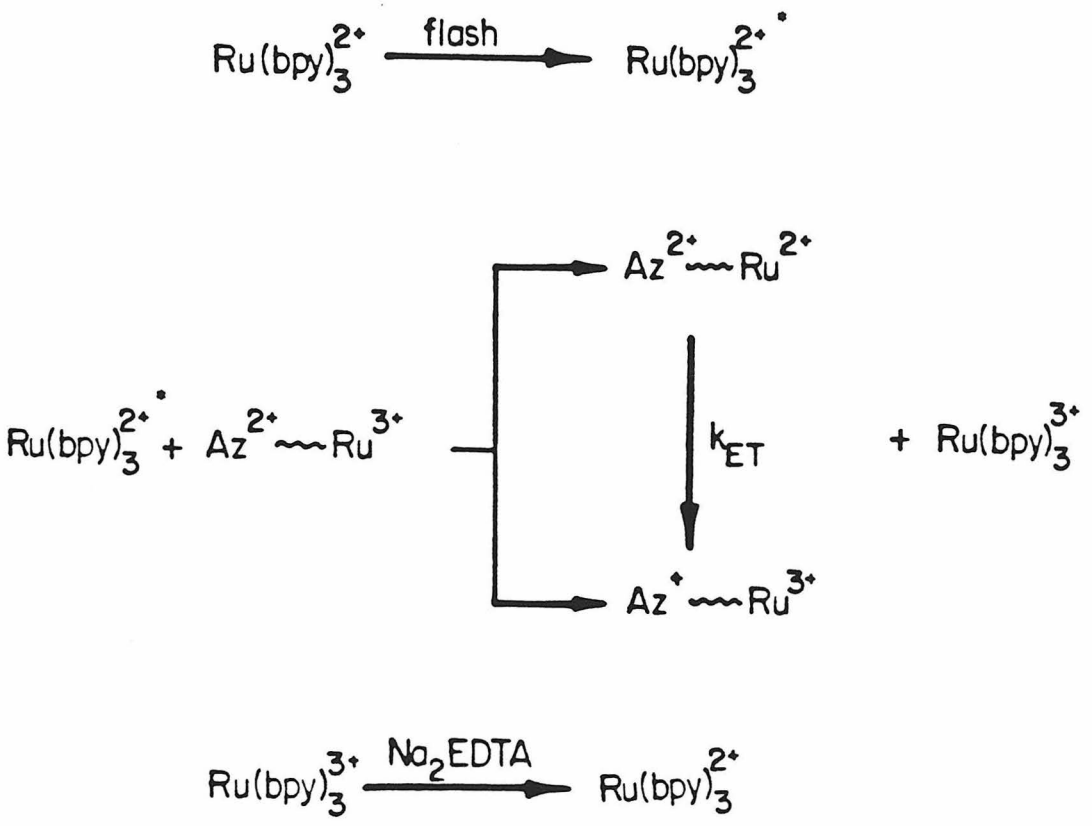
Ru(bpy)3 2+ flash Ru(bpy)3 2+*
Ru(bpy)3 2+* + Az 2+ ~ Ru 3+
Az 2+ ~ Ru 2+
kET
Az + ~ Ru 3+
+ Ru(bpy)3 3+
Ru(bpy)3 3+ Na2EDTA Ru(bpy)3 2+

photolysis experiments, of the following intramolecular electron transfer reaction:

$$[a_5Ru(His\text{-}83)]^{2+}\text{-}Az(Cu^{2+}) \longrightarrow [a_5Ru(His\text{-}83)]^{3+}\text{-}Az(Cu^{+})$$

Strict first-order kinetics are observed, yielding a rate constant of 1.9 s^{-1} that is temperature-independent from -8 to 53 ^{0}C,[29] as demonstrated in Figure 4.

The intramolecular long-range electron transfer kinetics of pentaammineruthenium modified azurins have also been investigated as a function of pH ranging from 5.0 to 9.0. Figures 5 and 6 show the pH-dependence of the electron transfer rate constant, k_{et}, for (a_5Ru)-Az and $(a_5Ru)_2$-Az, respectively. As shown in Figure 5, k_{et} of (a_5Ru)-Az, *i.e.*, $[a_5Ru(His\text{-}83)]$-Az, has been found to vary with pH. However, k_{et} of $(a_5Ru)_2$-Az demonstrates pH-independent behavior, as depicted in Figure 6.

Materials and Methods

All the native as well as the singly and doubly modified azurins were prepared by Dr. Nenad M. Kostić. *Pseudomonas aeruginosa* azurin, obtained from the Public Health Laboratory Service in England, has an A_{280}/A_{625} ratio of 1.72. Trypsin, treated with L-1-tosylamido-2-phenylethyl chloromethyl ketone, and cyanogen bromide were obtained from Worthington and Pierce Chemical Co., respectively. Ampholine

Figure 4. (A) First-order kinetic plot for the reduction of Cu^{II} in flash-generated $[a_5Ru^{II}(His\text{-}83)]\text{-}Az(Cu^{II})$ at 23 ^0C, and (B) temperature dependence of the rate constant for long-range $Ru^{II} \longrightarrow Cu^{II}$ electron transfer.

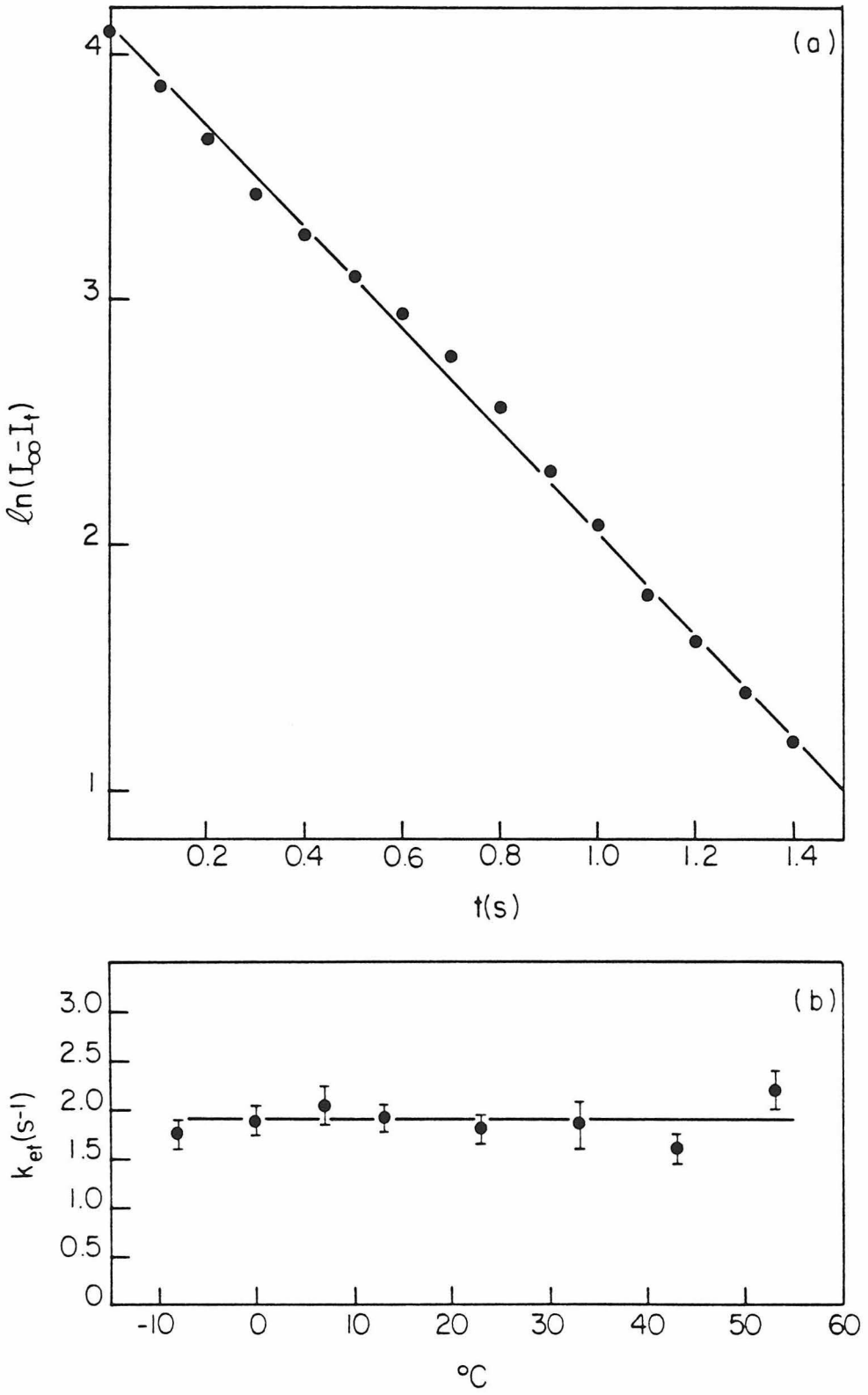
(a)
4
3
2
1
ℓn(I∞-It)
0.2
0.4
0.6
0.8
1.0
1.2
1.4
t(s)
(b)
3.0
2.5
2.0
1.5
1.0
0.5
0
kef(s-1)
-10
0
10
20
30
40
50
60
°C

Figure 5. The pH-dependence of the rate constant for long-range $Ru^{II} \longrightarrow Cu^{II}$ intramolecular electron transfer reaction in $[a_5Ru^{II}(His\text{-}83)]\text{-}Az(Cu^{II})$ at 23 ^{0}C.

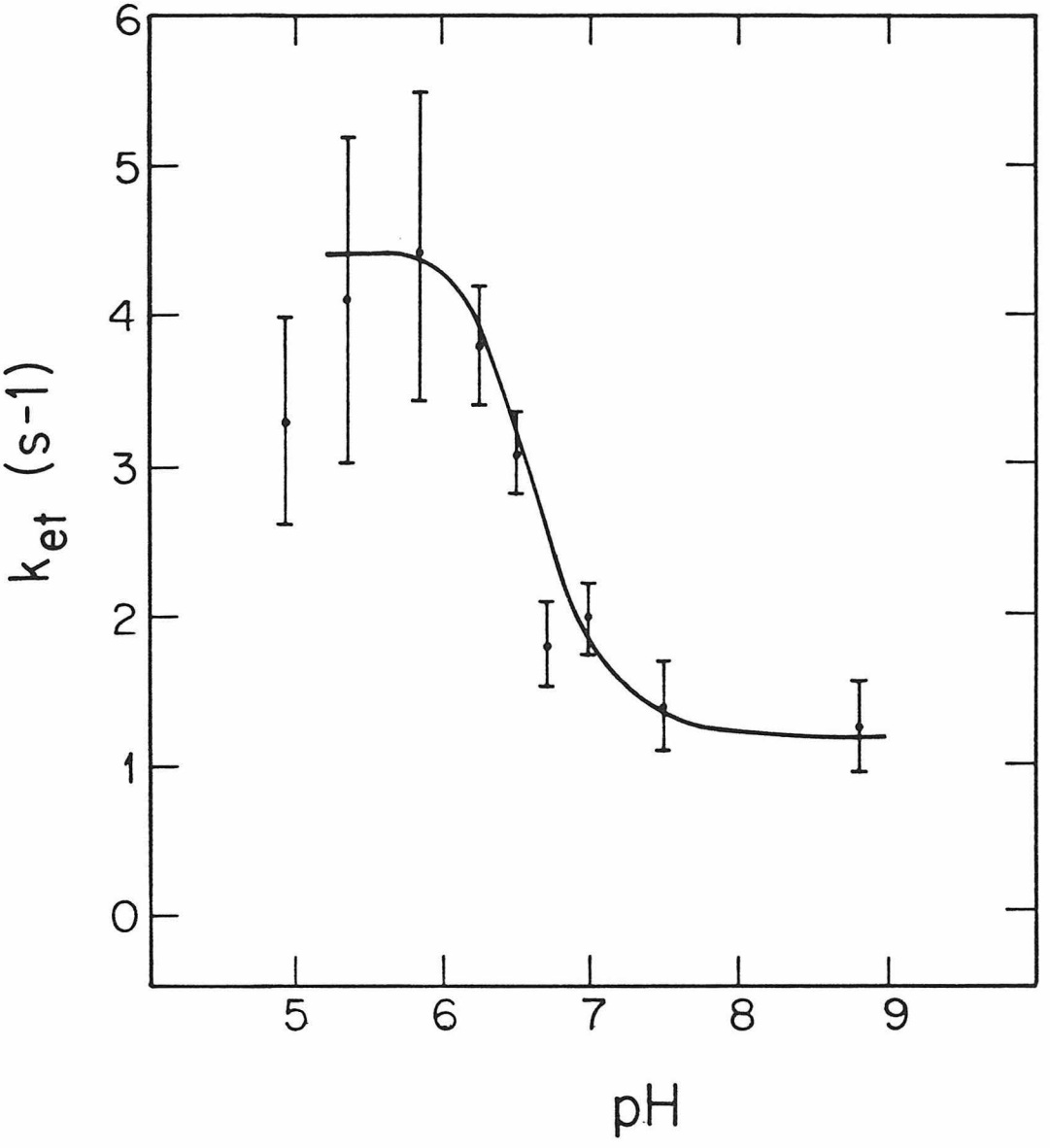
6
5
4
3
2
1
0
k_{et} (s-1)
5
6
7
8
9
pH

Figure 6. The pH-dependence of the rate constant for long-range $Ru^{II} \longrightarrow Cu^{II}$ intramolecular electron transfer reaction in $(a_5Ru^{II})_2$-Az(Cu^{II}) at 23 ^{0}C.

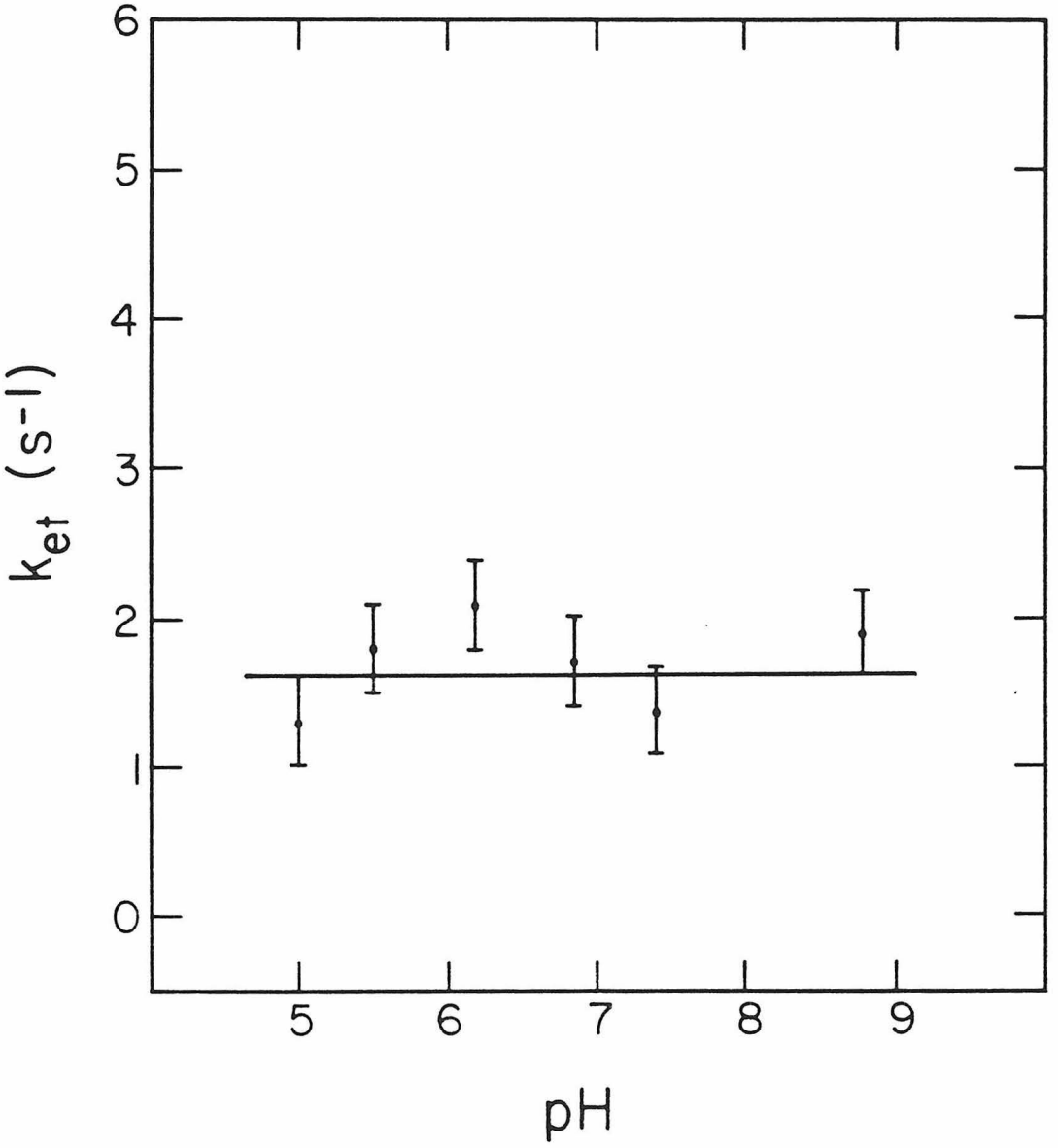
6
5
4
3
2
1
0
k_{et} (s-1)
5
6
7
8
9
pH

plates for isoelectric focusing (IEF) in the pH range 3.5 ~ 9.5 were obtained from LKB. Column chromatography of the modified azurin was carried out with Whatman CM-52 cellulose. $[a_5Ru(OH_2)](PF_6)_2$ was prepared according to a published procedure[35] with one slight modification (Na_2CO_3 was used instead of $BaCO_3$).[36] The complex $[a_5Ru(py)](ClO_4)_3$, was prepared as described previously.[37] Deionized water from a Barnstead NANOpure water purifier was employed in the preparation of all protein and buffer solutions. Ultrafiltration was performed with Amicon YM-5 membranes, under argon, with gentle stirring at 5 ^{0}C.

Azurin was allowed to react with a 50-fold excess of freshly prepared $[a_5Ru(OH_2)](PF_6)_2$, under argon, at room temperature, in 50 mM tris•HCl buffer (pH 7.2) for 3 hours. In a typical experiment, a deaerated solution of 27 mg of the ruthenium reagent in tris buffer was added anaerobically to a deaerated solution of 14 mg of azurin in the same buffer. The reaction mixture was deaerated briefly by evacuation and left under a constant pressure of argon, although argon gas was not permitted to bubble directly through the solution. The total volume was 10 ml, so that the concentration of the protein was 0.1 mM and of the ruthenium reagent, 5 mM. Small variations in the reagent ratio, concentrations, pH, or reaction time did not affect the properties of the modified protein and affected the yields only slightly. To stop the reaction, the ruthenium reagent was removed by repeated ultrafiltration of the reaction mixture into water or, 50 mM NH_4OAc buffer (pH 4.0). A solution of *ca.* 15 mg of

Na[Co(EDTA)] *ca.* 15-fold excess with respect to both Cu and Ru, in *ca.* 1 ml of either water or the NH_4OAc buffer, *ca.* 15-fold excess with respect to both Cu and Ru, was added to oxidize the concentrated protein. The oxidation was allowed to proceed for several hours in the unbuffered solution, or overnight in the NH_4OAc buffer. The oxidant was then removed by ultrafiltration into the pH 4.0 acetate buffer. Recovery of the protein from the reaction was 98 ~ 100%.

All three components of the reaction mixture were separated efficiently by cation-exchange chromatography on a column of CM-52 cellulose, previously equilibrated with pH 4.0, 50 mM NH_4OAc buffer. The separation was carried out at room temperature and the elution rate was *ca.* 100 ml/hr. The first fraction was eluted quickly with 50 mM buffer and elution with this buffer continued until the second band reached the bottom of the column. This second fraction was then eluted with pH 4.0, 75 mM NH_4OAc buffer. The third fraction, which had remained near the top of the column, was then eluted with 150 mM NaCl solution in pH 4.0, 50 mM NH_4OAc buffer. The average yields are follows: first fraction, 4.0 mg or 27%, second fraction, 4.9 mg or 34%, and third fraction, 2.7 mg or 18%, and the isoelectric points, *i.e.*, pI values in pH units, are the following: first fraction, 5.4, second fraction, 7.2, and third fraction, 8.1. The pI values did not change after exhaustive dialysis by ultrafiltration. When the labelling reaction was allowed to proceed for 5 ~ 7 hours, the yield of third fraction increased to *ca.* 28%, whereas the yield of second fraction decreased to *ca.* 22%.

Procedures for tryptic hydrolysis, separation of the resulting peptides by reversed-phase HPLC, and amino acid analysis[27,33] were used with minor modifications. A sample containing 5 ~ 6 mg of the second fraction, in 2 ml of water, was denatured by placing the sample in boiling water for 4 minutes prior to tryptic hydrolysis. The linear gradient for the HPLC separation of the tryptic peptides consisted of 45 ml each of phosphate buffer (49 mM KH_2PO_4/5.4 mM H_3PO_4, pH 2.85) and acetonitrile, the concentration of the latter increasing from 0% to 45%, the elution rate was 1 ml/min. The absorbance values were recorded at 220 nm, *i.e.*, the peptide bonds, and at 300 nm, which is near the absorption maximum, 303 nm, of $[a_5Ru(His)]^{3+}$.[38]

All peptide mapping experiments were performed in parallel on third fraction and native azurin. Protein samples were hydrolyzed by trypsin or by cyanogen bromide, CNBr. The solution of the denatured protein was 25 mM in NH_4HCO_3 and had a pH of 7.8. At the beginning of the digestion and again after 5 hours, 50 ml portions of a solution containing 2 mg trypsin per ml were added.

For hydrolysis by CNBr, 3 mg of the third fraction in 1.5 ml of water, were lyophilized to dryness and the residue dissolved in 1 ml of 70% HCOOH. A small lump of CNBr was added and the reaction allowed to proceed at room temperature in the dark for 16 hours. The sample was then diluted with 10 ml of water and lyophilized to dryness. Homoserine lactone was converted to homoserine by a published procedure.[39] A 1.8 mg sample of the protein, which had

been treated with CNBr, was dissolved in 0.5 ml of a 100 mM solution of pyridine in acetic acid at pH 6.48. The solution was heated in a sealed evacuated tube at 100 ^{0}C for one hour, the solvent then removed by an air stream at 40 ^{0}C, and the residue dissolved in 0.1 ml of 0.1% aqueous DF_3COOH. The HPLC separation of peptide was carried out in a similar manner to that of the second fraction. The phosphate buffer and the CH_3CN solutions were prepared using 0.1% aqueous CF_3COOH instead of pure water. Absorbance of the eluent was monitored at 220, 270, or 300 nm in different separations.

Formal reduction potentials at different temperatures, for native as well as singly and doubly pentaammineruthenium modified azurins, were determined at pH 7.0, 6.0, and 5.0 by using an optically transparent thin-layer electrode (OTTLE) cell in a non-isothermal configuration. The details of this methodology have been described in Chapter II. Five equivalents of $[a_5Ru(py)](ClO_4)_3$ was added to all the protein solutions as mediator-titrant. The OTTLE cell employed a gold minigrid as the working electrode, and optical path length was 0.48 mm. Potentials were applied across the thin-layer cell by using a Princeton Applied Research model 174A polarographic analyzer, and were accurately measured with a Keithley model 177 microvolt digital multimeter. The cell temperature was varied by using a variable temperature cell holder, and measured directly with an Omega Engineering precision microthermocouple connected to a Fluke model 2175A digital thermometer. The end of the thermocouple was placed in the protein solution in close proximity to the thin-layer

cavity. All visible spectra were obtained with a Cary 219 recording spectrophotometer.

Formal reduction potentials were determined by sequentially applying a series of potentials, $E_{appl.}$, to the gold minigrid electrode. Each potential was maintained until electrolysis ceased, so that the equilibrium value of the ratio of concentrations of oxidized to reduced forms of all redox couples in solution, [Ox]/[Red], was established as defined by the Nernst equation. Redox couples were incrementally converted from one oxidation state to the other by the series of applied potentials, for which each corresponding value of [Ox]/[Red] was determined from the spectra. Formal reduction potentials and n values were determined from plots of $E_{appl.}$ *vs.* log([Ox]/[Red]).

All solutions were deoxygenated prior to use by vacuum/argon cycling on a vacuum/purified-argon double manifold, and loaded into the OTTLE cell by using rubber septum caps and syringe techniques. The platinum wire auxiliary electrode was situated in a compartment containing deoxygenated mediator-titrant solution that was isolated from protein solution by a porous glass frit.

Results and Discussion

Pseudomonas aeruginosa azurin contains four histidines and six methionines per molecule. Because His-46, His-117, and Met-121 are coordinated to the copper atom, two histidines and five methionines

are potential sites of covalent binding to the a_5Ru-group.

In the case of the second fraction, since only the peptide that eluted at *ca.* 12 ml in the HPLC of the trypic hydrolyzate absorbs significantly at 300 nm, we concluded that only this peptide fragment contains an $[a_5Ru(His)]^{3+}$ unit, as shown in Figure 2, indicating that labelling takes place at a histidine residue in this particular protein fraction. The amino acid analysis also showed this peptide fragment to contain valine, isoleucine, alanine, histidine, threonine, and lysine, a composition that fits exactly the segment 80 ~ 85 of *Pseudomonas aeruginosa* azurin.[39] We conclude that a pentaammineruthenium group is attached to the imidazole ring of His-83. This Ru-N bond in $[a_5Ru(His\text{-}83)]$-Az is evidently not affected by denaturation of the sample at 100 ^{0}C, nor by the conditions under which tryptic hydrolysis is carried out.

The structure of azurin, [19,20] as shown in Figure 1, reveals that the imidazole of His-83 is located on the surface of the protein and protrudes into the surrounding medium. This exposure makes the imidazole easily accessible to the labelling reagent in solution. Several aspartic acid and glutamic acid residues are found in the vicinity of His-83, their negative charges presumably facilitate the attack of $[a_5Ru(OH_2)]^{2+}$ at His-83. The N1 atom in the imidazole ring of His-83 and the S atom of Cys-112 are 11.8 Å apart. Figure 3 shows the view of selected parts of the molecular skeleton of this modified azurin.

In the case of the third fraction, the tryptic peptide whose

composition corresponded to the segment 80 ~ 85 of *Pseudomonas aerugionsa* azurin exhibited strong absorbance at 300 nm, characteristic of the $[a_5Ru(His)]^{3+}$ chromophore. This establishes that the imidazole-bound a_5Ru-label is located at His-83 as in the singly-modified azurin described above.[27] The peptide whose composition corresponded to the segment 28-41 of the protein exhibited no absorbance at 300 nm. This evidence rules out a_5Ru-binding to His-35, the only histidine other than His-83 that is not coordinated to the copper atom. The two histidines bound to copper are not labelled, as evidenced by the UV-VIS, EPR, and resonance Raman spectra of the blue copper site.

Attempts to directly detect ruthenium bonded to a methionine side chain were unsuccessful.[40] The $[a_5RuS(CH_3)_2]^{3+/2+}$ complexes absorb appreciably ($\varepsilon \leqq 1{,}000\ M^{-1}\ cm^{-1}$) only at wavelengths lower than 290 nm,[41] where the absorbance due to the protein itself is overwhelming ($\varepsilon \leqq 10{,}000\ M^{-1}\ cm^{-1}$). For this reason, chromatograms of the corresponding tryptic peptides from native azurin and from the third fraction are very similar to each other. Next we turned to CNBr, a methionine-specific hydrolysis reagent. We first established that $[a_5RuS(CH_3)_2]$ is stable under the conditions used for hydrolysis and HPLC separation. Experiments with CNBr were based on the expectation that the ruthenium label should retard cleavage at the methionine to which it is bound. Although the CNBr did cleave at all the methionine residues in both native azurin and the third fraction, this cleavage was less than complete for both proteins so that no re-

tardation could be found. No conclusion about possible labelling of methionine could be drawn from the peptide-mapping experiments. A molecule of *Pseudomonas aeruginosa* azurin contains six methionine residues, one of which, Met-112, is coordinated to the copper atom. Of the remaining five, four are located near the protein surface and probably are accessible to $[a_5Ru(OH_2)]^{2+}$. The reduction potential of blue copper in native *Pseudomonas aeruginosa* azurin, and its temperature dependence, were investigated spectroelectrochemically in pH 7.0, 100 mM phosphate buffer.[42] Table 3 and Figure 7 summarize the electrochemical data of this experiment. In this chapter, formal reduction potentials and their temperature dependence of native azurin at pH 6.0 (Table 4, Figure 8), and at pH 5.0, (Table 5, Figure 9); of $[a_5Ru(His\text{-}83)]$-Az at pH 7.0 (Table 7, Figure 11), and at pH 5.0 (Table 8, Figure 12); as well as of $(a_5Ru)_2$-Az at pH 7.0 (Table 10, Figure 14) and at pH 5.0 (Table 11, Figure 15) have been presented. The phosphate buffer was used at pH 7.0 and at pH 6.0, however, acetate buffer was used instead at pH 5.0. In every case, the ionic strength was maintained at 100 mM.

The redox potentials and thermodynamic parameters of native azurin (Figure 10, Table 6), of $[a_5Ru(His\text{-}83)]$-Az (Figure 13, Table 9), and of $(a_5Ru)_2$-Az (Figure 16, Table 12) at pH 7.0, 6.0, and 5.0 have also been summarized, respectively. From these comparative plots, we can observe that the redox potentials become more positive as the pH values of protein solutions get lower. This phenomenon can be understood in terms of simple electrostatics. When the acidity of

Table 3. Temperature dependence of the formal reduction potentials, $E^{0\prime}$, for the blue-copper ion in *Pseudomonas aeruginosa* azurin, using nonisothermal thin-layer spectroelectrochemistry. Solution conditions: pH 7.0, μ = 100 mM, phosphate buffer.

Temperature (^{0}C)*	$E^{0\prime}$ (mV vs. NHE)†
6.8	320
10.5	319
10.9	319
15.1	318
16.1	313
20.0	312
24.9	309
25.0	309
30.3	303
35.2	300
40.8	299

* ± 0.2 ^{0}C

† ± 2 mV

Figure 7. Temperature dependence of the formal reduction potential, $E^{0\prime}$, for the type-1 copper center in *Pseudomonas aeruginosa* azurin, using nonisothermal thin-layer spectroelectrochemistry. Solution conditions: pH = 7.0, μ = 100 mM, phosphate buffer. Temperature range: 6.8 ~ 40.8 ^{0}C. A least squares fit of the data gave an $E^{0\prime}$ = 308 ± 2 mV at 25.0 ^{0}C and $(dE^{0\prime}/dT)_{25\ ^{0}C}$ = -7.00 x 10^{-4} V/^{0}C.

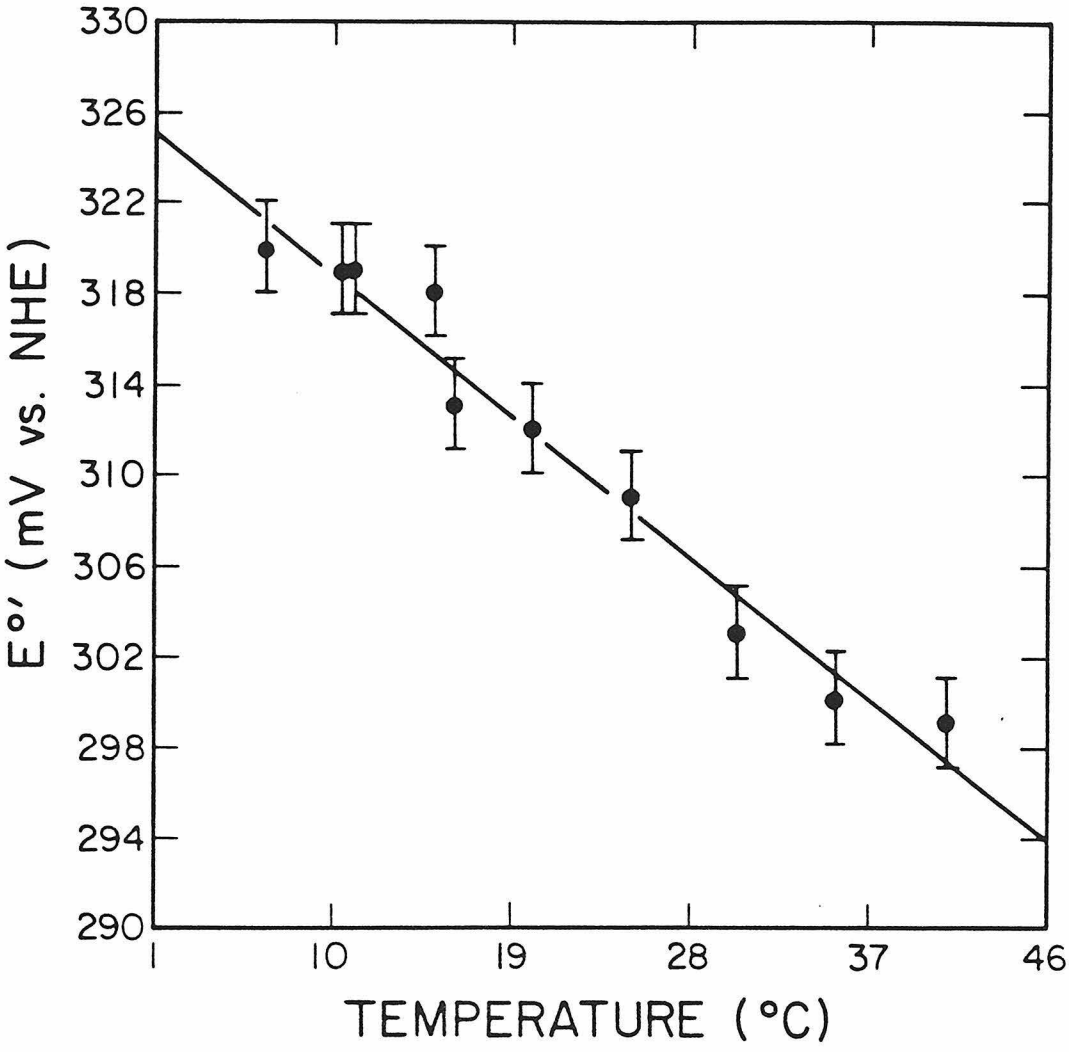
330
326
322
318
314
310
306
302
298
294
290
E°' (mV vs. NHE)
1
10
19
28
37
46
TEMPERATURE (°C)

Table 4. Temperature dependence of the formal reduction potentials, $E^{0\prime}$, for the blue-copper ion in *Pseudomonas aeruginosa* azurin, using nonisothermal thin-layer spectroelectrochemistry. Solution conditions: pH 6.0, μ = 100 mM, phosphate buffer.

Temperature (^{0}C)*	$E^{0\prime}$ (mV vs. NHE)†
3.9	333
9.7	329
15.2	327
20.2	324
25.0	325
30.2	320
34.2	318
41.6	316

* ± 0.2 ^{0}C

† ± 2 mV

Figure 8. Temperature dependence of the formal reduction potential, $E^{0\prime}$, for the type-1 copper center in *Pseudomonas aeruginosa* azurin, using nonisothermal thin-layer spectroelectrochemistry. Solution conditions: pH = 6.0, μ = 100 mM, phosphate buffer. Temperature range: 3.9 ~ 41.6 ^{0}C. A least squares fit of the data gave an $E^{0\prime}$ = 323 ± 2 mV at 25.0 ^{0}C and $(dE^{0\prime}/dT)_{25\ ^{0}C}$ = -4.44 x 10^{-4} V/^{0}C.

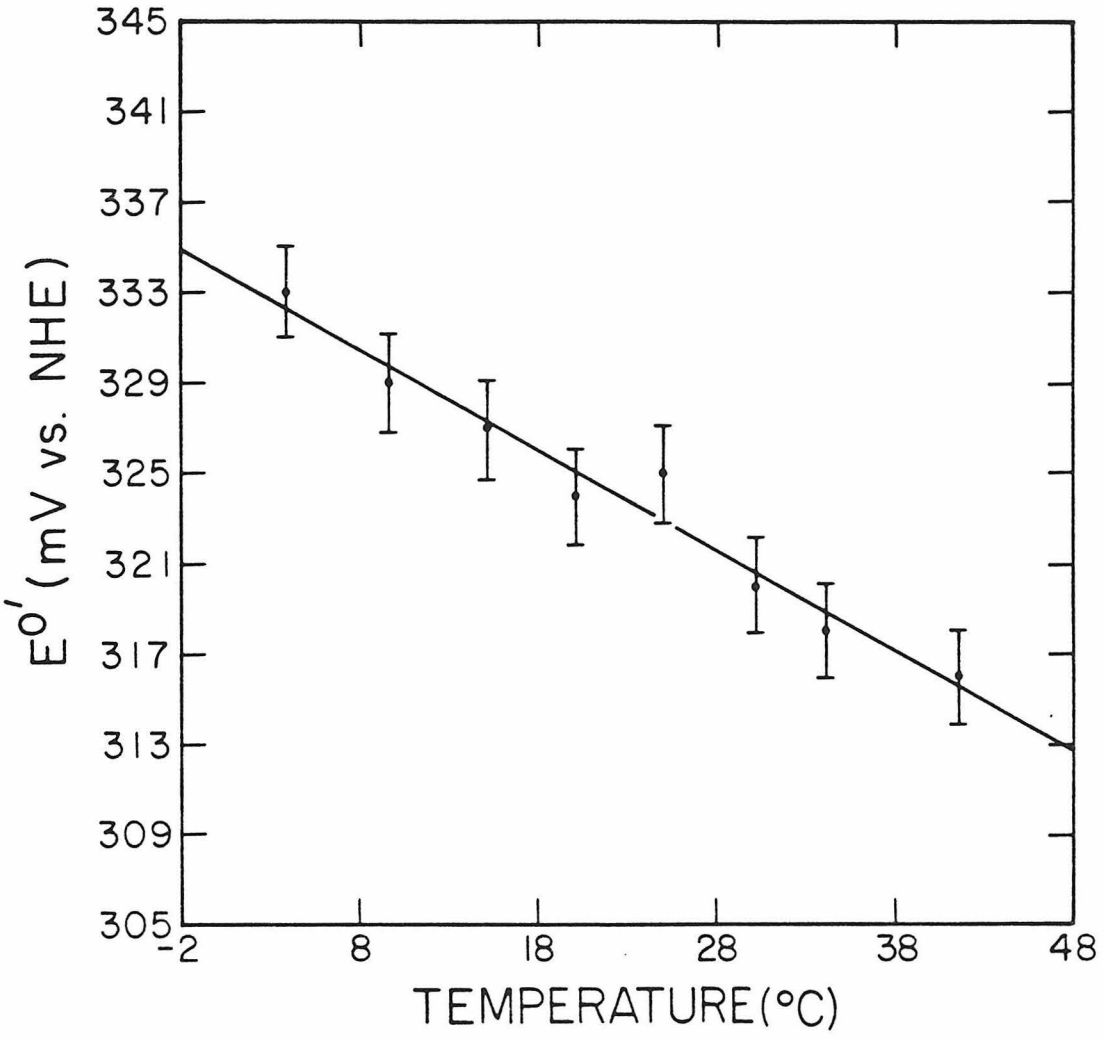
345
341
337
333
329
325
321
317
313
309
305
E°' (mV vs. NHE)
-2
8
18
28
38
48
TEMPERATURE (°C)

Table 5. Temperature dependence of the formal reduction potentials, $E^{0\prime}$, for the blue-copper ion in *Pseudomonas aeruginosa* azurin, using nonisothermal thin-layer spectroelectrochemistry. Solution conditions: pH 5.0, μ = 100 mM, acetate buffer.

Temperature (^{0}C)*	$E^{0\prime}$ (mV vs. NHE)†
3.3	363
9.6	365
10.6	359
15.3	362
17.8	368
19.8	364
22.8	369
25.4	372
28.8	372
32.3	374
35.2	376
40.2	376

* ± 0.2 ^{0}C

† ± 2 mV

Figure 9. Temperature dependence of the formal reduction potential, $E^{0\prime}$, for the type-1 copper center in *Pseudomonas aeruginosa* azurin, using nonisothermal thin-layer spectroelectrochemistry. Solution conditions: pH = 5.0, μ = 100 mM, acetate buffer. Temperature range: 3.3 ~ 40.2 ^{0}C. A least squares fit of the data gave an $E^{0\prime}$ = 370 ± 2 mV at 25.0 ^{0}C and $(dE^{0\prime}/dT)_{25\ ^{0}C}$ = 4.66 x 10^{-4} V/^{0}C.

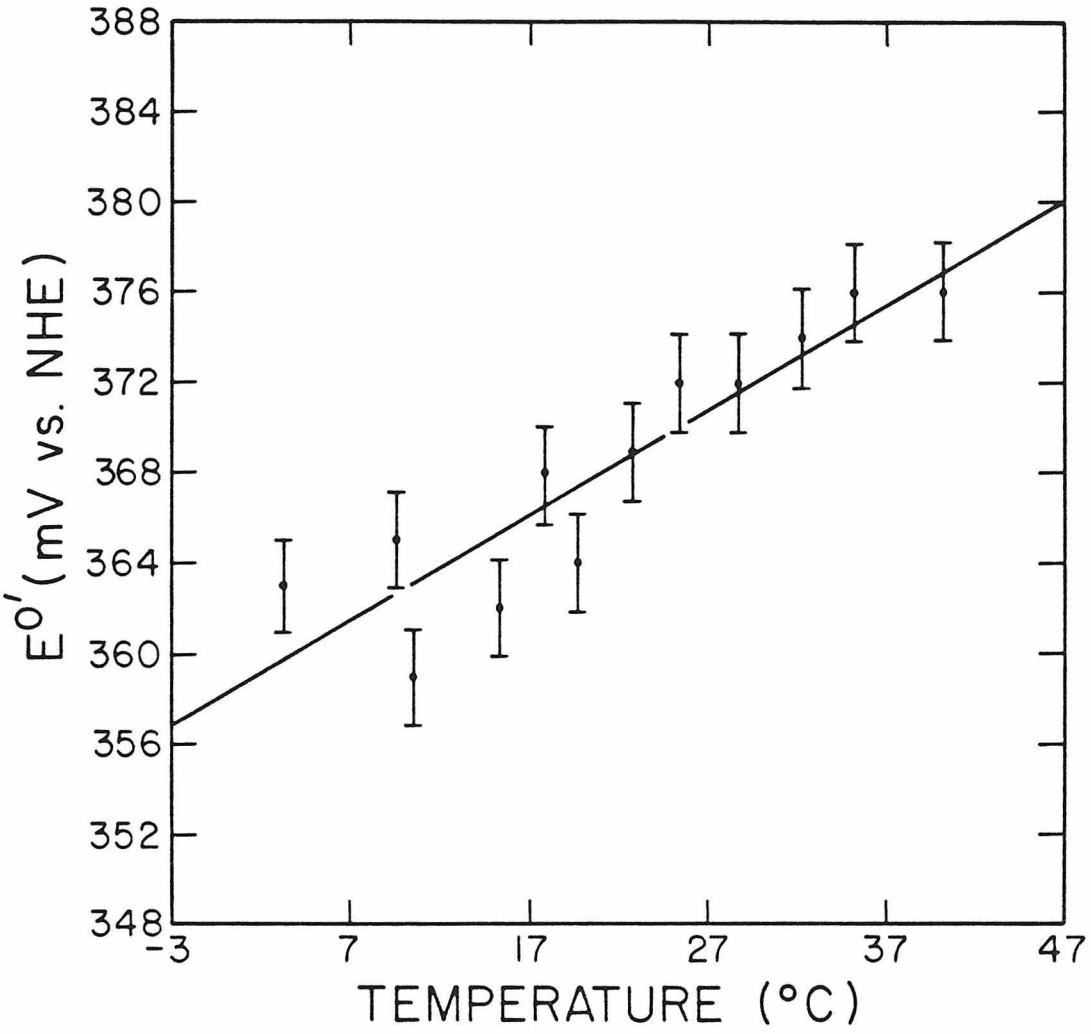
388
384
380
376
372
368
364
360
356
352
348
E°' (mV vs. NHE)
-3
7
17
27
37
47
TEMPERATURE (°C)

Figure 10. Temperature dependence of the formal reduction potential, $E^{0\prime}$, for the type-1 copper center in *Pseudomonas aeruginosa* azurin at pH 7.0 (Δ), at pH 6.0 (•), and at pH 5.0 (X). Solution conditions: μ = 100 mM, phosphate buffer (pH 6.0, pH 7.0) or acetate buffer (pH 5.0), 5 equivalents $[Ru(NH_3)_5(py)](ClO_4)_3$.

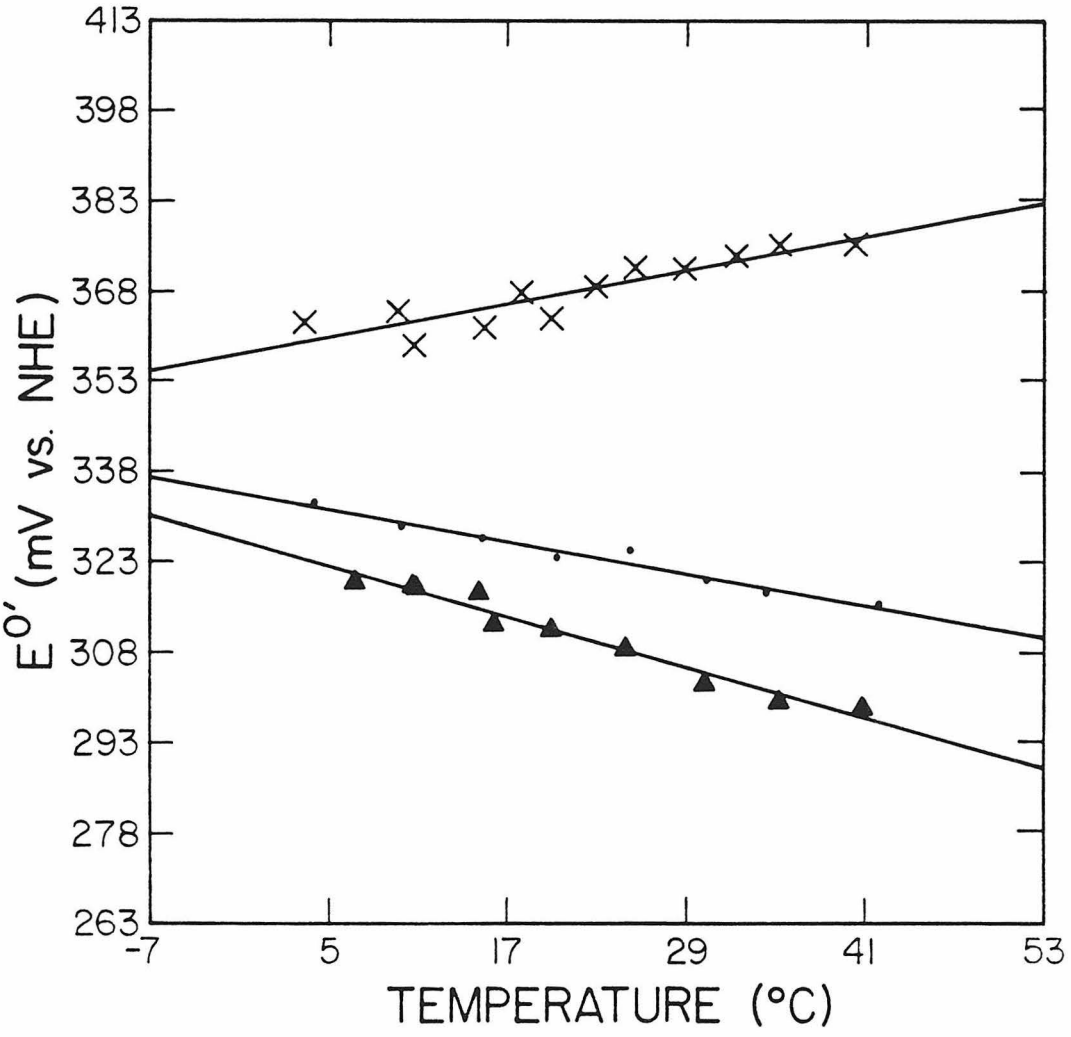
413
398
383
368
353
338
323
308
293
278
263
E°' (mV vs. NHE)
-7
5
17
29
41
53
TEMPERATURE (°C)

Table 6. Thermodynamic parameters for the reduction of the type-1 blue-copper center in native *Pseudomonas aeruginosa* azurin at three pH values. Solution conditions: μ = 100 mM, phosphate buffer (pH 6.0, pH 7.0), acetate buffer (pH 5.0), 25 ^{0}C.

	Native Az pH 7.0, 0.1 M Phosphate	**Native Az pH 6.0, 0.1 M Phosphate**	**Native Az pH 5.0, 0.1 M Acetate**
$E^{0\prime}$ at 25 ^{0}C (mV vs. NHE)	308	323	370
$\Delta S^{0\prime}$ (eu)	-31.7	-25.8	-4.9
$\Delta S^{0\prime}_{et}$ (eu)	16.1	-10.2	10.7
$\Delta G^{0\prime}$ (kcal/mol)	-7.10	-7.45	-8.53
$\Delta H^{0\prime}$ (kcal/mol)	-16.6	-15.2	-10.0

Table 7. Temperature dependence of the formal reduction potentials, $E^{0\prime}$, for the blue-copper ion in $[Ru(NH_3)_5(His\text{-}83)]$-azurin from *Pseudomonas aeruginosa*, using nonisothermal thin-layer spectroelectrochemistry. Solution conditions: pH 7.0, μ = 100 mM, phosphate buffer.

Temperature (^{0}C)*	$E^{0\prime}$ (mV vs. NHE)†
6.6	330
9.8	330
15.5	322
20.7	322
25.0	315
30.0	323
34.7	318
40.2	311

* ± 0.2 ^{0}C

† ± 2 mV

Figure 11. Temperature dependence of the formal reduction potential, $E^{0\prime}$, for the type-1 copper center in $[Ru(NH_3)_5(His\text{-}83)]$-azurin from *Pseudomonas aeruginosa*, using nonisothermal thin-layer spectroelectrochemistry. Solution conditions: pH = 7.0, μ = 100 mM, phosphate buffer. Temperature range: 6.6 ~ 40.2 ^{0}C. A least squares fit of the data gave an $E^{0\prime}$ = 320 ± 2 mV at 25.0 ^{0}C and $(dE^{0\prime}/dT)_{25\ ^0C}$ = -4.86 x 10^{-4} V/^{0}C.

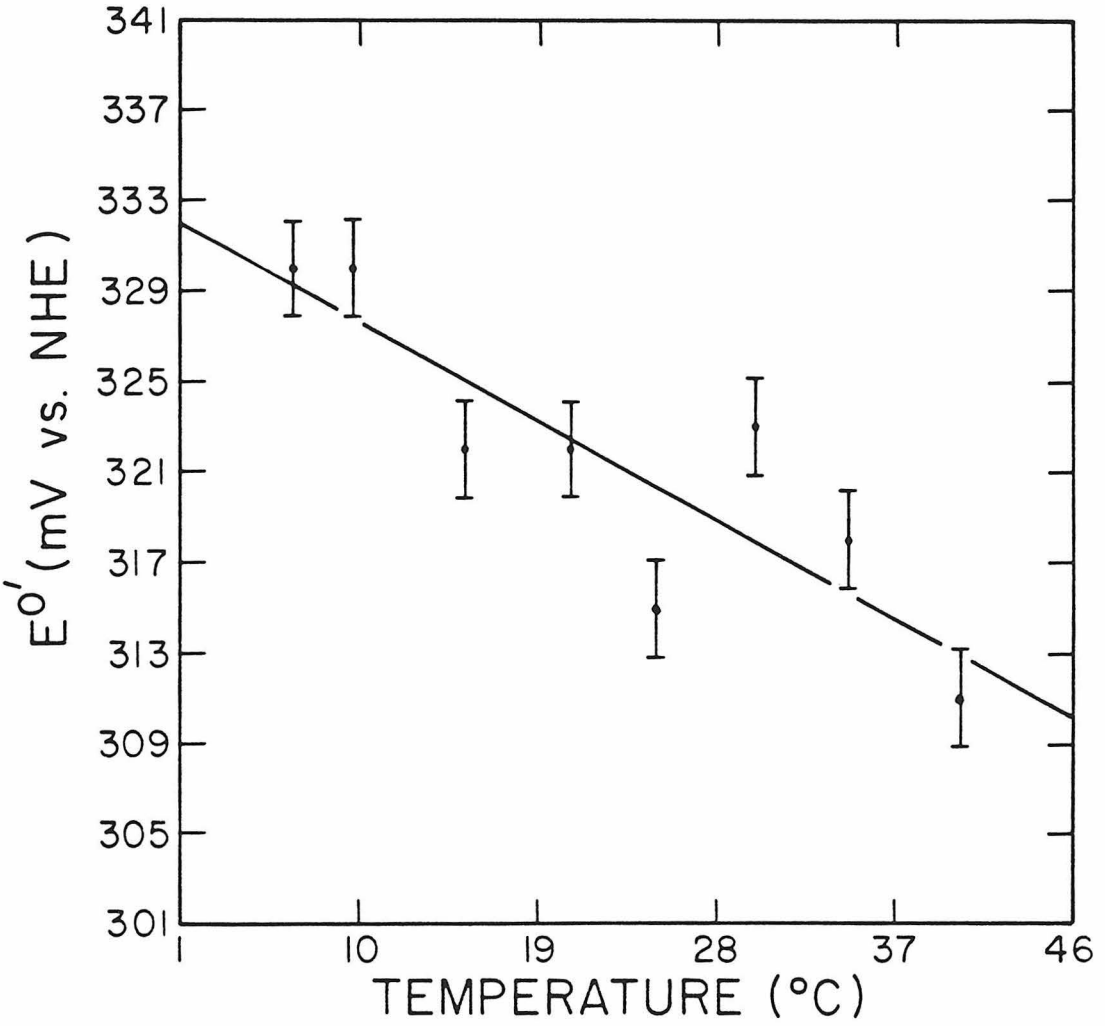
341
337
333
329
325
321
317
313
309
305
301
E°' (mV vs. NHE)
1
10
19
28
37
46
TEMPERATURE (°C)

Table 8. Temperature dependence of the formal reduction potentials, $E^{0\prime}$, for the blue-copper ion in $[Ru(NH_3)_5(His\text{-}83)]$-azurin from *Pseudomonas aeruginosa*, using nonisothermal thin-layer spectroelectrochemistry. Solution conditions: pH 5.0, μ = 100 mM, acetate buffer.

Temperature (^{0}C)*	$E^{0\prime}$ (mV vs. NHE)†
9.8	356
13.2	356
19.4	354
21.0	356
26.0	358
29.8	354
35.6	356

* ± 0.2 ^{0}C

† ± 2 mV

Figure 12. Temperature dependence of the formal reduction potential, $E^{0\prime}$, for the type-1 copper center in $[Ru(NH_3)_5(His\text{-}83)]$-azurin from *Pseudomonas aeruginosa*, using nonisothermal thin-layer spectroelectrochemistry. Solution conditions: pH = 5.0, μ = 100 mM, acetate buffer. Temperature range: 9.8 ~ 35.6 ^{0}C. A least squares fit of the data gave an $E^{0\prime}$ = 356 ± 2 mV at 25.0 ^{0}C and $(dE^{0\prime}/dT)_{25\ ^0C}$ = -4.37 x 10^{-6} V/^{0}C.

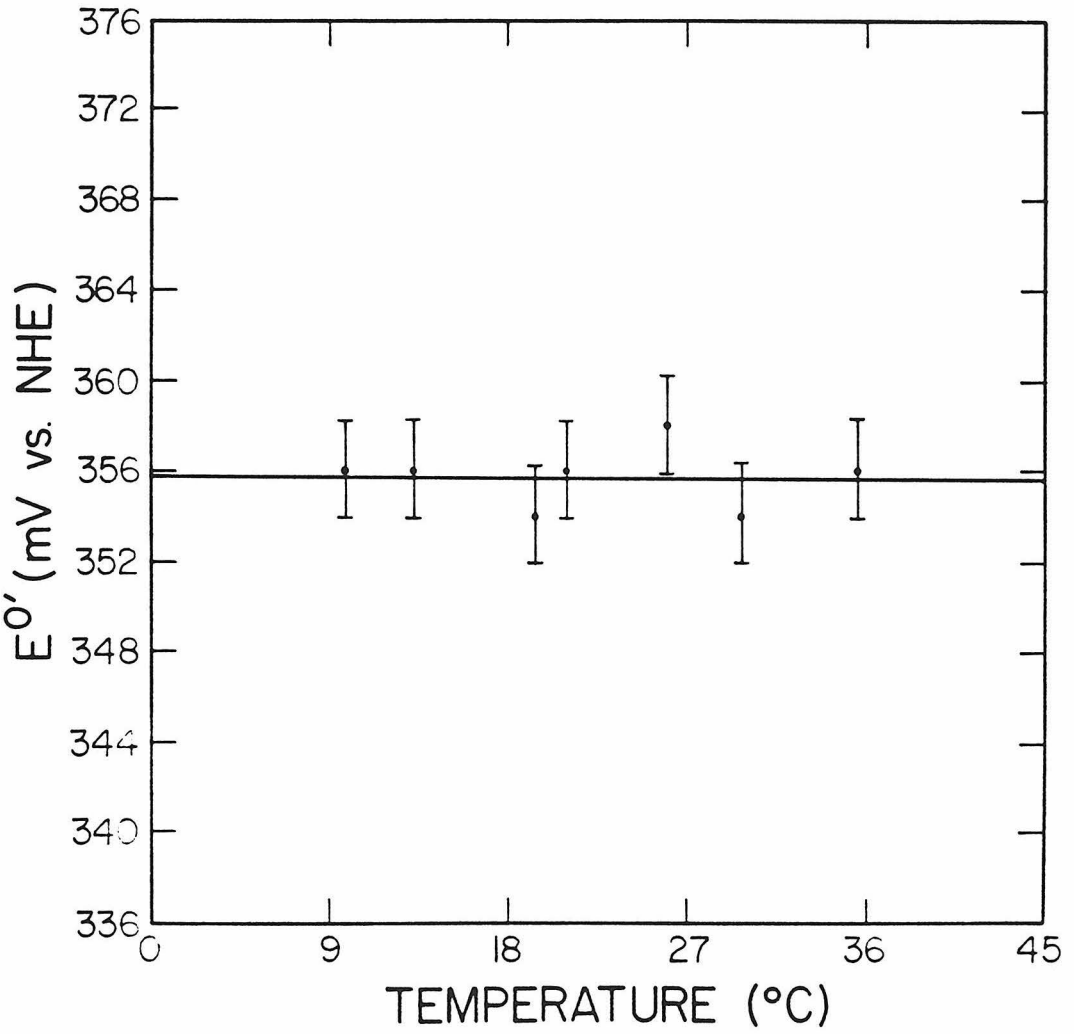
376
372
368
364
360
356
352
348
344
340
336
E°' (mV vs. NHE)
0
9
18
27
36
45
TEMPERATURE (°C)

Figure 13. Temperature dependence of the formal reduction potential, $E^{0\prime}$, for the type-1 copper center in $[Ru(NH_3)_5(His\text{-}83)]$-azurin from *Pseudomonas aeruginosa* at pH 7.0 (Δ) and at pH 5.0 (X). Solution conditions: μ = 100 mM, phosphate buffer (pH 7.0) or acetate buffer (pH 5.0), 5 equivalents $[Ru(NH_3)_5(py)](ClO_4)_3$.

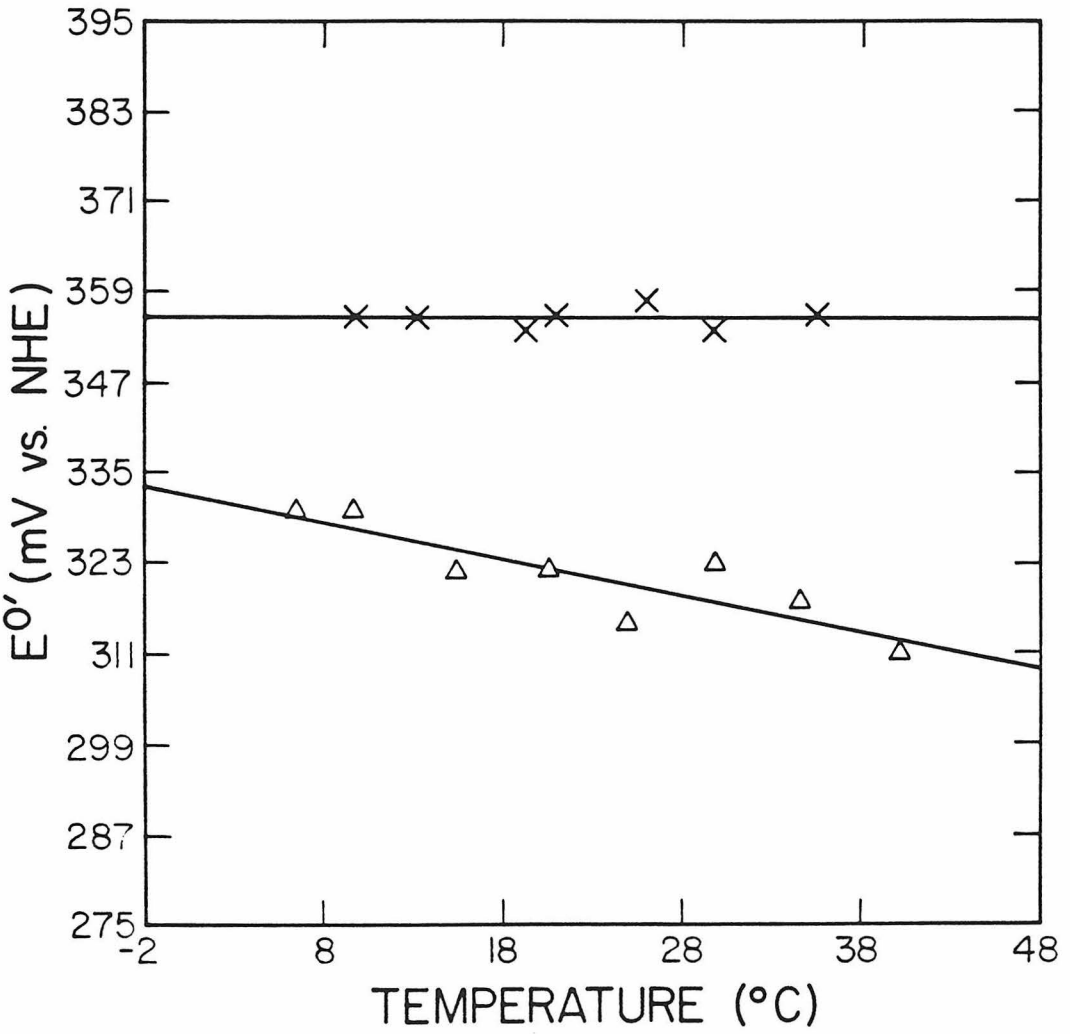
395
383
371
359
347
335
323
311
299
287
275
E°' (mV vs. NHE)
-2
8
18
28
38
48
TEMPERATURE (°C)

Table 9. Thermodynamic parameters for the reduction of the type-1 blue-copper center in $[Ru(NH_3)_5(His\text{-}83)]$-azurin from *Pseudomonas aeruginosa* at two pH values. Solution conditions: μ = 100 mM, phostate buffer (pH 7.0), acetate buffer (pH 5.0), 25 ^{0}C.

	(a_5Ru)-Az pH 7.0, 0.1 M Phosphate	**(a_5Ru)-Az pH 5.0, 0.1 M Acetate**
$E^{0\prime}$ at 25 ^{0}C (mV vs. NHE)	320	356
$\Delta S^{0\prime}$ (eu)	-26.8	-15.7
$\Delta S^{0\prime}_{et}$ (eu)	-11.2	-0.1
$\Delta G^{0\prime}$ (kcal/mol)	-7.39	-8.20
$\Delta H^{0\prime}$ (kcal/mol)	-15.4	-12.9

Table 10. Temperature dependence of the formal reduction potentials, $E^{0\prime}$, for the blue-copper ion in doubly pentaammineruthenium modified *Pseudomonas aeruginosa* azurin, using nonisothermal thin-layer spectroelectrochemistry. Solution conditions: pH 7.0, μ = 100 mM, phosphate buffer.

Temperature (^{0}C)*	$E^{0\prime}$ (mV vs. NHE)†
4.1	349
8.6	349
14.0	340
16.2	342
20.6	340
25.0	335
31.0	324
34.0	317
34.4	317
39.3	309

* ± 0.2 ^{0}C

† ± 2 mV

Figure 14. Temperature dependence of the formal reduction potential, $E^{0\prime}$, for the type-1 copper center in doubly pentaammineruthenium modified *Pseudomonas aeruginosa* azurin, using non-isothermal thin-layer spectroelectrochemistry. Solution conditions: pH = 7.0, μ = 100 mM, phosphate buffer. Temperature range: 4.1 ~ 39.3 ^{0}C. A least squares fit of the data gave an $E^{0\prime}$ = 330 ± 2 mV at 25.0 ^{0}C and $(dE^{0\prime}/dT)_{25\ ^{0}C} = -1.17 \times 10^{-3}$ V/^{0}C.

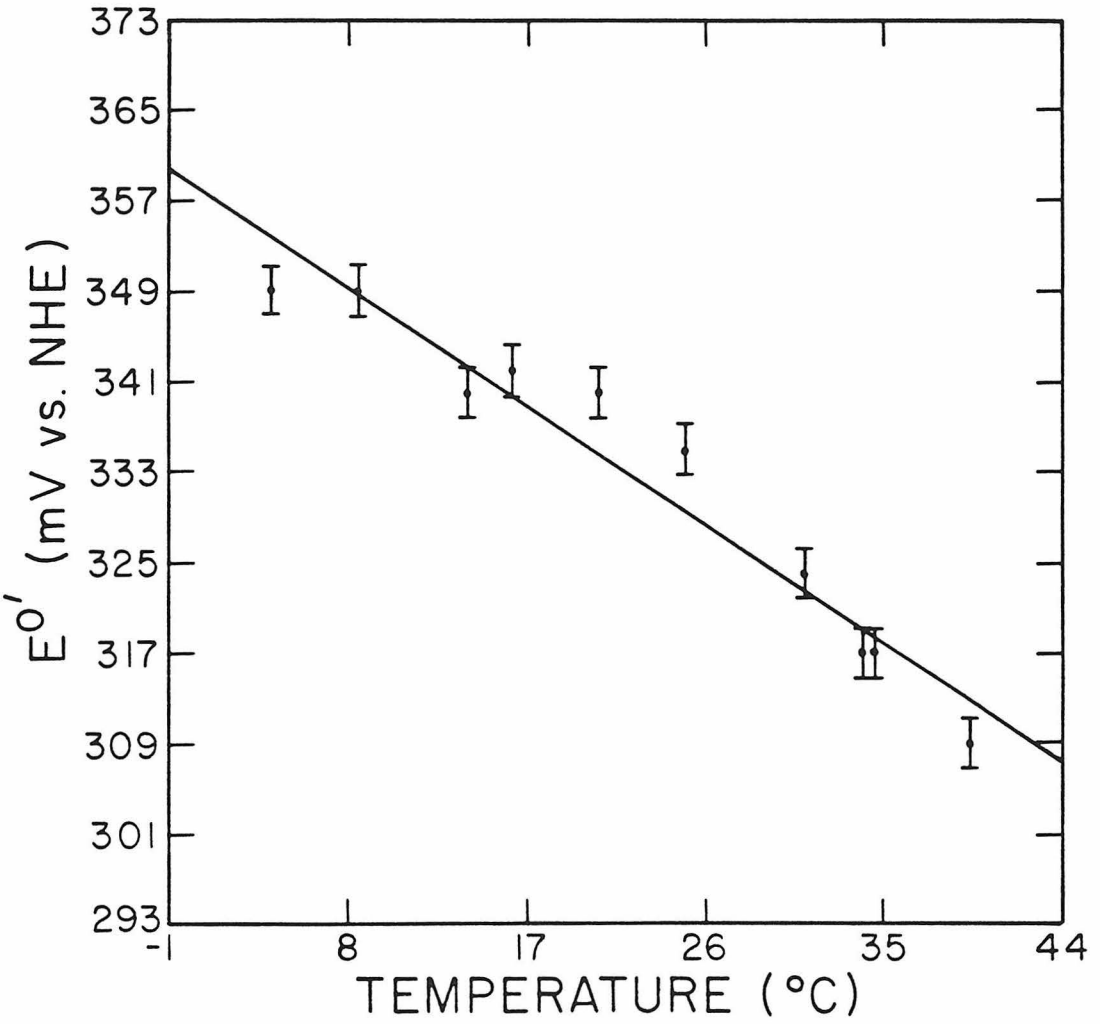
373
365
357
349
341
333
325
317
309
301
293
E°' (mV vs. NHE)
-1
8
17
26
35
44
TEMPERATURE (°C)

Table 11. Temperature dependence of the formal reduction potentials, $E^{0\prime}$, for the blue-copper ion in doubly pentaammineruthenium modified *Pseudomonas aeruginosa* azurin, using nonisothermal thin-layer spectroelectrochemistry. Solution conditions: pH 5.0, μ = 100 mM, acetate buffer.

Temperature (^{0}C)*	$E^{0\prime}$ (mV vs. NHE)†
4.0	377
11.2	371
15.1	370
20.0	373
25.2	371
30.6	365

* ± 0.2 ^{0}C

† ± 2 mV

Figure 15. Temperature dependence of the formal reduction potential, $E^{0\prime}$, for the type-1 copper center in doubly pentaammineruthenium modified *Pseudomonas aeruginosa* azurin, using non-isothermal thin-layer spectroelectrochemistry. Solution conditions: pH = 5.0, μ = 100 mM, acetate buffer. Temperature range: 4.0 ~ 30.6 ^{0}C. A least squares fit of the data gave an $E^{0\prime}$ = 369 ± 2 mV at 25.0 ^{0}C and $(dE^{0\prime}/dT)_{25\ ^{0}C} = -3.28 \times 10^{-4}$ V/^{0}C.

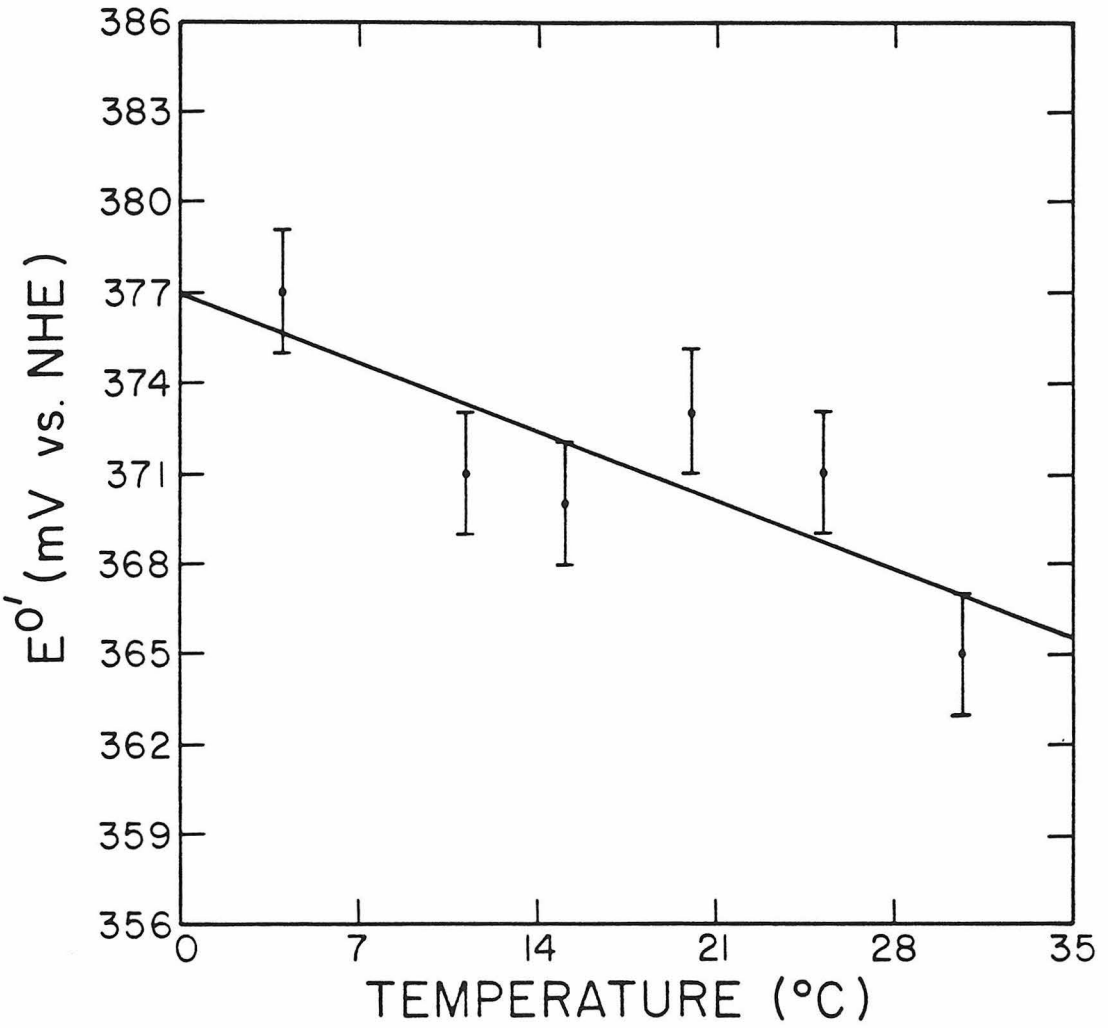
386
383
380
377
374
371
368
365
362
359
356
$E^{O'}$ (mV vs. NHE)
0
7
14
21
28
35
TEMPERATURE (°C)

Figure 16. Temperature dependence of the formal reduction potential, $E^{0\prime}$, for the type-1 copper center in doubly pentaammine-ruthernium modified *Pseudomonas aeruginosa* azurin at pH 7.0 (Δ) and at pH 5.0 (X). Solution conditions: μ = 100 mM, phosphate buffer (pH 7.0) or acetate buffer (pH 5.0), 5 equivalents $[Ru(NH_3)_5(py)](ClO_4)_3$.

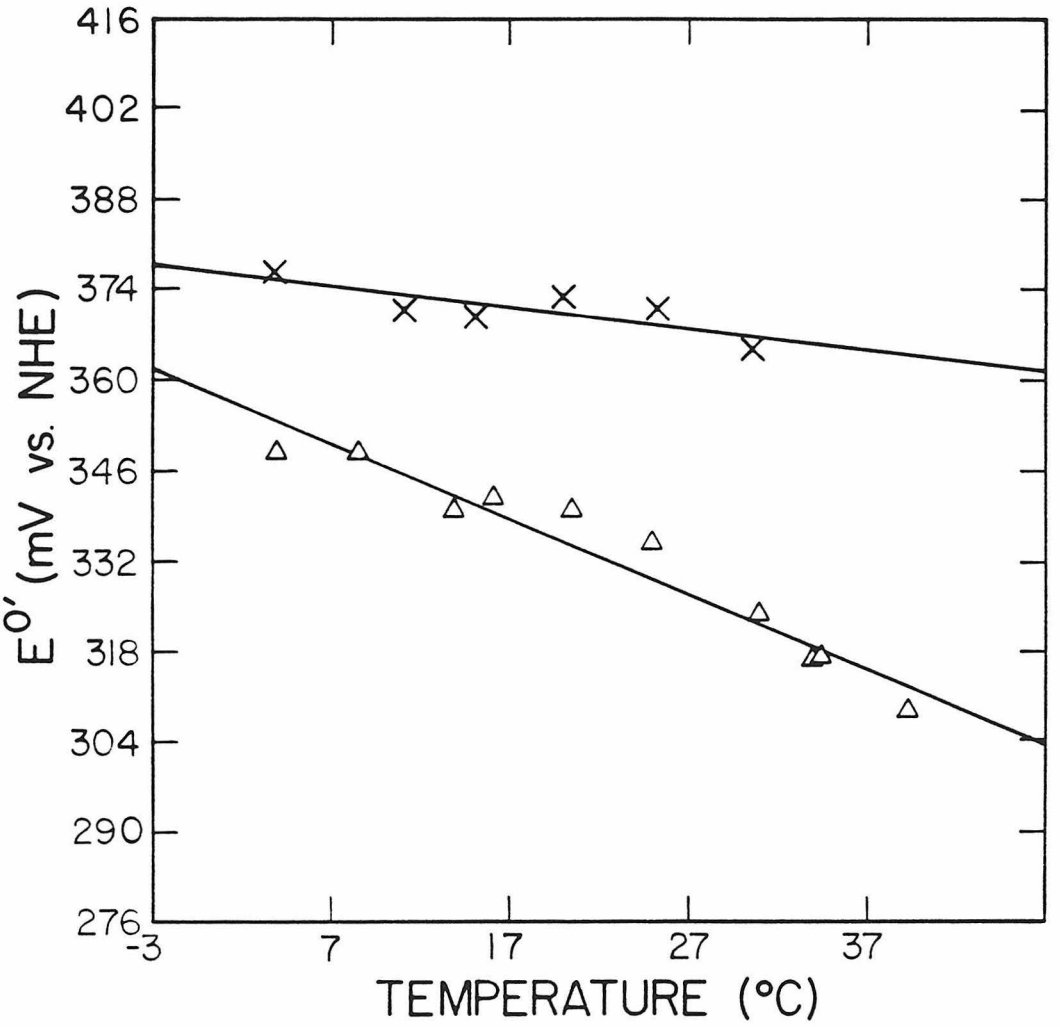
416
402
388
374
360
346
332
318
304
290
276
E°' (mV vs. NHE)
-3
7
17
27
37
TEMPERATURE (°C)

Table 12. Thermodynamic parameters for the reduction of the type-1 blue-copper center in doubly pentaammineruthenium modified *Pseudomonas aeruginosa* azurin at two pH values. Solutions conditions: μ = 100 mM, phosphate buffer (pH 7.0), acetate buffer (pH 5.0), 25 ^{0}C.

	$(a_5Ru)_2$-Az pH 7.0, 0.1 M Phosphate	$(a_5Ru)_2$-Az pH 5.0, 0.1 M Acetate
$E^{0\prime}$ at 25 ^{0}C (mV vs. NHE)	330	369
$\Delta S^{0\prime}$ (eu)	-42.5	-23.2
$\Delta S^{0\prime}_{et}$ (eu)	-26.9	-7.6
$\Delta G^{0\prime}$ (kcal/mol)	-7.60	-8.50
$\Delta H^{0\prime}$ (kcal/mol)	-20.3	-15.4

the protein environment increases, some amino acid residues become positively charged, and this facilitates the acceptance of an electron by the redox center. In native azurin, however, the difference in redox properties caused by the change in acidity is more dramatic than that in [a_5Ru(His-83)]-Az and in $(a_5Ru)_2$-Az. The effect of pentaammineruthemium labelling on proteins is a intriguing subject. As far as the protein structure is concerned, the available spectroscopic evidence suggests that the conformations of proteins have not been perturbed significantly.[27,33] It would be interesting to see whether or not the same can be said for the electrochemical and thermodynamic properties of the proteins upon labelling.

The formal reduction potentials and thermodynamic parameters of native, as well as singly and doubly pentaammineruthenium modified azurins, have been compared in pH 7.0, 100 mM phosphate buffer (Figure 17, Table 13) and in pH 5.0, 100 mM acetate buffer (Figure 18, Table 14).

At pH 7.0, the effect of a_5Ru-labeling on both the redox potentials and thermodynamic properties of the blue-copper center in azurin is quite small. However, at pH 5.0, the introduction of an a_5Ru-label produces quite a dramatic change in thermodynamic properties of azurin. The reaction entropies, $\Delta S^{0'}_{et}$, are 10.7 eu for native azurin, ~ 0.0 eu for [a_5Ru(His-83)]-Az, and -7.6 eu for $(a_5Ru)_2$-Az. This phenomenon indicates that protonation has a key effect on either the conformational, or electrostatic factors, influencing electron transfer to the blue copper site. The peptide

Figure 17. Temperature dependence of the formal reduction potential, $E^{0\prime}$, for the type-1 copper center in native (Δ), in $[Ru(NH_3)_5(His\text{-}83)]$-modified (•), and in doubly pentaammine -ruthenium modified (X) *Pseudomonas aeruginosa* azurins. Solution conditions: pH 7.0, μ = 100 mM, phosphate buffer.

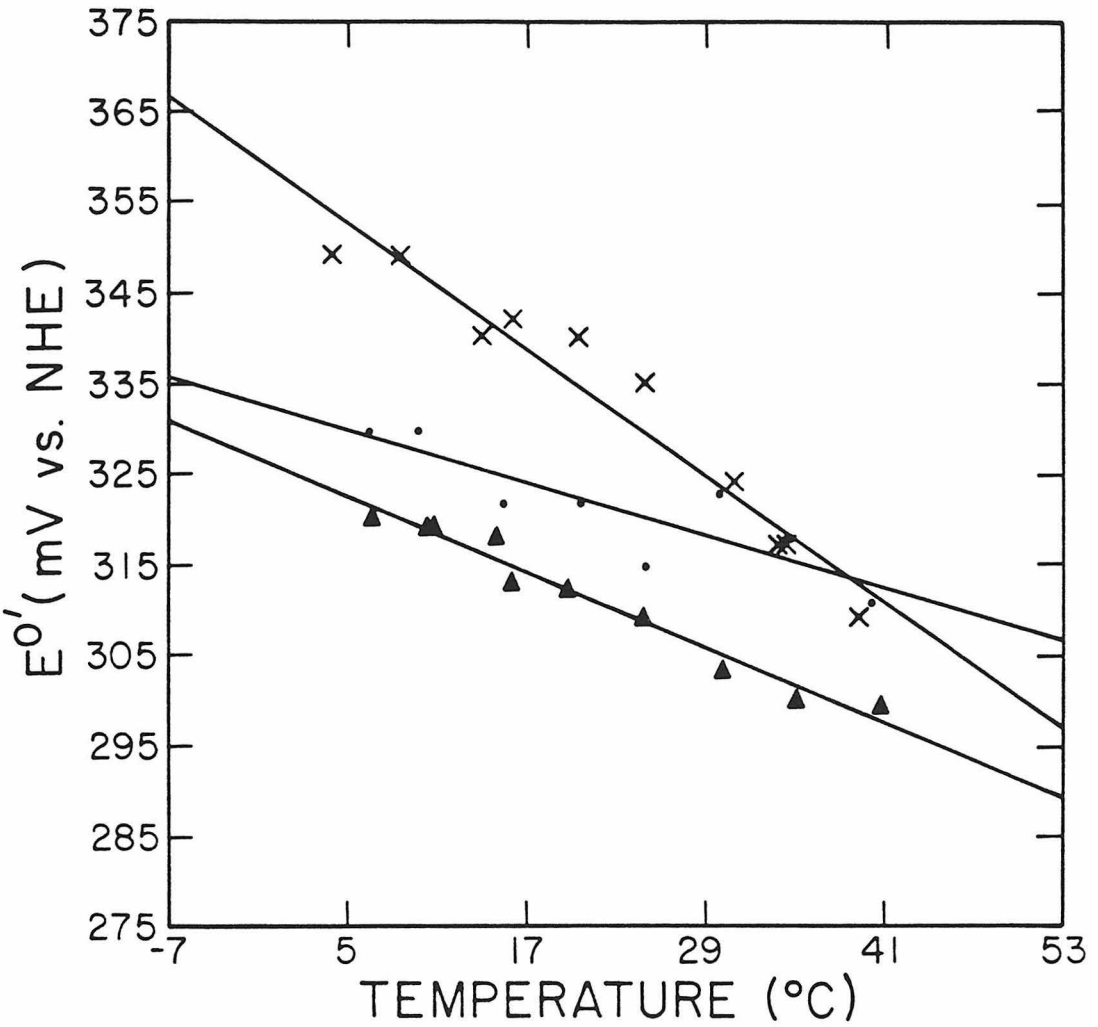
375
365
355
345
335
325
315
305
295
285
275
E°' (mV vs. NHE)
-7
5
17
29
41
53
TEMPERATURE (°C)

Table 13. Thermodynamic parameters for the reduction of the type-1 blue-copper centers in native, in $[Ru(NH_3)_5(His\text{-}83)]$-modified, and in doubly pentaammineruthenium modified *Pseudomonas aeruginosa* azurins at pH 7.0, μ = 100 mM, phosphate buffer, 25 ^{0}C.

	Native Az pH 7.0, 0.1 M Phosphate	(a_5Ru)-Az pH 7.0, 0.1 M Phosphate	$(a_5Ru)_2$-Az pH 7.0, 0.1 M Phosphate
$E^{0\prime}$ at 25 ^{0}C (mV vs. NHE)	308	320	330
$\Delta S^{0\prime}$ (eu)	-31.7	-26.8	-42.5
$\Delta S^{0\prime}_{et}$ (eu)	-16.1	-11.2	-26.9
$\Delta G^{0\prime}$ (kcal/mol)	-7.10	-7.39	-7.60
$\Delta H^{0\prime}$ (kcal/mol)	-16.6	-15.4	-20.3

Figure 18. Temperature dependence of the formal reduction potential, $E^{0\prime}$, for the type-1 copper center in native (•), in $[Ru(NH_3)_5(His\text{-}83)]$-modified (X), and in doubly pentaammine -ruthenium modified (Δ) *Pseudomonas aeruginosa* azurins. Solution conditions: pH 5.0, μ = 100 mM, acetate buffer.

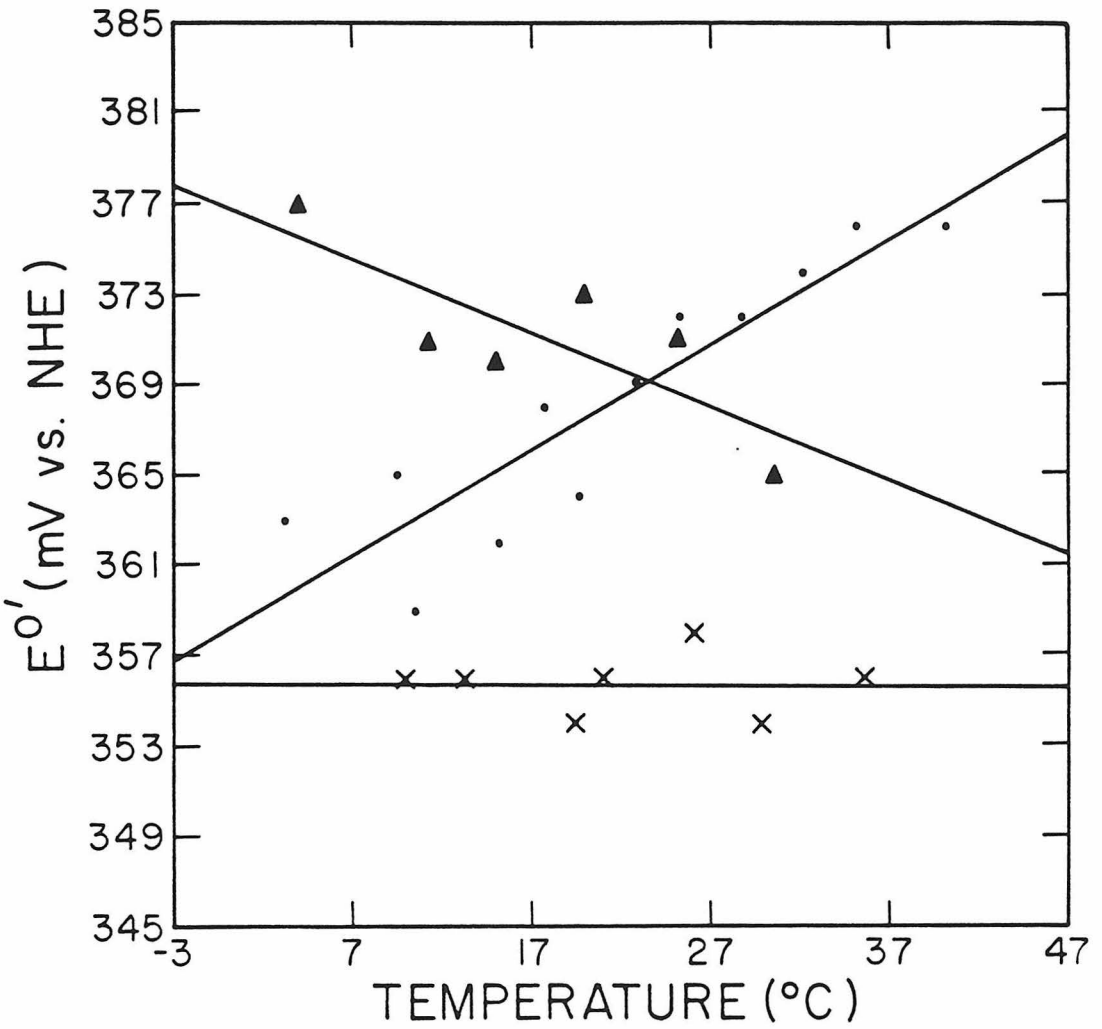
385
381
377
373
369
365
361
357
353
349
345
E^O' (mV vs. NHE)
-3
7
17
27
37
47
TEMPERATURE (°C)

Table 14. Thermodynamic parameters for the reduction of the type-1 blue-copper centers in native, in $[Ru(NH_3)_5(His\text{-}83)]$-modified, and in doubly pentaammineruthenium modified *Pseudomonas aeruginosa* azurins at pH 5.0, μ = 100 mM, acetate buffer, 25 ^{0}C.

	Native Az pH 5.0, 0.1 M Acetate	**(Rua_5)-Az pH 5.0, 0.2 M Acetate**	**$(RuA_5)_2$-Az pH 5.0, 0.1 M Acetate**
$E^{0\prime}$ at 25 ^{0}C (mV vs. NHE)	370	356	369
$\Delta S^{0\prime}$ (eu)	-4.9	-15.7	23.2
$\Delta S^{0\prime}_{et}$ (eu)	10.7	-0.1	-7.6
$\Delta G^{0\prime}$ (kcal/mol)	-8.53	-8.20	-8.50
$\Delta H^{0\prime}$ (kcal/mol)	-10.0	-12.9	-15.4

mapping analysis of $(a_5Ru)_2$-Az indicates that His-35 is not modified, and an unconfirmed methionine modification by a_5Ru- is suggested instead. It is difficult to draw a definite conclusion in the case of doubly modified azurin, however, if an a_5Ru- modification on His-83, which is 11.8 Å from the copper site, can decrease $\Delta S^{0\prime}_{et}$ by ~ 11 eu, then it is reasonable that a second a_5Ru-modification, near or distant from the copper center, can have an equivalent effect of the order of 7.6 eu, on the reaction entropy along the same transition direction.

The pH-dependence of the formal reduction potential at 25 ^{0}C for the blue-copper center in native, in $[Ru(NH_3)_5$(His-83)]-modified, and in doubly pentaammineruthenium modified *Pseudomonas aeruginosa* azurins is shown in Figure 19. It is clearly shown that the redox potential of the blue-copper center in native azurin has a dramatic change while pH value of the protein solution changed from 6.0 to 5.0. It is interesting to notice that the pH-dependent phenomena of formal reduction potentials of the blue-copper center in $[Ru(NH_3)_5$(His-83)]-modified and in doubly pentaammineruthenium modified azurins are quite similar. The observation is in conflict with the pH-dependent behaviors of rate constant for long-range $Ru^{II} \longrightarrow Cu^{II}$ intramolecular electron transfer reaction in $[Ru(NH_3)_5$(His-83)]-modified and in doubly pentaammineruthenium modified azurins, which is shown in Figures 5 and 6. By the comparison of these data thus leads us to conclude that the reason for pH-inpendence of electron transfer rate constant for $Ru^{II} \longrightarrow Cu^{II}$ in doubly pentaammineruthe-

Figure 19. The pH-dependence of the formal reduction potential, $E^{0\prime}$, for the blue-copper center in native (Δ), in $[Ru(NH_3)_5(His\text{-}83)]$-modified (O), and in doubly pentaammineruthenium modified (X) *Pseudomonas aeruginosa* azurins. Solution condition: μ = 100mM, phosphate buffer (pH 6.0, and pH 7.0) or acetate buffer (pH 5.0), 5 equivalents $[Ru(NH_3)_5(py)](ClO_4)_3$.

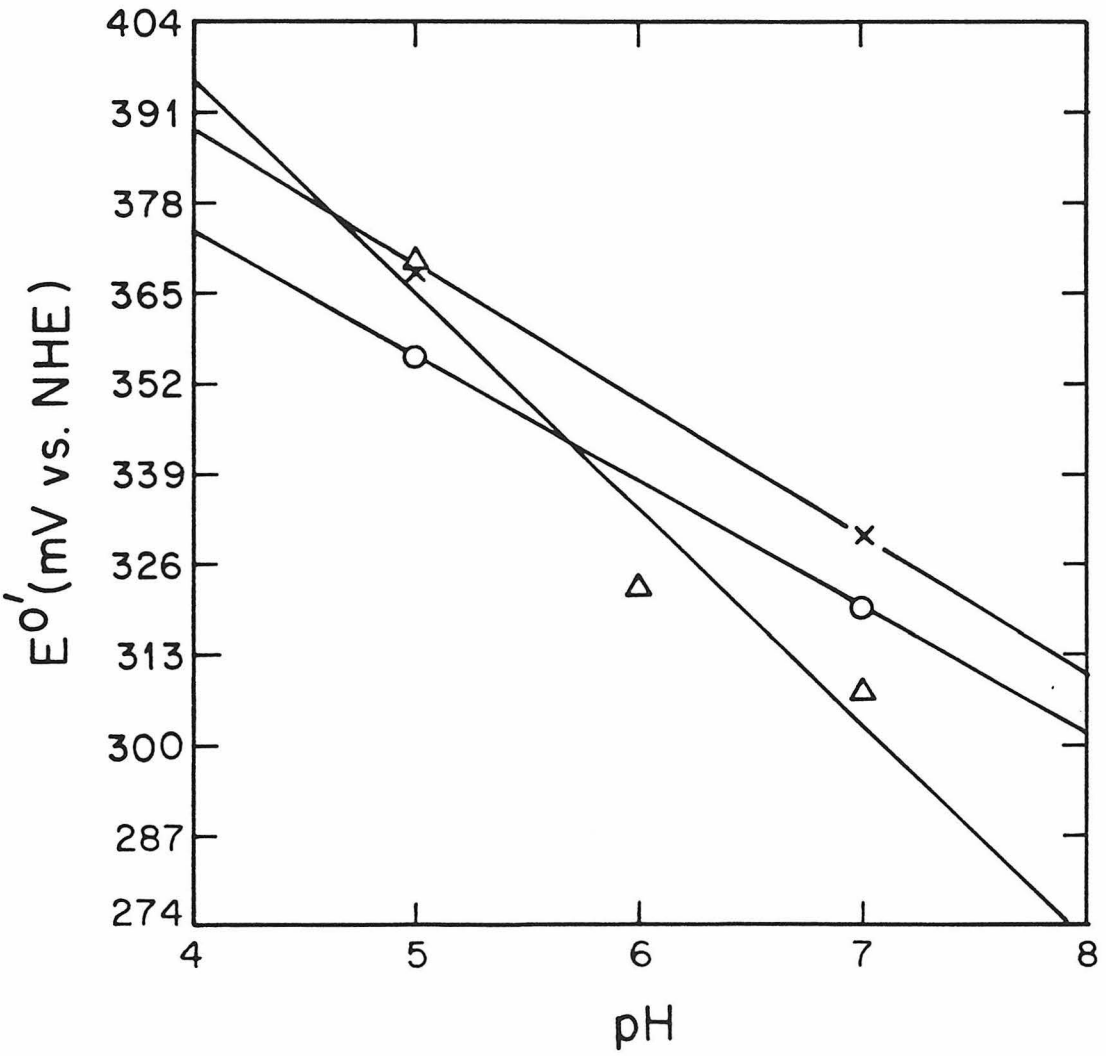
404
391
378
365
352
339
326
313
300
287
274
4
5
6
7
8
pH
E°'(mV vs. NHE)

nium modified azurin in the domain ranging from pH 9.0 to pH 5.0 is not due to the factor of driving force. The increase in driving force causing by the solvent acidification must be compensated out by some other factor which we are not able to identify at the present time. Since this situation is not present in singly modified $[Ru(NH_3)_5(His\text{-}83)]$-Az, the second a_5Ru- modifier must be responsible to pH-independent electron transfer kinetics in $(a_5Ru)_2$-Az.

References

1. Fee, J. A., in *Structure and Bonding*, Volume 23, Dunitz, J. D., Hemmerich, P., Holm, R. H., Ibers, J. A., Jørgensen, C. K., Neilands, J. B., Reinen, D., and Williams, J. P., eds., Springer-Verlag, Berlin, 1975, P. 1.

2. Malkin, R., and Malmström, B. G., in *Advances in Enzymology and Related Areas of Molecular Biology*, Volume 33, Nord, F. F., ed., Wiley, New York, 1970, P. 177.

3. Sutherland, I. W., and Wilkinson, J. F., *J. Gen. Microbiol.*, **30**, 105 (1963).

4. Horio, T., *J. Biochem. (Tokyo)*, **45**, 195 (1958).

5. Verhoeven, W., and Takeda, Y., in *Inorganic Nitrogen Metabolism*, McElroy, W. D., and Glass, B., eds., Johns Hopkins Press, Baltimore, 1956, P. 159.

6. Adman, E. T., in *Topics in Molecular and Structural Biology, Volume 6, Metalloproteins, Part 1: Metal Proteins with Redox Roles*, Harrison, P. M., ed., MacMillan Press, London, 1985, P. 1.

7. Rydén, L., in *Copper Proteins and Copper Enzymes*, Volume I, Lontie, R., ed., CRC Press, Boca Raton, 1984, P. 157.

8. Farver, O., and Pecht, I., in *Metal Ions in Biology, Volume 3, Copper Proteins*, Spiro, T. G., ed., Wiley, New York, 1981, P. 151.

9. Lappin, A. G., in *Metal Ions in Biological Systems, Volume 13, Copper Proteins*, Sigel, H., ed., Marcel Dekker, New York, 1981, P. 15.

10. Gray, H. B., and Solomon, E. I., in *Metal Ions in Biology, Volume 3, Copper Proteins*, Spiro, T. G., ed., Wiley, New York, 1981, P. 1.

11. Solomon, E. I., Hare, J. W., Dooley, D. M., Dawson, J. H., Stephens, P. J., and Gray, H. B., *J. Am. Chem. Soc.*, **102**, 168 (1980).

12. Solomon, E. I., Hare, J. W., and Gray, H. B., *Proc. Natl. Acad. Sci. USA*, **73**, 1389 (1976).

13. Cass, A. E. G., and Hill, H. A. O., in *Copper Proteins and Copper Enzymes*, Volume I, Lontie, R., ed., CRC Press, Boca

Raton, 1984, P. 63.

14. Markley, J. L., Ulrich, E. L., Berg, S. P., and Krogmann, D. W., *Biochemistry*, ***14***, 4428 (1975).

15. Boas, J. F., in *Copper Proteins and Copper Enzymes*, Volume I, Lontie, R., ed., CRC Press, Boca Raton, 1984, P. 5.

16. Loehr, T. M., and Sanders-Loehr, J., in *Copper Proteins and Copper Enzymes*, Volume I, Lontie, R., ed., CRC Press, Boca Raton, 1984, P. 115.

17. Co, M. S., and Hodgson, K. O., in *Copper Proteins and Copper Enzymes*, Volume I, Lontie, R., ed., CRC Press, Boca Raton, 1984, P. 93.

18. Tullius, T. D., Frank, P., and Hodgson, K. O., *Proc. Natl. Acad. Sci. USA*, *75*, 4069 (1978).

19. Adman, E. T., and Jensen, L. H., *Isr. J. Chem.*, ***21***, 8 (1981).

20. Adman, E. T., Stenkamp, R. E., Sieker, L. C., and Jensen, L. H., *J. Mol. Biol.*, ***123***, 35 (1978).

21. Peisach, J., and Blumberg, W. E., *Arch. Biochem. Biophys.*, ***165***, 691 (1974).

22. Crutchley, R. J., Ellis, W. R., Jr., and Gray, H. B., in *Frontiers in Bioinorganic Chemistry*, Xavier, A. V., ed., VCH erlagsgesellschaft, Weinheim, F. R. G., 1986, P. 679.

23. Mayo, S. L., Ellis, W. R., Jr., Crutchley, R. J., and Gray, H. B., *Science*, ***233***, 948 (1986).

24. Gray, H. B., *Chem. Soc. Rev.*, ***15***, 17 (1986).

25. Crutchley, R. J., Ellis, W. R., Jr., and Gray, H. B., *J. Am. Chem. Soc.*, ***107***, 5002 (1985).

26. Isied, S. S., Kuehn, C., and Worosila, G., *J. Am. Chem. Soc.*, ***106***, 1722 (1984).

27. Margalit, R., Kostić, N. M., Che, C.-M., Blair, D. F., Chiang, H.-J., Pecht, I., Shelton, J. B., Shelton, J. R., Schroeder, W. A., and Gray, H. B., *Proc. Natl. Acad. Sci. USA*, ***81***, 6554 (1984).

28. Nocera, D. G., Winkler, J. R., Yocom, K. M., Bordignon, E., and Gray, H. B., *J. Am. Chem. Soc.*, ***106***, 5145 (1984).

29. Kostić, N. M., Margalit, R., Che, C.-M., and Gray, H. B., *J. Am. Chem. Soc.*, ***105***, 7765 (1983).

30. Yocom, K. M., Winkler, J. R., Nocera, D. G., Bordignon, E., and Gray, H. B., *Chem. Scr.*, ***21***, 29 (1983).

31. Isied, S. S., Worosila, G., and Atherton, S. J., *J. Am. Chem. Soc.*, ***104***, 7659 (1982).

32. Winkler, J. R., Nocera, D. G., Yocom, K. M., Bordignon, E., and Gray, H. B., *J. Am. Chem. Soc.*, ***104***, 5798 (1982).

33. Yocom, K. M., Shelton., J. B., Shelton, J. R., Schroeder, W. A., Worosila, G., Isied, S. S., Bordignon, E., and Gray, H. B., *Proc. Natl. Acad. Sci. USA*, ***79***, 7052 (1982).

34. Kostić, N. M., unpublished results.

35. Curtis, J. C., Sullivan, B. P., and Meyer, T. J., *Inorg. Chem.*, ***22***, 224 (1983).

36. Kirschner, S., in *Inorganic Syntheses*, Volume 5, Moeller, T., ed., McGraw-Hill, New York, 1957, P. 186.

37. Cummins, D., and Gray, H. B., *J. Am. Chem. Soc.*, ***99***, 5158 (1977).

38. Sundberg, R. J., and Gupta, G., *Bioinorg. Chem.*, ***3***, 39 (1973).

39. Ambler, R. P., and Brown, L. H., *Biochem. J.*, ***104***, 784 (1967).

40. Kostić, N. M., Shelton, J. B., Shelton, J. R., Schroeder, W. A., Blair, D. F., Chiang, H.-J., and Gray, H. B., in Preparation.

41. Stein, C. A., and Taube, H., *Inorg. Chem.*, ***18***, 1168 (1979).

42. Taniguchi, V. T., Sailasuta-Scott, N., Anson, F. C., and Gray, H. B., *Pure Appl. Chem.*, ***52***, 2275 (1980).

CHAPTER V

RUTHENIUM-MODIFIED PROTEINS.

REACTIONS OF *cis*-$[Ru(NH_3)_4(OH_2)_2]^{2+}$ AND

cis-$[Ru(en)_2(OH_2)_2]^{2+}$ WITH AZURIN, MYOGLOBIN, AND CYTOCHROME *c*

Introduction

The electron transport chains involved in the metabolic processes necessary for the survival of all organisms, function as a series of consecutive electron transfer reactions between pairs of proteins which have evolved to couple efficiently for energy conservation. In order to understand what factors control the rate of electron transfer through the intervening polypeptide chains, scientists have investigated reactions involving proteins and redox-active transition metal complexes as artificial substrates.[1-12] However, the kinetics of many of these protein – inorganic complex electron transfer reactions were found to be second order and bimolecular mechanisms were proposed.[6,13]

Among the various factors controlling long-range electron transfer kinetics, the distance between redox centers is one of the most important.[14] In an effort to investigate the distance dependence of long-range electron transfer, a novel approach has consisted of the modification of metalloproteins with redox-active inorganic complexes, and measurement of the kinetic and thermodynamic parameters for intramolecular electron transfer between the inorganic label and the native metal site in the protein interior.[15-25]

Recent experiments have demonstrated that the surface histidines of proteins react rapidly with $[Ru(NH_3)_5(OH_2)]^{2+}$, and derivatives of horse heart cytochrome *c*,[25] *Pseudomonas aeruginosa* azurin,[18] and sperm whale myoglobin[15,16,21] have been characterized. We have begun

an investigation of the binding of other ruthenium-amine complexes with proteins, because of the need for electron transfer experiments with variations in the reaction driving force. Complexes of the types *cis*- and *trans*-$[Ru^{II}L_4(OH_2)_2]^{2+}$ in which L_4 denotes four mono-dentate amines, or two bi-dentate amines, or a tetra-dentate amine, are particularly attractive in this context, because their chemistry is well worked out.[26,27] In this chapter, the products of the reactions of horse heart myoglobin, *Pseudomonas aeruginosa* azurin, and horse heart cytochrome *c* with *cis*-$[Ru(NH_3)_4(OH_2)_2]^{2+}$ and *cis*-$[Ru(NH_3)_4(OH2)_2]^{2+}$ are described.[28] The formal reduction potential and thermodynamic parameters of *cis*-$[Ru(en)_2(OH)$(His-33)]-horse heart cytochrome *c* are also investigated by spectroelectrochemistry.

Materials and Methods

Sperm whale and horse heart myoglobins (Sigma Chemical Co.) were purified before use by ion exchange chromatography on Whatman CM-52 cellulose and eluted with pH 7.8, 50 mM tris•HCI buffer at 4 ^{0}C. The major myoglobin components were the last to come off the column and had pI *ca.* 8.1. *Pseudomonas aeruginosa* azurin obtained from the Public Health Laboratory Service in England, has an A_{280}/A_{625} ratio of 1.72.

Trypsin treated with L-1-tosylamido-2-phenylethyl chloromethyl ketone was obtained from Worthington. Baker reagent grade acetonitrile was used for HPLC. *cis*-$[Ru(NH_3)_4Cl_2]^+$,[26] *cis*-

$[Ru(en)_2Cl_2]^+$,[27] and $[Ru(NH_3)_5(py)](ClO_4)_3$[29] were prepared according to published procedures. Deionized water from a Barnstead NANOpure water purifier was used throughout. Ultrafiltration was performed with Amicon YM-5 membranes under argon with gentle stirring at 5 ^{0}C.

A solution of *cis*-$[Ru(NH_3)_4(OH_2)_2]^{2+}$ (**1**) or *cis*-$[Ru(en)_2(OH_2)_2]^{2+}$ (**2**) was generated by Zn(Hg) reduction of *cis*-$[Ru(NH_3)_4Cl_2]^+$ or *cis*-$[Ru(en)_2Cl_2]^+$ in tris•HCl or phosphate buffer (pH 6.5) under an inert atmosphere for 1 hour.[27] *cis*-$[Ru(en)_2(OH)$(His-81)]-horse heart myoglobin (**A**) was prepared by mixing **1**, which was generated by Zn(Hg) reduction of 50 mg *cis*-$[Ru(en)_2Cl_2]ClO_4$ in 15 ~ 20 ml phosphate, and 50 mg horse heart myoglobin for 4 ~ 5 hours. (*cis*-$[Ru(en)_2(OH)$(His)$]_2$-horse heart cytochrome *c* (**C**) were synthesized by mixing **1**, which was generated by Zn(Hg) reduction of 50 mg *cis*-$[Ru(en)_2Cl_2]ClO_4$ in 15 ~ 20 ml tris•HCl, and 50 mg horse heart myoglobin and 50 mg horse heart cytochrome *c*, respectively, for 24 hours. *cis*-$[Ru(en)_2(OH)$(His-83)]-*Pseudomonas aeruginosa* azurin (**D**) was made by mixing **1**, which was generated by Zn(Hg) reduction of 7 mg *cis*-$[Ru(en)_2Cl_2]ClO_4$ in 10 ml tris•HCl, and 12 mg *Pseudomonas aeruginosa* azurin for 4 hours. *cis*-$[Ru(NH_3)_4(OH)$(His-83)]-*Pseudomonas aeruginosa* azurin (**E**) was obtained by mixing **2**, which was generated by Zn(Hg) reduction of 7 mg *cis*-$[Ru(NH_3)_4Cl_2]Cl$ in 10 ml tris•HCl, and 10 mg of *Pseudomonas aeruginosa* azurin for 4 hours.

The procedures for tryptic hydrolysis used in peptide mapping experiments, separation of the resulting peptides by reversed-phase HPLC, and amino acid analysis, have been described previously.[18,25]

A sample containing 5 ~ 6 mg of modified proteins in 2 ml of water, was denatured for 4 minutes in boiling water prior to tryptic hydrolysis. The linear gradient, for the HPLC separation of the tryptic peptides, consisted of 45 ml each of phosphate buffer (49 mM KH_2PO_4/5.4 mM H_3PO_4, pH 2.85) and acetonitrile, the concentration of the latter increasing from 0% to 45%, and the elution rate was 1 ml/min. Absorbance measurements were recorded at 220 nm for the peptide bonds in **A**, **B**, **D**, and **E**; *ca.* 450 nm for *cis*-$[Ru(en)_2(OH)(His)]$ in **A**, **B**, and **D**; and 370 nm for *cis*-$[Ru(NH_3)_4(OH)(His)]$ in **E**.

In cyclic voltammetry experiments, a Princeton Applied Research model 174A polarographic analyzer was used in conjunction with a Hewlett-Packard 7004B X-Y recorder. A Keithley model 177 microvolt digital multimeter was used to confirm the starting potential prior to a scan. The all-glass cell consisted of two compartments, separated by a sintered glass disk. It was also equipped with a side arm for degassing the sample. The working electrode consisted of a gold disk measuring 3 mm in diameter, and the auxiliary electrode was a coil of platinum wire. The reference electrode was a saturated NaCl calomel electrode (SSCE). The supporting electrolyte was 100 mM $NaClO_4$ in pH 7.0, 100 mM phosphate buffer. All solutions were deoxygenated by bubbling with argon for several minutes prior to use.

Formal reduction potentials for the heme center in *cis*-$[Ru(en)_2(OH)(His\text{-}33)]$-horse heart cytochrome *c*, at pH 7.0, were determined at different temperatures by using an optically transpa-

rent thin-layer electrode (OTTLE) cell in a nonisothermal configuration. The details of this methodology are given in Chapter II. Five equivalents of $[Ru(NH_3)_5(py)](ClO_4)_3$ were introduced to the protein solution as mediator-titrant. The OTTLE cell employed a gold minigrid as the working electrode, and the optical path length was 0.48 mm. Potentials were applied across the thin-layer cell by using a Princeton Applied Research model 174A polarographic analyzer, and were accurately measured with a Keithley model 177 microvolt digital multimeter. The cell temperature was varied by using a variable temperature cell holder, and measured directly with an Omega Engineering precision microthermocouple connected to a Fluke model 2175A digital thermometer. The thermocouple was situated in the protein solution in close proximity to the thin-layer cavity. All visible spectra were obtained with a Cary 219 recording spectrophotometer.

Formal reduction potentials were determined by sequentially applying a series of potentials, $E_{appl.}$, to the gold minigrid electrode. Each potential was maintained until electrolysis ceased, so that the equilibrium value of the ratio of concentrations of oxidized to reduced forms of all redox couples in solution, [Ox]/[Red], was established as defined by the Nernst equation. Redox couples were incrementally converted from one oxidation state to the other by the series of applied potentials, for which each corresponding value of [Ox]/[Red] was determined from the spectra. Formal reduction potentials and n values were determined from plots of $E_{appl.}$ *vs.* log([Ox]/[Red]).

The protein solution was deoxygenated prior to use in experiments by vacuum/argon cycling on a vacuum/purified-argon double manifold, and loaded into the OTTLE cell by using rubber septum caps and syringe techniques. The platinum wire auxiliary electrode was situated in a compartment containing deoxygenated mediator-titrant solution that was isolated from the protein solution by a porous glass frit.

Results and Discussion

The modification reactions, and the properties of the ruthenated proteins, are summarized in Table 1. In most preparations, the reaction was quenched by applying the solution to a Sephadex G-25 column, and the ruthenated proteins were then oxidized by $[Co(dipic)_2]^-$ and purified by standard procedures.[18,25] For horse heart myoglobin, both 1:1 (**A**) and 2:1 (**B**) derivatives were isolated. Tryptic peptide analyses showed conclusively that the sites of modification in the 1:1 ruthenated proteins are His-81 for horse heart myoglobin and His-83 for *Pseudomonas aeruginosa* azurin. In product **C**, the absence of the His-33 C-2 proton peak at δ = 8.84 ppm in the high-field ^1H NMR spectrum, as shown in Figure 1, strongly indicates that His-33 of horse heart cytochrome *c* is labelled with *cis*-$[Ru(en)_2(OH_2)_2]^{2+}$.

Preliminary UV-VIS circular dichroism measurements indicate that the conformations of the proteins are not perturbed significantly by the ruthenium complexes, a finding that is in accord with previous

Table 1. Preparation and characterization of ruthenated proteins.

Reaction[a]	Product	pI	E_f° (V vs. NHE)[b]
1 and 50 mg Mb^h, 4-5 h	cis-$[Ru(en)_2(OH)](His\text{-}81)Mb^h$ (A)	8.2	-0.12
1 and 50 mg Mb^h, 24 h	cis-$[Ru(en)_2(OH)]_2Mb^h$ (B)	9.2	-0.13
1 and 50 mg cyt c, 24 h	cis-$[Ru(en)_2(OH)](His\text{-}33)$cyt c (C)	c	0.265[d]
1 and 12 mg Az, 4h	cis-$[Ru(en)_2(OH)](His\text{-}83)$Az (D)	7.2	-0.09
2 and 10 mg Az, 4h	cis-$[Ru(NH_3)_4(OH)](His\text{-}83)$Az (E)	7.2	-0.10 0.30[e]

[a] **1** was generated by Zn(Hg) reduction of 50 mg (A,B,C) or 7 mg (D) cis-$[Ru(en)_2Cl_2]ClO_4$ in 15-20 mL phosphate (A) or 15-20 mL tris·HCl (B,C) or 10 mL tris·HCl (D); **2** was generated by Zn(Hg) reduction of 7 mg cis-$[Ru(NH_3)_4Cl_2]Cl$ in 10 mL tris·HCl.

[b] Ru(III)/(II) at pH 7.2 and 25°C unless noted otherwise.

[c] Not determined.

[d] cyt c [Fe(III)/(II)].

[e] Az[Cu(II)/(I)].

Figure 1. Proton NMR spectra (Bruker WH 500) of (A) horse heart cytochrome *c* and (B) *cis*-[$Ru(en)_2(OH)$(His-33)]-horse heart cytochrome *c* in the region of imidazole ^1H resonances. Solution conditions: pH 5.5, D_2O/DCl; internal DSS).

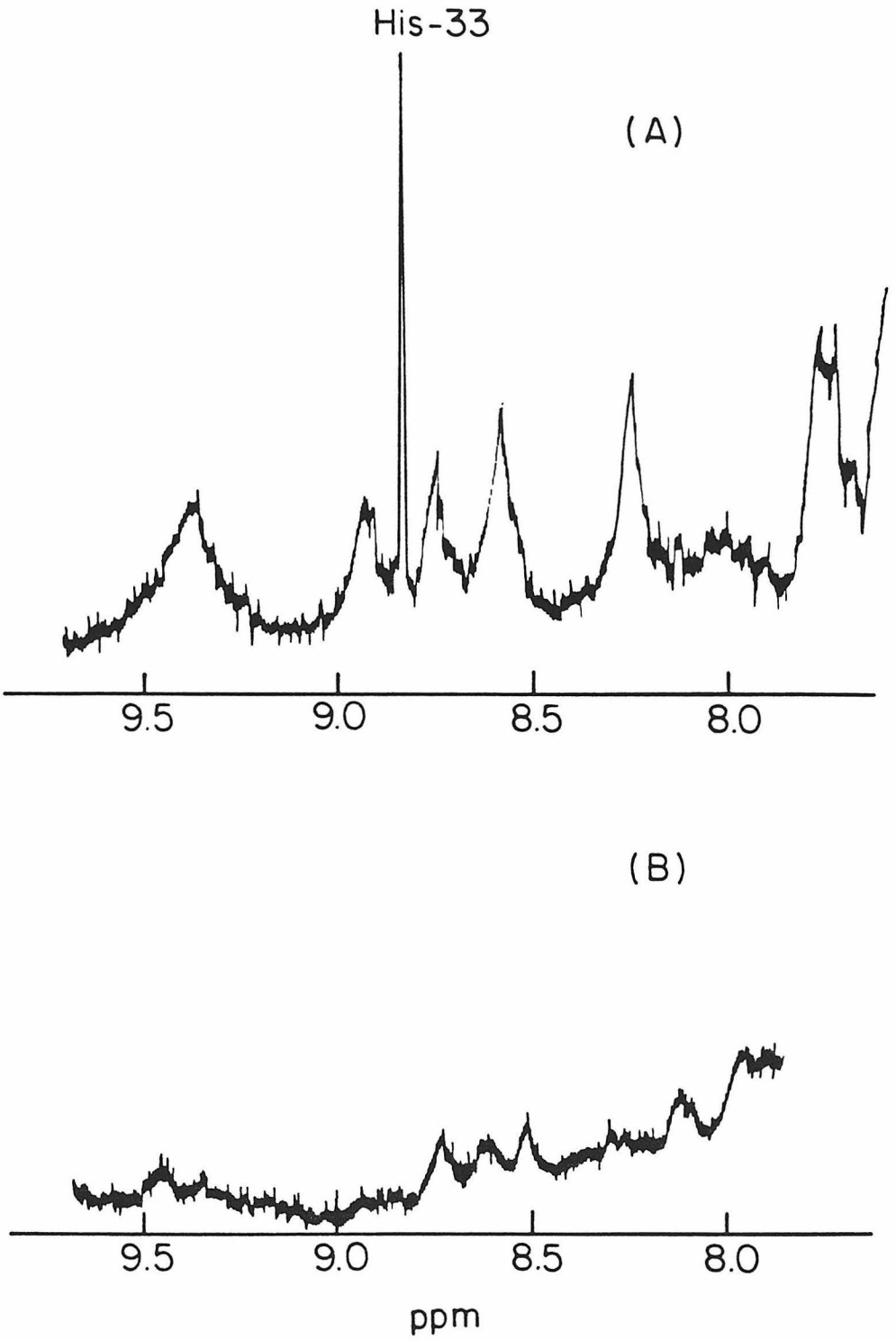
His-33
(A)
9.5
9.0
8.5
8.0
(B)
9.5
9.0
8.5
8.0
ppm

work on $Ru(NH_3)_5$-proteins.[15,16,18,21,25,30] Spectroelectrochemical measurements on **C** show that the structure of the redox-active metal site (heme c) is intact in the modified protein.

At pH 7.2, and in tris•HCI buffer, the $E^{0\prime}$ values of *cis*-$[Ru(en)_2(OH)(His)]^{2+/+}$ in products **A** ~ **D** are in the range -0.07 to -0.13 V *vs.* NHE; these $E^{0\prime}$ values are comparable to that found for *cis*-$[Ru(NH_3)_4(OH)(His)]^{2+/+}$ (-0.10 V *vs.* NHE) in product **E**. The electrochemical results suggest that the sites of ruthenium-amine binding in products **A** ~ **E** are similar. The decrease in $E^{0\prime}$ from *trans*-$[Ru(NH_3)_3(Im)(OH_2)]^{3+}$ (0.12 V)[26] to *cis*-$[Ru(NH_3)_4(OH)(His)]^{2+}$ (-0.10 V) to *trans*-$[Ru(NH_3)_4(Im)(SO_4)]^{+}$ (-0.37 V)[31] parallels the decreasing charge on the Ru(III)-amine complexes. Thus the observed pH dependence of the $E^{0\prime}$ values (*e.g.*, **C**: pH 7.2, -0.13 V; pH 4.0, 0.013 V) of the ruthenium-amine derivatives, is consistent with the formulation *cis*-$[Ru(en)_2(OH)(His)]^{2+}$ at pH 7.2.

The UV-VIS absorption spectra of **D** and **E** in Figure 2, clearly show the blue copper signature; the bands at ~ 390 and 430 nm are probably due to *cis*-$[Ru(NH_3)_4(OH)(His)]^{2+}$ and *cis*-$[Ru(en)_2(OH)(His)]^{2+}$ respectively. A similar UV-VIS absorption spectrum has been found for *cis*-$[Ru(en)_2(OH)(His\text{-}81)]$-horse heart myoglobin ($\lambda_{max}$ ~ 450 nm). Virtually the same UV-VIS absorption spectrum is obtained from the product of the reaction of *cis*-$[Ru(en)_2(OH_2)_2]^{2+}$ with imidazole, under similar conditions.

It appears that *cis*-$[Ru(en)_2(OH_2)_2]^{2+}$ is very similar to $[Ru(NH_3)_5(OH_2)]^{2+}$ as a protein modification reagent. With horse

Figure 2. UV-VIS absorption spectra of (A) *cis*-[$Ru(en)_2$(OH)(His-83)]-azurin from *Pseudomonas aeruginosa* and (B) *cis*-[$Ru(NH_3)_4$(OH)(His-83)]-azurin from *Pseudomonas aeruginosa.* Solution conditions: pH 7.2, 25 ^{0}C, tris•HCl buffer.

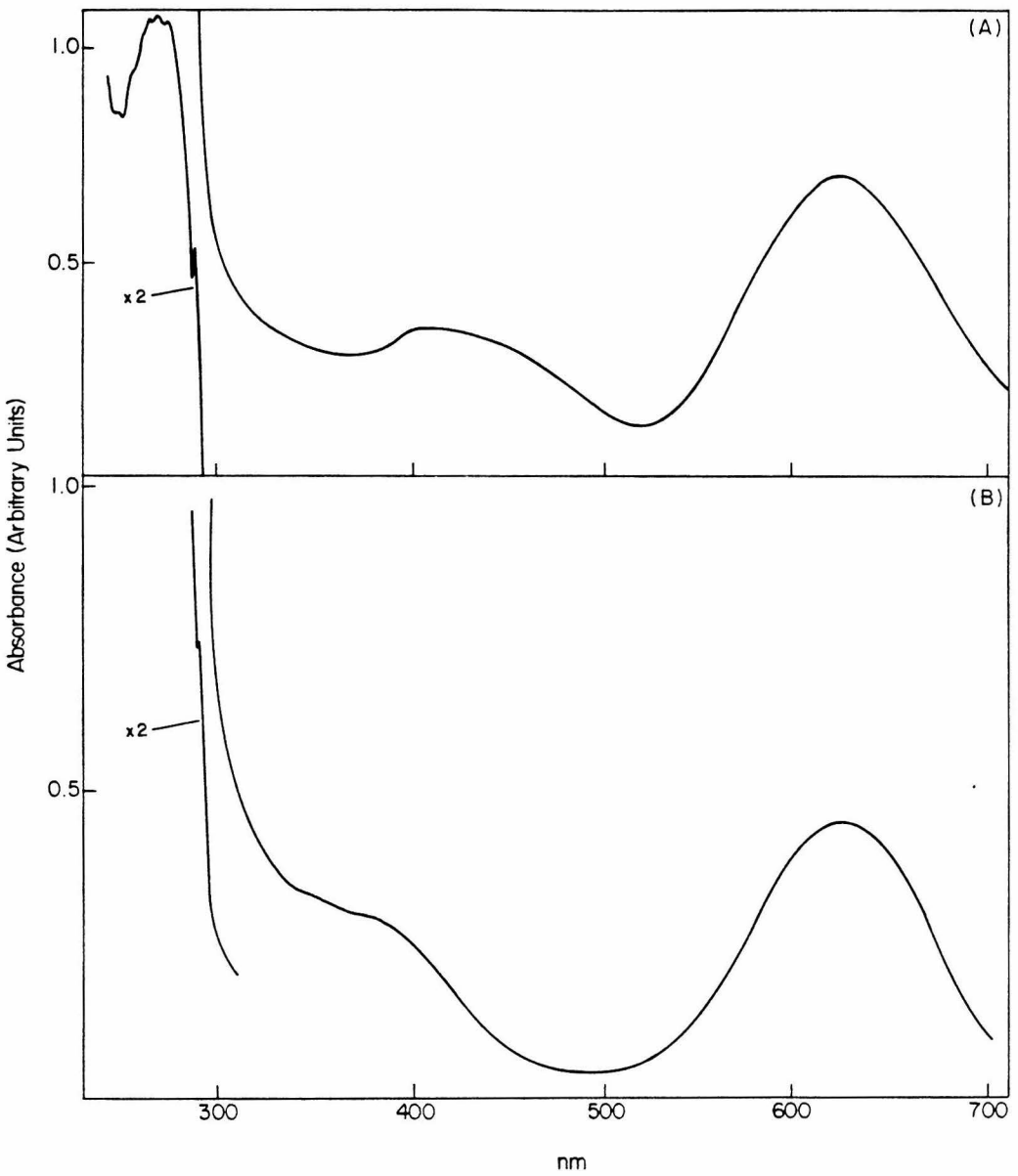
(A)
(B)
1.0
0.5
x2
Absorbance (Arbitrary Units)
300
400
500
600
700
nm

heart cytochrome *c* and *Pseudomonas aeruginosa* azurin, the same histidine (His-33 and His-83, respectively) are labelled; and, with horse heart myoglobin, His-81, which is one of the major products of the reaction[15,16,21] of $[Ru(NH_3)_5(OH_2)]^{2+}$ with sperm whale myoglobin, is readily modified.

The formal reduction potential of the heme center in *cis*-$[Ru(en)_2(OH)(His\text{-}33)]$-horse heart cytochrome *c*, was determined by spectroelectrochemistry in pH 7.0, 100 mM phosphate buffer. Figure 3 shows the overlay spectra and absorbance changes at different values of the applied potentials. The value of 265 ± 2 mV *vs.* NHE at 25 ^{0}C is very similar to the formal reduction potential of native horse heart cytochrome *c*, which is 260 ± 2 mV under identical conditions.[32] The results for the temperature dependence of the formal reduction potential of *cis*-$[Ru(en)_2(OH)(His\text{-}33)]$-horse heart cytochrome *c* are presented in Table 2 and illustrated in Figure 5. The derived thermodynamic parameters are as follows: $\Delta S^{0\prime}$, -24.4 ± 1.2 eu; $\Delta S^{0\prime}_{et}$, -8.8 ± 1.2 eu; $\Delta G^{0\prime}$, -6.11 ± 0.05 kcal/mol; and $\Delta H^{0\prime}$, -13.4 ± 0.4 kcal/mol. Table 3 and Figure 6 present the electrochemical results of native horse heart cytochrome *c*.[32] Comparative summarization of the electrochemical and thermodynamic properties of native and *cis*-$[Ru(en)_2(OH)(His\text{-}33)]$-modified horse heart cytochrome *c* are shown in Table 4 and in Figure 7.

The formal reduction potentials of the Ru sites in the *cis*-$[Ru(en)_2(OH)(His)]^{2+}$-proteins are roughly 0.25 V lower than those of the $Ru(NH_3)_5^{3+}$ analogues. In line with this finding, neither **A** nor **B**

Figure 3. Thin-layer spectroelectrochemistry of *cis*-$[Ru(en)_2(OH)(His\text{-}33)]$-horse heart cytochrome *c*. Solution conditions: pH 7.0, μ = 100 mM, phosphate buffer, 16.6 ^{0}C. Protein concentration: 0.26 mM. Redox mediator: $[Ru(NH_3)_5(py)](Cl0_4)_3$, 1.30 mM. Overlay spectra and absorbance changes at different values of the applied potentials in mV *vs.* SCE.

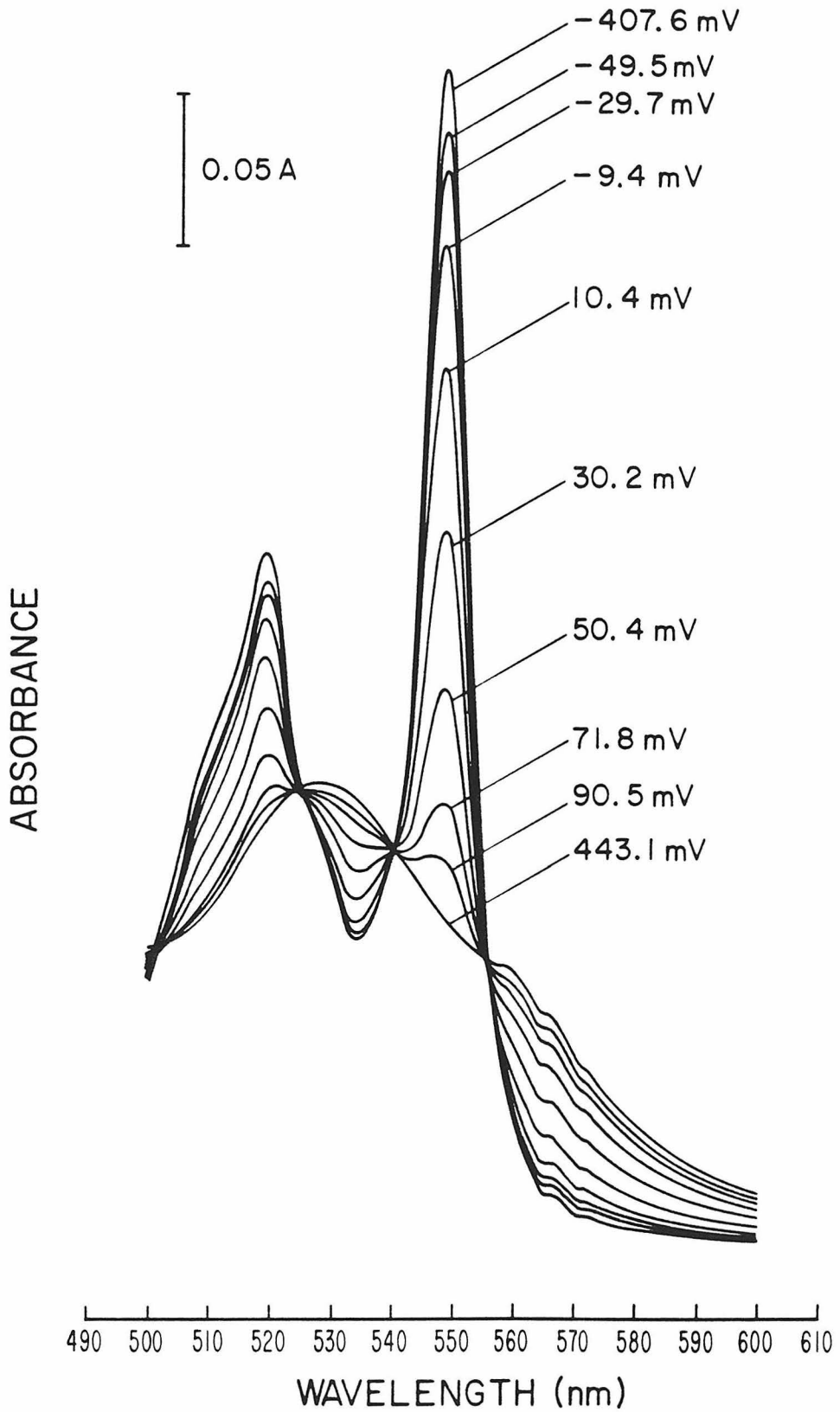
-407.6 mV
-49.5 mV
-29.7 mV
-9.4 mV
10.4 mV
30.2 mV
50.4 mV
71.8 mV
90.5 mV
443.1 mV
0.05 A
ABSORBANCE
490 500 510 520 530 540 550 560 570 580 590 600 610
WAVELENGTH (nm)

Figure 4. Nernst plot of the absorbance changes at 549 nm during a spectroelectrochemical titration of the iron center in *cis*-[Ru(en)$_2$(OH)(His-33)]-horse heart cytochrome *c*. The circles represent experimental points, and the line is a least squares fit of the $E_{appl.}$ *vs.* log([Ox]/[Red]). The fit yielded $E^{0\prime}$ = 265 mV *vs.* NHE and Nernst slope = 61 mV. Solution conditions: pH = 7.0, μ = 100 mM, phosphate buffer, 25.0 ^{0}C, 5 equivalents [Ru(NH$_3$)$_5$(py)](Cl0$_4$)$_3$.

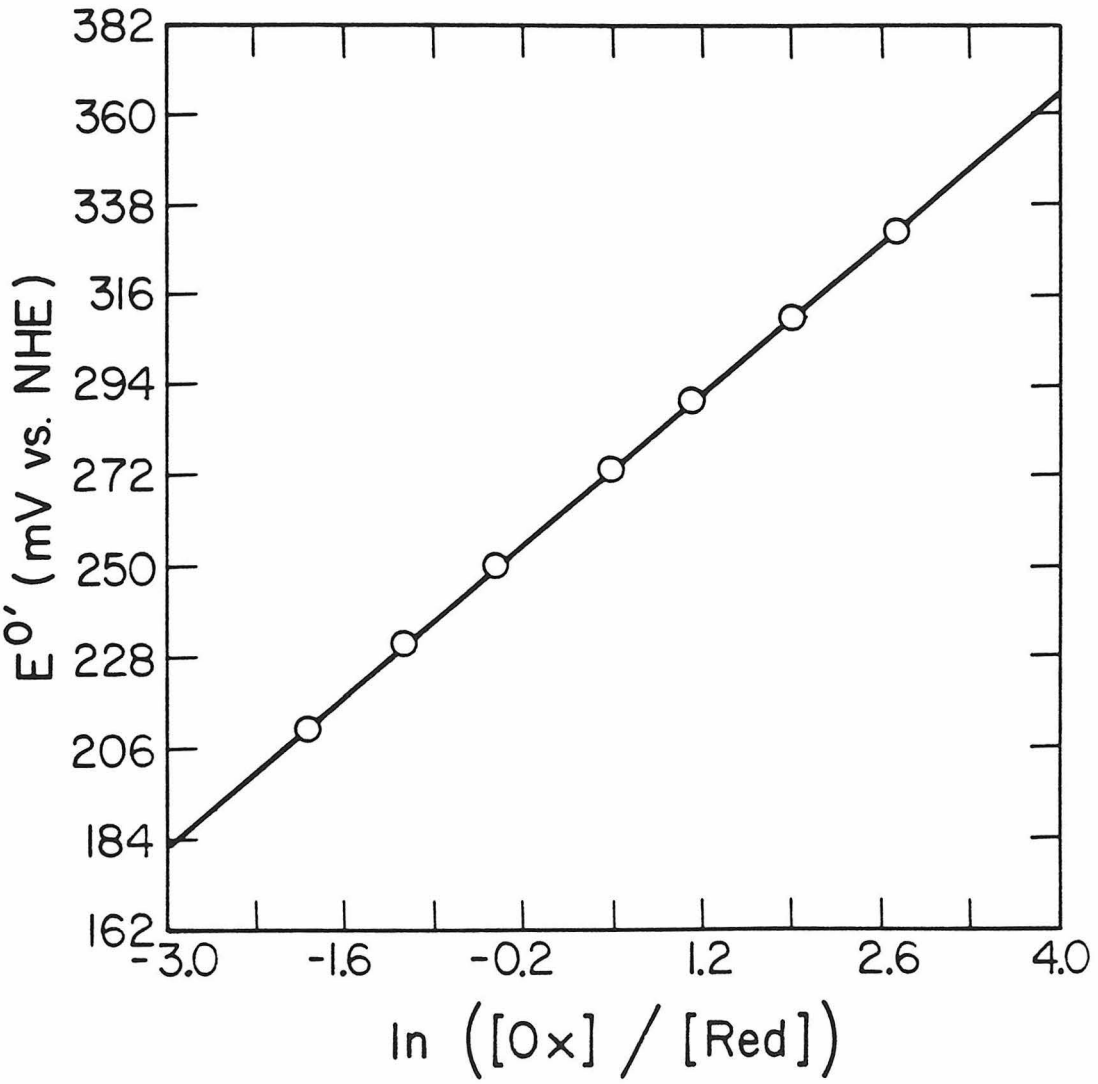
382
360
338
316
294
272
250
228
206
184
162
E°' (mV vs. NHE)
-3.0
-1.6
-0.2
1.2
2.6
4.0
ln ([Ox] / [Red])

Table 2. Temperature dependence of the formal reduction potentials, $E^{0\prime}$, for the heme center in *cis*-[Ru(en)$_2$(OH)(His-33)]-horse heart cytochrome *c*, using nonisothermal thin-layer spectroelectrochemistry. Solution conditions: pH 7.0, μ = 100 mM, phosphate buffer.

Temperature (^{0}C)*	$E^{0\prime}$ (mV vs. NHE)†
9.2	271
16.6	269
25.0	265

* ± 0.2 ^{0}C

† ± 2 mV

Figure 5. Temperature dependence of the formal reduction potentials, $E^{0\prime}$, for the heme center in *cis*-[$Ru(en)_2(OH)$(His-33)]-horse heart cytochrome *c*, using nonisothermal thin-layer spectroelectrochemistry. Solution conditions: pH 7.0, μ = 100 mM, phosphate buffer. Temperature range: 9.2 ~ 25.0 ^{0}C. A least squares fit of the data gave an $E^{0\prime}$ = 265 ± 2 mV at 25 ^{0}C and $(dE^{0\prime}/dT)_{25\ ^0C}$ = -3.82 x 10^{-4} V/^{0}C.

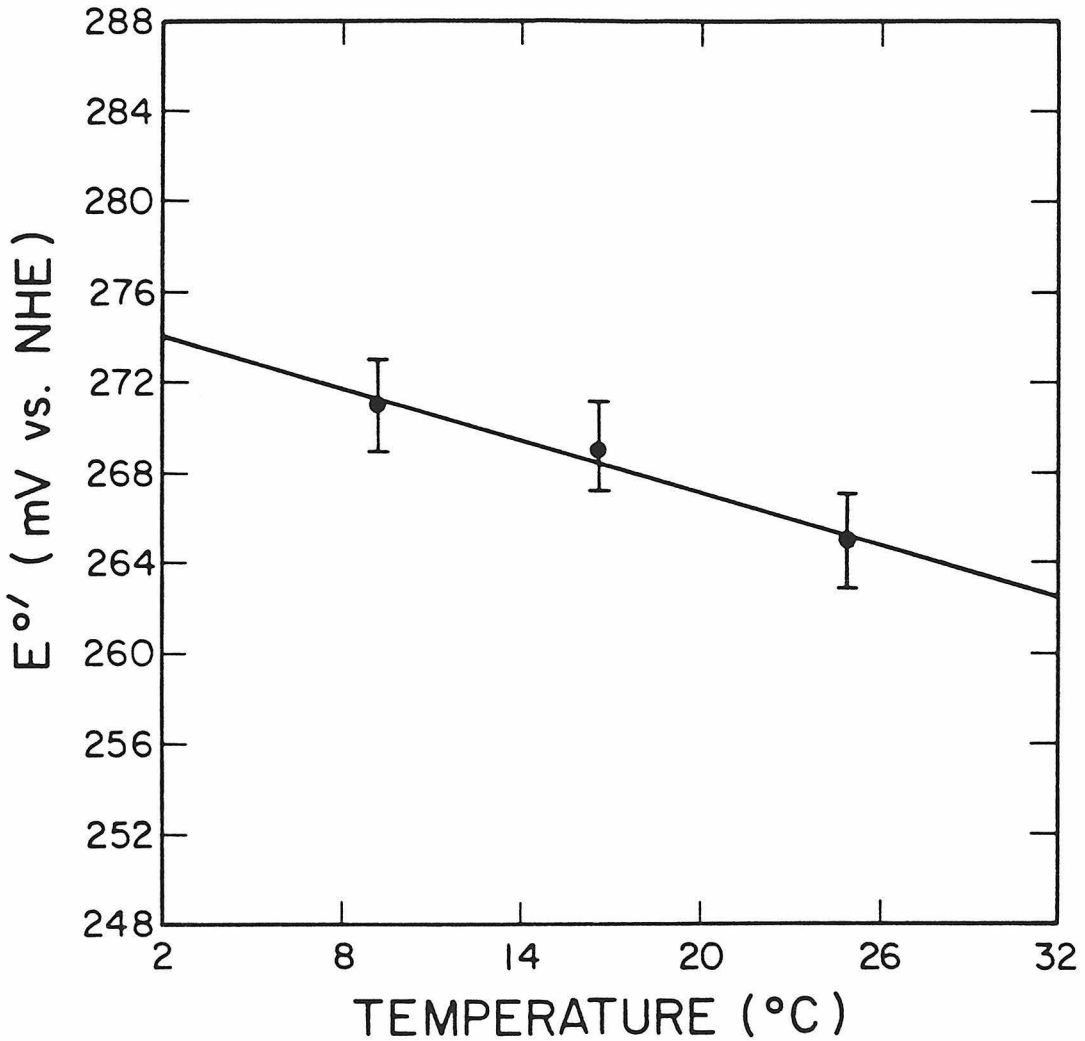
288
284
280
276
272
268
264
260
256
252
248
E°′ (mV vs. NHE)
2
8
14
20
26
32
TEMPERATURE (°C)

Table 3. Temperature dependence of the formal reduction potentials, $E^{0\prime}$, for the heme center in native horse heart cytochrome *c*, using nonisothermal thin-layer spectroelectrochemistry. Solution conditions: pH 7.0, μ = 100 mM, phosphate buffer.

Temperature (^{0}C)*	$E^{0\prime}$ (mV vs. NHE)†
8.6	269
9.2	270
15.5	267
16.8	265
19.8	262
20.2	263
24.4	262
29.8	257
30.6	258
35.2	254
39.4	253

* ± 0.2 ^{0}C

† ± 2 mV

Figure 6. Temperature dependence of the formal reduction potential, $E^{0\prime}$, for the heme center in native horse heart cytochrome *c*, using nonisothermal thin-layer spectroelectrochemistry. Solution conditions: pH = 7.0, μ = 100 mM, phosphate buffer. Temperature range: 8.6 ~ 39.4 ^{0}C. A least squares fit of the data gave an $E^{0\prime}$ = 260 ± 2 mV at 25.0 ^{0}C and $(dE^{0\prime}/dT)_{25\ ^{0}C}$ = -5.61 x 10^{-4} V/^{0}C.

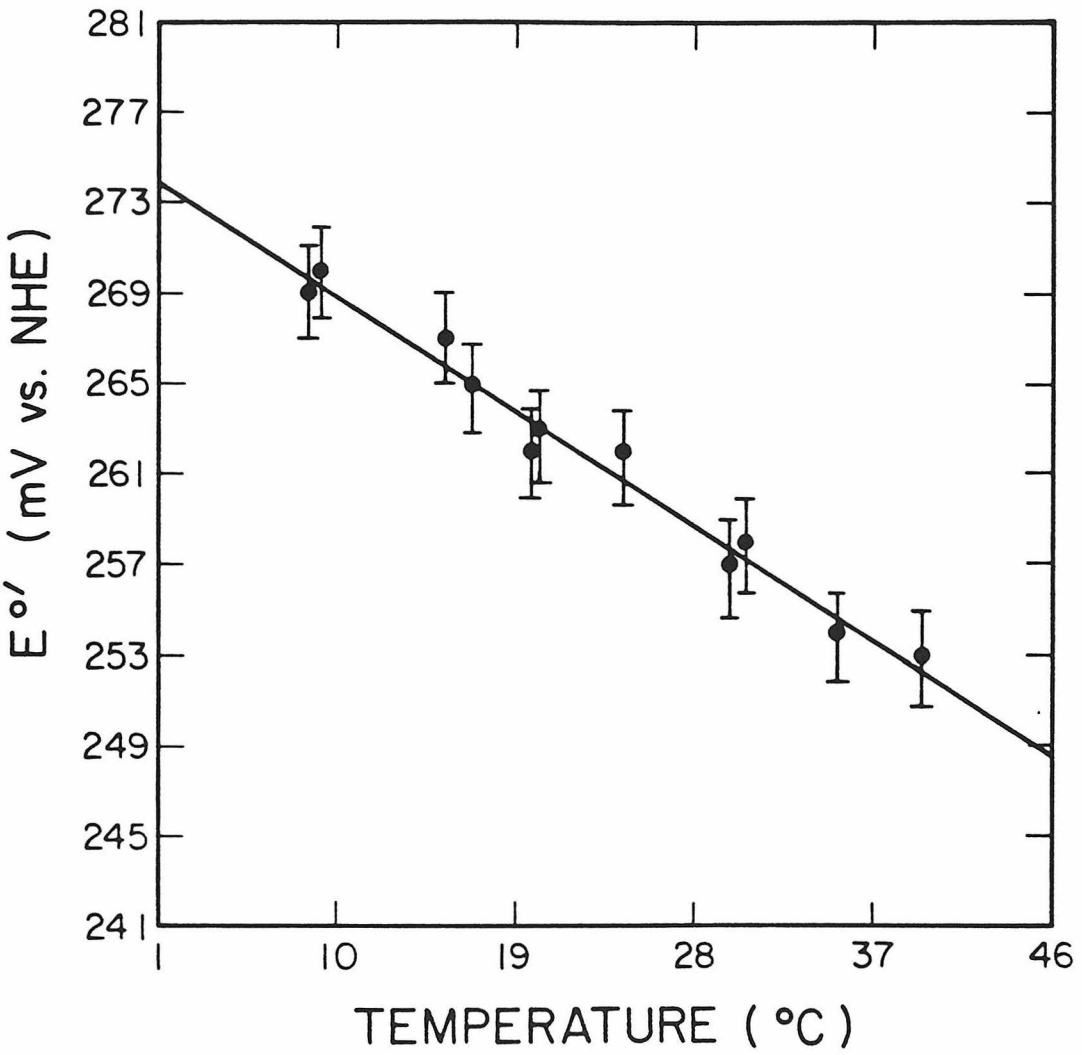
281
277
273
269
265
261
257
253
249
245
241
E°′ (mV vs. NHE)
1
10
19
28
37
46
TEMPERATURE (°C)

Figure 7. Temperature dependence of the formal reduction potential, $E^{0\prime}$, for the heme centers in native (O) and in *cis*-[$Ru(en)_2(OH)$(His-33)]-modified (X) horse heart cytochrome c. Solution conditions: pH 7.0, μ = 100 mM, phosphate buffer.

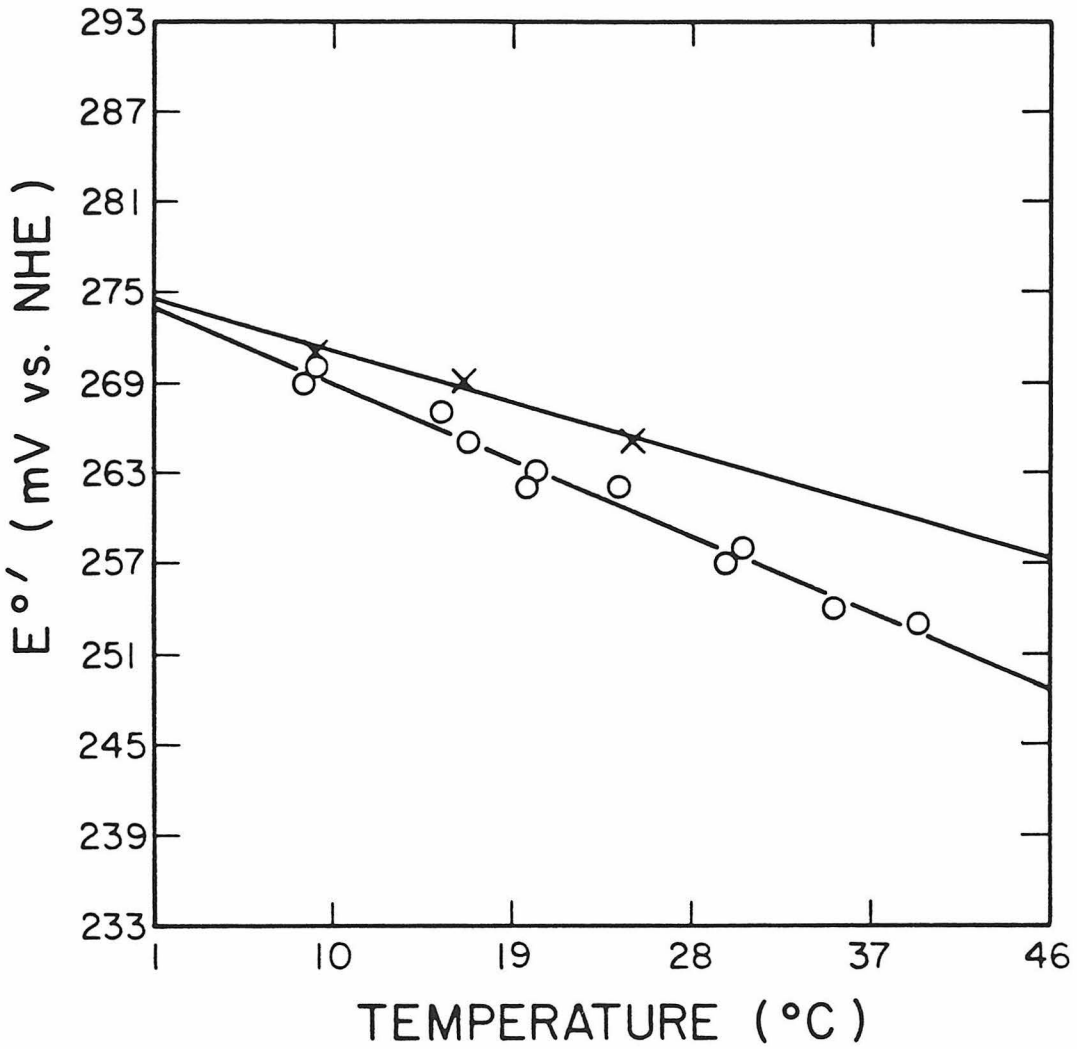
293
287
281
275
269
263
257
251
245
239
233
E°′ (mV vs. NHE)
1
10
19
28
37
46
TEMPERATURE (°C)

Table 4. Thermodynamic parameters for the reduction of the heme centers in native and in *cis*-[$Ru(en)_2(OH)$(His-33)]-modified horse heart cytochrome *c* at pH 7.0, μ = 100 mM, phosphate buffer, 25 ^{0}C.

	Native Cyt. *c* pH 7.0, 0.1 M Phosphate	*cis*-[Ru(en)$_2$(OH)(His-33)]-Cyt. *c* pH 7.0, 0.1 M Phosphate
$E^{0\prime}$ at 25 ^{0}C (mV vs. NHE)	260	265
$\Delta S^{0\prime}$ (eu)	-28.5	-24.4
$\Delta S^{0\prime}_{et}$ (eu)	-12.9	-8.8
$\Delta G^{0\prime}$ (kcal/mol)	-6.00	-6.11
$\Delta H^{0\prime}$ (kcal/mol)	-14.5	-13.4

catalyzes the aerial oxidation of ascorbate. This lack of reactivity in the low potential derivatives suggests that electron transfer from ascorbate to Ru(III) plays a key role in the observed[21] catalytic activity of $(Ru(NH_3)_5)_3$-sperm whale myoglobin.

References

1. Brunschwig, B. S., DeLaive, P. J., English, A. M., Goldberg, M., Gray, H. B., Mayo, S. L., and Sutin, N., *Inorg. Chem.*, ***24***, 3742 (1985).

2. English, A. M., Lum, V. R., DeLaive, P. J., and Gray, H. B., *J. Am. Chem. Soc.*, ***104***, 870 (1982).

3. Mauk, A. G., Bordignon, E., and Gray, H. B., *J. Am. Chem. Soc.*, ***104***, 7654 (1982).

4. Gray, H. B., Coyle, C. L., Dooley, D. M., Grunthaner, P. J., Hare, J. W., Holwerda, R. A., McArdle, J. V., McMillin, D. R., Rawlings, J., Rosenberg, R. C., Sailasuta, N., Solomon, E. I., Stephens, P. J., Wherland, S., and Wurzbach, J. A., in *Advances in Chemistry Series, No. 162, Bioinorganic Chemistry-II*, Raymond, K. N., ed., American Chemical Society, Washington, D. C., 1977, P. 145.

5. McArdle, J. V., Coyle, C. L., Gray, H. B., Yoneda, G. S., and Holwerda, R. A., *J. Am. Chem. Soc.*, ***99***, 2483 (1977).

6. Holwerda, R. A., Wherland, S., and Gray, H. B., in *Annual Review of Biophysics and Bioengineering*, Volume 5, Mullins, L. J., ed., Annual Reviews Inc., Palo Alto, 1976, P. 363.

7. Cummins, D., and Gray, H. B., *Inorg. Chem.*, ***20***, 3712 (1981).

8. Holwerda, R. A., Knaff, D. B., Gray, H. B., Clemmer, J. D., Crowley, R., Smith, J. M., and Mauk, A. G., *J. Am. Chem. Soc.*, ***102***, 1142 (1980).

9. McArdle, J. V., Yocum, K., and Gray, H. B., *J. Am. Chem. Soc.*, ***99***, 4141 (1977).

10. Coyle, C., and Gray, H. B., *Biochem. Biophys. Res. Comm.*, ***73***, 1122 (1976).

11. Wherland, S., and Gray, H. B., *Proc. Natl. Acad. Sci. USA*, ***73***, 2950 (1976).

12. McArdle, J. V., Gray, H. B., Creutz, C., and Sutin, N., *J. Am. Chem. Soc.*, ***96***, 5737 (1974).

13. Wherland, S., and Gray, H. B., in *Biological Aspects of Inorganic Chemistry*, Addison, A. W., Cullen, W. R., Dolphin, D., and James, B. R., eds., Wiley, New York, 1977, P. 289.

14. Hush, N. S., *Coord. Chem. Rev.*, ***64***, 135 (1985).

15. Crutchley, R. J., Ellis, W. R., Jr., and Gray, H. B., in *Frontiers in Bioinorganic Chemistry*, Xavier, A. V., ed., VCH erlagsgesellschaft, Weinheim, F. R. G., 1986, P. 679.

16. Crutchley, R. J., Ellis, W. R., Jr., and Gray, H. B., *J. Am. Chem. Soc.*, ***107***, 5002 (1985).

17. Isied, S. S., Kuehn, C., and Worosila, G., *J. Am. Chem. Soc.*, ***106***, 1722 (1984).

18. Margalit, R., Kostić, N. M., Che, C.-M., Blair, D. F., Chiang, H.-J., Pecht, I., Shelton, J. B., Shelton, J. R., Schroeder, W. A., and Gray, H. B., *Proc. Natl. Acad. Sci. USA*, ***81***, 6554 (1984).

19. Nocera, D. G., Winkler, J. R., Yocom, K. M., Bordignon, E., and Gray, H. B., *J. Am. Chem. Soc.*, ***106***, 5145 (1984).

20. Kostić, N. M., Margalit, R., Che, C.-M., and Gray, H. B., *J. Am. Chem. Soc.*, ***105***, 7765 (1983).

21. Margalit, R., Pecht, I., and Gray, H. B., *J. Am. Chem. Soc.*, ***105***, 301 (1983).

22. Yocom, K. M., Winkler, J. R., Nocera, D. G., Bordignon, E., and Gray, H. B., *Chem. Scr.*, ***21***, 29 (1983).

23. Isied, S. S., Worosila, G., and Atherton, S. J., *J. Am. Chem. Soc.*, ***104***, 7659 (1982).

24. Winkler, J. R., Nocera, D. G., Yocom, K. M., Bordignon, E., and Gray, H. B., *J. Am. Chem. Soc.*, ***104***, 5798 (1982).

25. Yocom, K. M., Shelton., J. B., Shelton, J. R., Schroeder, W. A., Worosila, G., Isied, S. S., Bordignon, E., and Gray, H. B., *Proc. Natl. Acad. Sci. USA*, ***79***, 7052 (1982).

26. Tweedle, M. F., and Taube, H., *Inorg. Chem.*, ***21***, 3361 (1982).

27. Poon, C. K., Che, C.-M., and Kan, Y. P., *J. Chem. Soc., Dalton Trans.*, 128 (1980).

28. Che, C.-M., Margalit, R., Chiang, H.-J., and Gray, H. B., *Inorg. Chim. Acta*, ***135***, 33 (1987).

29. Cummins, D., and Gray, H. B., *J. Am. Chem. Soc.*, ***99***, 5158 (1977).

30. Toi, H., La Mar, G. N., Margalit, R., Che, C.-M., and Gray, H. B., *J. Am. Chem. Soc.*, ***106***, 6213 (1984).

31. Isied, S. S., and Kuehn, C. G., *J. Am. Chem. Soc.*, ***100***, 6754 (1978).

32. Taniguchi, V. T., Ellis, W. R., Jr., Cammarata, V., Webb, J., Anson, F. C., and Gray, H. B., in *Advances in Chemistry Series, No. 201, Electrochemical and Spectrochemical Studies of Biological Redox Components,* Kadish, K. M., ed., American Chemical Society, Washington, D. C., 1982, P. 51.

CHAPTER VI

SYNTHESIS AND SPECTROELECTROCHEMISTRY OF [Ru(MpIX)(DMSO) dicarboxylic acid]-RECONSTITUTED MYOGLOBIN

Introduction

In studies of long-range electron transfer reactions of metalloenzymes, two different kinds of hemoproteins have been chosen for investigation, *viz.*, horse heart cytochrome *c*[1-5] and sperm whale myoglobin.[6,7] The prosthetic groups of cytochrome *c* and myoglobin are identical in each case, *i.e.*, iron-protoporphyrin IX, commonly called heme, and the molecular structure of the basic heme unit is shown in Figure 1.

Cytochrome *c* is present in all organisms possessing mitochondrial respiratory chains, and its conformation has remained essentially constant for at least one billion years.[8] It's role in the respiratory process is to carry electrons from the QH_2-cytochrome *c* reductase complex, the second energy-conserving site, to cytochrome *c* oxidase, the third energy-conserving site.[9,10]

Cytochrome *c*[11-15] consists of a single polypeptide chain of 104 amino acid residues and has a molecular weight of around 12,500 daltons. The three-dimensional structure of reduced cytochrome *c* from tuna is shown in Figure 2.[16] It contains very little α-helix and no β-pleated sheet. The protein is roughly spherical, with a diameter of 34 Å. The heme of cytochrome *c* is covalently attached to the protein by two thioether linkages between the vinyl groups of the heme and cysteine-14 and cysteine-17 residues of the protein. The iron atom is also axially ligated by the sulfur atom of a methionine-80 residue and by the nitrogen atom of a histidine-18 residue.

Figure 1. Molecular structure of iron protoporphyrin IX, which is the prosthetic group in cytochrome *c* and in myoglobin.

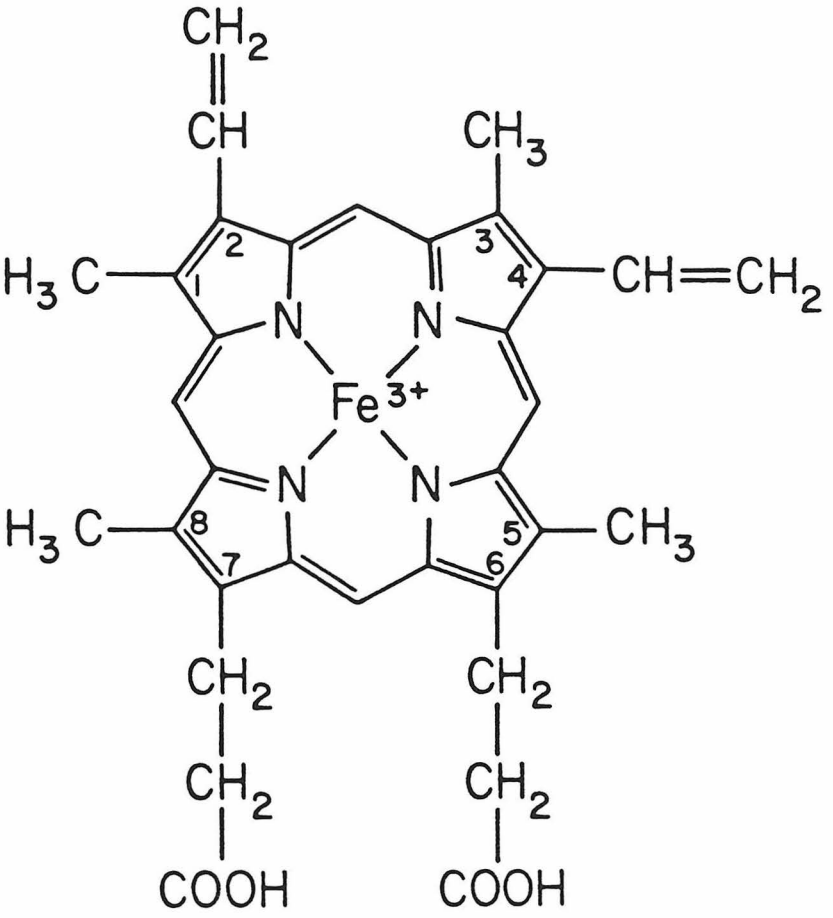
CH2
CH
CH3
H3C
2
1
3
4
CH=CH2
N
N
Fe3+
N
N
H3C
8
7
5
6
CH3
CH2
CH2
CH2
CH2
COOH
COOH

Figure 2. X-ray crystallographic structure of the polypeptide backbone of tuna cytochrome *c* in the reduced form.

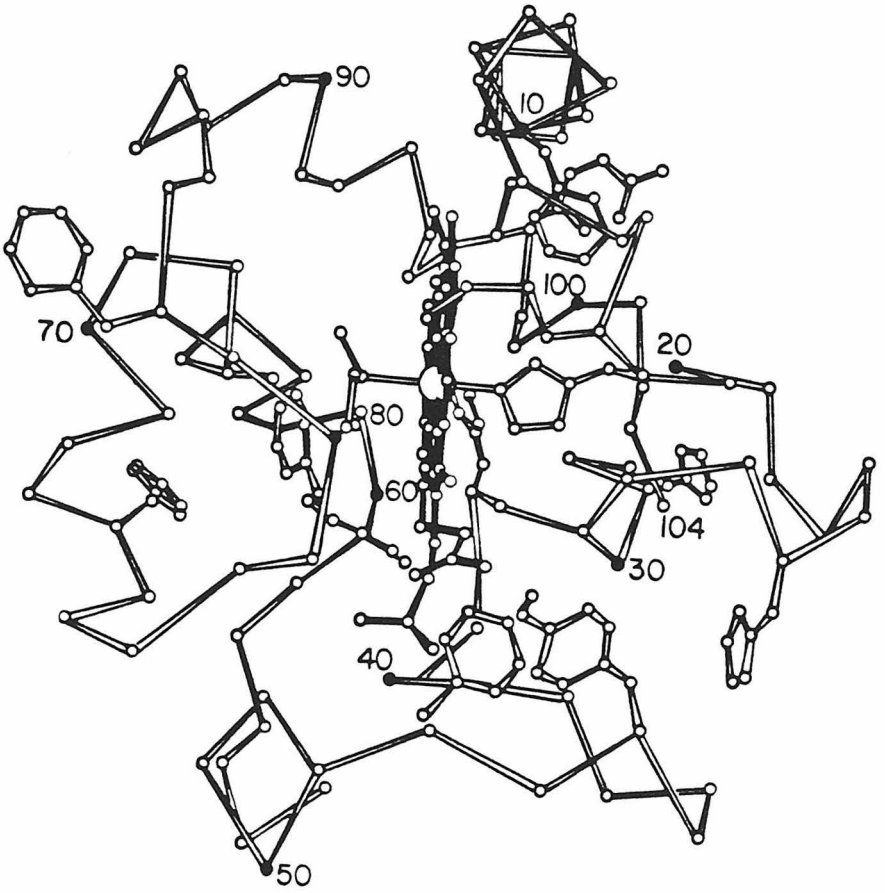
90
10
100
70
20
80
60
104
30
40
50

Myoglobin shows no structural similarity to cytochrome *c*. In vertebrates, myoglobin facilitates the transport of oxygen in muscle and serves as a reserve supply of oxygen in the tissue.[17] It combines reversibly with molecular dioxygen, which it takes up from the blood and passes on to mitochondria in muscle. *In vivo* its iron atom remains ferrous, but *in vitro* it autoxidizes to the ferric metmyoglobin in which the sixth ligand at the iron is water.

The elucidation of the three-dimensional structure of myoglobin by John C. Kendrew,[18] was a landmark in molecular biology, and a structural model of metmyoglobin, based on these X-ray crystallographic studies,[19-21] is illustrated in Figure 3.[22] Further structural studies on oxymyoglobin[20] and deoxymyoglobin[23] have demonstrated the details of the mechanism and structure-function relationship of the oxygen binding process in myoglobin. Myoglobin contains a single polypeptide chain of 153 amino acid residues, with a molecular weight of around 17,800 daltons. The amino acid sequence of sperm whale myoglobin[24] is shown in Figure 4.[6] The most striking structural feature of myoglobin lies in its irregularity, and its total lack of symmetry. It is extremely compact, the overall dimensions are *ca.* 45 x 35 x 25 Å, with very little interior room for water molecules. About 75% of the main chain is folded in an α-helical conformation. The interior consists almost entirely of non-polar residues, the only polar residues inside myoglobin being two histidines, *viz.*, a proximal histidine-93, which is the fifth coordination ligand for the iron atom, and a distal histidine-64,

Figure 3. X-ray crystallographic structure of the polypeptide backbone of sperm whale myoglobin in the oxidized form. The amino acid residues are identified by the single-letter code.

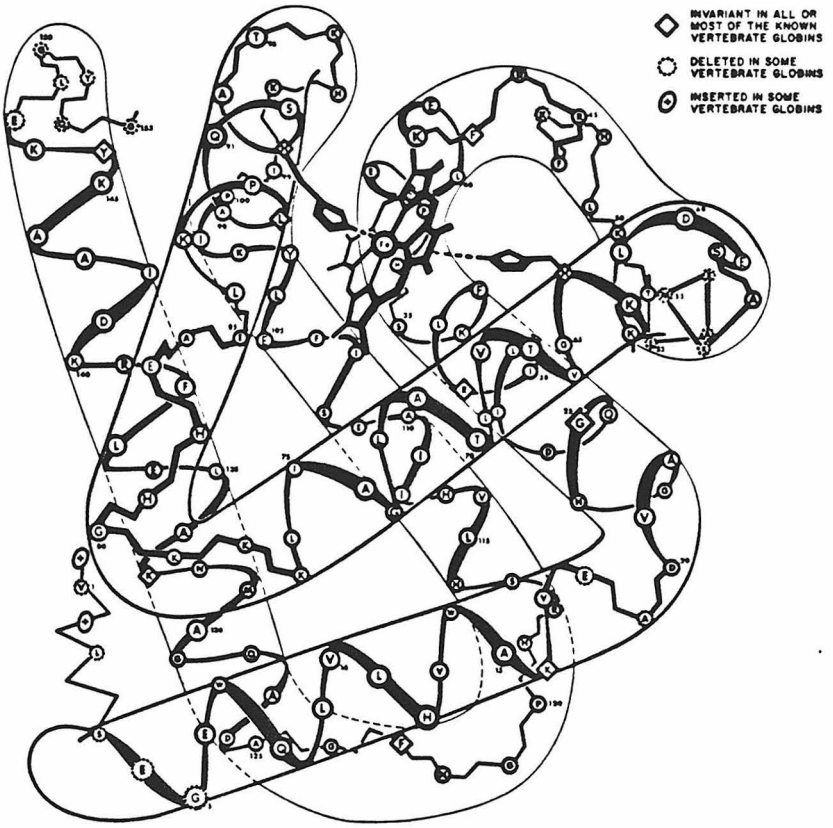
INVARIANT IN ALL OR MOST OF THE KNOWN VERTEBRATE GLOBINS
DELETED IN SOME VERTEBRATE GLOBINS
INSERTED IN SOME VERTEBRATE GLOBINS

Figure 4. The amino acid sequence of sperm whale myoglobin. Peptide T1 through T23 were obtained after digestion of myoglobin with trypsin.

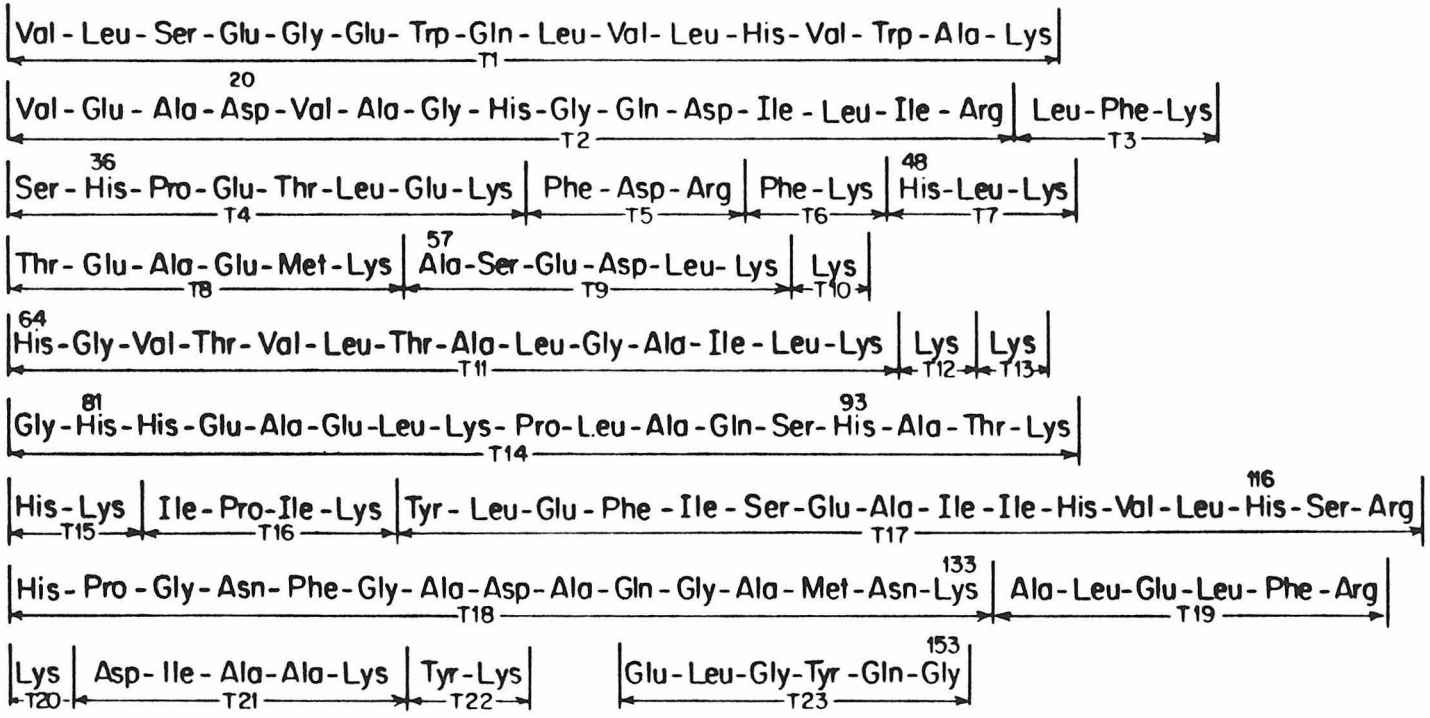
Val - Leu - Ser - Glu - Gly - Glu - Trp - Gln - Leu - Val - Leu - His - Val - Trp - Ala - Lys
T1
20
Val - Glu - Ala - Asp - Val - Ala - Gly - His - Gly - Gln - Asp - Ile - Leu - Ile - Arg
T2
Leu - Phe - Lys
T3
36
Ser - His - Pro - Glu - Thr - Leu - Glu - Lys
T4
Phe - Asp - Arg
T5
Phe - Lys
T6
48
His - Leu - Lys
T7
Thr - Glu - Ala - Glu - Met - Lys
T8
57
Ala - Ser - Glu - Asp - Leu - Lys
T9
Lys
T10
64
His - Gly - Val - Thr - Val - Leu - Thr - Ala - Leu - Gly - Ala - Ile - Leu - Lys
T11
Lys
T12
Lys
T13
81
Gly - His - His - Glu - Ala - Glu - Leu - Lys - Pro - Leu - Ala - Gln - Ser - 93 His - Ala - Thr - Lys
T14
His - Lys
T15
Ile - Pro - Ile - Lys
T16
Tyr - Leu - Glu - Phe - Ile - Ser - Glu - Ala - Ile - Ile - His - Val - Leu - 116 His - Ser - Arg
T17
His - Pro - Gly - Asn - Phe - Gly - Ala - Asp - Ala - Gln - Gly - Ala - Met - Asn - 133 Lys
T18
Ala - Leu - Glu - Leu - Phe - Arg
T19
Lys
T20
Asp - Ile - Ala - Ala - Lys
T21
Tyr - Lys
T22
Glu - Leu - Gly - Tyr - Gln - 153 Gly
T23

which is close to the position of the sixth coordination site of the iron atom. The sixth coordination site of the heme unit is the binding site for oxygen. The heme iron in myoglobin is high-spin in both ferric and ferrous oxidation states, in contrast to the low-spin heme iron in cytochrome *c*,[25,26] and the spin state of the heme certainly plays an important role in the control of the electron transfer kinetics of heme-containing oxidase and oxygenase enzymes.[27] Although the spin state itself will probably not determine the redox kinetics of a heme site, a change in heme geometry is expected to result in slow electron transfer.[28,29] Tables 1[2,7] and 2[1,4,30] compare thermodynamic and kinetic data for the intramolecular electron transfer reaction in ruthenated horse heart cytochrome *c* and sperm whale myglobin. It shows that the reorganization energy of the myoglobin high spin heme is much larger than that for the low spin heme in cytochrome *c*.

Ruthenium substituted heme, whose structure is depicted in Figure 5, is low-spin in both the +3 and +2 states. It appeared therefore, that substituting myoglobin with ruthenium porphyrin, would allow study of the effects of changing both the driving force and the reorganization energy, on the intramolecular electron transfer rate.

Materials and Methods

Ruthenium porphyrin[31] compounds were synthesized by Dr. Chi-Ming

Table 1. Thermodynamic parameters for the reduction of the heme centers in native and in $(NH_3)_5Ru^{3+/2+}$ modified horse heart cytochrome *c* as well as in native and $(NH_3)_5Ru^{3+/2+}$ modified sperm whale myoglobin. Solution conditions: pH 7.0, μ = 100 mM, phosphate buffer, 25 ^{0}C.

Measure	a_5Ru(His-33)Cyt *c*	Native Cyt *c*	Native Mb $Fe^{3+/2+}$	Modified Mb $Fe^{3+/2+}$	Modified Mb $a_5Ru^{3+/2+}$
$E^{0\prime}$(mV vs. NHE)	270 ± 2	260 ± 2	60 ± 2	65 ± 2	86 ± 2
$\Delta G^{0\prime}$(kcal/mol)	-6.22 ± 0.05	-6.00 ± 0.05	-1.36 ± 0.05	-1.51 ± 0.05	-1.98 ± 0.05
$\Delta S^{0\prime}$(cal/deg•mol)	-29.2 ± 0.8	-28.5 ± 1.2	-39.2 ± 1.2	-37.6 ± 1.2	4.2 ± 1.2
$\Delta H^{0\prime}$(kcal/mol)	-14.9 ± 0.3	-14.5 ± 0.4	-13.0 ± 0.4	-12.7 ± 0.4	-0.7 ± 0.4

Table 2. Intramolecular long-range electron transfer kinetics in $(NH_3)_5Ru^{3+/2+}$ modified horse heart cytochrome *c* and sperm whale myoglobin.

	Edge-to-edge distance between $[a_5Ru(His)^{3+/2+}$ and heme ($Fe^{3+/2+}$) (Å)	Ru^{2+}-PFe^{3+} $\longrightarrow$ Ru^{3+}-PFe^{2+} k_1 (sec^{-1})
$[a_5Ru(His-33)]$-Cyt. *c*	12.1	30*
		50†
$[a_5Ru(His-48)]$-Mb	14.6	0.019‡

*Flash photolysis.

†Pulse radiolysis.

‡Backward rate constant k_{-1} is 0.041 sec^{-1}.

Figure 5. Molecular structure of ruthenium mesoporphyrin IX.

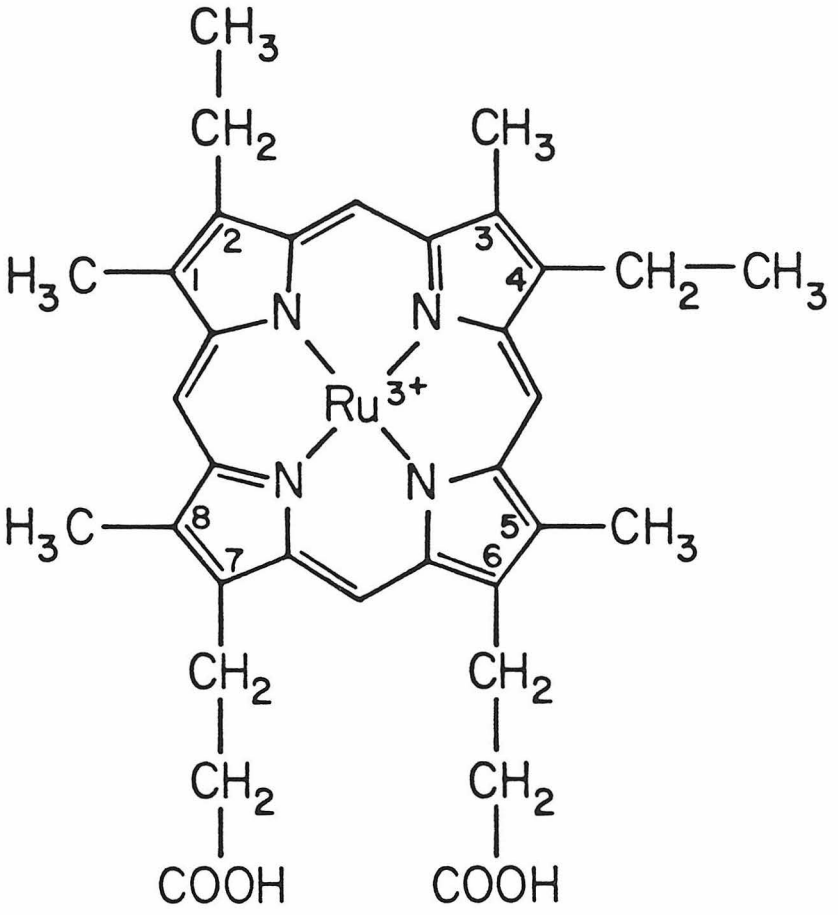
CH3
CH2
CH3
H3C
CH2—CH3
N
N
Ru3+
N
N
H3C
CH3
CH2
CH2
CH2
CH2
COOH
COOH

Che. Equal weights of ruthenium dodecacarbonyl ($Ru_3(CO)_{12}$, Strem Chemical Co.) and mesoporphyrin IX dimethyl ester (Sigma Chemical Co.) were refluxed under nitrogen, in toluene for 24 hours. The toluene was removed by under reduced pressure, and the residue dissolved in 50:50 ethanol/dichloromethane and refluxed under nitrogen for an additional 30 minutes. The solid residue was chromatographed over neutral alumina using dichloromethane as eluting solvent. The dichloromethane was again removed under reduced pressure, and the solid residue was washed with petroleum ether and dried in vacuum to give ruthenium(II)(CO) mesoporphyrin IX dimethyl ester. The ruthenium(II)(CO) mesoporphyrin IX dicarboxylic acid was prepared by refluxing the dimethyl ester derivative in ethanol containing 2% potassium hydroxide for at least six hours to remove the dimethyl ester. The ethanol was removed by rotary evaporation, and the solid residue was recrystallized from acetone/water. The visible spectrum of ruthenium(II)(CO) mesoporphyrin IX dicarboxylic acid in dimethyl sulfoxide (DMSO) is shown in Figure 6.

$Ru^{II}(MpIX)(DMSO)_2$ dicarboxylic acid was prepared by degassing a dimethyl sulfoxide solution of $Ru^{II}(MpIX)(CO)$ dicarboxylic acid through five freeze-thaw cycles and irradiating with a 1,000-watt tungsten lamp. The light of wavelength shorter than 300 nm was filtered out. After every nine to ten hours irradiation, the sample was degassed again through five freeze-thaw cycles. The result was monitored spectroscopically as shown in Figure 7. For 32.5 mg of $Ru^{II}(MpIX)(CO)$ dicarboxylic acid in 20 ml dimethyl sulfoxide, the

Figure 6. Absorption spectra of ruthenium(II)(CO) mesoporphyrin IX dicarboxylic acid in dimethyl sulfoxide (DMSO). The wavelengths of peaks are 548, 516, 399, and 341 nm.

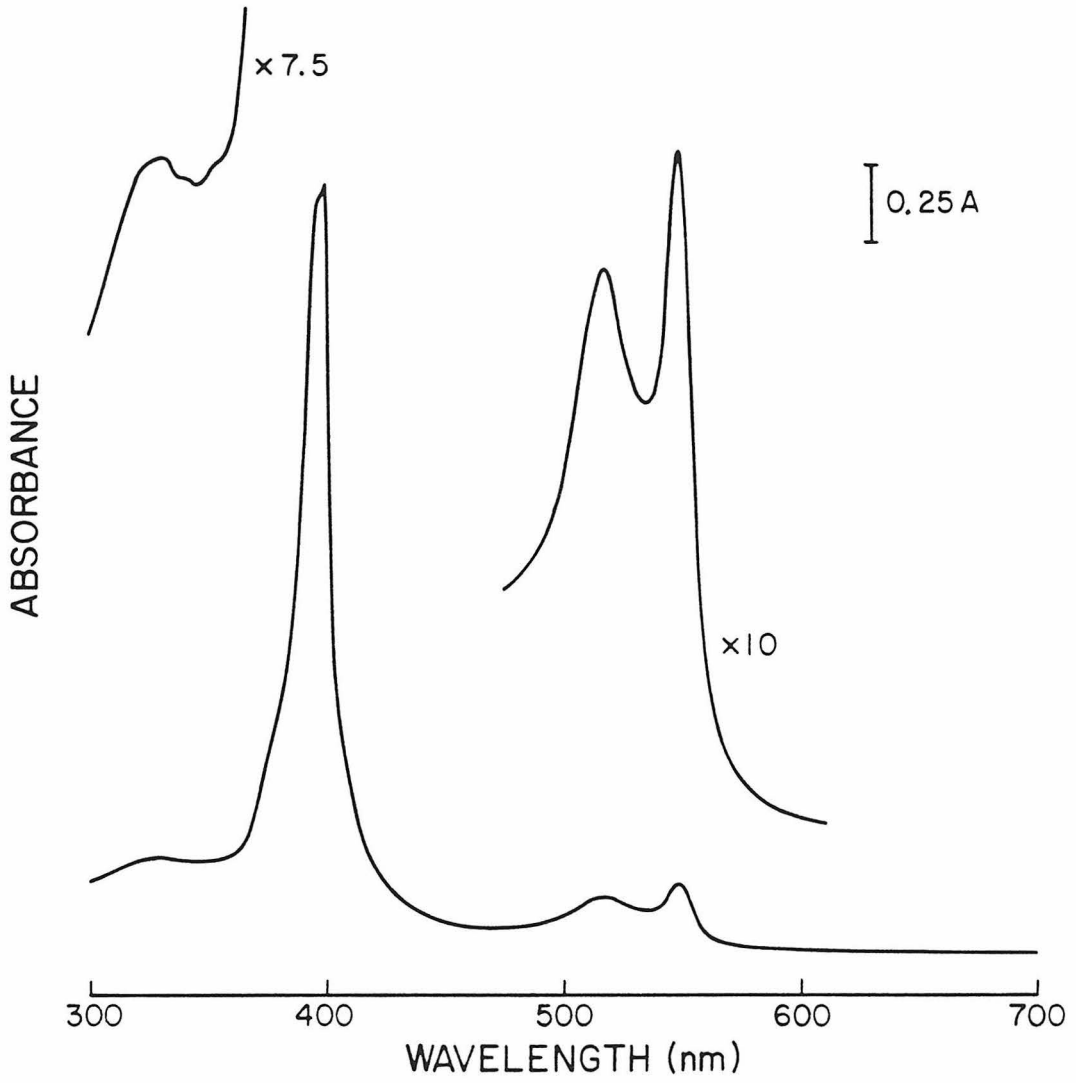
×7.5
0.25 A
ABSORBANCE
×10
300
400
500
600
700
WAVELENGTH (nm)

Figure 7. The overlay spectra of photolysis of Ru^{II}(MpIX)(CO) dicarboxylic acid in dimethyl sulfoxide as a function of time. After every irradiation of *ca.* ten hours, the sample was degassed through five freeze-thaw cycles. The spectrum marked with 195.5 hr corresponds to the final product, Ru^{II}(MpIX)$(DMSO)_2$ dicarboxylic acid. The wavelengths of peaks before photolysis are 548 and 518 nm.

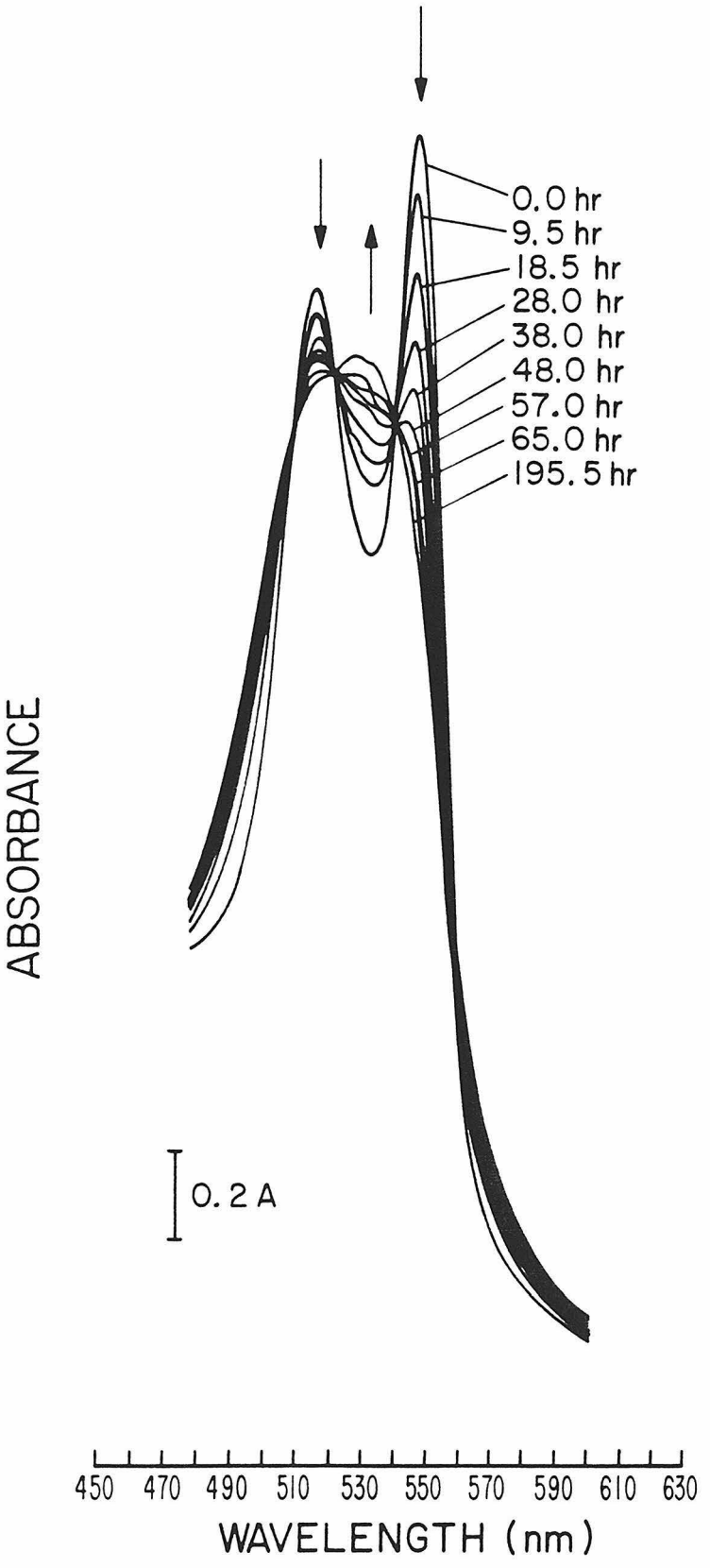
0.0 hr
9.5 hr
18.5 hr
28.0 hr
38.0 hr
48.0 hr
57.0 hr
65.0 hr
195.5 hr
ABSORBANCE
0.2 A
450 470 490 510 530 550 570 590 610 630
WAVELENGTH (nm)

total irradiation time is around 196 hours.

Sperm whale myoglobin (Sigma Chemical Co.) was purified before use by ion exchange chromatography on Whatman CM-52 cellulose, and eluted with pH 7.8, 50 mM tris•HCI buffer at 4 ^{0}C. The major myoglobin component was the last to come off the column and had pI = 8.11. Ultrodex granulated gel and ampholytes (pH 7 ~ 9 and 9 ~ 11) were purchased from LKB. The synthesis of $K_4[W(CN)_8]\cdot 2H_2O$ was described previously.[32] The preparation of all protein and buffer solutions employed deionized water from Barnstead NANOpure water purifier.

In the preparation of apo-myoglobin,[33] the tris•HCl buffer was removed by ultrafiltration into water using Amicon YM-5 membranes under argon with gentle stirring at 5 ^{0}C. The protein solution of low ionic strength was adjusted to pH 2.3 ~ 2.5 by dropwise additions of 0.1 M HCl and immediately mixed with an equal volume of ice-cold 2-butanone. The mixture was vigorously shaken for 1 minute and allowed to stand at 4 ^{0}C for 30 minutes until the deeply colored upper layer of butanone phase which contained the heme was well separated from the colorless lower layer of aqueous phase which contained the apo-protein. The aqueous phase was treated twice more with 2-butanone and dialyzed against two changes of 10 mM sodium bicarbonate solution followed by three changes of water to remove the dissolved butanone. Then the apo-protein solution was dialyzed three times against tris•HCI buffer of pH 7.2, 50 mM.

The syntheses of Ru(CO)Mb[34] and RuMb[35] have been described

elsewhere. The solvent used to introduce ruthenium porphyrin into the cavity of apo-myoglobin was DMSO instead of dimethylformamide (DMF) or pyridine. The freshly prepared apo-myoglobin was mixed with $Ru^{II}(MpIX)(DMSO)_2$ dicarboxylic acid. The protein concentration was 1 mM, and half the stoichiometric amount of $Ru^{II}(MpIX)(DMSO)_2$ dicarboxylic acid was added dropwise to apo-myoglobin with gentle stirring. The process of mixing was carried out in an inert atmosphere free glove box. After mixing for one hour, the solution was passed through a column of Sephadex G-25 which had been previously equilibrated with 50 mM tris•HCI buffer pH 7.2. The eluted protein was then desalted by ultrafiltration into water. The salt free aqueous protein solution then further purified by isoelectric focusing (IEF).

The methodology of preparative flat-bed isoelectric focusing has been described in great detail.[36,37] The 2% ampholyte solutions used to make the pH 7 ~ 10 gradient gels were pretreated by ultrafiltration to get rid of any high molecular weight component. The [Ru^{II}(MpIX)(DMSO) dicarboxylic acid]-reconstituted myoglobin, 0.3 g in 2 ml water, was pipetted onto the gel surface as a narrow zone near the anode. After running for 20 hours at 8 watts constant power, and with the temperature maintained at 10 ^{0}C, IEF purification was complete. Two very closely-running narrow bands were resolved in the IEF gel. Both bands were collected although only the band with higher pI value, *i.e.*, the band closer to the cathode, was investigated by spectroelectrochemistry. Extensive ultrafiltration was used

to remove ampholyte from the protein solution, which was removed from the IEF gel with tris buffer. The protein was again purified by ion exchange chromatography on CM-52 cellulose, and eluted with pH 7.8, 50 mM tris•HCI buffer at 4 ^{0}C. The protein eluent was then dialyzed extensively against pH 7.0, 100 mM phosphate buffer. The UV-VIS spectrum of [Ru^{II}(MpIX)(DMSO) dicarboxylic acid]-reconstituted myoglobin is shown in Figure 8. The protein concentration used in spectroelectrochemical experiments was 1.25 mM, which was based on a calculation using a molar extinction coefficient at 280 nm of 35,000 $M^{-1}cm^{-1}$. One equivalent of $K_4[W(CN)_8]•2H_2O$ was introduced to the protein solution as mediator-titrant. The absorption spectrum of $K_4[W(CN)_8]•2H_2O$ is shown in Figure 9.

Formal reduction potentials at different temperatures, for [Ru(MpIX)(DMSO) dicarboxylic acid]-reconstituted myoglobin, were determined by using an optically transparent thin-layer electrode (OTTLE) cell in a nonisothermal configuration. A summarized description of this technique is given in Chapter II. The OTTLE cell employed a gold minigrid as the working electrode material, and the optical path length was 0.49 mm. Potentials were applied across the thin-layer cell by using a Princeton Applied Research model 174A polarographic analyzer, and were accurately measured with a Keithley model 177 microvolt digital multimeter. The cell temperature was varied by using a variable temperature cell holder, and measured directly with an Omega Engineering precision microthermocouple connected to a Fluke model 2175A digital thermometer. The

Figure 8. The UV-VIS absorption spectrum of [Ru^{II}(MpIX)(DMSO) dicarboxylic acid]-reconstituted sperm whale myoglobin in pH 7.0, μ = 100 mM, phosphate buffer. The wavelengths of peaks are 522, 400, 381, 351, and 274 nm.

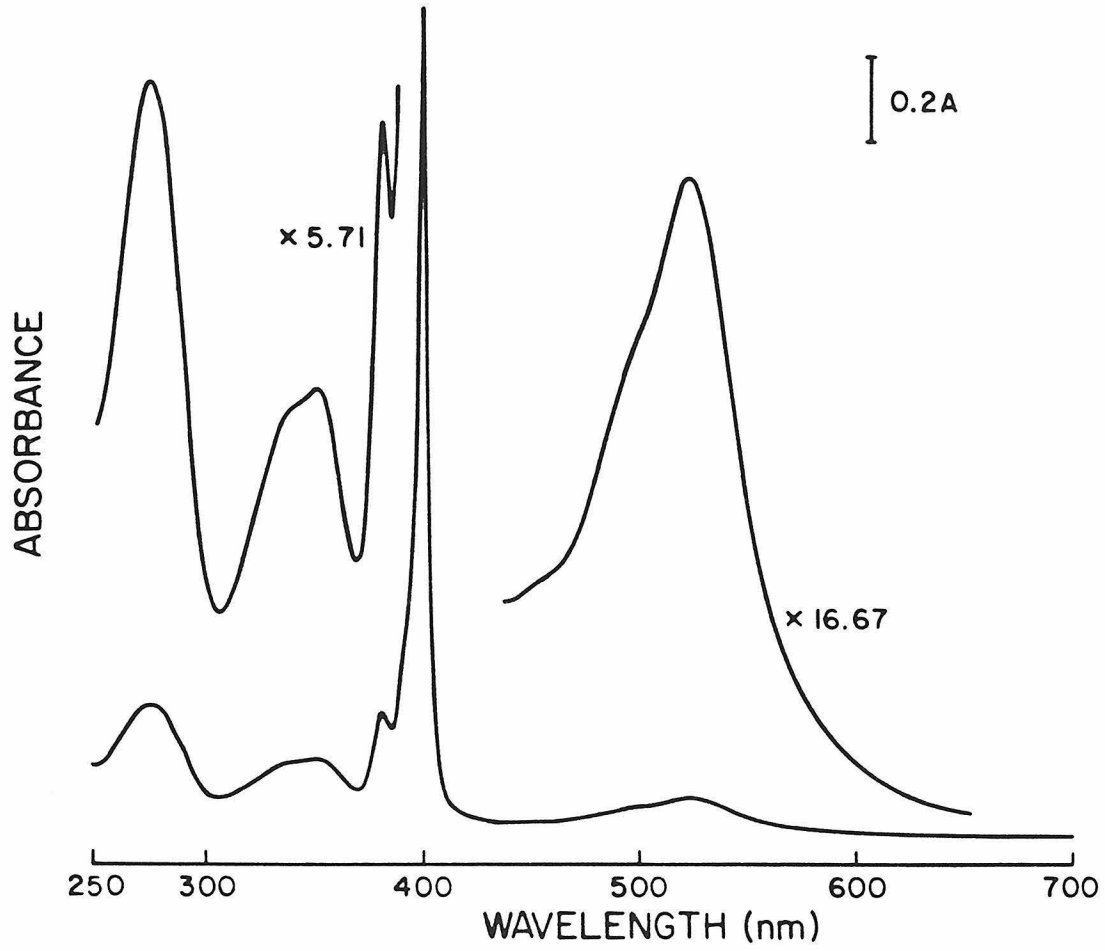
0.2A
× 5.71
× 16.67
ABSORBANCE
250
300
400
500
600
700
WAVELENGTH (nm)

Figure 9. The absorption spectrum of $K_4[W(CN)_8]\cdot 2H_2O$ in pH 7.0, μ = 100 mM, phosphate buffer. The wavelengths of peaks are 429 and 370 nm.

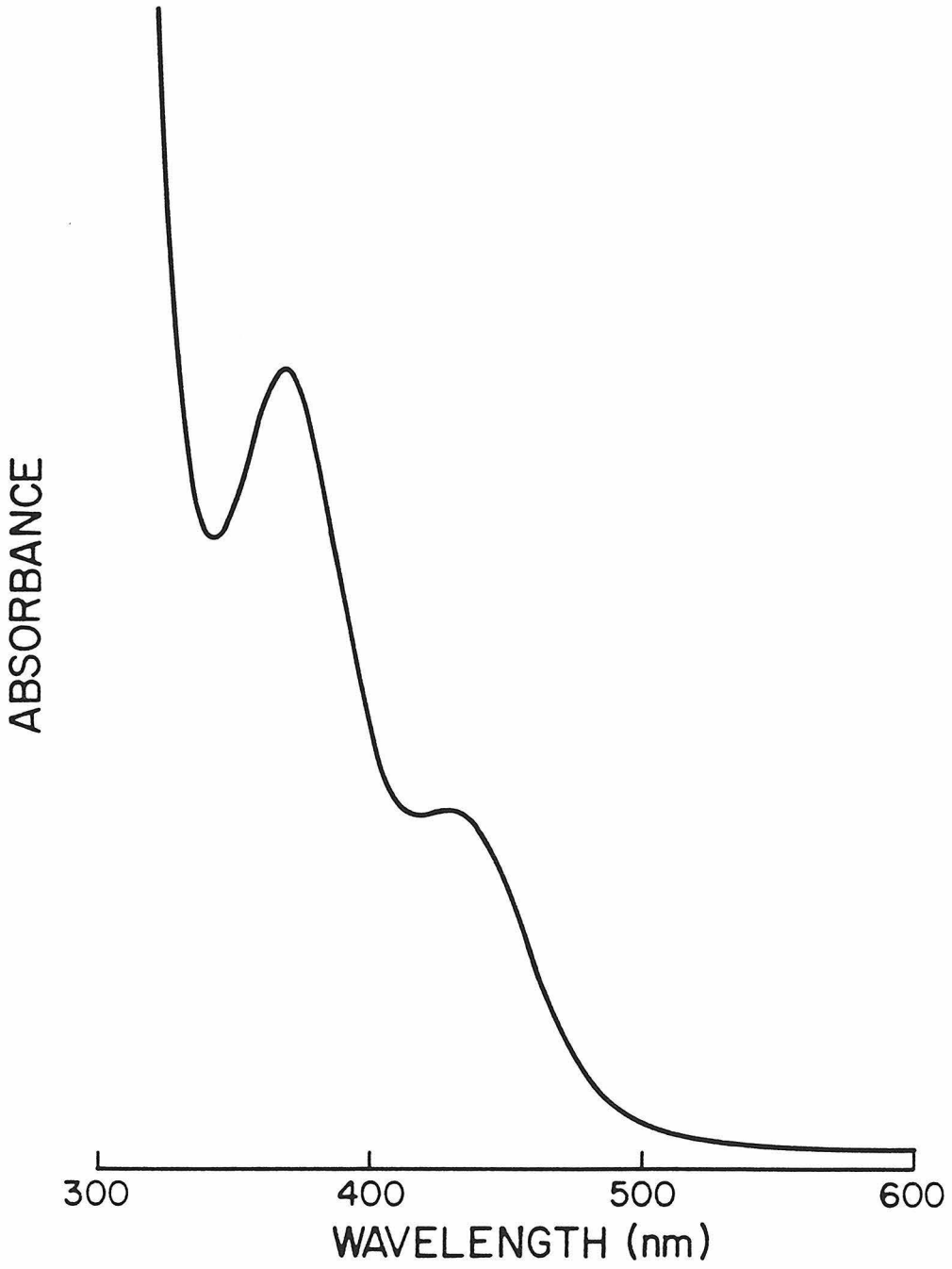
ABSORBANCE
300
400
500
600
WAVELENGTH (nm)

thermocouple was situated in the protein solution in close proximity to the thin-layer cavity. All visible spectra were obtained with a Cary 219 recording spectrophotometer.

Formal reduction potentials were determined by sequentially applying a series of potentials, $E_{appl.}$, to the gold minigrid electrode. Each potential was maintained until electrolysis had ceased, so that the equilibrium value of the ratio of concentrations of oxidized to reduced forms of all redox couples in solution, [Ox]/[Red], was established as defined by the Nernst equation. Redox couples were incrementally converted from one oxidation state to the other by the series of applied potentials, for which each corresponding value of [Ox]/[Red] was determined from the spectra. Formal reduction potentials and n values were determined from plots of $E_{appl.}$ *vs.* log([Ox]/[Red]).

All solution were deoxygenated prior to use by vacuum/argon cycling on a vacuum/purified argon double manifold, and loaded into the OTTLE cell by using rubber septum caps and syringe techniques. The platinum wire auxiliary electrode was situated in a compartment containing deoxygenated mediator-titrant solution that was isolated from the protein solution by a porous glass frit.

Results and Discussion

A typical thin-layer spectroelectrochemical experiment with [Ru^{II}(MpIX)(DMSO) dicarboxylic acid]-reconstituted sperm whale

myoglobin is shown in Figure 10. Because both $[W(CN)_8]^{3-}$ and $[W(CN)_8]^{4-}$ absorb quite weak above 500 nm,[38] all absorbance changes at 523 nm are mainly due to the absorption of ruthenium porphyrin center and can be analyzed directly. In Figure 11, a least squares analysis of the 523 nm Nernst plot gives a midpoint potential of 540 mV *vs.* NHE and a slope of 61 mV at 13.0 ^{0}C.

The protein could be reversibly cycled between its fully oxidized and fully reduced forms, and the value of $E^{0\prime}$ calculated for the ruthenium center was independent of the direction of the experiment.

The temperature dependence of the formal reduction potential of the ruthenium center is shown in Table 3 and Figure 12. A least squares fit of these data gives an $E^{0\prime}$, at 25 ^{0}C, of 514 mV *vs.* NHE, and $(dE^{0\prime}/dT)_{25\ ^0C}$ = -2.06 mV/^{0}C. The partial molal ionic entropy difference between the reduced and oxidized halves of the redox couple of interest, *i.e.*, the electron transfer reaction entropy, $\Delta S^{0\prime}_{et}$, is directly proportional to the temperature coefficient of the nonisothermal cell:

$$\Delta S^{0\prime}_{et} = F \bullet (dE^{0\prime}/dT)_{25\ ^0C}$$

in which F is the Faraday constant. The $\Delta S^{0\prime}_{et}$ for the ruthenium center is therefore calculated to be -47.6 ± 1.2 eu. The entropy for the complete cell reaction, $\Delta S^{0\prime}$, adjusted to the NHE scale, is -63.2 ± 1.2 eu, when a value of -15.6 eu is assumed for ΔS^0_{et} (NHE).[39] The

Figure 10. Thin-layer spectroelectrochemistry of [Ru(MpIX)(DMSO) dicarboxylic acid]-reconstituted sperm whale myoglobin. Solution conditions: pH 7.0, μ = 100 mM, phosphate buffer, 3.0 ^{0}C. Protein concentration: 1.25 mM. Redox mediator: $K_4[W(CN)_8]\cdot 2H_2O$, 1.20 mM. Overlay spectra and absorbance changes at different values of the applies potentials in mV *vs.* SCE. This particular experiment was carried out on oxidation of the protein, *i.e.*, from $Ru^{II} \longrightarrow Ru^{III}$.

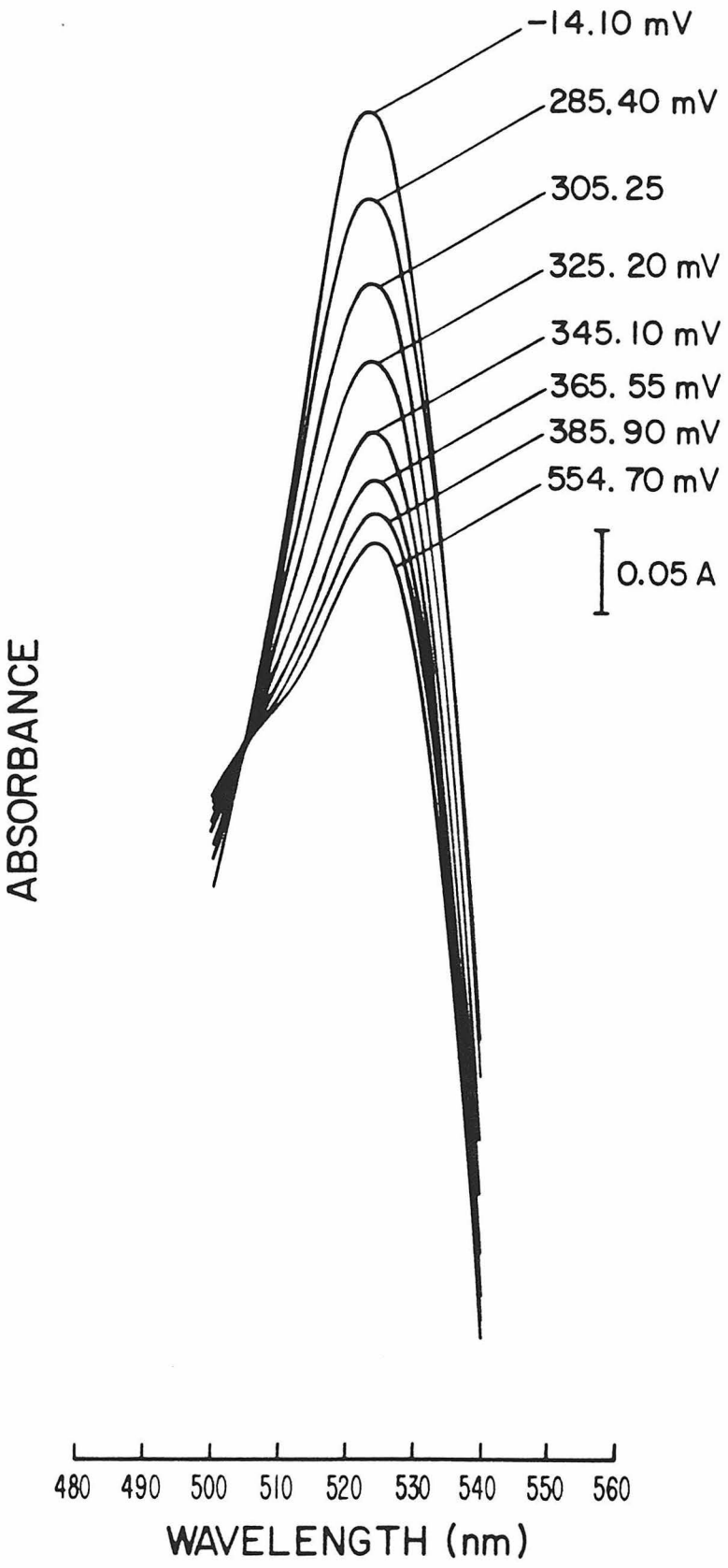
-14.10 mV
285.40 mV
305.25
325. 20 mV
345. 10 mV
365. 55 mV
385. 90 mV
554. 70 mV
0.05 A
ABSORBANCE
480 490 500 510 520 530 540 550 560
WAVELENGTH (nm)

Figure 11. Nernst plot of the absorbance changes at 523 nm during a spectroelectrochemical titration of ruthenium center in [Ru(MpIX)(DMSO) dicarboxylic acid]-reconstituted sperm whale myoglobin. The circles represent experimental points, and the line is a least squares fit of the $E_{appl.}$ *vs.* log([Ox]/[Red]). The fit yielded $E^{0\prime}$ = 540 mV *vs.* NHE and Nernst slope = 61 mV. Solution conditions: pH 7.0, μ = 100 mM, phosphate buffer, 13.0 ^{0}C, 1 equivalent $K_4[W(CN)_8]\cdot 2H_2O$.

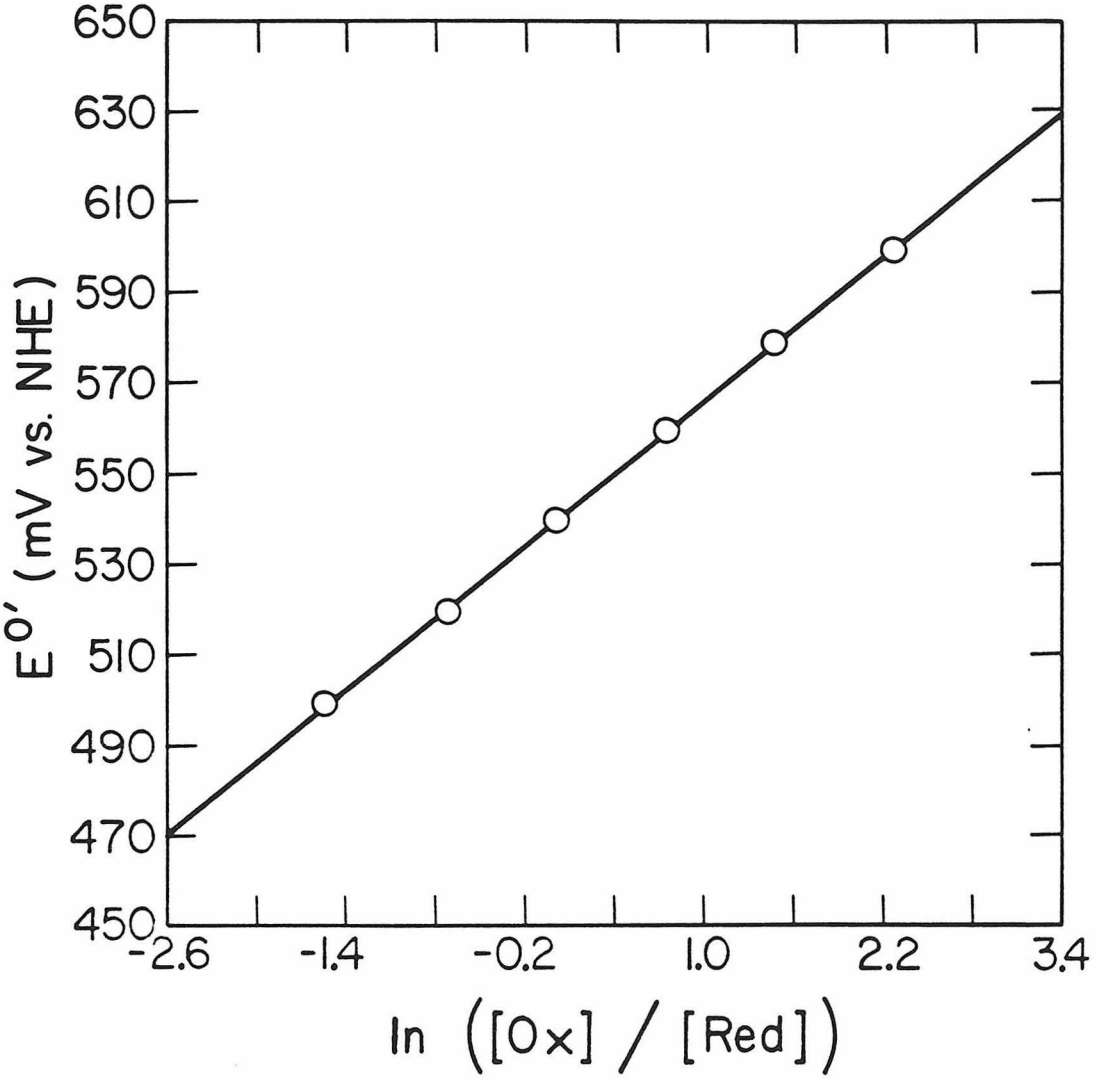
650
630
610
590
570
550
530
510
490
470
450
E°' (mV vs. NHE)
-2.6
-1.4
-0.2
1.0
2.2
3.4
ln ([Ox] / [Red])

Table 3. Temperature dependence of the formal reduction potentials, $E^{0\prime}$, for [Ru(MpIX)(DMSO) dicarboxylic acid]-reconstituted sperm whale myoglobin, using nonisothermal thin-layer spectroelectrochemistry. Solution conditions: pH 7.0, μ = 100 mM, phosphate buffer.

Temperature (^{0}C)*	$E^{0\prime}$ (mV vs. NHE)†
3.0	565
8.0	536
13.0	540
18.0	533
23.0	518
28.0	519
33.0	491
38.8	483

* ± 0.2 ^{0}C

† ± 2 mV

Figure 12. Temperature dependence of the formal reduction potentials, $E^{0\prime}$, for [Ru(MpIX)(DMSO) dicarboxylic acid]-reconstituted sperm whale myoglobin, using nonisothermal thin-layer spectroelectrochemistry. Solution conditions: pH 7.0, μ = 100 mM, phosphate buffer. Temperature range: 3.0 ~ 38.8 ^{0}C. A least squares fit of the data gave an $E^{0\prime}$ = 514 ± 2 mV at 25 ^{0}C and $(dE^{0\prime}/dT)_{25\ ^{0}C}$ = -2.06 x 10^{-3} V/^{0}C.

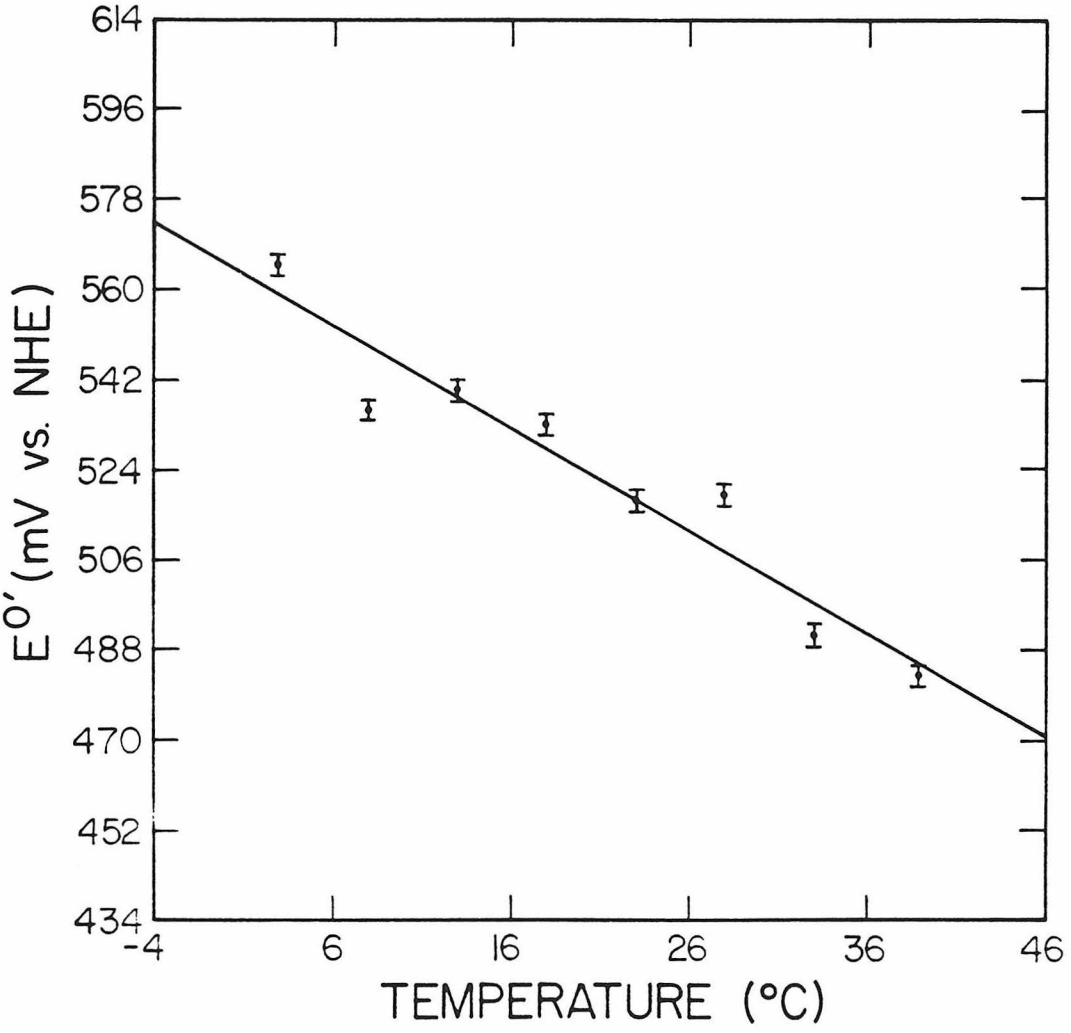
614
596
578
560
542
524
506
488
470
452
434
E°' (mV vs. NHE)
-4
6
16
26
36
46
TEMPERATURE (°C)

corresponding reaction enthalpy, $\Delta H^{0\prime}$, is -30.7 ± 0.4 kcal/mol, and reaction free energy change, $\Delta G^{0\prime}$, is -11.85 ± 0.05 kcal/mol.

The most interesting observation from the spectroelectrochemical experiment, lies in the relatively high value determined for the formal reduction potential, and in the very negative value found for the reaction entropy, $\Delta S^{0\prime}_{et}$. The $E^{0\prime}$ value of 514 *vs.* NHE, gives some indication of the nature of the coordination sphere around ruthenium ion. According to previous investigations of model ammineruthenium complexes containing hydrogen sulfide and related sulfur ligands,[40] those systems in which the coordination sphere consists of five nitrogens and one sulfur are most likely to have their redox potentials around 500 ~ 700 mV *vs.* NHE. With reference to this finding, it is quite possible that the ruthenium ion is coordinated by the four pyrrolic nitrogens from the porphyrin, one nitrogen from the imidazole ring of the proximal histidine F8, *i.e.*, histidine-93, and one sulfur from dimethyl sulfoxide. However, the formal redox potential of $[Ru(NH_3)_5(DMSO)]^{3+/2+}$ is 1,000 mV *vs.* NHE in 0.1 M HCl solution.[40]

In Figure 13, the reaction entropies for the redox couples of some transition metal complexes, in addition to native and modified metalloproteins, are summarized.[6,7,41-45] In contrast to transition metal complexes, the reaction entropies of a large number of metalloproteins are found to range from 0 eu to -16 eu. In the case of [Ru(MpIX)(DMSO) dicarboxylic acid]-reconstituted sperm whale myoglobin, the value of $\Delta S^{0\prime}_{et}$ is exceptionally negative, -47.6 eu.

Figure 13. Reaction entropies of redox couples for selected transition metal complexes as well as native and modified metalloproteins.

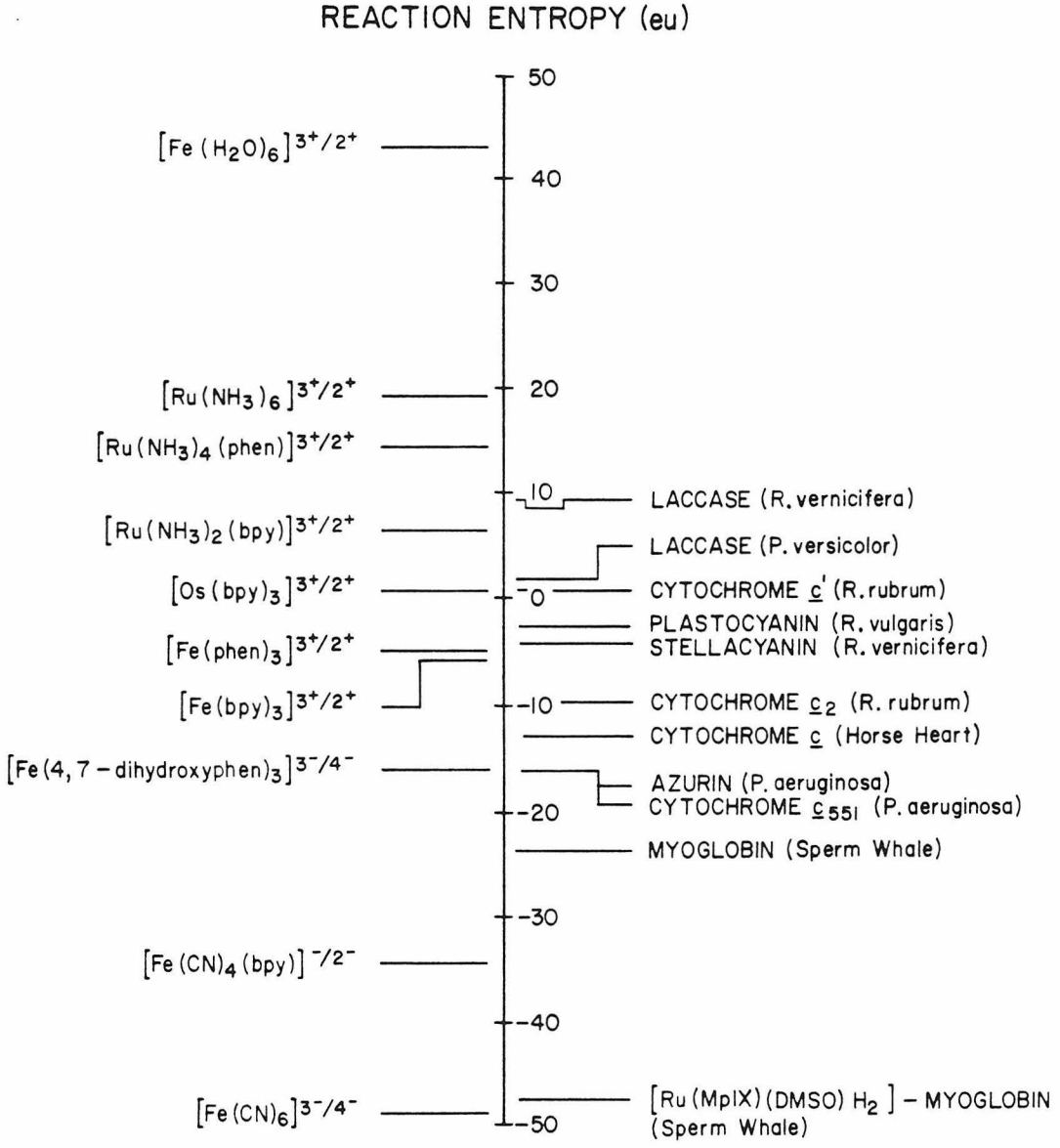
REACTION ENTROPY (eu)
50
40
30
20
10
0
-10
-20
-30
-40
-50
$[Fe(H_2O)_6]^{3+/2+}$
$[Ru(NH_3)_6]^{3+/2+}$
$[Ru(NH_3)_4(phen)]^{3+/2+}$
$[Ru(NH_3)_2(bpy)]^{3+/2+}$
$[Os(bpy)_3]^{3+/2+}$
$[Fe(phen)_3]^{3+/2+}$
$[Fe(bpy)_3]^{3+/2+}$
$[Fe(4,7-dihydroxyphen)_3]^{3-/4-}$
$[Fe(CN)_4(bpy)]^{-/2-}$
$[Fe(CN)_6]^{3-/4-}$
LACCASE (R. vernicifera)
LACCASE (P. versicolor)
CYTOCHROME c' (R. rubrum)
PLASTOCYANIN (R. vulgaris)
STELLACYANIN (R. vernicifera)
CYTOCHROME c_2 (R. rubrum)
CYTOCHROME c (Horse Heart)
AZURIN (P. aeruginosa)
CYTOCHROME c_{551} (P. aeruginosa)
MYOGLOBIN (Sperm Whale)
$[Ru(MpIX)(DMSO)H_2]$ – MYOGLOBIN (Sperm Whale)

According to the spectroelectrochemistry of native sperm whale myoglobin, which has been investigated by Dr. Walther R. Ellis, Jr., native myoglobin has been found to possess quite a negative reaction entropy, -23.6 eu.[6,7] Since myoglobin functions as an oxygen carrier, this measurement was made under strictly anaerobic conditions, in order to prevent formation of oxymyoglobin upon reduction of the protein. The formal reduction potential, and its temperature dependence, for native sperm whale myoglobin, are presented in Table 4 and Figure 14.[45] The comparative plot of the temperature dependence of the formal reduction potentials of native and [Ru(MpIX)(DMSO) dicarboxylic acid]-reconstituted myoglobins is shown in Figure 15. The electrochemical and thermodynamic parameters of native and histidine-48 pentaammineruthenium-modified, in addition to [Ru(MpIX)(DMSO) dicarboxylic acid]-reconstituted, sperm whale myoglobins, are summarized in Table 5.

The heme iron in myoglobin is significantly displaced from the heme plane in both of the available oxidation states, and is highspin in each case. The out-of-plane distances are 0.40 Å for aquometmyoglobin, 0.55 Å for deoxymyoglobin, and 0.33 Å for oxymyoglobin. The axial water ligand of metmyoglobin dissociates from the iron upon reduction of the protein, and this process ought to lead to a positive value for the reaction entropy. However, a quite negative $\Delta S^{0\prime}_{et}$ has been observed instead.[45]

The results in Table 6 show that the transition from aquometmyoglobin to deoxymyoglobin is associated with a movement of

Table 4. Temperature dependence of the formal reduction potentials, $E^{0\prime}$, for the heme center in native sperm whale myoglobin, using nonisothermal thin-layer spectroelectrochemistry. Solution conditions: pH 7.0, μ = 100 mM, phosphate buffer. This experiment was done in anaerobic condition and the formation of oxymyoglobin was prevented upon reduction of the metmyoglobin.

Temperature (^{0}C)*	$E^{0\prime}$ (mV vs. NHE)†
4.9	79
7.5	77
12.5	71
14.9	70
20.0	64
25.0	60
30.0	54
35.0	48
39.8	44
44.8	38

* ± 0.2 ^{0}C

† ± 2 mV

Figure 14. Temperature dependence of the formal reduction potentials, $E^{0\prime}$, for native sperm whale myoglobin, using thin-layer spectroelectrochemistry. Solution condition: pH 7.0, μ = 100 mM, phosphate buffer. Temperature range: 4.9 ~ 44.8 ^{0}C. A least squares fit of the data gave an $E^{0\prime}$ = 59 ± 2 mV at 25 ^{0}C and $(dE^{0\prime}/dT)_{25\ ^{0}C} = -1.03 \times 10^{-3}$ V/^{0}C.

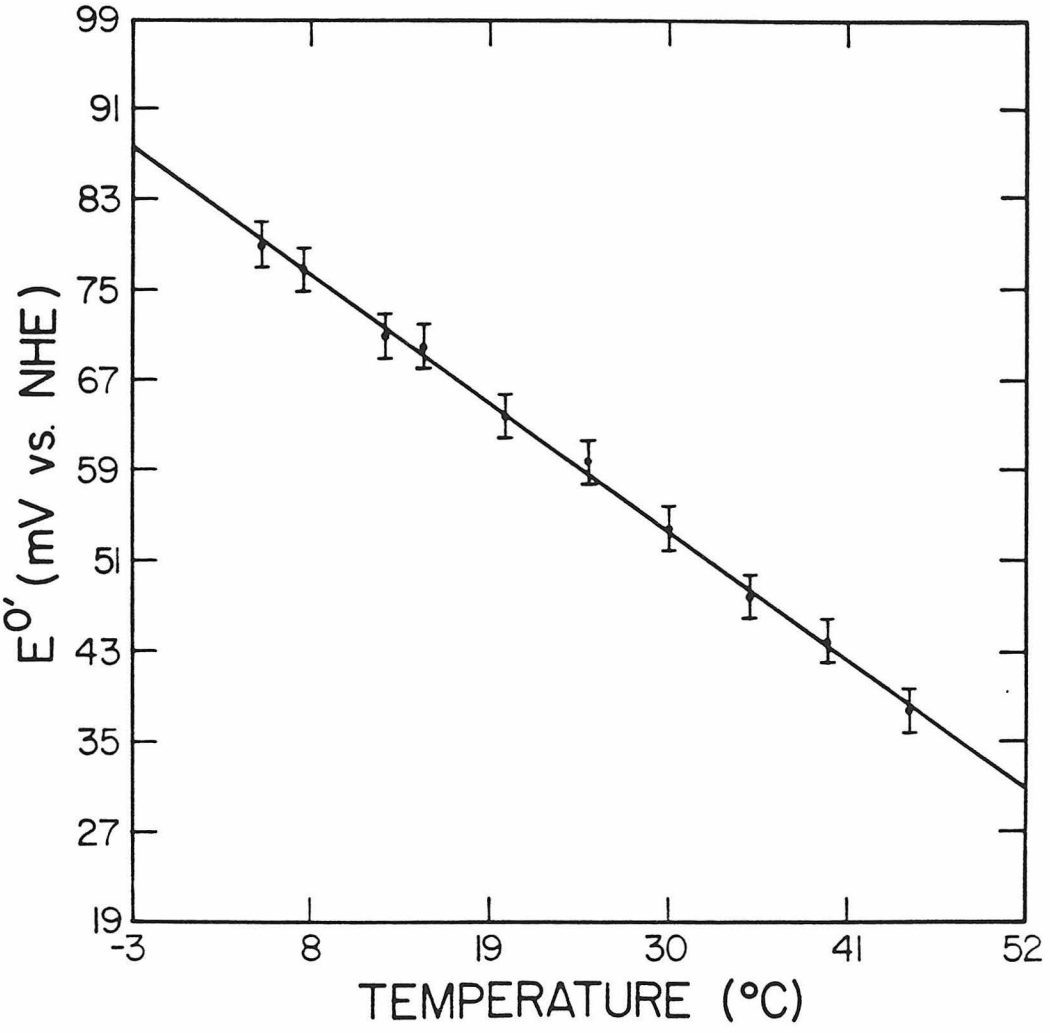
99
91
83
75
67
59
51
43
35
27
19
E°' (mV vs. NHE)
-3
8
19
30
41
52
TEMPERATURE (°C)

Figure 15. Temperature dependence of the formal reduction potentials, $E^{0\prime}$, for the native sperm whale myoglobin (Δ) and for the [Ru(MpIX)(DMSO) dicarboxylic acid]-reconstituted sperm whale myoglobin (•).

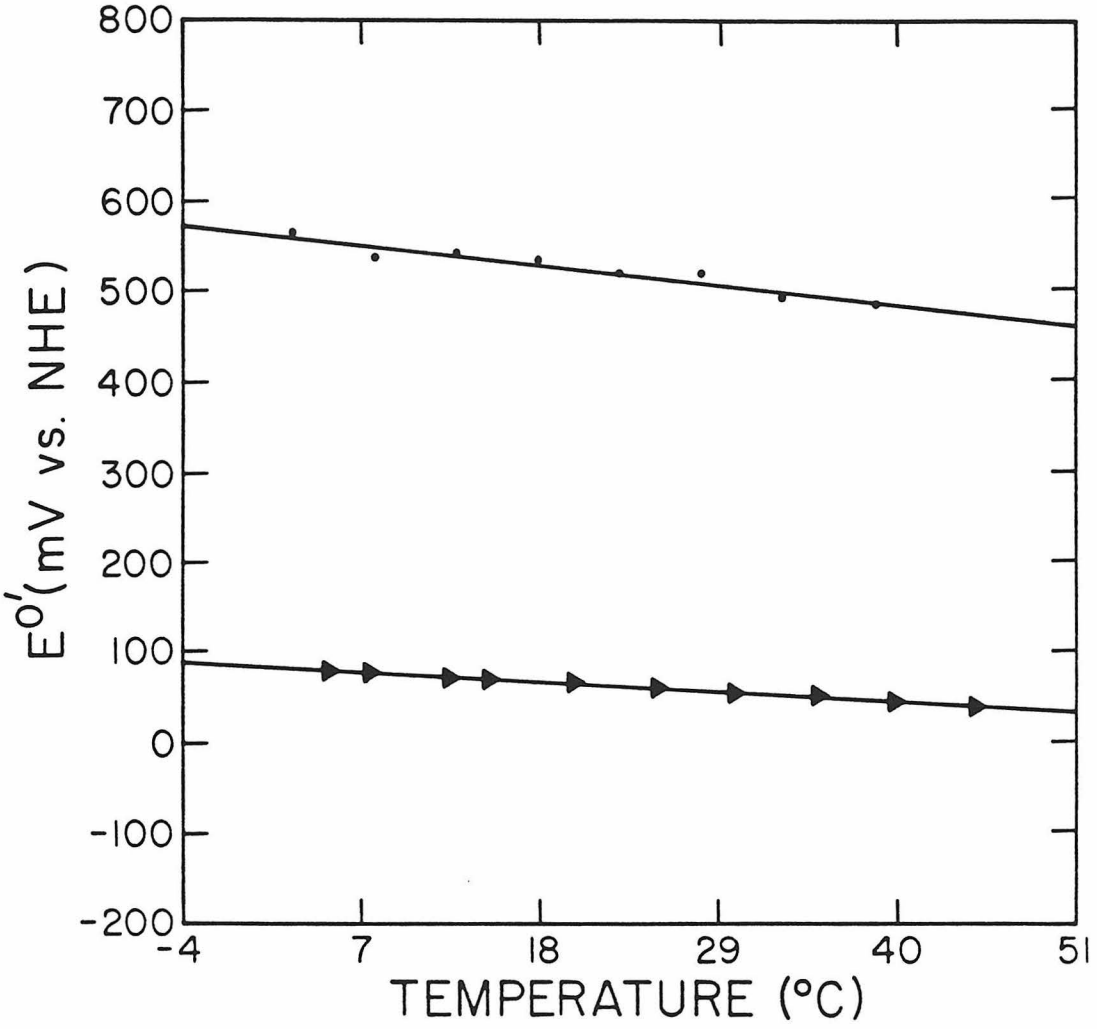
800
700
600
500
400
300
200
100
0
-100
-200
E°'(mV vs. NHE)
-4
7
18
29
40
51
TEMPERATURE (°C)

Table 5. Thermodynamic parameters for the reduction of iron centers in native and in [$Ru(NH_3)_5$(His-48)]-modified sperm whale myoglobins, as well as of ruthenium center in [Ru(MpIX)(DMSO) dicarboxylic acid]-reconstituted sperm whale myoglobin. Solution conditions: pH 7.0, μ = 100 mM, phosphate buffer, 25 ^{0}C.

	Native S.W. Mb $Fe^{3+/2+}$	[a_5Ru(His-48)]-S.W. Mb $Fe^{3+/2+}$	[Ru(MpIX)(DMSO) diacid]-S.W. Mb $Ru^{3+/2+}$
$E^{0\prime}$ (mV vs. NHE)	59	65	514
$\Delta G^{0\prime}$ (kcal/mol)	-1.36	-1.51	-11.85
$\Delta S^{0\prime}$ (eu)	-39.2	-37.6	-63.2
$\Delta S^{0\prime}_{et}$ (eu)	-23.6	-22.0	-47.6
$\Delta H^{0\prime}$ (kcal/mol)	-13.0	-12.7	-30.7

Table 6. Heme geometry in myoglobin derivatives.

Distance	Deoxy-Mb*	Aquo-Met-Mb†	Oxy-Mb‡
Fe-heme plane	0.55	0.40	0.33
His F8-heme plane	2.6	2.5	2.3

*Reference 17.

†Reference 16.

‡Reference 20.

the iron atom and proximal histidine F8 away from the porphyrin plane, of the order of 0.15 Å and 0.1 Å respectively. The distance between the iron center and the coordinating nitrogen in the imidazole ring of proximal histidine F8, becomes 0.05 Å shorter. However, this kind of change in the coordination sphere of the metal ion does not seem to be the main factor accounting for the large negative value found for the reaction entropy. The most convincing explanation for the phenomenon probably lies in a dramatic contraction of the protein structure, leaving little interior space for water molecules.

The question of rationalizing the large negative value found for the reaction entropy of [Ru(MpIX)(DMSO) dicarboxylic acid]-sperm whale myoglobin is an interesting problem, and will probably require much more work before a satisfactory solution is found. The dissociation of dimethyl sulfoxide, following the transition from Ru(II) to Ru(III), seems unlikely to occur. A low-spin ruthenium-substituted heme is expected in both +2 and +3 oxidation states. The most reasonable explanation lies in the protein itself becoming more rigid, leading to stonger internal solvent-protein interactions, with a greater degree of ordering in the solvation at the protein surface following reduction of the protein.

References

1. Isied, S. S., Kuehn, C., and Worosila, G., *J. Am. Chem. Soc.*, ***106***, 1722 (1984).

2. Nocera, D. G., Winkler, J. R., Yocom, K. M., Bordignon, E., and Gray, H. B., *J. Am. Chem. Soc.*, ***106***, 5145 (1984).

3. Yocom, K. M., Winkler, J. R., Nocera, D. G., Bordignon, E., and Gray, H. B., *Chem. Scr.*, ***21***, 29 (1983).

4. Winkler, J. R., Nocera, D. G., Yocom, K. M., Bordignon, E., and Gray, H. B., *J. Am. Chem. Soc.*, ***104***, 5798 (1982).

5. Yocom, K. M., Shelton., J. B., Shelton, J. R., Schroeder, W. A., Worosila, G., Isied, S. S., Bordignon, E., and Gray, H. B., *Proc. Natl. Acad. Sci. USA*, ***79***, 7052 (1982).

6. Crutchley, R. J., Ellis, W. R., Jr., and Gray, H. B., in *Frontiers in Bioinorganic Chemistry*, Xavier, A. V., ed., VCH erlagsgesellschaft, Weinheim, F. R. G., 1986, P. 679.

7. Crutchley, R. J., Ellis, W. R., Jr., and Gray, H. B., *J. Am. Chem. Soc.*, ***107***, 5002 (1985).

8. Keilin, D., *The History of Cell Respiration and Cytochromes*, Cambridge University Press, Cambridge, 1966.

9. Hatefi, Y., in *Annual Review of Biochemistry*, Richardson, C. C., ed., Annual Reviews Inc., Palo Alto, 1985, P. 1015.

10. Dixit, B. P. S. N., and Vanderkooi, J. M., in *Current Topics in Bioenergetics*, Volume 13, Lee, C. P., ed., Academic, Orlando, 1984, P. 159.

11. Takano, T., and Dickerson, R. E., *J. Mol. Biol.*, ***153***, 79 (1981).

12. Takano, T., and Dickerson, R. E., *J. Mol. Biol.*, ***153***, 95 (1981).

13. Dickerson, R. E., *Sci. Amer.*, ***242***, 137 (1980).

14. Salemme, F. R., in *Annual Review of Biochemistry*, Volume 46, Snell, E. E., ed., Annual Reviews Inc., Palo Alto, 1977, p. 299.

15. Dickerson, R. E., *Sci. Amer.*, ***226***, 58 (1972).

16. Takano, T., Kallai, O. B., Swanson, R., and Dickerson, R. E., *J. Biol. Chem.*, ***248***, 5244 (1973).

17. Wittenberg, J. B., *Physiol. Rev.*, ***50***, 559 (1970).

18. Kendrew, J. C., Dickerson, R. E., Strandberg, B. E., Hart, R. G., Davies, D. R., Phillips, D. C., and Shore, V. C., *Nature*, ***185***, 442 (1960).

19. Takano, T., *J. Mol. Biol.* ***110***, 537 (1977).

20. Takano, T., *J. Mol. Biol.*, ***110***, 569 (1977).

21. Watson, H. C., in *Progress in Stereochemistry*, Volume 4, Aylett, B. J., and Harris, M. M., eds., Butterworths, London, 1969, P. 299.

22. Matthews, B. W., in *The Proteins*, Volume 3, Third Edition, Neurath, H., and Hill, R. L., eds., Academic, New York, 1977, P. 403.

23. Phillips, S. E. V., *Nature*, ***273***, 247 (1978).

24. Edmundson, A. E., *Nature*, ***205***, 883 (1965).

25. Rifkind, J. M., in *Inorganic Biochemistry*, Volume 2, Eichhorn, G. L., ed., Elsevier, Amsterdam, 1973, P. 832.

26. Antonini, E., and Brunori, M., eds., *Hemoglobin and Myoglobin in Their Reactions with Ligands*, North-Holland, Amsterdam, 1971.

27. Poulos, T. L., and Finzel, B. C., in *Peptide and Protein Reviews*, Volume 4, Hearn, M. T. H., ed., Marcel Dekker, New York, 1984, P. 115.

28. Backes, W. L., Tamburini, P. P., Jansson, I., Gibson, G. G., Sligar, S. G., and Schenkman, J. B., *Biochemistry*, ***24***, 5130 (1985).

29. Fisher, M. T., and Sligar, S. G., *Biochemistry*, ***24***, 6696 (1985).

30. Mayo, S. L., Ellis, W. R., Jr., Crutchley, R. J., and Gray, H. B., *Science*, ***233***, 948 (1986).

31. Bonnet, J. J., Eaton, S. S., Eaton, G. R., Holm, R. H., and Ibers, J. A., *J. Am. Chem. Soc.*, ***95***, 2141 (1973).

32. Goodenow, E. L., and Garner, C. S., *J. Am. Chem. Soc.*, ***77***, 5268 (1955).

33. Yonetani, T., *J. Biol. Chem.*, ***242***, 5008 (1967).

34. Srivastava, T. S., *Biochim. Biophys. Acta*, ***491***, 599 (1977).

35. Paulson, D. R., Addison, A. W., Dolphin, D., and James, B. R., *J. Biol. Chem*, ***254***, 7002 (1979).

36. Winter, A., Pelmutter, H., and Davies, H., LKB Application Note, No. 198 (1980).

37. Radola, B. J., *Biochim. Biophys. Acta*, ***386***, 181 (1974).

38. Perumareddi, J. R., Liehr, A. D., and Adamson, A. W., *J. Am. Chem. Soc.*, ***85***, 249 (1963).

39. Taniguchi, V. T., Sailasuta-Scott, N., Anson, F. C., and Gray, H. B., *Pure Appl. Chem.*, ***52***, 2275 (1980).

40. Kuehn, C. G., and Taube, H., *J. Am. Chem. Soc.*, ***98***, 689 (1976).

41. Taniguchi, V. T., Ellis, W. R., Jr., Cammarata, V., Webb, J., Anson, F. C., and Gray, H. B., in *Advances in Chemistry Series, No. 201, Electrochemical and Spectrochemical Studies of Biological Redox Components*, Kadish, K. M., ed., American Chemical Society, Washington, D. C., 1982, P. 51.

42. Taniguchi, V. T., Malmström, B. G., Anson, F. C., and Gray, H. B., *Proc. Natl. Acad. Sci. USA*, ***79***, 3387 (1982).

43. Yee, E. L., and Weaver, M. J., *Inorg. chem.*, ***19***, 1077 (1980).

44. Hanania, G. I. H., Irvine, D. H., Eaton, W. A., and George, P., *J. Phys. Chem.*, ***71***, 2022 (1967).

45. Ellis, W. R., Jr., Ph.D. Thesis, California Institute of Technology, Pasadena, United States, 1986.